Influence of different silica sources as an alternative to conventional sodium silicate in fly ash geopolymer concrete

by

Ntebaleng Lekhera

Dissertation submitted in fulfilment of the requirements for the degree

MASTER of ENGINEERING in CIVIL ENGINEERING

in the

Department of Civil Engineering

of the

Faculty of Engineering, Built Environment and Information Technology

at the

Central University of Technology, Free State

Supervisor: Dr R. Gopinath

Co-supervisor: Dr A. Naghizadeh

Co-supervisor: Mr W. Strydom

BLOEMFONTEIN

2026

DECLARATION OF INDEPENDENT WORK

I, Ntebaleng Lekhera, student number _____, do hereby declare that this research project submitted to the Central University of Technology, Free State, for the Degree MASTER OF ENGINEERING: CIVIL ENGINEERING, is my own independent work; and complies with the Code of Academic Integrity, as well as other relevant policies, procedures, rules and regulations of the Central University of Technology, Free State; and has not been submitted before to any institution by myself or any other person in fulfilment (or partial fulfilment) of the requirements for the attainment of any qualification.

_____ 11/02/2026

SIGNATURE OF STUDENT DATE

PUBLICATIONS

Lekhera, N., Naghizadeh, A. & Gopinath, R. 2023. Effect of waste-derived alkali activators on compressive strength of fly ash geopolymer mortar. *Concrete Beton* 174(1): 10–14. Available in: https://concretesocietysa.org.za/issues/issue174//offline/download.pdf

ACKNOWLEDGEMENTS

I would like to acknowledge and express my gratitude to the Central University of Technology, Free State, for awarding the research grant that facilitated this study.

Special appreciation goes to my supervisor, Dr R. Gopinath, and my co-supervisors, Dr A. Naghizadeh and Mr W. Strydom for their invaluable support, guidance, and contributions to the success and completion of this study. Their assistance, corrections, recommendations, and words of encouragement were instrumental throughout this journey.

I am also thankful to the Department of Engineering Sciences at the University of the Free State for granting access to their laboratory, which was crucial for completing the experimental programme.

Lastly, I extend my deepest gratitude to my family and friends for their unwavering support throughout this endeavour. A heartfelt thank you to my husband, Mr T. Tlebere, and my beloved daughter, M.J. Tlebere, for their love, understanding, and encouragement.

TABLE OF CONTENTS

LIST OF FIGURES

LIST OF TABLES

LIST OF ABBREVIATIONS

AAB	Alkali-activated binder
AAC	Alkali-activated concrete
AAFS	Alkali-activated fly ash-slag
AAM	Alkali-activated material
ACI	American Concrete Institute
AS	Australian Standard
A-S-H	Aluminosilicate hydrate
ASTM	American Society for Testing and Materials
BS EN	British Standard
C-A-S-H	Calcium-aluminium-silicate-hydrate
C-S-H	Calcium silicate hydrate
EHS	Environmental Health and Safety
FTIR	Fourier transform infrared [spectroscopy]
GGBS	Ground granulated blast-furnace slag
GPC	Geopolymer concrete
GWP	Glass waste powder
HMNS	High-magnesium nickel slag
ITZ	Interfacial Transition Zone
L/S	Liquid to solid
LOI	Loss on ignition
N-A-S-H	Sodium aluminosilicate hydrate
OPC	Ordinary Portland Cement
PC	Portland Cement
RHA	Rice husk ash
rpm	Revolutions per minute
SANS	South African National Standard
SEM	Scanning electron microscopy/microscope
SF	Silica fume
SS/SH	Solid to solid to heat

USA	United States of America
Vicat	Vicatronic automatic recording apparatus
XRD	X-ray diffraction
XRF	X-ray fluorescence

LIST OF UNITS

°	Degree(s)
°C	Degree(s) Celsius
µm	Micrometre(s)
g	Gram(s)
g/cm³	Gram(s) per cubic centimetre
kg	Kilogram(s)
kg/m²	Kilogram(s) per square metre
kg/m³	Kilogram(s) per cubic metre
kg/m³	Kilograms per cubic metre
kg/t	Kilogram(s) per ton
kN/min	Kilonewton per minute
kV	Kilovolt
L	Litre
M	Molar concentration
m²/g	Square metre(s) per gram
mA	Milliampere
ml	Millilitre(s)
mm	Millimetre(s)
mm/√*h*	Millimetres per square root of hour
mol/kg	Mole(s) per kilogram
MPa	Megapascal
mS/cm	milliSiemens/centimeter
nm	Nanometre(s)
wt.%	Percentage by weight
θ	Phase angle
µm	Micrometre(s)
$	United States dollar(s)

LIST OF CHEMICAL SYMBOLS

Al_2O_3	Alumina
Al^{3+}	Aluminium ions
$Al_{4.68}Si_{1.32}O_{9.66}$	Mullite
$Al_6P_6O_{12}$	Berlinite
AlO_4	Aluminate
Ca	Calcium
$Ca(OH)_2$	Calcium hydroxide
$Ca_{12}Fe_7.54Si_{12}O_{48}$	Andradite
Ca^{2+}	Calcium ions
$CaMg(CO_3)_2$	Dolomite
$Ca_4Mn_8O_{16}$	Marokite
CaO	Calcium oxide
Cl^-	Chloride ions
CO_2	Carbon dioxide
Cs	Caesium
CsOH	Caesium hydroxide
$MgFe_2O_4$	Magnesioferite
$Fe_{24}O_{32}$	Magnetite
Fe_2O_3	Iron oxide
$(Ca,Mg,Fe)(Mg,Fe)Si_2O_6$	Pigeonite
H^+	Hydrogen ions
H_2	Dihydrogen gas
H_2O	Water
H_2SO_4	Sulphuric acid
HCl	Hydrochloric acid
HNO_3	Nitric acid
K	Potassium
$K(AlSi_2O_6)$	Leucite
K_2O	Potassium oxide

K_2O_3Si	Potassium silicate
KOH	Potassium hydroxide
Li	Lithium
LiOH	Lithium hydroxide
Mg	Magnesium
Mg_4O_4	Periclase
$MgAl_2O_4$	Spinel
MgO	Magnesium oxide
$MgSO_4$	Magnesium sulphate
MnO	Manganese oxide
MOH	Metal hydroxide
Na	Sodium
Na^+	Sodium ions
$NaAlSi_2O_6$	Jadeite
Na_2CO_3	Sodium carbonate
Na_2O	Sodium oxide
Na_2SiO_3	Sodium silicate
Na_2SO_4	Sodium sulphate
$NaAl_2O_2$	Sodium aluminate
NaOH	Sodium hydroxide
NOx	Nitrogen oxide
O_2	Oxygen
OH^-	Hydroxide ions
P_2O_5	Phosphorus pentoxide
Rb	Rubidium
RbOH	Rubidium hydroxide
SiO_2	Quartz
Si^{4+}	Silicon ions
Si_8	Silicon
SiO	Silicon monoxide
SiO_2	Silicon dioxide

SiO_4	Silicate
SO2	Sulphur oxide
SO_3	Sulphur trioxide
Ti_2O_4	Rutile
TiO_2	Titanium dioxide

ABSTRACT

The production of Portland Cement (PC) is known for its substantial carbon emissions. Geopolymer offers an alternative to PC as a binder in concrete. Fly ash is a commonly utilised source material in geopolymers due to its extensive availability and good performance. While the elimination of lime calcination reduces the environmental impact of geopolymer binders, the use of conventional sodium silicate as an activator has been questioned by several studies due to its environmental implications. The production of sodium silicate involves high temperatures of up to 1 300 °C, which leads to an increased carbon footprint. The aim of this study was to substitute sodium silicate with silica source materials such as silica fume, rice husk ash, and glass waste powder, which are industrial and agricultural by-products.

The study investigated the viability of these by-products as activators in fly ash geopolymer. The alkali-activator solution was prepared using sodium hydroxide via a hydrothermal method, while fly ash was blended with ground granulated blast-furnace slag (GGBS) to control flow workability and setting time, as well as to enhance compressive strength. The study utilised various parameters for the mixture, including the ratio of alkali-activator solution to fly ash, the ratio of silica sources to sodium hydroxide, the concentration of sodium hydroxide solution, and the GGBS ratio. In total, 70 batches of mortar and 15 batches of concrete mixtures were prepared, using mortar cubes of 50 mm and 100 mm in size, respectively. These cubes were used to assess the compressive strengths of the mortars at seven or 28 days, and of the concrete at three, seven, 28, and 90 days, following the guidelines of American Society for Testing and Materials (ASTM C109:2021). Additionally, the flow workability and setting time of fresh mortars were evaluated according to ASTM C230 (2008) and ASTM C807 (2020). Durability was assessed through durability index tests (oxygen permeability, water sorptivity, and chloride conductivity indexes), and microstructural analysis that utilised X-ray diffraction and scanning electroscope microscopy techniques.

The results of the compressive strength tests, flow workability assessments, setting time measurements, durability index, and microstructural studies were analysed. In general, the compressive strength demonstrated an upward trend relative to the influence of each

parameter (such as the silica source / sodium hydroxide) ratio, sodium hydroxide concentration, GGBS ratio, etc.). However, the findings also revealed that this increase could only occur to a certain extent, as a notable decline was observed upon exceeding specific ratios. Workability and setting time measurements were conducted to evaluate the fresh properties of the fly ash geopolymer when GGBS was introduced. The results for both parameters indicated a decrease with higher dosages of GGBS. To maintain acceptable workability flow, GGBS incorporation had to be limited to below 40% in the mix.

Conversely, higher dosages of GGBS prolonged the setting time for this type of geopolymer, which may be advantageous in most cases, especially when working on-site. Durability index testing was performed on a mixture comprising 70% fly ash and 30% GGBS geopolymer activated with 6 M silica fume at a ratio of 1.3. The oxygen permeability index results demonstrated enhanced resistance to gas penetration overall. Water sorptivity and porosity showed favourable durability when the GGBS content remained below 30% but deteriorated when it surpassed 30% GGBS. Chloride conductivity indicated strong durability, especially with a GGBS content of 40% and higher. Microstructural analyses revealed undissolved fly ash in the samples. Nonetheless, with an increase in the molarity of the sodium hydroxide, a denser matrix and a reduced quantity of undissolved fly ash particles were observed. Furthermore, the findings indicated that incorporating more GGBS into the mixture resulted in a rougher surface of the sample. The inclusion of GGBS also led to enhanced mechanical properties of fly ash-based geopolymers.

These findings highlight the potential of geopolymer concrete, activated with sustainable materials, as a viable and eco-friendly alternative to PC in the construction phase. This approach contributes to reduced carbon emissions and promotes circular economy practices.

Keywords: geopolymer, silica fume, rice husk ash, glass waste powder, sodium silicate

CHAPTER 1:
INTRODUCTION

1.1 Background

Concrete is one of the most important materials used in the construction industry. It is a popular building material due to its relatively low cost, availability, remarkable durability, and the ability to be formed into any shape or size (Singh et al., 2019). The primary binding material in concrete is Portland Cement (PC). PC production is increasing by 9% annually worldwide, with approximately four billion tonnes produced each year (Singh et al., 2019; Ali, 2025). Since its invention in the early 1800s, PC has become the world's second most consumed material after water (H_2O) (Faris et al., 2017; Rosen, 2021). Cement production requires a calcium (Ca) source, typically limestone, as well as a silicon (Si_8) source such as clay or sand (Xiao Kun Lu et al., 2024). These raw materials are finely ground and mixed before being fed into a rotary cement kiln, where a clinker is produced. A clinker is formed by firing a mixture of clay and limestone at temperatures above 1 300 °C (Ige et al., 2021). These reactions occur at extremely high temperatures and result in the emission of carbon dioxide (CO_2) and other greenhouse gases that are responsible for global warming.

According to Singh et al. (2020), greenhouse gas emissions from PC production amount to approximately 1.5 billion tonnes per year, representing 7% to 8% of total emissions from various sectors worldwide. In Figure 1.1, Lowitt (2020) illustrates that the calcining process accounts for 50% of carbon dioxide emissions, which makes it an unavoidable aspect of PC clinker production. Approximately 40% of greenhouse gas emissions in cement production stem from the use of fuel to generate the high temperatures necessary for the calcining process (i.e., heating limestone to produce lime), which distinguishes the cement industry from others. In contrast, the primary source of greenhouse gas emissions in other industries is predominantly the combustion of fuels for energy purposes. However, in cement production, a significant portion of emissions arises from the specific thermal requirements of the calcining process rather than direct fuel combustion for energy.

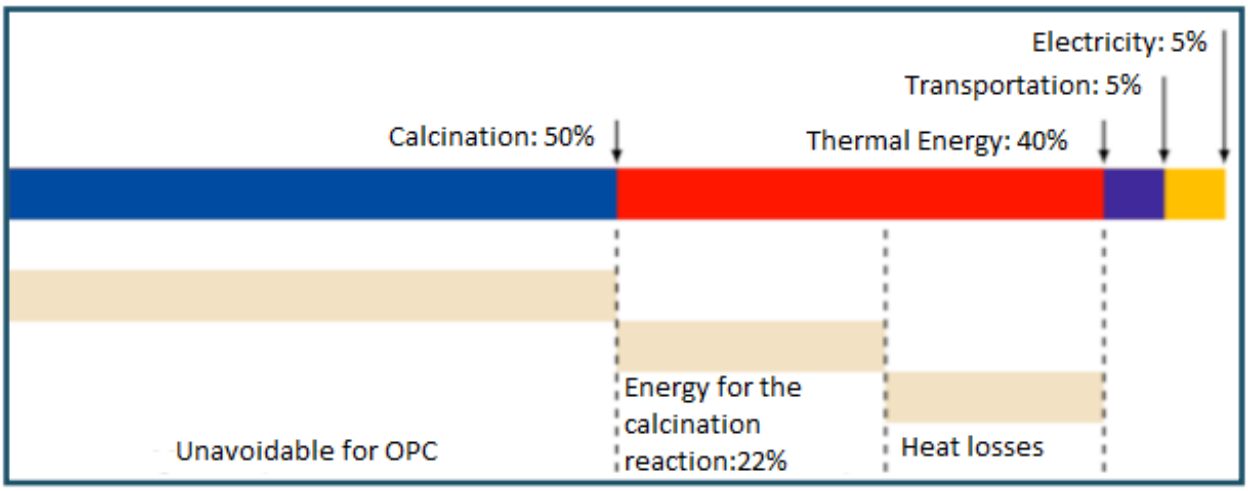

Figure 1.1: Carbon dioxide emissions during cement production

Source: Lowitt (2020)

South Africa produced 13.78 million tonnes of cement in the 2023 financial year and approximately 15 million tonnes in 2024, while global cement production was approximately 4.17 billion tonnes (Global Cement, 2023). This accounted for roughly 0.33% of global production, which may seem like a small fraction of total output. However, its steady growth reflects ongoing infrastructure development and housing initiatives (Jessa & Ajidahum, 2024). Generally, the production of one ton of PC results in the release of approximately one ton of carbon dioxide, which makes it necessary to develop more environmentally friendly concrete alternatives to replace PC (Hariz et al., 2017; Jessa & Ajidahum, 2024). These alternatives may include various types of low-carbon or carbon-neutral cements, such as fly ash-based geopolymers, slag-based cements, or calcium aluminate cements; among others. By replacing PC with these greener alternatives, it is possible to reduce the overall carbon emissions associated with cement production. Fly ash-based geopolymers are considered more sustainable than PC because they utilise industrial by-products, thereby reducing waste and conserving natural resources. Their production avoids the high-temperature calcination process required for PC, which significantly lowers energy consumption and carbon emissions. Additionally, their superior durability and chemical resistance extend the lifespan of structures, which minimises maintenance and lifecycle emissions. However, the exact environmental impact of these alternatives may vary, and their widespread adoption

depends on factors such as cost, the availability of raw materials, and regulatory support. Many researchers have suggested adopting geopolymer cement as an alternative to PC, as it presents a promising way to reduce both greenhouse gas emissions and energy consumption in the cement industry (Adjei et al., 2021; Singh et al., 2019; Singh & Middendorf, 2020; Carreño-Gallardo et al., 2018).

The main factor in environmental sustainability is to reduce carbon emissions and minimise waste materials disposed of in landfills. The development of innovative recycling techniques that not only divert waste from landfills but also transform it into new marketable products is significantly important and should be considered (Keawthun et al., 2014; Besklubova et al., 2025). The drive to use waste material as an alternative to sodium silicate (Na_2SiO_3) in alkaline solutions serves as a remedy for the recycling of agricultural, industrial, and municipal wastes (Rajan & Kathirvel, 2021; Billong et al., 2021; Rivera et al., 2018). This innovative technology can also be implemented in developing countries such as South Africa to improve waste management and promote the production of sustainable and cleaner geopolymers using renewable resources.

The history of geopolymer materials dates back to the early 20th century, with the first known patent for a geopolymer-like substance granted to a chemist and engineer named Wilhelm Kühl from Germany in 1908 (Faris et al., 2017). According to Faris et al. (2017), Kühl's patent outlined a process involving the reaction of a solid precursor material containing aluminium dioxide or alumina (Al_2O_3) and silicon dioxide or silica (SiO_2), specifically vitreous slag, with an alkaline source such as alkali sulphate or carbonate. This reaction resulted in the formation of a solid material comparable to PC in terms of its binding and structural properties. Kühl's patent marked one of the earliest documented instances of using an alkali-activated binder (AAB) system akin to what we now refer to as geopolymer materials. However, the term "geopolymer" itself was not widely used at that time, and the understanding of the underlying chemistry and material properties was not as developed as it is today.

The term "geopolymer" gained prominence much later, particularly in the 1970s, when French researcher Joseph Davidovits began investigating alkali-activated materials (AAMs) derived from industrial by-products. Davidovits is often credited with popularising

the term “geopolymer” and advancing research in this area. He emphasised the use of fly ash and other aluminosilicate-rich materials as precursors, activated by alkali solutions to form geopolymers. His work laid the foundation for the modern understanding and development of geopolymer science and technology (Davidovits, 1989; 1991; 2013; 2018). Over the years, geopolymer research has expanded, and its potential applications have grown beyond cementitious materials to include fire-resistant materials, high-temperature coatings, waste encapsulation, and more. Geopolymers are valued for their reduced environmental impact compared to traditional cement-based materials due to their utilisation of industrial by-products and lower carbon emissions (Azad & Samarakoon, 2021).

Geopolymerisation is the reaction of aluminosilicate materials (such as fly ash, slag, or clay) with alkali activators (including silicate, potassium silicate [K_2O_3Si], potassium hydroxide [KOH], and sodium hydroxide [NaOH]) at mild temperatures, as illustrated in Figure 1.2 (Singh & Middendorf, 2020; Joshi & Kadu, 2012; Xu & Van Deventer, 2000). However, growing interest in sustainability, cost reduction, and simplifying mix designs has led researchers to investigate whether NaOH alone can effectively activate aluminosilicate precursors. Studies show that although sodium silicate improves silica availability and generally enhances geopolymer strength, NaOH-only activation can still yield viable geopolymer binders, particularly in systems rich in reactive aluminosilicates such as slag, red mud, fly ash, and metakaolin. In a study by Mariyappan and Somasundaram (2025), an investigation of red mud–based geopolymer mortars activated solely with low-molarity NaOH (0.5M–2M) was conducted. The results showed the highest compressive strength in non-carbonated samples was achieved at 0.5M, whereas carbonated samples peaked at 2M NaOH. Microstructural analysis (XRD, SEM) confirmed formation of geopolymer gels and sodium carbonate in carbonated conditions. Effective geopolymerization at very low NaOH concentrations, attributed to the inherent alkalinity of red mud. These findings demonstrated that NaOH-only activation is feasible when the precursor itself contains sufficient soluble alkalis. Sodium potassium hydroxide and sodium, as well as potassium silicate solutions, are the most commonly used alkali activators in geopolymerisation (Nikolov et al., 2017). The alkaline solution contains a high concentration of hydroxide ions (OH^-), typically greater than 5 M (molar

concentration). This high alkalinity enables the solution to dissolve the amorphous fraction of solid powders, such as fly ash or slag, which are used as raw materials in geopolymer production. The solution also contains sodium or potassium silicate, commonly known as water glass, which is a soluble silicate compound that provides a source of soluble silicon dioxide for the geopolymerisation reaction. Silicon dioxide is an essential component in geopolymer formation, as it reacts with alumina from the solid powders to form the geopolymer binder (Kamseu et al., 2017).

Furthermore, Kamseu et al.'s (2017) study stated that among the two solutions, sodium/potassium silicate raises the most concerns regarding the effective and efficient sustainability of geopolymers, as its production involves energy-intensive processes and potentially harmful chemicals. The presence of soluble silicate, particularly sodium silicate, in a geopolymer activating solution is known to produce a denser and more compact material with higher mechanical strength than hydroxide-activated geopolymers (Sambucci et al., 2021). Additionally, a study by Abdulla, Kamarudin, Mohammed, Nizar, Rafiza and Zarina (2011) showed that mixing a sodium silicate solution with a sodium hydroxide solution improved the interaction between the aluminosilicate material and the solution. Moreover, the sodium silicate activator dissolves quickly and bonds the aluminosilicate material particles together. The dissolution of solid sodium silicate is an endothermic reaction. As the modulus (molar ratio of silicon dioxide to sodium oxide [Na_2O] in the sodium silicate) increases, the dissolution rate and solubility of vitreous silicates decrease due to the formation of more stable, less soluble species. However, sodium silicate production involves the calcination of sodium carbonate (Na_2CO_3) and quartz (silicon dioxide) at temperatures ranging from 1 400 to 1 500 °C, which results in large amounts of carbon dioxide being produced as a by-product, which is then emitted into the environment (Turner & Collins, 2013; Rodríguez et al., 2013).

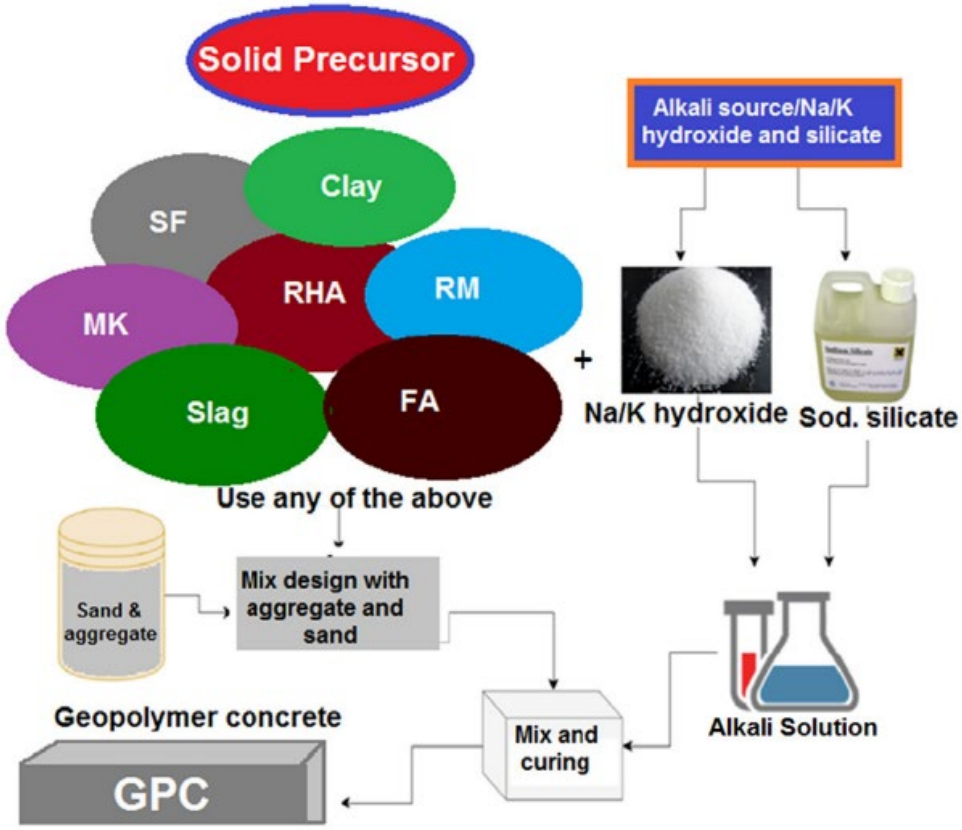

Figure 1.2: Process of geopolymerisation

Source: Singh and Middendorf (2020)

There is substantial literature regarding the properties of good activators. The activator must:

- be able to trigger and ensure the full reaction with the precursor in the desired time (too long reaction times may result in low early-age strength, while too short reaction times may result in fast setting problems);
- be available at a low cost and in sufficient quantity;
- have a low environmental impact; and
- allow for simple and cost-effective synthesis (Vinai & Soutsos, 2019).

Several alternative silica sources have been proposed to replace sodium silicate, including waste glass, bamboo leaves, silica fume (SF), nano-silica, and rice husk ash (RHA) (Rajan & Kathirvel, 2021; Bernal et al., 2015; Luukkonen et al., 2018). Researchers have focused on hydrothermal processes as a means of producing silicate solutions

(Tong et al., 2018; Delgado-Plana et al., 2024; Adeleke et al., 2023). These solutions are used as activators in AABs. In the study by Tong et al. (2014), the mix used a blend of fly ash and ground granulated blast-furnace slag (GGBS) as precursors. Mortars made with the RHA-derived sodium silicate solution (produced via a hydrothermal process) achieved about 60 MPa at 28 days, which is comparable to mortars activated with commercial sodium silicate solutions. The study also highlighted that AABs using RHA-derived activators are more durable in aggressive environments compared to PC-based systems. Delgado-Plana et al. (2024) focused on synthesising solid sodium silicate from waste glass and used it in one-part AAMs. In this study, the activator modulus (Ms = SiO_2/Na_2O) was tested at 0.5, 1.0, and 1.5. The Na_2O dosage was 10, 20, and 30 g per 100 g of precursor. The compressive strength obtained was 35.8 MPa at Ms 1.0 and 20 g Na_2O per 100 g precursor. In another study, Adeleke et al. (2023) synthesised sodium silicate from SF and used it in geopolymer concrete (GPC). The highest compressive strength achieved was 62.6 MPa at an activator-to-precursor ratio of 0.9 and an SS/NaOH ratio of 1.2/0.8. Microstructural analysis confirmed the formation of a dense aluminosilicate gel, and durability indicators such as water absorption and chemical resistance were comparable to mixes using commercial sodium silicate. Although it has been explored, there are few studies that focus on waste-derived activators with blended systems (e.g., slag and fly ash). Instead of employing conventional methods to produce sodium silicate, recent studies have proposed alternative approaches, such as the hydrothermal process and alkaline fusion method (Rajan & Kathirvel, 2021; Vinai & Soutsos, 2019). The studies further indicate that by using the hydrothermal process, researchers can achieve the desired results while potentially reducing energy consumption and emissions by more than 70% compared to PC-based concrete. Consequently, this study adopted the hydrothermal process to convert the industrial and agricultural by-products used as alternative silica sources.

1.2 Problem statement and research significance

Existing literature indicates a potential decrease in global warming of 40% to 44% through the adoption of geopolymer technology instead of PC (Jalal et al., 2024; Abbas et al., 2024). However, these studies also express reservations about potential secondary costs

associated with the production and transportation of geopolymer materials. While the primary focus of the studies was on the reduction in global warming potential, the researchers acknowledged that achieving this reduction may involve trade-offs and additional complexities related to the entire lifecycle of geopolymer materials. Most of the aluminosilicate materials for geopolymers are industrial byproducts such as fly ash and GGBS. In 2022, the global fly ash generation reached was 592 million tonnes and over 60% of global fly ash is consumed by the construction industry, mainly in concrete. Despite this, significant volumes remain unused, especially in Asia, leading to large stockpiles near coal power plant and this can be cited as a major environmental waste-management challenge. While in 2024, more than 310 million tonnes of blast furnace slag was produced globally. Approximately 65% of this (200 million tonnes) is processed into GGBS each year. However, even with relatively high reuse rates, large unused quantities still require disposal, and steel production itself produces vast emissions. One of the most common alkali activators used during geopolymer synthesis is sodium silicate, which provides mechanical durability to the system. However, sodium silicate is obtained through an expensive and polluting process that requires temperatures above 1 300 °C, which results in significant carbon dioxide emissions (Toniolo, 2018; Rajan & Kathirvel, 2021).

Furthermore, the production of sodium silicate emits approximately 1.514 kg of CO_2 per kilogram, excluding the energy used for raw material extraction. This figure is relatively high compared to Ordinary Portland Cement (OPC), which averages 0.85 to 0.95 kg CO_2 per kilogram. However, OPC is used in much larger quantities in concrete mixes, making its overall environmental impact significantly greater. In contrast, geopolymers use sodium silicate in smaller proportions alongside low-carbon precursors like fly ash or slag, which have near-zero emissions since they are industrial by-products. The overall global warming potential of GPC is still 40% to 44% lower than that of OPC, due to reduced binder content and the avoidance of limestone calcination. The production of sodium silicate also generates dust, nitrogen oxides (NOx), and sulphur oxides (SO_2), which contribute to air pollution; this process is therefore not considered environmentally friendly (Kaduku et al., 2015). The use of industrial or agricultural by-products as a reactive silica source in geopolymer binders can help to reduce the environmental impact of commercial

sodium silicate production (Rajan & Kathirvel, 2021). For instance, SF is a waste product from silicon and ferrosilicon alloy industries, already generated as part of another industrial process. In 2023 it had a global annual production of 560 million which is mostly used in concrete. Using it as a reactive silica source therefore avoids the need to manufacture additional sodium silicate, directly reducing upstream emissions. Additionally, using SF as an alternative silica source can reduces waste disposal, limit land occupation, and prevent particulate pollution associated with SF stockpiling (Adeleke et al., 2023). Global RHA production was measured in the range of thousands of kilotonnes, with rice-producing countries (China, India, Indonesia). Approximately 40–48% is used in concrete, steel and silica industries. Producing RHA requires lower energy than producing commercial sodium silicate because burning is often part of biomass energy generation or existing agricultural processing. Another factor is that ash can be collected with minimal additional processing. These facts confirm that RHA serves as a silica-rich alternative requiring far less embodied energy than industrial silicate production (Billong et al., 2021). About 130 million tonnes of glass is produced annually worldwide. Only 21% (27 million tonnes) of glass is recycled globally. Glass is non-biodegradable, and the vast majority ends in landfills (due to contamination, ineffective collection, and lack of reuse streams). Thus, incorporating GWP in geoplymer concrete can also minimises landfill burden which reduces environmental impacts associated with waste disposal (Delgado-Plana et al., 2025). The use of the hydrothermal process for producing sodium silicate significantly reduces CO_2 emissions compared to the conventional process. By using lower temperatures and avoiding high-energy calcination, hydrothermal methods can cut emissions by more than 50%. Previous studies on sodium silicate production and its application in concrete have notable gaps. Most research lacks a comparison of various alternative materials; most studies are primarily based on one alternative material, and there is limited standardisation of chemical properties for waste-derived sodium silicate, which affects consistency in concrete performance. Furthermore, long-term durability under aggressive conditions remains underexplored. The development of geopolymers, particularly alkali activators, based on by-product materials represents a significant economic and environmental benefit and offers an alternative to commercial sodium silicate. Silica-based by-product materials used as activators in

geopolymer binders can potentially improve the mechanical and durability properties of concrete. Furthermore, the incorporation of these materials not only positively impacts the environment by eliminating sodium silicate from the activation process but also promotes sustainable approaches to converting waste into valuable resources. This study aims to advance sustainable construction by exploring the use of RHA, glass waste powder (GWP), and SF as alternative silica sources to replace commercial sodium silicate in fly ash-based GPC. The significance of this research lies in its potential to address two critical challenges: reducing the environmental footprint of geopolymer production and promoting circular economy principles through the recycling of industrial and agricultural waste. By minimising reliance on energy-intensive sodium silicate, this study could substantially lower the carbon emissions associated with geopolymer technology, which will make it a more viable alternative to PC.

1.3 Research aim and objectives

The aim of this study was to assess the influence of different silica sources as an alternative to conventional sodium silicate in fly ash-GPC.

The following research objectives were formulated for the study:

- To characterise the various silica sources that can be used as alternatives to conventional sodium silicate.
- To determine the optimum proportions of various silica sources based on the fresh and hardened properties of fly ash and fly ash / GGBS geopolymer mortar. To conduct microstructural and analytical studies to understand the variation in the hardened properties of fly ash and fly ash / GGBS geopolymer mortars with different silica activators.
- To determine the viability of the optimum mix with respect to the durability characteristics of fly ash-GPC incorporated with GGBS.

1.4 Research Questions

The current study addresses the following questions:

- **Characterisation:** How do the physical, chemical, and mineralogical characteristics of different silica sources compare when considered as alternatives to conventional sodium silicate in fly ash–based geopolymer systems?
- **Proportioning:** What is the optimum mix required to achieve target workability and strength in fly ash and fly ash/GGBS geopolymer mortars?
- **Mechanisms:** How do SEM and XRD observations vary across silica sources, and how do these microstructural signatures explain differences in hardened performance?
- **Durability:** To what extent is the optimum silica-based activator mix durable (e.g., sulfate resistance, acid resistance, water absorption/permeability) when scaled to concrete with GGBS?

1.5 Scope and limitations of research

The preparation of geopolymers using by-product materials can be effective for sustainable development; however, this is limited by the availability, cost, and accessibility of these materials. This study investigated the substitution of sodium silicate with alternative by-products such as SF, RHA, and GWP. For instance, in regions such as South Africa, where rice is not produced, developing RHA-based geopolymers can be challenging, as this material would need to be imported. This not only limits the feasibility of production but also increases the associated costs. Additionally, the process of preparing effective sodium silicate from alternative by-products relies heavily on the methodology used. Several parameters influence the dissolution of these by-products, including:

- The process temperature and duration of the alkaline solution: The temperature and duration of the alkaline solution can affect the dissolution rate and efficiency of the by-products. Higher temperatures and longer durations may enhance dissolution, although the effect can vary depending on the nature of the by-product. For by-products with a rapid dissolution rate, such as SF, higher temperatures can accelerate the process. However, this rapid dissolution can lead to bubbling and overflow of the solution.

- Sodium hydroxide concentration: Higher concentrations usually accelerate dissolution; however, a solution with higher molarity may lead to increased costs.
- Alkali-activator solution filtration method: The method used to filter the alkali-activator solution after the dissolution process can influence the purity and quantity of the final product.

1.6 Outline of the dissertation

The dissertation contains five chapters. A schematic breakdown and summary of each chapter is given below.

Chapter 1: Introduction

This chapter introduces the study and provides a brief background, the problem statement and research significance, the aim and objectives of the research, the scope and limitations of the research, as well as the thesis structure.

Chapter 2: Literature Review

This chapter provides a detailed literature review on the chemistry of geopolymerisation, the environmental impacts of sodium silicate, as well as its replacement using alternative silica sources. The mechanical properties and durability characteristics of fly ash geopolymer mortar and concrete are also discussed in detail.

Chapter 3: Methodology

This chapter provides comprehensive explanations of the different materials used and their quantities, which are depicted in the mix design provided for the investigation. Additionally, the chapter offers an in-depth overview of the various testing and measurement techniques employed in the study, such as flow workability and setting time measurement, compressive strength tests, and durability index testing, which includes the oxygen permeability index, water sorptivity index, and chloride conductivity index tests.

Chapter 4: Results and Discussions

This chapter provides a detailed analysis and discussion of the obtained test results. It offers an in-depth examination of the results from the compressive strength test in relation

to various parameters. The results of the flow workability and setting time tests are also discussed. Additionally, the durability index test results for fly ash / GGBS concrete are analysed. Finally, the microstructural results are interpreted using advanced technology from the Geotechnical Department at the University of the Free State.

Chapter 5: Conclusions and Recommendations

This chapter concludes the study and provides a summary of the results presented in Chapter 4. It also explores the recommendations that emanated from the study.

CHAPTER 2:
LITERATURE REVIEW

2.1 Background

Concrete has become the most widely used building material on the planet. PC serves as a binder in concrete due to its numerous advantages, including acceptable compressive strength, resistance to chemical attack, and long-term durability. However, the production of PC has a significantly negative impact on the environment. The cement industry is identified as one of the largest users of carbon-based fuels and accounts for 5% to 8% of global carbon dioxide emissions (Singh et al., 2019; Naghizadeh & Ekolu, 2017; Amran et al., 2021). In 2016, South African cement plants emitted an average of 671 kg of carbon dioxide per ton of cement produced. While this figure exceeds the global average of 642 kg carbon dioxide per ton of cement, it is still better than several regions, including the Middle East (712 kg), Russia (707 kg), and North America (745 kg). Although South Africa's emissions fall within the mid-range when compared globally, it remains critical to prioritise efforts to decarbonise the cement industry (Lowitt, 2020).

Climate change has recently sparked extensive debate around the world, with experts discussing its potential consequences for the way society operates, particularly for vulnerable populations in less developed regions. Within this debate, there is growing agreement that climate change is more than just an issue of energy efficiency or industrial carbon emissions, as the approach to pursuing development and economic growth has proven to be highly unsustainable from an ecological perspective (Bernal et al., 2016). As a result, there is an urgent need to develop new and sustainable approaches to material manufacturing and consumption as a critical component of the effort to reduce waste generation. This also necessitates maximising waste conversion into valuable resources.

As the need to reduce global carbon dioxide emissions grows due to their contribution to climate change, geopolymer cements are becoming the focus of increased research efforts. Geopolymer cements offer potential advantages over traditional PC in terms of their lower carbon footprint (Živica et al., 2015; Singh et al., 2015). They are typically produced by activating aluminosilicate materials, such as industrial by-products or natural

minerals, with alkali solutions. The reported range of carbon dioxide equivalent values for GPC compared to PC is quite substantial. Estimates suggest that GPC could have carbon dioxide equivalent emissions as much as 80% lower than those of PC (Turner & Collins, 2013). Geopolymers also possess excellent mechanical strength and resistance to aggressive environments, which presents an opportunity to improve both environmental and engineering performance simultaneously when compared to traditional technology (Fifinatasha et al., 2013). Researchers such as Aliques-Granero et al. (2019), Aiken et al. (2018), Lahoti et al. (2019), Shill et al. (2020), Karthiyaini (2016), and Vafaei et al. (2018) have thoroughly studied the benefits of geopolymer cements, including fire resistance, chemical corrosion resistance, high mechanical strength, and excellent durability. Figure 2.1 presents the benefits of GPC.

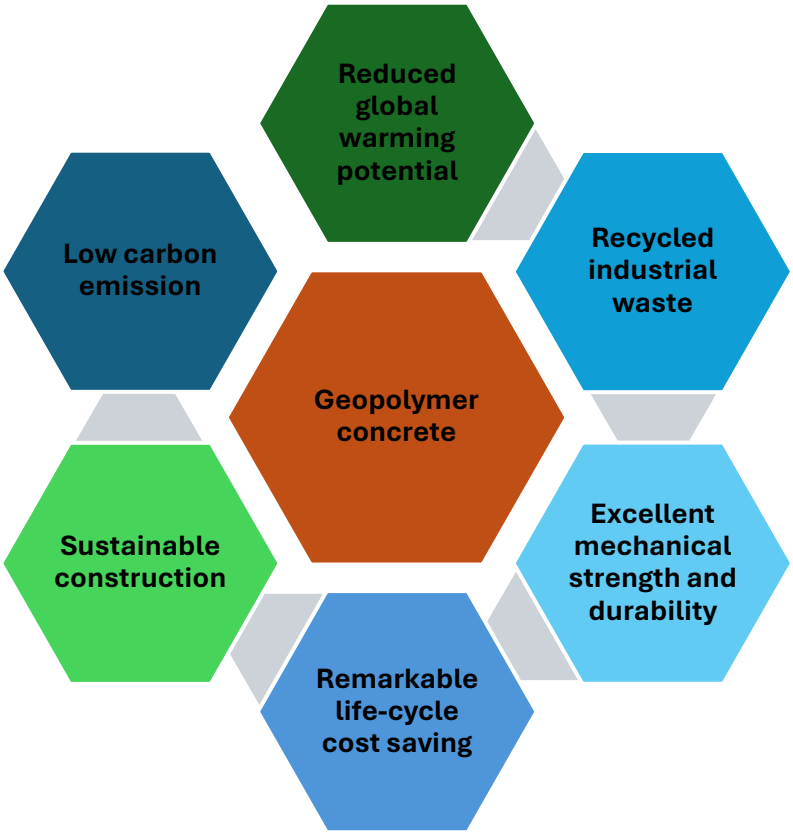

Figure 2.1: Benefits of geopolymer concrete (GPC) in sustainable construction

Source: Aliques-Granero et al. (2019); Aiken et al. (2018); Lahoti et al. (2019); Shill et al. (2020); Karthiyaini (2016); Vafaei et al. (2018)

Geopolymers have a wide range of potential applications due to their numerous beneficial properties (Fifinatasha et al., 2013). These materials have garnered significant attention as promising options for building restoration because of their excellent characteristics since their discovery. As a result, the building industry has become a major user of geopolymer technology, particularly in the form of geopolymer cement, which is regarded as a “green” alternative to traditional cement and concrete (Cong & Cheng, 2021). Geopolymers have also been utilised in commercial airports and mainline railway sleepers in Australia. Additionally, they can be employed for the repair of degraded concrete in rigid pavements at military bases (Cong & Cheng, 2021; Shill et al., 2020; Lee et al., 2016). Furthermore, geopolymers can immobilise and encapsulate hazardous elemental wastes in their matrix, and they can be used to produce ceramics, adhesives, binders in the precast industry, coatings, and various construction materials (Fifinatasha et al., 2013).

Geopolymers are inorganic polymers produced by the reaction of aluminosilicate materials with alkali activators at mild temperatures, which results in amorphous to semi-crystalline polymeric structures containing Si-O-Al and Si-O-Si bonds (Abdullah et al., 2011). These materials are now employed in large-scale concrete production and can provide technical and environmental benefits over PC (Passuello et al., 2017; Duxson et al., 2007). The most commonly used alkali activators in geopolymerisation are sodium/potassium hydroxide and sodium/potassium silicate solutions (Nikolov et al., 2017). However, the production of sodium silicate solution for the alkali-activator in geopolymers entails heating sodium carbonate and quartz at temperatures between 1 400 and 1 500 °C (Kamseu et al., 2017). This process generates substantial quantities of carbon dioxide as a by-product. Manufacturing silica particles from renewable sources or waste materials therefore serves as a good example of sustainability (Azad & Samarakoon, 2021).

Valuable by-products in the industrial, agricultural, and municipal sectors are currently underutilised or discarded, yet they possess the potential for further valorisation and recycling through alkali activation (Bernal et al., 2016). The desire to valorise additional industrial wastes and by-products, along with the aim of reducing the cost of producing

geopolymer binders, has prompted the development of alternative alkali activators. These are based on the combination of alkalis with waste-derived amorphous silica sources such as SF, RHA, and GWP. These alternatives can exhibit comparable or even higher effectiveness when compared to traditional alkali activators based on soluble silicate alkalis (Bernal et al., 2016; Passuello et al., 2017; Palomo et al., 1999). A schematic process of geopolymerisation is shown in Figure 2.2, which includes the use of industrial, agricultural, and municipal wastes and by-products.

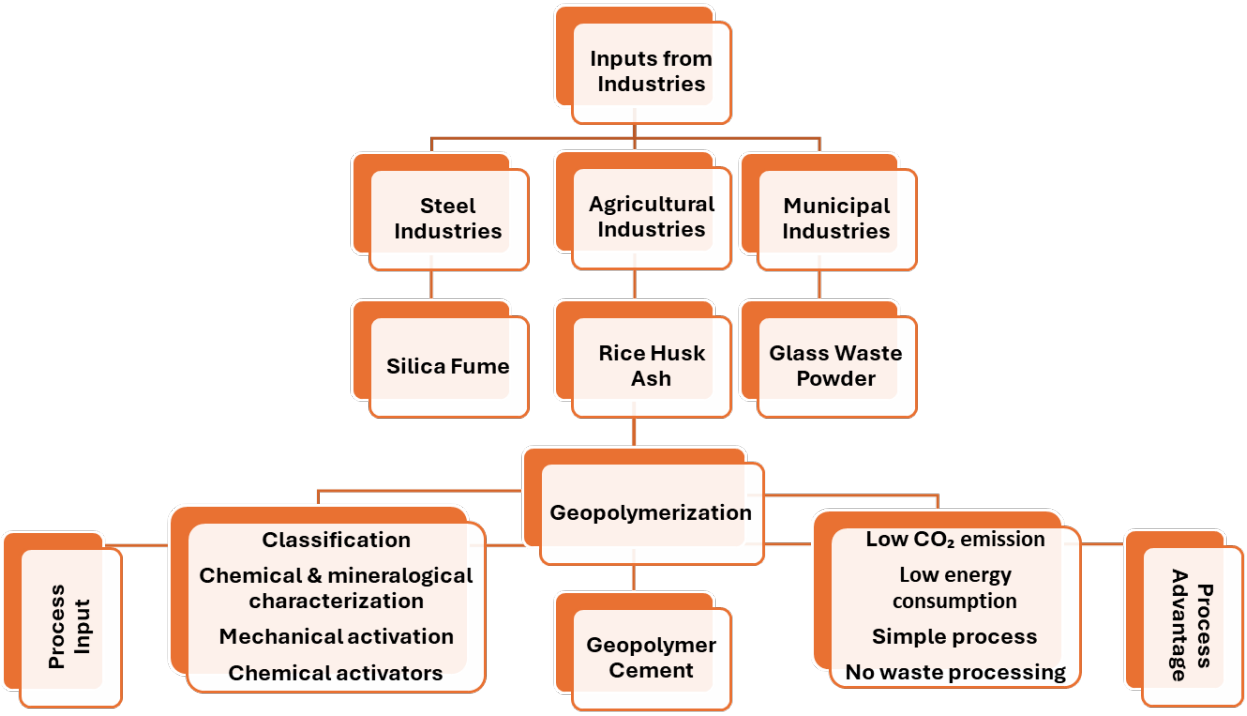

Figure 2.2: Process diagram for valuable wastes and by-products through geopolymer synthesis
Source: Azad and Samarakoon (2021)

Geopolymers generally minimise greenhouse gas emissions. However, sodium silicate, a key component of the alkaline activator in geopolymers, presents challenges regarding sustainability. This research proposes an alternative alkaline activator by blending sodium hydroxide with various silica-based waste materials, including SF, RHA, and GWP. This approach aimed to reduce the carbon footprint of the binder while ensuring the effective and efficient sustainability of geopolymer materials.

2.2 Mechanism of geopolymerisation

Geopolymer binders consist of reactive solid components such as silicon oxides (SiO_2) and aluminium (Al_2O_3), along with an alkali-activator solution. When these two components (the reactive solids and the alkali-activation solution) react, they form an aluminosilicate network that ranges from amorphous to partially crystalline. This process results in a hardened, water-resistant product. The compact three-dimensional network that develops during hardening is known as geopolymer, and the entire process is referred to as geopolymerisation (Al Bakri et al., 2011; Cong & Cheng, 2021).

Geopolymer binders are amorphous to semi-crystalline three-dimensional silico-aluminate structures. The three types of geopolymer structures are poly(sialate) (-Si-O-Al-O-), poly(sialate-siloxo) (-Si-O-Al-O-Si-O-), and poly(sialate-disiloxo) (-Si-O-Al-O-Si-O-Si-O-). Geopolymers with poly(sialate-siloxo) and poly(sialate-disiloxo) structures tend to exhibit greater rigidity, stability, and strength compared to those with poly(sialate) structures (Al Bakri et al., 2011).

Poly(sialate) compounds are proposed as the chemical designation for silico-aluminate-based geopolymers. The term “sialate” is derived from silicon-oxo-aluminate. In the network structure of poly(sialate), silicate (SiO_4) and aluminate (AlO_4) tetrahedra alternate and are linked by shared oxygen (O_2) atoms. Positive ions such as Na^+, K^+, Li^+, Ca^{2+}, Ba^{2+}, NH_4^+, and H_3O^+ are present in the framework to balance the charge of Al^{3+} ions in IV-fold coordination. The empirical formula for poly(sialates) is:

$$Mn\text{-}(SiO_2)z\text{-}(AlO_2)n,\ Wh_2O$$

Where:

- M represents a cation like potassium (K), sodium (Na), or calcium (Ca).
- n represents the degree of polycondensation.
- z can take values of 1, 2, or 3, indicating the silicon/aluminium ratio.
- Wh_2O signifies water molecules that are present.

The z value in the empirical formula determines the silicon/aluminium ratio of the poly(sialate) compound. There are three types of poly(sialates) based on the silicon/ aluminium ratio, as shown in Figure 2.3:

- Poly(sialate) with a 1:1 silicon/aluminium ratio (z = 1)
- Poly(sialate-siloxo) with a 2:1 silicon/aluminium ratio (z = 2)
- Poly(sialate-disiloxo) with a 3:1 silicon/aluminium ratio (z = 3)

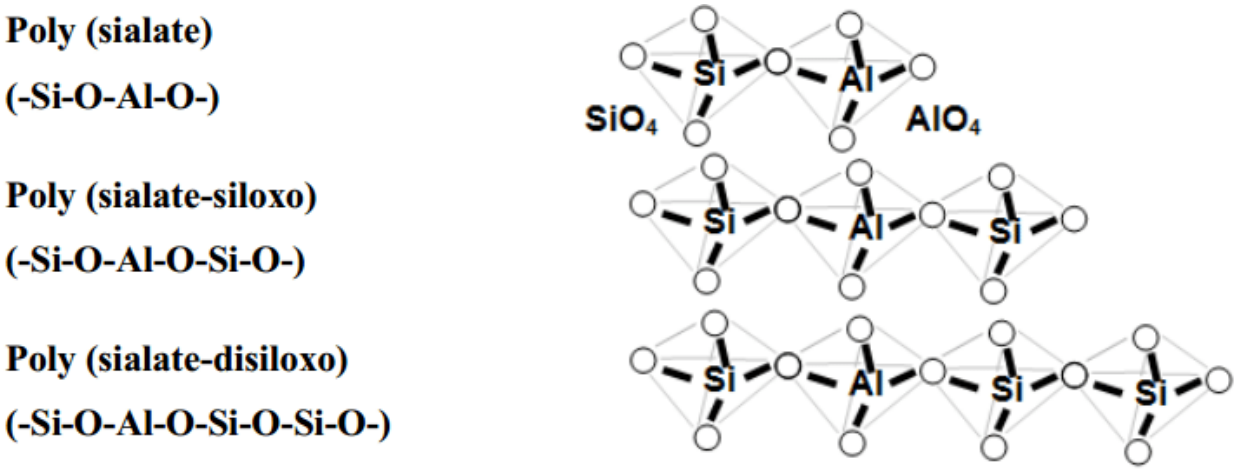

Figure 2.3: Poly(sialates) in IV-fold coordination

Source: Škvára (2011)

Geopolymerisation is the process of producing geopolymer through the polycondensation reaction of aluminosilicate material (precursor) and alkali activators. Several proposed mechanisms suggest that the geopolymerisation process entails three distinct but interconnected stages: (1) the dissolution of silicon and aluminium atoms from the precursor via the action of hydroxide ions, (2) the transportation or oligomerisation of precursor ions into monomers, and (3) setting or polycondensation/polymerisation of monomers into polymeric structures (Fifinatasha et al., 2013; Duxson et al., 2007; Provis & Deventer, 2007).

In the geopolymer process, intermediate molecules called oligomers form during the early stages of polymerisation. These molecules are larger than monomers but smaller than polymers. Several types of oligomers are produced during the dissolution and reorganisation of aluminosilicate; these oligomers connect to form large polymers. When

oligomers join, the hydroxide groups at their ends meet and share an oxygen atom and releases water. There are two types of geopolymerisation processes: conventional and advanced geopolymerisation (Amritphale et al., 2019).

2.2.1 Conventional geopolymerisation

The conventional process uses a solution chemistry mechanism in which amorphous aluminosilicate, such as fly ash, reacts with a sodium hydroxide-sodium silicate solution to form geopolymeric gel, as depicted in Figure 2.4. Consequently, geopolymer formation follows the bimolecular nucleophilic substitution mechanism. Although the mechanism of geopolymerisation reactions via solution chemistry is complex and not fully understood, these reactions can be categorised into the following stages:

- Association: In the initial step, the amorphous aluminosilicate material, like fly ash, interacts with the sodium hydroxide-sodium silicate solution. Sodium hydroxide dissociates into sodium ions (Na^+) and hydroxide ions (OH^-) in solution. The hydroxide ions can interact with the aluminosilicate structure, which initiates the geopolymerisation process. This association step prepares the reactants (aluminosilicate material and activator solution) for the subsequent reactions.
- Dissociation: The hydroxide ions in the sodium hydroxide solution interact with the amorphous aluminosilicate. This interaction can lead to the breaking of bonds in the aluminosilicate structure, which creates sites with exposed reactive species, such as aluminium and silicon atoms with available lone pairs of electrons. This dissociation step generates the necessary reactive centres for further reactions.
- Oligomerisation: In this step, the reactive species on the surface of the aluminosilicate particles start to react with each other. Alumina and silica species can undergo nucleophilic attacks, which is a chemical process where electron-rich species donate electrons to electron-deficient species, which leads to the formation of oligomers. These oligomers are the building blocks of geopolymeric gel. The nucleophilic attack involves the hydroxide ions acting as nucleophiles that attack the reactive centres, which results in the formation of covalent bonds.

- Auto-polycondensation: As oligomers form, they continue to react and polymerise through a series of condensation reactions. During this auto-polycondensation step, the reactive species link together to form a three-dimensional network of covalent bonds. This network grows and develops into the geopolymeric gel structure. This process involves the elimination of water molecules as by-products.

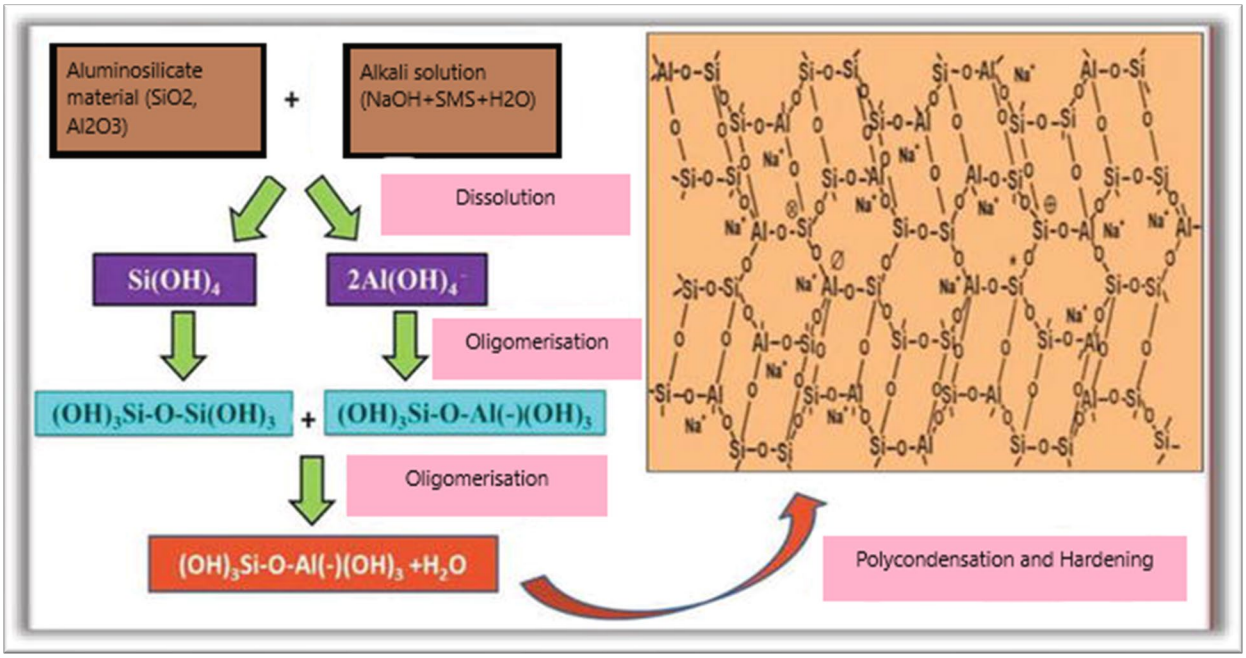

Figure 2.4: Stages of the geopolymerisation process

Source: Amritphale et al. (2019)

2.2.2 Advanced geopolymerisation

Advanced geopolymerisation is a method for producing geopolymers using an innovative solid-state chemistry mechanism, as shown in Figure 2.3 (Amritphale et al., 2019; Cong & Cheng, 2021). Unlike the conventional process, which involves preparing an initial solution of alkali and then mixing it with source materials, the advanced process is a one-part system. In this system, the tailored geopolymeric precursors are provided in solid powder form, and only water is needed to convert them into advanced geopolymeric material. The tailored precursors are produced by mechanochemically dry-grinding raw materials for eight hours (Toniolo, 2018). The basic raw materials used are vitreous silica- and alumina-containing by-product materials, such as fly ash and GGBS. These raw

materials can be activated with sodium hydroxide, with or without sodium silicate. The addition of water is all that is required to form geopolymeric material from this solid powder. The advanced process includes solid-state reactions during the dry-grinding phase, which enable the tailoring of raw materials and the sequencing of reactions among them for the preparation of geopolymeric materials. These geopolymeric materials are as simple to use on-site as ordinary PC.

In the initial steps of the reaction, the solid-state mechanism involved in advanced geopolymerisation differs from that of conventional geopolymerisation. As a result, the plausible chemical reaction mechanism for advanced geopolymerisation can be understood as follows:

- Dissociation: In the advanced geopolymerisation process, the initial step is dissociation. This is brought about by mechanochemical activation, where the glassy silica/alumina phase in fly ash is subjected to mechanical forces for an extended period (eight hours in this case). This mechanical activation leads to the breaking of bonds in the glassy silica/alumina phase. Unlike conventional geopolymerisation, where solution chemistry is involved, the advanced process starts with solid-state dissociation. This process results in the generation of unstable silanon species (Si=O) from the siloxane (Si-O-Si) bonds.
- Association: The unstable silanon species generated during the dissociation process are active and can rapidly transform into silanol (Si-OH) species even in the presence of a small amount of water. The next step is the association of these silanol intermediates with water molecules to form silanol complexes. This step involves the interaction between the reactive silanol species and water molecules, which facilitates the formation of water-associated silanol species.
- Auto-polycondensation: In the presence of water, the formed silanol species can further react with other reactive species, such as aluminosilicate components, to form Si-O-Al linkages. This auto-polycondensation reaction involves the condensation of silanol and aluminosilicate species to create a three-dimensional network. This network structure gradually forms the geopolymeric gel. As this gel forms and matures, it results in the creation of an advanced geopolymeric material.

When this material is dried, it exhibits significantly enhanced properties such as increased mechanical strength, improved durability, reduced porosity, and better fire resistance compared to conventionally formed geopolymers.

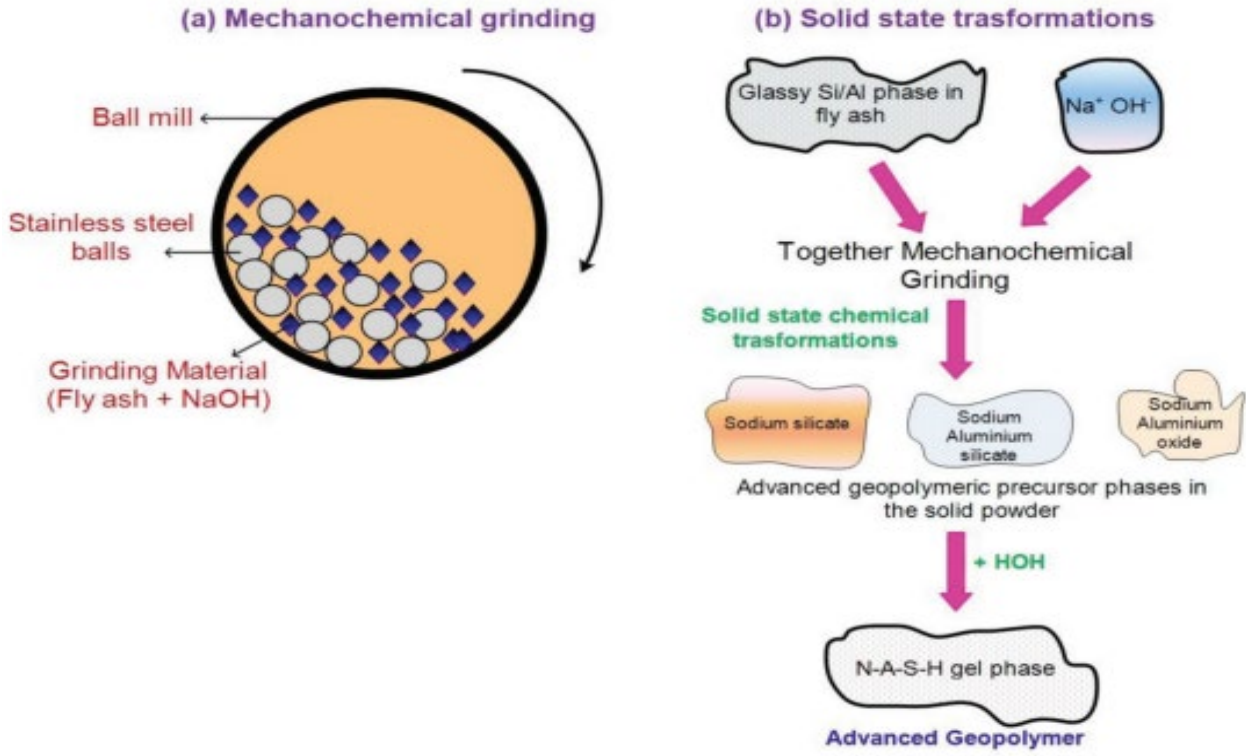

Figure 2.5: Mechanochemical raw material grinding and the creation of advanced geopolymeric precursor phases as a result of solid-state chemical reactions

Source: Amritphale et al. (2020).

2.2.3 pH levels in the geopolymerisation process

Identifying the appropriate pH values for pore solutions is crucial for maintaining the stability of hydration products in cementitious materials (Tang et al., 2015). PC, which is rich in calcium oxide (CaO), produces calcium hydroxide ($Ca(OH)_2$) when mixed with water; consequently, the pore solution in PC concrete remains highly alkaline. In contrast, geopolymers primarily rely on alkali solutions for activation, which results in pore solutions with higher initial alkalinity compared to PC (Han et al., 2023).

For OPC binders, the hydration process involves the formation of various hydration products, including calcium silicate hydrate (C-S-H) gel and calcium hydroxide. These

products form through a series of chemical reactions between the cement particles and water, with the C-S-H gel being a key component that provides strength and durability to the cementitious matrix.

Conversely, AABs follow a different activation mechanism. These binders are formed by the reaction of aluminosilicate precursors (such as fly ash or slag) with alkaline activators, which can include alkalis such as sodium hydroxide or sodium silicate solutions. The pH of the alkali-activated mixture is alkaline from the outset due to the presence of these alkaline activators. In AABs, the reaction between the aluminosilicate precursors and the alkaline activators leads to the formation of various types of hydrated gels, including sodium aluminosilicate hydrate (N-A-S-H) gel and other amorphous or crystalline phases, depending on the specific binder composition and activation conditions.

2.3 Raw materials in geopolymers

Geopolymer production can utilise a variety of raw materials with high silicon and aluminium content, including natural minerals, calcined clays, industrial wastes, and by-products such as fly ash, slag, red mud, or waste glass, as well as mixtures of these materials (Bilgil, 2018). The precursor material used in geopolymerisation technology is determined by competitive cost, availability, and specific application. The properties of the final geopolymer products are influenced by the selection and preparation of raw materials. Using waste materials and by-products from other industries can be economically advantageous and environmentally beneficial. Different applications may require specific properties from the geopolymer product. Depending on the intended use, the precursor material is chosen to match the desired characteristics of the final product. For instance, different materials are selected for applications that demand high compressive strength, compared to those that prioritise low thermal conductivity (Mucsi & Ambrus, 2018). For example, metakaolin can produce geopolymers with excellent mechanical properties, including high compressive strength, which makes it suitable for structural applications. In contrast, geopolymers derived from fly ash tend to have lower thermal conductivity compared to traditional materials such as concrete, which makes them suitable for thermal insulation applications.

Geopolymers can be divided into two main classes based on the calcium content of the precursor: low calcium content precursors and high-calcium content precursors. The most common low calcium content precursors are fly ash and metakaolin, which produce an N-A-S-H-type gel (Na_2O-Al_2O_3-SiO_2-H_2O) through major reaction pathways involving sodium, aluminium, and silicon components present in the precursors. In contrast, GGBS is the most common high-calcium content precursor, producing a calcium-aluminium-silicate-hydrate (C-A-S-H) type gel (CaO-Al_2O_3-SiO_2-H_2O) through the reaction of calcium, aluminium, and silicon components from the precursor (Samson et al., 2017).

Furthermore, Samson et al. (2017) explain that geopolymers derived from low-calcium content precursors typically exhibit good stability and favourable mechanical properties, which makes them suitable for a range of applications. Conversely, geopolymers derived from high-calcium content precursors, such as GGBS, often exhibit unique properties, including improved resistance to certain aggressive environments (e.g., acidic conditions) due to the presence of calcium.

2.3.1 Fly ash

Fly ash is widely available throughout the world, which has prompted waste management proposals (Bernal et al., 2016). In South Africa, a significant amount of fly ash is disposed of each year due to coal being the country's primary source of energy. South Africa generates approximately 36 million tonnes of coal fly ash annually from Eskom (the state-owned electricity company) power stations (Naghizadeh & Ekolu, 2017). However, only a small portion, around 7%, of the fly ash produced by Eskom is used beneficially (Reynolds-Clausen & Singh, 2019). Most of the fly ash that is not utilised is stored in ash dams and landfills. This raises concerns about the long-term management of these storage sites and the potential environmental implications. The issue of fly ash utilisation is crucial in South Africa due to both environmental and economic considerations (Reynolds-Clausen & Singh, 2019). Proper utilisation of fly ash in construction materials can reduce waste, lower carbon emissions, and contribute to sustainable development. As a result, GPC based on fly ash is a viable solution to address the abundance of fly ash.

Fly ash has been widely used in PC concrete to partially substitute PC as the binding material (Qaidi et al., 2022). Over the past decade, numerous researchers have identified fly ash as an excellent geopolymer binder due to its physical and chemical properties that facilitate geopolymerisation reactions (Lloyd & Rangan, 2010; Ridtirud et al., 2011; Kaduku et al., 2015). Fly ash is generally divided into Class F (low calcium oxide content) and Class C (high calcium oxide content). Class F fly ash is derived from sub-bituminous coals and contains more than 20% calcium oxide and exhibits both pozzolanic and cementitious properties. In contrast, Class C fly ash comes from bituminous and anthracite coals. It contains lower levels of calcium oxide and is primarily pozzolanic in nature (Joshi & Kadu, 2012). The high aluminosilicate content in fly ash increases reactivity and promotes a higher degree of geopolymerisation in an alkaline environment, while also helping to reduce hydration heat and thermal cracking. The formation of aluminosilicate gel and early strength gain in fly ash-based geopolymers have been demonstrated with early high-temperature curing, which accelerates geopolymerisation due to the higher activation energy required by fly ash. Through their amorphous nature, fly ash-based geopolymers exhibit superior durability against acid and alkali attacks compared to other geopolymer binders (Mishra et al., 2022).

The pH value of fly ash can influence the setting time of fly ash-based GPC. Fly ash with a pH value above 11 is highly likely to experience flash setting (hardening within five minutes of mixing), whereas fly ash with a pH value between 8 and 11 tends to set rapidly (Antoni et al., 2016). The pH value of fly ash is closely linked to its calcium oxide content. Another study indicated that fresh GPC, particularly those based on high-calcium fly ash, tends to have a short setting time (Chindaprasirt & Ridtirud, 2020). However, the high calcium oxide levels in fly ash are advantageous because they can produce concrete with high compressive strength. This benefit arises from the presence of both polymerisation and hydration reactions in high-calcium fly ash-based geopolymer. In contrast, GPC made with low-calcium fly ash shows no indication of setting for up to 120 minutes after mixing (Antoni et al., 2016).

Another study explained that when fly ash is exposed to alkali solutions, a process of dissolution occurs (Fernández-Jiménez et al., 2005). This means that the alkali solution

interacts with the fly ash particles, which causes the aluminium and silicon components in the particles to dissolve. Fernández-Jiménez et al. (2005) proposed a descriptive model to explain the activation process of fly ash. This model envisions the activation process as a series of steps. Initially, the alkali solution attacks the fly ash particles, which causes them to “open up” and expose smaller spheres within. These smaller spheres are also subject to dissolution by the alkali solution. As the dissolution process takes place, reaction products are formed both on the inside and outside of the fly ash particles. These reaction products are likely the result of the chemical reactions between the dissolved aluminium, silicon, and other elements in the alkali solution. The researchers suggest that the activation of fly ashes can be compared to a zeolitisation process, which involves the formation of zeolites, a group of minerals with unique porous structures. In this context, the zeolitisation process does not reach its final phase, but some of the principles of zeolite formation are applicable to the activation of fly ash. Figure 2.6A is a scanning electron microscopy (SEM) image that depicts the characteristic morphology of the original fly ash. The ash is composed of a series of spherical vitreous particles that vary in size, with diameters ranging from 200 to 10 μm. Figure 2.6B illustrates the initial changes observed in the microstructure of the fly ash system resulting from the caustic dissolution attack followed by thermal curing for five hours at 85 °C.

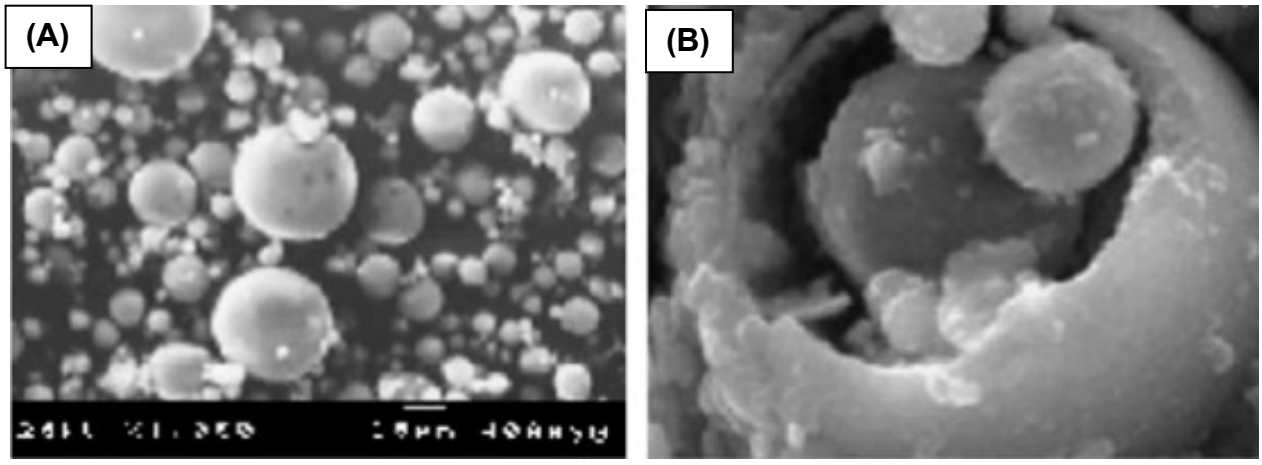

Figure 2.6: Microstructure of alkali activation of fly ash: (A) original fly ash and (B) sodium hydroxide-activated fly ash particles

Source: Fernández-Jiménez et al. (2005).

2.3.2 Metakaolin

Metakaolin is one of the most common source materials that contain aluminosilicates in GPC. It is produced by calcining natural clays such as kaolin at moderate temperatures (Albidah et al., 2021). Geopolymerisation is the reaction of silicon and aluminium found in natural source materials such as metakaolin. Metakaolin generally consists of particles smaller than 5 μm, and this small particle size contributes to its high reactivity and surface area. Additionally, metakaolin can be activated by various materials, such as alkali metal hydroxides (e.g., sodium hydroxide) and water glass (sodium silicate solution). These activators trigger chemical reactions that further enhance the reactivity of metakaolin and its contribution to the cementitious matrix. Numerous studies have been conducted on metakaolin-based geopolymers, which all yielded positive results (Duxson et al., 2007; Granizo et al., 2007; Li et al., 2010; Lancellotti et al., 2013; Samson et al., 2017). The goal of the study conducted by Samson et al. (2017) was to assess and compare the performance of AAMs made from either single pure precursors (one precursor) or blended precursors (two precursors), activated with two different levels of alkali-activator content (15% and 25% dry extract of alkaline solution). The findings indicated that AAMs made solely from metakaolin exhibited a moderate setting time, whereas those made solely from GGBS had a rapid setting time. Blends of metakaolin and GGBS showed significantly lower shrinkage values compared to other AAMs. Both metakaolin and GGBS AAMs demonstrated good mechanical properties, with metakaolin-GGBS blends exhibiting high early compressive strength. Albidah et al. (2021) reported on a thorough experimental investigation aimed at exploring the impact of various mix design factors on the characteristics of fresh and hardened metakaolin-based GPC. The study examined parameters such as workability, the development of compressive strength over time, splitting tensile strength, and water absorption. Seventeen different GPC mixes, along with two reference cement concrete mixes, were analysed. The results revealed that workability improved as the sodium silicate to sodium hydroxide (solids) ratio increased up to a certain threshold (identified as 2.5 in this study). However, the workability of metakaolin-based GPC was found to be highly influenced by the aggregate content, as even a slight increase in aggregate content could lead to a significant reduction in workability. Notably, for a given water-to-solids (or cement) ratio, metakaolin-based GPC

exhibited better slump values compared to cement concrete. The compressive strength increased with an increase in the sodium silicate to sodium hydroxide ratio and alkaline solids to metakaolin ratio, up to a certain threshold depending on the mix's molar ratios. Splitting tensile strength remained relatively consistent across the mixes. In comparing metakaolin-based GPC with cement concrete mixes, water absorption for geopolymer mixes was either equivalent to or higher than that of cement concrete.

2.3.3 Granulated blast-furnace slag (GGBS)

GGBS is a by-product obtained from the iron industry, specifically from blast furnaces. When blast-furnace slag is rapidly cooled and then finely ground to a particle size similar to that of cement, it becomes GGBS (Bouaissi et al., 2019). This process produces a material with hydraulic properties, which means it can react with water to form cementitious compounds. GGBS can be used independently or in combination with fly ash to create alkali-activated concrete (AAC) / GPC cured at an ambient temperature. It offers strong mechanical properties while requiring a relatively low amount of activator. Nevertheless, this approach presents certain practical challenges, such as the rapid setting of high-calcium alkali-activated systems. Chemical admixtures commonly used as retarders in PC applications have not proven suitable for AABs. In fact, some of these admixtures have been found to adversely affect compressive strength. So far, no new chemical admixtures have been identified to address this issue.

In comparisons, the mechanical strength of slag-based AAC outperformed that of PC-based concrete with similar levels of binder and water content, as well as curing temperature. Additionally, the strength development of slag-based AAC was shown to be less impacted by changes in binder content than PC concrete. Slag-based AAC also exhibited lower water absorption and total porosity than PC concrete. However, these properties tend to decrease as the binder content increases (Rafeet et al., 2017).

In a recent study, the effects of GGBS and sodium chloride (NaCl) molarity on the mechanical, durability, and microstructural properties of fly ash-blended GPC were thoroughly investigated. Fly ash and GGBS were combined in various ratios (0, 10, 20, 30, and 40%) to create GPC. The mechanical properties and durability features, such as

the rapid chloride permeability test and accelerated corrosion test, of fly ash-GGBS-blended GPC were examined. Micro-level properties were assessed using X-ray diffraction (XRD) and SEM tests.

The results indicated that increasing the GGBS content decreased the workability of GPC samples by 12% to 37%, and higher sodium hydroxide molarity also significantly reduced the slump value. The mechanical properties improved with a 40% GGBS replacement. Durability properties (porosity, water absorption, rapid chloride permeability test, and accelerated corrosion test) also improved with higher GGBS content and a 10 M sodium hydroxide solution. Calcite in GGBS supported the geopolymeric reaction in the pore structure, which enhances the formation of Ca^{2+}, Si^{4+}, and Al^{3+} ions, which in turn boost the generation of geopolymer products. This leads to better microstructural properties at 10 M sodium hydroxide, with improved C-A-S-H gel formation. A denser microstructure was observed with a 40% GGBS replacement with fly ash and 10 M sodium hydroxide, which indicates that GGBS particles filled the pores and thus strengthened the geopolymeric structure (Bellum et al., 2022).

Another study investigated the mechanical and microstructural properties of geopolymer paste and concrete made from fly ash, GGBS, and high-magnesium nickel slag (HMNS) (Bouaissi et al., 2019). The specimens were tested at different ages (seven, 14, and 28 days), and the percentage of GGBS ranged from 0% to at least 40%, as shown in Figure 2.5. The results indicated that for GGBS replacement levels below 30%, the compressive strength of the geopolymer paste specimens increased over time. This suggests that incorporating GGBS into the mixture is beneficial for both early and long-term development of compressive strength. However, after the 14-day mark, the compressive strength began to decrease over time, with a further reduction observed at 40% GGBS replacement. This decrease in compressive strength is attributed to the presence of excess calcium content sourced from the GGBS. This excess calcium content is inactive and unreacted in the mixture, which is thought to interfere with the condensation process and hinder the formation of a continuous network of geopolymer gels. The study found that geopolymer paste and concrete with a mix of 70% fly ash, 20% GGBS, and 10%

HMNS exhibited superior mechanical properties, achieving a compressive strength of 55.6 megapascals (MPa) and a splitting tensile strength of 4.57 MPa.

Morphological and microstructural analyses revealed the formation of additional crystalline phases. XRD results indicated the presence of C-S-H, C-A-S-H, and new gel phases such as magnesium vanadium molybdenum oxide and calcium beryllium praseodymium oxide ($CaBePrO_3$), primarily sourced from GGBS and HMNS, which provide calcium (Ca) and magnesium (Mg), respectively. SEM analysis showed that the GPC had a highly compacted structure with a dense matrix and fewer pores. Energy-dispersive X-ray analysis, in conjunction with SEM images and Fourier transform infrared (FTIR) spectroscopy results, confirmed that partially replacing fly ash with GGBS and HMNS enhances the mechanical properties of the GPC. This enhancement is attributed to the formation of new crystalline phases due to the incorporation of Ca^{2+} and Mg^{2+} into the geopolymer gel. Consequently, the combination of fly ash, GGBS, and HMNS leads to the formation of ternary gels such as C-S-H, A-S-H, and Na-Al(Mg)-Si-H, which results in improved mechanical properties of the geopolymer products (Bouaissi et al., 2019).

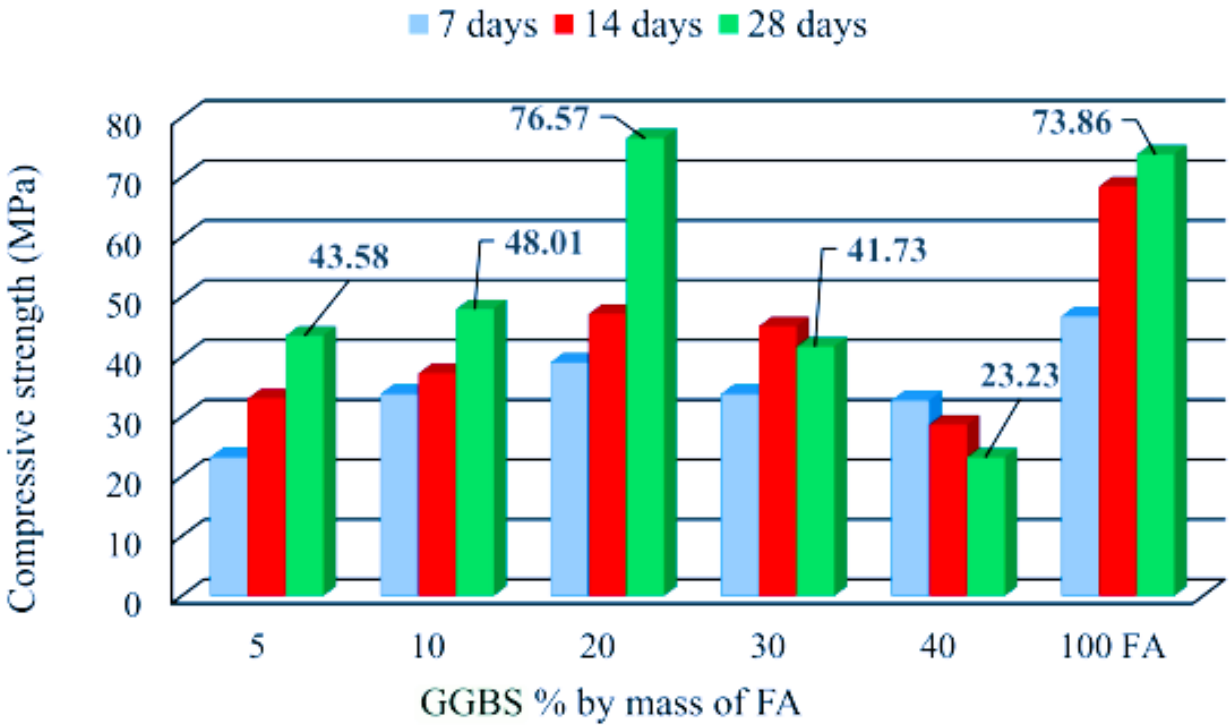

Figure 2.7: Compressive strength of fly-ash based paste with varying GGBS replacement
Source: Bouaissi et al. (2019)

2.4 Alkali activators

The purpose of the alkali-activator in an AAB (geopolymer) is to activate the binder during the geopolymerisation process (Karthiyaini, 2016). Alkali activators are produced in various ways, but they are typically made from a combination of alkaline solution and water glass (Faris et al., 2017). The alkaline solution serves as a catalyst for the geopolymerisation reaction by facilitating the transformation of aluminosilicate precursors into a durable and chemically stable geopolymer binder. It must be designed to allow for the rapid dissolution of the raw materials, in order to result in a swift increase in the concentration of aluminate and silicate units.

2.4.1 Effect of alkali-activator type on the properties of geopolymer binders

The key functions of the alkali-activator solution include initiating the reaction in the geopolymerisation process, activating the precursors, and controlling the pH level by maintaining an alkaline environment to promote the rapid dissolution of the precursor material. The alkali-activator typically used in geopolymer synthesis is often a combination of alkali hydroxides and alkali silicates (Faris et al., 2017). Furthermore, the most commonly used alkali activators in geopolymerisation are a combination of sodium or potassium hydroxide and sodium or potassium silicate solutions (Nikolov et al., 2017). Additionally, sodium-based solutions are frequently employed as alkaline activators in geopolymer synthesis due to their low cost and widespread availability.

2.4.1.1 Alkali hydroxide

Alkali hydroxide is a strong base composed of a metal alkali cation and a hydroxide anion (Fatima et al., 2023). Also known as metal hydroxide (MOH), alkali hydroxide is extremely corrosive. The metal alkali cations can include sodium (Na), potassium (K), lithium (Li), rubidium (Rb), or caesium (Cs), with sodium and potassium hydroxide being the most commonly used (Provis & Van Deventer, 2009). An advantage of sodium hydroxide and potassium hydroxide is their high solubility in water, which can reach up to 20 mol/kg water at 25 °C. Both metal hydroxides are widely used as activators in AABs, particularly when combined with Class F fly ash binders (Faris et al., 2017). In contrast, lithium

hydroxide (LiOH), rubidium hydroxide (RbOH), and caesium hydroxide (CsOH) are unsuitable for use as activators due to their high cost, instability, and low water solubility, especially in the case of lithium, which has a solubility of only 5.4 mol/kg water at 25 °C (Monnin & Dubois, 2005).

Previous studies have shown that with sodium hydroxide solution concentrations above 10 M, the rate of polymerisation decreases, which leads to reduced strength. However, a higher content of alkaline activator results in increased compressive strength (Hanjitsuwan et al., 2014). The molarity of the sodium hydroxide solution is crucial for determining the strength of the geopolymer. Higher concentrations of sodium hydroxide are required to effectively break down chemical bonds in fly ash particles, particularly in Class F fly ash. This breakdown process is essential for releasing the necessary oxides and initiating the geopolymerisation reaction. Understanding the relationship between sodium hydroxide concentration, fly ash composition, and bond breakdown is vital for optimising the geopolymerisation process and achieving the desired properties in the resulting geopolymer materials.

A study by Hamidi et al. (2016) drew a similar conclusion regarding the dissolution of silica and alumina from fly ash, which was significantly affected by the concentration of sodium hydroxide. The study showed that higher sodium hydroxide concentrations promoted the dissociation of active components in the fly ash. This enhanced dissociation results in a larger amount of raw material reacting to form the geopolymer network, thus contributing to improved geopolymerisation. Additionally, while increasing the sodium hydroxide concentration can enhance the geopolymerisation process, there is an upper limit beyond 10 M, which may have negative effects. Very high concentrations of hydroxide ions from excessive sodium hydroxide may disrupt the geopolymerisation process, which can result in an inefficient reaction and potentially hindering the development of the desired geopolymeric structure.

The work of Xu and Van Deventer (2003) suggests that geopolymer formulations using potassium hydroxide as an alkali-activator tend to exhibit higher compressive strength compared to those using sodium hydroxide. When potassium hydroxide was used, the average compressive strength of all the minerals was 11 MPa, which was 42% greater

than that achieved with sodium hydroxide. This observation indicates that the choice of alkali-activator can significantly impact the mechanical properties of the geopolymers. Palomo et al. (1999) offer a different perspective by suggesting that sodium hydroxide-based geopolymers can yield higher compressive strength than potassium hydroxide-based geopolymers under certain conditions. Factors that influence this observation include variations in curing temperature and time, as well as the ratio of alkali-activator to aluminosilicate materials. The research further suggests that the compressive strength of geopolymer materials is not solely determined by the type of alkali-activator used; variations in curing temperature and duration, along with the ratio of alkali-activator to aluminosilicate materials, can lead to different strength outcomes.

A study by Rahim et al. (2014) utilised sodium hydroxide as the sole activator for geopolymer and focused on the effects of sodium hydroxide concentration. The study investigated how varying sodium hydroxide concentrations, in relation to curing time and temperature, affected the mechanical properties of a non-sodium silicate fly ash-based geopolymer. Samples were prepared by combining fly ash with 8, 10, and 12 M of sodium hydroxide, which were then cured for one, seven, and 28 days at room temperature and 60 °C. The findings in Figure 2.8 indicate that, regardless of the curing duration, the highest alkali concentration of 12 M exhibited the shortest setting time and the highest compressive strength. The maximum compressive strength obtained during curing at 60 °C was 59.81 MPa after seven days. At room temperature, the maximum strength achieved was 17.71 MPa after 28 days of curing.

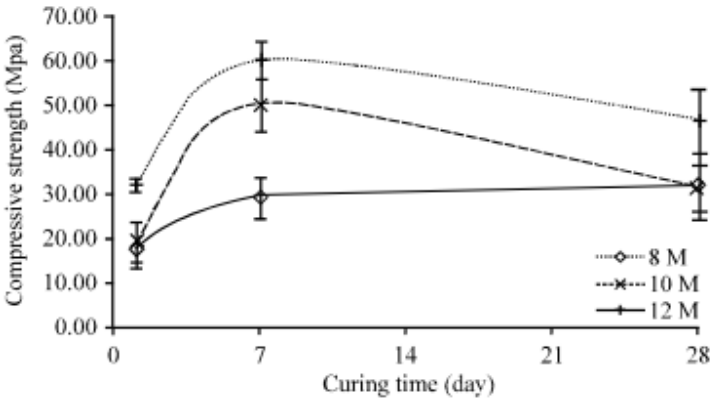

Figure 2.8: Compressive strength versus curing time with variation of sodium hydroxide concentration

Source: Rahim et al. (2014)

2.4.1.2 Alkali silicates

Alkali silicates are important chemical compounds that serve as effective activators for AABs. Like alkali hydroxides, these alkali silicates contain metal cations, the most common of which are sodium and potassium, which are used as activators in AABs (Provis & Van Deventer, 2009). One of the most common silicates employed as an activator is sodium silicate. Sodium silicate is produced through a high-temperature fusion process, in which high-purity quartz sand and sodium carbonate or soda are heated to temperatures ranging from 1 300 to 1 500 °C. This fusion results in the formation of an amorphous glass material (EHS, 2021). Sodium silicate is a generic term for a range of chemical compounds with the general formula $Na_2O{\cdot}nSiO_2$, where “n” represents the ratio of silicon dioxide to sodium oxide. It is available in both aqueous solutions and solid forms. The compound is commonly referred to as water glass when in its soluble form, due to its glassy appearance when dry (Toniolo, 2018).

Sodium silicate has various industrial applications, including its use as an adhesive, binder, sealant, detergent ingredient, and in geopolymerisation processes. The specific properties and uses of sodium silicate can vary based on the ratio of silica / sodium oxide, as well as other factors such as concentration and pH. There are several methods for producing sodium silicate, including hydrothermal and alkaline fusion methods (Ling, 2018). The most commonly used method is the alkaline fusion method, which involves

melting a mixture of high-purity silica sand and sodium carbonate at high temperatures of around 1 100 to 1 200 °C. In contrast, the hydrothermal method involves the reaction of silica-rich materials with an alkaline solution under high pressure and temperature conditions. Furthermore, the most commonly used sodium silicates in geopolymer cements have a silicate modulus of 2 to 3.3 and a solid content of 37 to 48 wt.% (Naghizadeh & Ekolu, 2017). Other metal silicates are rarely used in geopolymer cement due to limited sources, high costs, drawbacks, and low solubility, particularly when used on a large scale.

2.4.1.3 Combination of alkali silicate (sodium silicate) and alkali hydroxide (sodium/potassium hydroxide)

Sodium silicate cannot be used as an independent activating agent, as it lacks the activation potential to initiate the pozzolanic reaction on its own. It is combined with sodium hydroxide or potassium hydroxide as a reinforcing agent to increase alkalinity and overall geopolymer strength (Naghizadeh & Ekolu, 2017; Ling, 2018). A combination of sodium silicate solution and sodium hydroxide is the most common alkaline liquid used in alkali activation. Typically, sodium silicate provides soluble silica for polymerisation, enhances mechanical strength and durability, and influences workability and setting time. Additionally, sodium hydroxide dissolves aluminosilicate materials to release reactive species and controls the rate and efficiency of the dissolution process. However, there are some drawbacks to using alkali hydroxide and silicate solutions. These include difficulties in handling on-site due to their highly alkaline nature, which poses health and safety risks; variations in molarity that can lead to inconsistent performance; and the costs, embodied energy, and environmental impact associated with the production of activators, particularly sodium silicate, which is typically produced by melting sodium carbonate and silicon dioxide at temperatures ranging from 1 200 to 1 400 °C. This industrial process produces a significant amount of carbon dioxide.

A study by Zerfu and Ekaputri (2016) states that the optimal compressive strength is achieved with a mass ratio of alkaline liquid to fly ash of 0.35 and a mass ratio of sodium silicate to sodium hydroxide of 2.50, as shown in Figure 2.9. Additionally, a 12 M

concentration of sodium hydroxide is the most recommended solution, even though it provides slightly less strength compared to 14 M and 16 M concentrations, which result in a denser and less workable paste. Figure 2.10 clearly illustrates that the compressive strength of GPC increases with the molarity of the alkaline solution.

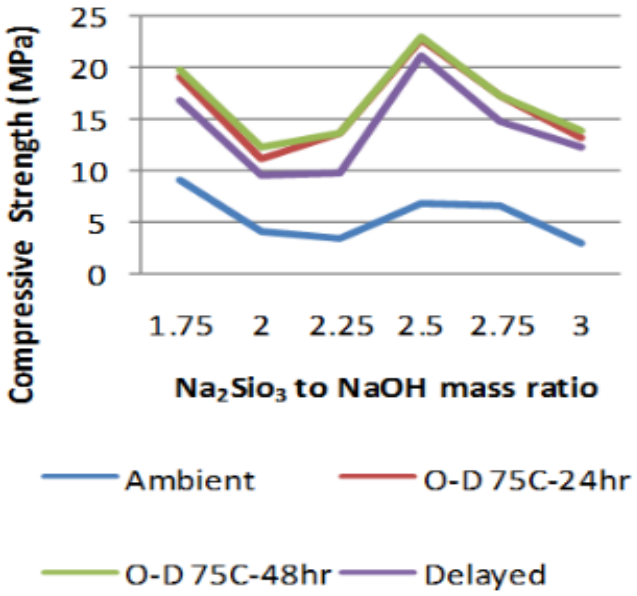

Figure 2.9: Effect of mass ratio of sodium silicate to sodium hydroxide for ambient and oven dry curing

Source: Zerfu and Ekaputri (2016)

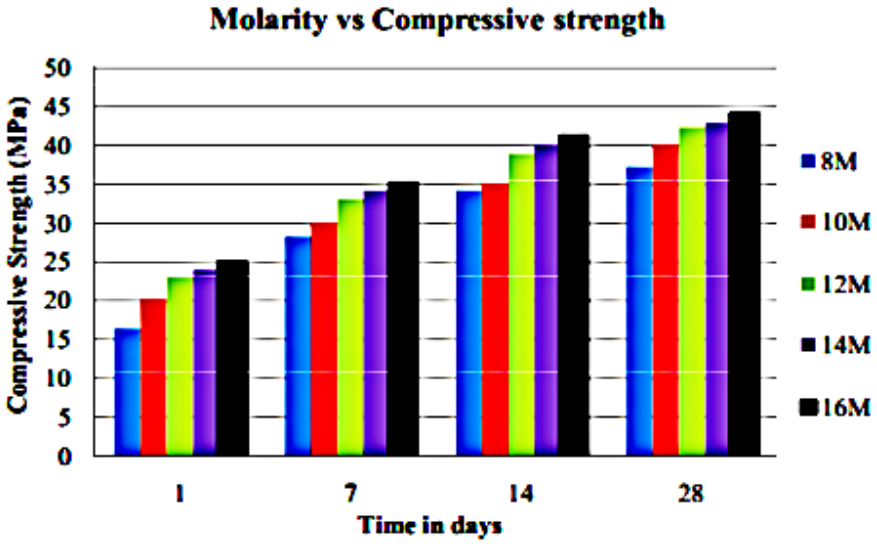

Figure 2.10: Strength gain with variations in molarities

Source: Zerfu and Ekaputri (2016)

A study by Jegan et al. (2023) compared the effects of two alkali activators on strain-hardening geopolymer composites by replacing Class F fly ash with GGBS: 4 M sodium hydroxide and a combination of 4 M sodium hydroxide with sodium silicate. The activator containing sodium silicate was found to be superior, in terms of higher strain capacity, to the one containing only sodium hydroxide. This superiority can be attributed to the presence of silicon dioxide in the sodium silicate, which enhanced the properties of the geopolymer.

2.4.2 Effect of silicon dioxide / sodium oxide molar ratio

Sodium silicate is a mixture of sodium oxide and silicate with water. Its general formula is $Na_2O/nSiO_2$, where n represents the silicate modulus, indicating the number of moles of silica per mole of sodium oxide (Naghizadeh & Ekolu, 2017). The silicon dioxide / sodium oxide molar ratio, also known as the module, is a critical parameter in geopolymer design. Variations in the module are well known to significantly alter the degree of polymerisation of the dissolved species in the reacting solution, which influences the mechanics and overall characteristics of the synthesised gel product (Ling, 2018). Commercial liquid sodium silicate products can be produced with a wide range of silicon dioxide / sodium oxide mass ratios, typically ranging from 1.60 to 3.30 (Passuello et al., 2017). A lower ratio (1.6 to 2.0) results in a more alkaline solution, which can accelerate the setting time and reduce workability. In contrast, a higher ratio (3.0 to 3.3) produces a less alkaline solution, which slows down the setting time and can improve workability. In terms of mechanical strength, a lower ratio can result in higher early strength due to the rapid polymerisation process. However, if the ratio is too low, it may cause excessive shrinkage and cracking, which will negatively affect long-term durability.

On the other hand, a higher ratio may lead to increased long-term strength, as the slower reaction allows for more complete polymerisation and denser microstructure formation. However, very high ratios might result in lower early strength and extended curing times. A related study discovered that a sodium silicate to sodium hydroxide ratio of 1.5 yielded the highest compressive strength for fly ash-based geopolymer cement mortars when a sodium silicate solution with a silicate modulus of 2.33 and a solid content of 46 wt% was

mixed with a 10 M sodium hydroxide solution (Ridtirud et al., 2011). A study by Lin et al. (2012), which examined the effect of the silicon dioxide / sodium oxide ratio on the compressive strength of thin film transistor liquid crystal display waste glass-metakaolin-based geopolymers, reported similar results. The findings indicated that compressive strength increased as the silicon dioxide / sodium oxide ratio was raised from 0.8 to 2.0.

The combination of sodium silicate solution and sodium hydroxide improves mechanical properties beyond the capabilities of a hydroxide activator alone (Naghizadeh & Ekolu, 2019). Furthermore, sodium silicate is rarely used on its own as an activating agent because it lacks sufficient hydroxide ions to initiate the pozzolanic reaction independently. Instead, it is typically combined with sodium hydroxide to boost alkalinity and enhance overall strength. Although the dissolution of aluminium-silicon species increases as the concentration of the alkali solution rises, excessive concentrations of sodium hydroxide or potassium hydroxide in the aqueous phase reduce the sodium oxide to silicon dioxide ratio and, consequently, hinder polycondensation. As a result, the concentration of alkali hydroxide in the activator solution must be limited to produce a high-strength gel phase (Zuda et al., 2006; Majidi, 2009). According to the relevant literature, the concentration of sodium hydroxide is effective in the range of 8 M to 16 M (Joshi & Kadu, 2012; Hanjitsuwan et al., 2014; Handayani et al., 2021). Concentrations higher than this can lead to excessive heat generation, non-uniform morphology, and/or diminished mechanical properties. Various recommendations exist in the literature regarding the appropriate mixing ratio for these substances. For example, a study by Jegan et al. (2023) stated that a fly ash-based geopolymer with a sodium oxide to silicon dioxide ratio of 0.4 produced the most workable mortar and paste, which achieved the highest mean compressive strength of 13.74 MPa. The study further explained that a higher sodium oxide to silicon dioxide ratio leads to the formation of more alumina-silicate gel, as it enables greater dissolution of silica and alumina in the reaction compared to the gel formation at ratios of 0.2 and 0.3.

In a study by Ling (2018), the impact of key design parameters, including the sodium oxide to silicon dioxide molar ratios (1.0, 1.5, and 2.0), solute concentration in the alkaline solution, liquid-to-fly-ash mass ratio, and the temperature and duration of curing, on the

setting time, compressive strength, and heat of hydration behaviours of high-calcium fly ash geopolymer mixtures was examined. The results showed that increasing the sodium oxide to silicon dioxide molar ratio from 1.0 to 1.5 accelerated the setting time but decreased strength, total heat generation, reaction time, and geopolymerisation peak time. However, for mixtures with a 2.0 modulus, the initial setting time decreased as the concentration increased across all liquid-to-fly ash ratios. This is likely because a higher percentage of soluble silica in the geopolymer system slows down the dissolution of fly ash, whereas increased concentration may help to dissolve silicon and aluminium ions from the fly ash.

On the other hand, the rate at which solid sodium silicate dissolves, as well as the solubility of vitreous (glassy) silicates, is influenced by the modulus. Higher moduli generally lead to slower dissolution rates and decreased solubility of vitreous silicates. In other words, higher sodium oxide to silicon dioxide ratios can make the dissolution process less efficient.

In a study by Leong et al. (2016), the sodium silicate to sodium hydroxide (solid to solid to heat [SS/SH]) ratio varied from 0.5 to 3.0. An 8 M sodium hydroxide solution, combined with a sodium silicate solution having a silicate modulus of 3.22 and a solid content of 38%, was used as the alkali-activator. The SS/SH mass ratio significantly affected the mechanical properties. Compressive strength increased as the SS/SH ratio rose from 0.5 to 2.0, then decreased linearly as the SS/SH ratio increased from 2.0 to 3.0. The highest compressive strength was observed in samples with an SS/SH ratio of 2.0.

A study by Tchakoute et al. (2013) observed and reported specific effects on the properties of the GPC as they varied the sodium oxide to silicon dioxide ratio. The study found that as the sodium oxide to silicon dioxide ratio was increased from 0.7 to 1.4 in the activator solution. The compressive strength of the resulting geopolymer-based concrete increased. This suggests that higher sodium oxide to silicon dioxide ratios contributed to improved mechanical performance, likely due to optimised geopolymerisation reactions. However, the results also showed that the setting time of the GPC decreased. The findings align with the literature review by Naghizadeh and Ekolu (2017), which used a sodium oxide to silicon dioxide ratio range of 0.7 to 1.4 (as shown in Figure 2.11) for

producing different types of geopolymer cements. This indicates that the geopolymer material solidified and gained structural integrity faster as the sodium oxide to silicon dioxide ratio was increased. The increase in compressive strength and the decrease in setting time with higher sodium oxide to silicon dioxide ratios suggest that careful tuning of this ratio can lead to more desirable and efficient geopolymerisation reactions that result in improved material performance. This is because a higher sodium oxide to silicon dioxide ratio provides more silica available for reaction, which results in a more extensive and interconnected network of silicate and aluminate bonds that contribute to higher compressive strength. Additionally, faster setting times mean that the material can reach its final hardened state faster, which reduces the likelihood of defects or weaknesses developing during the curing process.

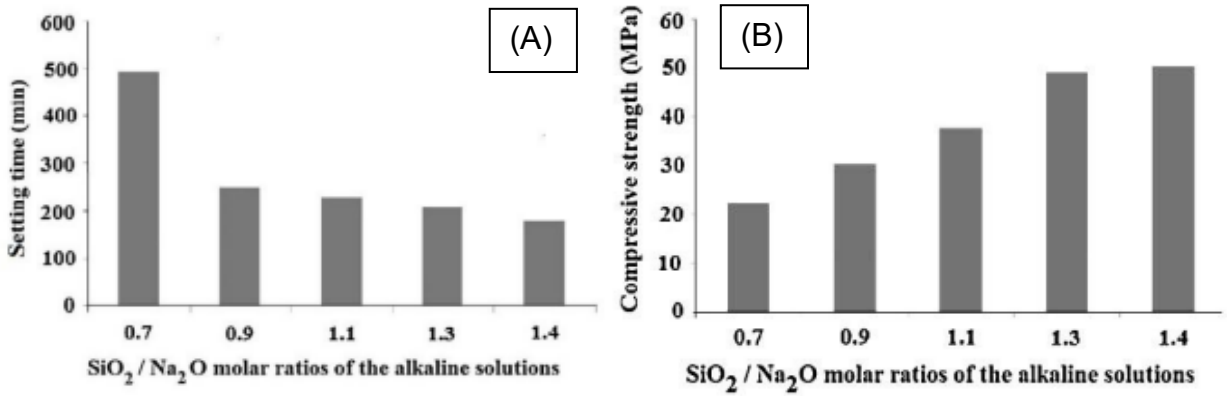

Figure 2.11: (A) Setting time of the volcanic ash-based geopolymers and (B) compressive strength of the volcanic ash-based geopolymers

Source: Naghizadeh and Ekolu (2017)

2.4.3 Effect of water content on GPC

Water is just as important in GPC as it is in regular concrete. It serves as the medium in the reaction model of geopolymerisation and participates in several intermediate reactions during geopolymer formation, such as dissolution and polycondensation (Xie & Kayali, 2013). The total mass of water consists of the water in the hydroxide and silicate solutions, as well as the mass of additional water added to the mixture. Water plays a critical role in controlling the speed of the geopolymerisation reaction. The reaction rate must be balanced to ensure that it is slow enough to allow for the complete dissolution of

raw materials while being fast enough to enable the formation of a dense network with reasonable compressive strength (Toniolo, 2018). This can be attributed to the fact that higher water content usually slows down the reaction by diluting the concentration of reactive species, whereas lower water content results in a more concentrated solution that accelerates the reaction but may make the mixture too viscous to handle. Furthermore, excessive water can lead to the formation of too many pores in the gel, which will weaken the final material. This observation aligns with the results of Vora and Dave (2013), where GPC mixes were cast using additional water of 10% (Mix 7A), 15% (Mix 7B), and 20% (Mix 7C) by fly ash mass of 428 kg/m³ for each mix. The results showed a 33% decrease in compressive strength for concrete Mix 7C compared to concrete Mix 7A. The conclusion was that the compressive strength of GPC reduced as the water-to-geopolymer solids ratio increased.

According to Toniolo (2018), the quantity of water is determined by various parameters, including the source materials, particle size, shape, distribution, and specific surface area. In geopolymers, water is often added to enhance the workability of the mixture, which makes it easier to handle, mix, and place. The water content affects the viscosity and flow of the geopolymer paste, which allows it to be shaped into the desired forms before it sets.

Understanding the role of water in the creation of geopolymers is critical. Water ejected from the geopolymer matrix during the curing and subsequent drying phases forms discontinuous nanopores in the matrix, which enhances geopolymer performance (Karthiyaini, 2016). In this context, geopolymer performance improves due to the nanopores distributing stress more evenly throughout the material, thereby reducing the likelihood of cracks and leading to an overall increase in compressive strength. Additionally, the presence of these nanopores can enhance the material's resistance to chemical attacks, which contributes to its long-term durability.

Superplasticisers or additional water can be added to improve the workability of mortar. In a study by Chindaprasirt et al. (2007), the use of superplasticisers had a negative impact on the strength of the geopolymer. As a result, adding more water appears to yield greater strength than adding superplasticisers. This is because the effectiveness of

superplasticisers is highly dependent on the specific mix design and dosage used. However, adding more water usually enhances workability, which improves the compaction of the mix and reduces the presence of voids, which leads to denser and stronger concrete. This aligns with the findings of Aliabdo et al. (2016), which indicate that the workability of concrete is significantly affected by the extra water content; adding more water thus enhances the concrete's workability, as seen in Figure 2.12. The optimum additional water content was determined to be 30 kg/m³, which had minimal impact on the properties of the geopolymer.

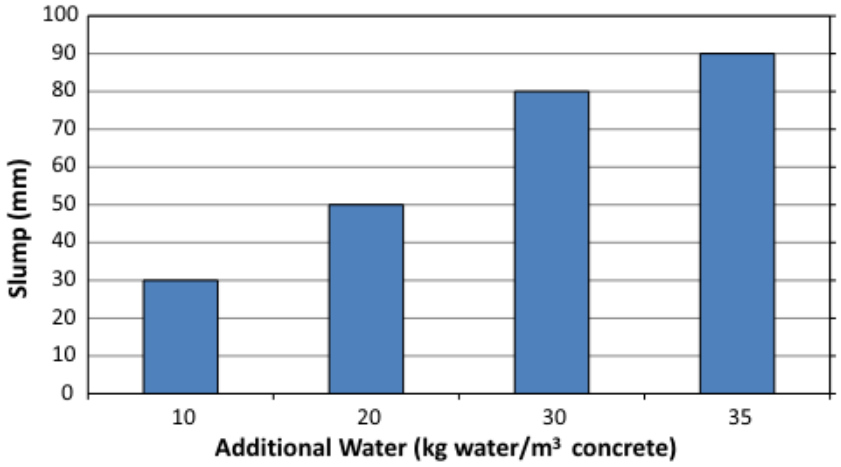

Figure 2.12: Effect of additional water content fly ash-based GPC slump

Source: Aliabdo et al. (2016)

2.5 Environmental impacts of sodium silicate

Sodium silicate has been widely used as an alkaline activator in GPC, which results in significant mechanical strength development and low permeability, which are associated with a stable and dense structure (Tong et al., 2018). However, the production of sodium silicate poses environmental challenges, as it increases embodied energy and carbon dioxide emissions due to its manufacturing process (Faris et al., 2017; Tong et al., 2018). This process typically entails calcining sodium carbonate and quartz sand (silica) at temperatures ranging from 1 400 to 1 500 °C, which generates carbon dioxide from the decomposition of sodium carbonate, as well as from the combustion of fuel used to achieve these high temperatures. Additionally, the process produces dust, nitrogen

oxides, and sulphur oxides, all of which contribute to air pollution (Kaduku et al., 2015). Moreover, this process is highly costly.

Sodium silicate is an amorphous glass that can be dissolved in water to create silicate solutions. When dissolved, the substance breaks down into silica that is identical to natural dissolved silica. Silica does not bioconcentrate as it moves up the food chain (Occidental Chemical Corporation, 2013). Due to its high pH levels, sodium silicate can be extremely toxic. It is generally hazardous to aquatic organisms but only slightly toxic to terrestrial ones (Occidental Chemical Corporation, 2013). The production of sodium silicate can also significantly increase other environmental impacts, such as freshwater ecotoxicity, by up to 1000%.

Sodium silicates are characterised by their density and viscosity, as well as the silica to sodium oxide ratio, or molar ratio (EHS, 2021). There are several applications for sodium silicate. It aids in the reduction of porosity in various masonry materials such as concrete, stucco, and plasters. Sodium silicate is commonly used in drilling fluids to support borehole walls and prevent collapse. It is particularly beneficial when drilling into argillaceous strata that contain swelling clay minerals such as smectite or montmorillonite (EHS, 2021).

The total annual output of sodium silicate is estimated to be around 12 million tonnes (Assi et al., 2020). China is the world's largest producer of sodium silicate, with 42% of global output. Western Europe and the United States of America (USA) are the next major producers, with 1.9 and 1.42 million tonnes produced each year, respectively. Figure 2.13 illustrates the production capacities of sodium silicate around the world (Assi et al., 2020).

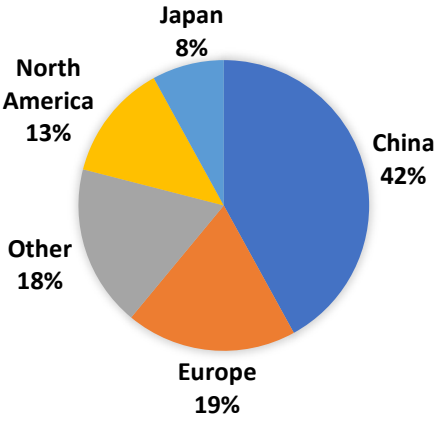

Figure 2.13: Sodium silicate production around the world

Source: Assi et al. (2020)

Sodium silicate is primarily used in the manufacturing of silicate derivatives, such as aluminosilicates, silicates, and zeolites. According to Assi et al. (2020), 35% of sodium silicate is utilised for precipitated silica, which is commonly used in industries such as rubber, plastics and polymers, adhesives and sealants, and agriculture, in Europe. This differs from the global use of sodium silicate, estimated at 71% in the following applications (shown in Figure 2.14):

- Detergents (25%)
- Catalysts (17%)
- Pulp and paper (12%)
- Elastomers (9%)
- Food and health (8%)
- Other (29%)

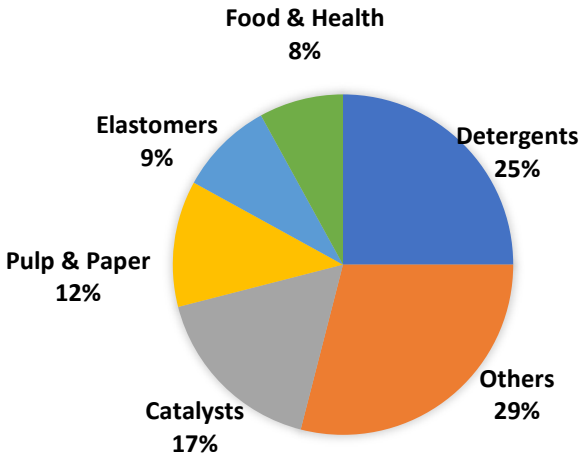

Figure 2.14: Applications of sodium silicate around the world

Source: Assi et al. (2020)

According to the study by Mohamed Ismail et al. (2020), the market value of sodium silicate was estimated at $8.8 billion in 2017 and was expected to reach $11.7 billion by 2024. Consequently, the rising demand for detergents, precipitated silica, adhesives, sealants, construction materials, pulp and paper, water treatment, metal casting, and food preservation appears to be driving the sodium silicate market.

As the production of sodium silicate has been reported to be detrimental to society, this study aimed to advocate for change. Specifically, the study sought to provide alternative products that can replace sodium silicate, particularly in the main applications that account for a higher percentage of its use. It is believed that this approach could also lead to a reduction in the cost of this material.

2.6 Replacing sodium silicate with alternative silica sources

In fly ash-GPC, sodium silicate as an activator is known to yield a more compact and dense material with higher mechanical strength (Fernández-Jiménez et al., 2005). However, the production of this material has a negative impact on the environment and represents the most expensive component in the production of geopolymers. The development of alternative activators with lower carbon dioxide footprints and improved sustainability for GPC is therefore crucial. This could lead to a significant reduction in the

environmental impact of AABs, particularly in terms of global warming potential (Tong et al., 2018). Additionally, concretes with strengths ranging from 35 MPa to 70 MPa were investigated, and preliminary cost analyses indicated that they were 30% to 35% less expensive than those produced with commercially available chemicals and 4% to 16% less expensive than PC concrete (Vinai & Soutsos, 2019; Bianco et al., 2021).

Efforts to reduce the cost and environmental impact of activators have focused on hydrothermal procedures (methods where the reaction between precursors and alkaline activators occurs under elevated temperature conditions) that manufacture silicate solutions from by-products such as condensed SF, RHA, and GWP. These silica-based waste materials have the potential to replace commercial sodium silicate in the production of fly ash geopolymers.

Tong et al. (2018) introduced a hydrothermal method for producing a sodium silicate solution by dissolving RHA in a sodium hydroxide solution under the following conditions: 3 M sodium hydroxide solution, a heating temperature of 80 °C, and a processing time of three hours. Their study concluded that waste-derived sodium silicate resulted in a 55% reduction in activation costs, as well as improved environmental conditions.

According to an experiment conducted by Assi et al. (2016), employing high external temperatures accelerates the geopolymerisation of fly ash-based GPC with SF, as it provides the necessary energy to enhance the interaction between the fly ash and the activating solution. This experiment demonstrated that fly ash-based GPC with SF is better suited for hot weather conditions, as significant compressive strength can be achieved within seven days at high average temperatures ranging from 40 to 45 °C. However, while there is an increase in energy costs associated with using higher external temperatures, the application of this type of concrete may be limited to prestressed and precast constructions. Such considerations led the researchers to believe that external temperature has a significant impact on cost, which supports the use of fly ash-based GPC with an activating solution of SF and sodium hydroxide (Assi et al., 2016). In a study by Živica (2006), the results indicated that SF is a highly effective alkali-activator for the binder system. According to the data, the favourable impact of the SF activator appears to be based on its ability to accelerate the synthesis of C-S-Hs and densify the developing

pore structure. Torres-Carrasco and Puertas (2015) also concluded that waste glass is a suitable alternative to commercial sodium silicate hydrates, which are widely used to create geopolymers by activating aluminosilicate materials such as fly ash.

2.6.1 Glass waste

Glass waste is a type of municipal solid waste that has caused major environmental difficulties due to its non-biodegradability and a poor recycling rate of roughly 10%, primarily owing to contamination from impurities and mixed colours (Xiao et al., 2020). In the USA, 12.5 million tonnes of waste glass are produced each year, with only 20% being recycled. Containers account for about 80% of all glass waste. In Hong Kong, 44 000 tonnes of domestic glass waste are produced annually, in addition to approximately 20 000 tonnes generated by the commercial sector. Of this total of 64 000 tonnes, only 8 000 tonnes of waste glass are recycled (Rivera et al., 2018). In Italy, the percentage of glass rejected by the so-called “closed loop” due to impurities and limitations (such as colour and composition) has been estimated to be between 6% and 15% (Vinai & Soutsos, 2019). According to a lifecycle assessment study conducted in Cape Town, South Africa, which has a rising population of 3.7 million people, between 150 000 and 300 000 tonnes of glass waste are generated each year, with only 20 000 to 60 000 tonnes being recycled (Rivera et al., 2018). Furthermore, the study noted that recycling glass containers instead of discarding them in landfills can result in a 27% energy saving and a 37% decrease in greenhouse gas emissions.

The recovered glass is typically used as a raw material for manufacturing abrasives, as glass powders for metal cleaning, as coarse aggregates in asphalt or concrete mixtures, and as a pozzolan in blended cements (Rivera et al., 2018). Glass waste is incorporated into geopolymers due to its chemical and physical uniformity, as well as its high content of amorphous silica. It undergoes a milling process that produces a by-product called GWP. GWP can be used as precursors, aggregates, or to develop activator solutions for GPC. One study proposed using glass waste as a source of reactive silica in geopolymer mixes. The researchers found that adding 15 g of glass waste (<45 µm) to 100 ml of 10 M sodium hydroxide to form an alkali-activator resulted in the highest compressive strength

of 37 MPa when cured for 28 days (Torres-Carrasco & Puertas, 2015). The inclusion of alkali sources such as glass cullet is advantageous in the production of geopolymers (Cyr et al., 2012). Glass cullet serves as a source of silica or alkalis in metakaolin or fly ash-based geopolymers. Specifically, using waste as a silica source in the manufacturing of sodium silicate as a substitute for commercial sodium silicates significantly reduces the environmental impact and carbon footprint of alkaline cement production (Rivera et al., 2018).

Another study proposed the production of sodium silicate by blending GWP, sodium hydroxide, and water at temperatures ranging from 150 °C to 330 °C for one to two hours. Fly ash and fly ash / GGBS blends served as precursors for AAB mortars produced with this sodium silicate. The results indicated that the compressive strengths were comparable to or better than those of commercial activators (sodium silicate and sodium hydroxide). At 28 days, the highest strength of 58 MPa was achieved with fly ash / GGBS mortars activated by powder activator at 150 °C (Vinai & Soutsos, 2019).

There are two types of manufacturing techniques that focus on the utilisation of glass waste for the development of low-cost, environmentally friendly silicate solutions (Vinai & Soutsos, 2019):

- The hydrothermal technique involves synthesising geopolymers by treating precursor materials at high temperatures and pressures in an aqueous solution. In this case, the glass is heated in an alkaline solution, which results in a silica dissolution rate of approximately 72%. While temperatures below 100 °C indicated that the process was feasible, the dissolution rate remained low. To enhance dissolution, the temperature was increased to a range of 150 to 250 °C.
- The thermochemical/fusion technique involves high-temperature processing of precursor materials with solid alkaline activators. In this case, the process combined glass and sodium hydroxide powders at extremely high temperatures of 500 °C, 650 °C, and 700 °C to 1 300 °C. The conversion of glass to sodium silicate was significant; however, the solubility of the resulting powder at ambient pressure

was low. This necessitated reheating at 175 °C for at least one hour, yet it still did not fully dissolve.

2.6.2 Silica fume (SF)

SF is a by-product of the smelting process for silicon and ferrosilicon alloys. High-purity quartz, which contains silicon and oxygen in the form of silica, is subjected to a reduction process. This typically involves heating the quartz to extremely high temperatures, up to 2 000 °C, and reacting it with a reducing agent such as carbon. This process separates the silicon from the oxygen in the silica, which produces silicon and silicon monoxide (SiO) vapour as by-products. As the high-purity quartz is reduced at these high temperatures, silicon monoxide vapour is generated. This vapour contains silicon and oxygen atoms and exists in a gaseous state. The silicon monoxide vapour, which is highly reactive, can undergo oxidation when it encounters oxygen or other oxidising agents present in the production environment. This oxidation process converts the silicon monoxide vapour back into solid silicon dioxide particles. The newly formed silica particles are extremely fine and typically non-crystalline and thus lack a well-defined crystalline structure. These particles are often referred to as undensified SF. Undensified SF consists of a high percentage of non-crystalline silica. The exact composition can vary but typically falls within the range of 85% to 99% silica. The non-crystalline nature of these particles makes them highly reactive and suitable for various applications, such as enhancing the properties of concrete and other construction materials. SF is a promising nanoparticle that can be added to geopolymers either as a precursor or a substitute and can also serve as an alkaline activator. This is due to its highly effective pozzolanic properties, extreme fineness, and high silica content (Lee et al., 2016). It is known to have spherical particles, which can act like small ball bearings that facilitate movement between solid particles in a mixture. This can potentially reduce friction between the solid particles, which allows for better flowability. However, despite this potential benefit, the overall effect of SF on workability also depends on its high surface area, which tends to increase water demand and can counteract improved flowability. According to Wang et al. (2022), SF particles are extremely fine and have a high specific surface area compared to other materials such as fly ash or calcium aluminate cement. This increased surface area can lead to

unique interactions with water and other components in the mixture, with particle surface area ranging from 13 000 to 30 000 kg/m² (Billong et al., 2021). Wang et al. (2022) also noted that the inclusion of a small amount of SF can indeed enhance flowability due to its lubricating effect, which reduces friction between solid particles. However, when a higher dosage of SF is used, it can absorb a significant amount of water onto its surface. This water absorption can lead to a decrease in the free water content in the mixture, making it less fluid, and, in turn, reducing flowability. The addition of SF to geopolymers, in particular, is said to improve their performance capabilities and result in the formation of a more highly polymerised product with high acid resistance (Lee et al., 2016).

Previous research has investigated the effect of SF as an alkali-activator in GPC. Okoye et al. (2016) examined the effects of different SF dosages in fly ash-based GPC activated with sodium hydroxide and sodium silicate, which was cured in an oven at 100 °C. The results indicated that the addition of SF enhanced the compressive strength of the GPCs. Furthermore, the compressive strength of fly ash-based geopolymer improved with an increase in nano-silica content by up to 2%, which was attributed to the densification of the microstructures and a well-connected interlocking morphology (Lee et al., 2016). Additionally, the fine SF particles filled the spaces between the sand particles, which contributed to a reduction in porosity and enhanced mechanical characteristics.

The effectiveness of using SF-based sodium silicate in producing metakaolin and GGBS-based geopolymers was investigated. Undensified SF was dissolved in a 10 M hydroxide solution to create a sodium silicate alternative solution. The results indicate that pastes with sodium silicate alternative exhibited slightly higher 28-day strength compared to those with commercial sodium silicate solution for both precursor materials. However, commercial sodium silicate led to a more rapid strength gain than sodium silicate alternative. For GGBS-based pastes, approximately 72% of the 28-day strength was achieved at seven days using a sodium silicate alternative, while 88% was achieved using commercial sodium silicate. For metakaolin-based pastes, the strength development was even faster, with equivalent values of 79% and 92%, respectively. Overall, compressive strength test results suggest that SF can be used to produce an sodium silicate alternative for viable geopolymer binders, which will enhance sustainability (Billong et al., 2021).

2.6.3 Rice husk ash (RHA)

RHA, a by-product of paddy rice production, has been identified as a potential source of amorphous silica that can be easily transformed into alkali silicates while requiring little energy. Rice husk is the tough protective covering that surrounds a rice grain and, on average, accounts for 20% of total paddy rice production. Since 2002, annual global paddy rice production has remained significant, reaching over 952 million tonnes in 2016, with corresponding rice husk of 238 million tonnes (Food and Agriculture Organization, 2018; Tong et al., 2018). Furthermore, approximately 1.7 tonnes of RHA are produced annually through the incineration of rice husk. RHA has been thoroughly examined as a possible source of silicate and, more recently, has been investigated as a silica source to produce sodium silicate, which is typically used for the alkali activation of geopolymers.

The environmental issue is the valorisation of RHA as a so-called by-product at small-scale levels via a low-temperature hydrothermal process with sodium hydroxide to obtain a silicate gel, which is a critical requirement for the geopolymerisation process. Until now, based on published data (Bernal et al., 2015; Kamseu et al., 2017; Tong et al., 2018; Lima et al., 2021), the reutilisation of RHA as an alternative source of silica to produce eco-friendly materials has been satisfactory and has proven that it can be used to replace commercial silicate for AAMs.

In the production of metakaolin-based geopolymer and fired clay brick-based geopolymer, RHA-based silicate was used as a partial substitute for commercial silicate (Kamseu et al., 2017). Three initial concentrations of sodium hydroxide (8, 10, and 12 M) were examined to determine the optimal dissolution and formation of silica oligomers that can serve as binders during geopolymerisation. The results from FTIR and XRD analyses indicated that RHA-sodium hydroxide-sodium silicate solutions possessed properties comparable to those of standard commercial sodium silicate.

A previous study evaluated the mechanical properties and structural changes of alkali-silicate activated slag cements exposed to high temperatures, using sodium silicates derived from SF and RHA. Similar reaction products were observed regardless of the type of silicate, with minor differences in the composition of the C-S-H gels, which resulted in

varying strength losses after high-temperature exposure. Cements produced with alternative activators demonstrated higher compressive strengths compared to those with commercial silicate. All samples maintained strengths above 50 MPa after exposure to 600 °C; however, only the specimens made with the RHA-based activator retained measurable strength after exposure to 800 °C. The study revealed that silicate-activated slag binders, whether activated with commercial silicate solutions or sodium silicates from SF or RHA, remain stable up to 600 °C (Bernal et al., 2015).

The initial and final setting times of geopolymer mortars using RHA-derived solution were both faster than those of the commercial solution (Tong et al., 2018). This implies that the silicates in the RHA-derived solution were more readily available for the reaction, which confirms the high activation potential of RHA-derived sodium silicates. The compressive strength values of mortar samples prepared with waterglass derived from RHA were similar to those prepared with commercial activators (Control 1), as illustrated in Figure 2.15. This similarity indicates that the quantity and reactivity of dissolved silicates in the RHA-derived solution matched those in the commercial sodium silicate solution. This comparability suggests that RHA-derived waterglass can effectively serve as an alternative to commercial sodium silicate in producing geopolymers with comparable strength.

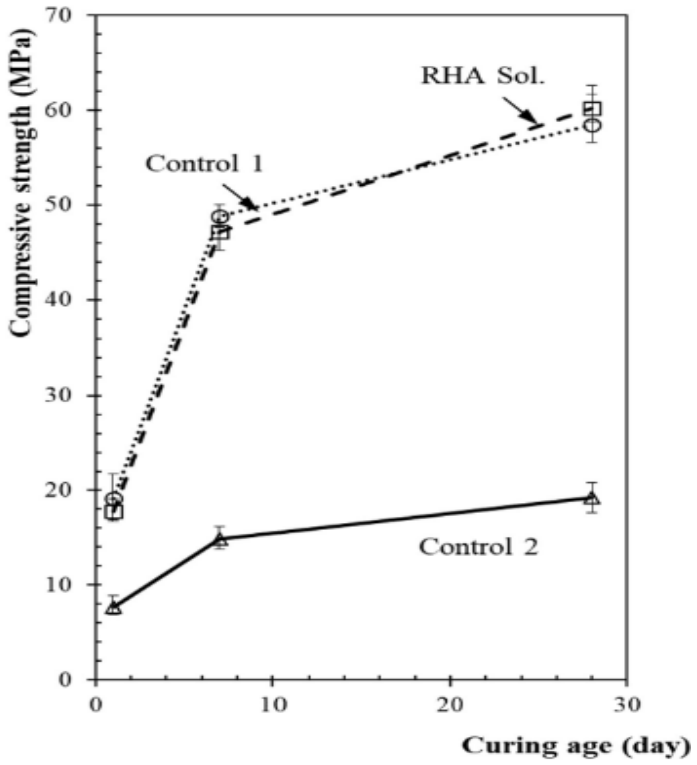

Figure 2.15: Compressive strength of mortars activated with RHA-derived and commercial alkaline solutions

Source: Tong et al. (2018)

2.7 pH of the alkali-activator solution

pH is a measure of the acidity or alkalinity of a solution and is widely used in various fields. It provides valuable information about the chemical properties of a solution (Grubb et al., 2007). The pH scale ranges from 0 to 14. A neutral solution has a pH of 7, while an acidic solution has a pH value of less than 7. A basic (alkaline) solution has a pH value of greater than 7. Typically, concrete is highly alkaline at the beginning of its life, with a pH of around 13. In any solution, both hydrogen ions (H^+) and hydroxide ions (OH^-) are present. Solutions with a higher concentration of hydrogen ions are termed acidic, while those with a higher concentration of hydroxide ions are termed basic (alkaline). When an acidic solution is mixed with water, the equilibrium shifts to the left, which results in a decrease in the concentration of hydroxide ions. Conversely, when a basic solution is mixed with water, the equilibrium also shifts to the left, but this time it leads to a decrease in the concentration of hydrogen ions (Oyebisi et al., 2021).

The findings from a relevant study indicated that a higher alkali pH significantly enhances the strength performance of GPC. Specifically, a pH value of 14 resulted in strength levels five times higher than those observed at a pH of 12. Consequently, it was concluded that the optimal pH range for the most effective polymerisation and higher strength in the GPC fresh mix is between 13 and 14 (Khale & Chaudhary, 2007). Another study showed that increasing the silicon/sodium ratio makes the solution less strongly alkaline due to the addition of more silica. When the silicon/sodium ratio is high, fewer hydroxide ions are concentrated on the surfaces of these particles, which results in slower reactions and, eventually, lower compressive strength (Han et al., 2023).

Different silica sources (e.g., SF, RHA, and GWP) have unique chemical compositions and solubility characteristics. These properties affect the overall alkalinity of the solution. For instance, certain silica sources dissolve more readily in sodium hydroxide, which contributes to a higher pH. Additionally, sodium hydroxide is a strong alkali, and its concentration in the solution directly impacts the pH level. Higher concentrations of sodium hydroxide increase the number of hydroxide ions in the solution, which raises the pH. For example, an 8 M sodium hydroxide solution will have a lower pH than a 10 M sodium hydroxide solution. The ratio of silica to sodium hydroxide in the activator is therefore very important (Chindaprasirt et al., 2007). Higher silica / sodium hydroxide ratios indicate a greater amount of silica relative to sodium hydroxide. Increasing the silica content in the system relative to sodium hydroxide can lead to a decrease in pH. Silica reacts with sodium hydroxide to form silicate species, which can reduce the free hydroxide ions in solution as they are consumed in the reaction. This reaction may slightly lower the pH as the system transitions to a more stable silicate-dominated environment. However, lower silica / sodium hydroxide ratios would still maintain high pH levels due to the abundant sodium hydroxide, but they might result in different reaction kinetics and gel properties (Hanjitsuwan et al., 2014).

2.8 Fresh and hardened properties of geopolymer mortar/concrete

The primary purpose of testing geopolymer mortar samples and concrete samples is to investigate and evaluate their properties under specific conditions. This involves studying

both the residual properties (properties after exposure to certain conditions) and the normal engineering properties (properties under standard conditions) of geopolymers based on low-calcium fly ash and blended with other materials. Initially, the geopolymer binder is a fluid resin that transitions into a paste, which eventually sets and hardens into a highly resistant material. The properties of fresh geopolymer mortar are assessed through workability and setting time tests, while the mechanical performance of the hardened mortar is evaluated using compressive strength tests (Al-Majidi, 2017).

2.8.1 Setting time of geopolymer mortar

Setting time is an important property of concrete and is categorised into initial and final setting times, to reflect the concrete's degree of rigidity. The initial setting time is defined as the moment when the penetration resistance reaches 3.5 MPa, while the final setting time occurs when it reaches 27.6 MPa (ASTM C403-08). Additionally, the initial setting time for OPC with a strength class of 42.5 should exceed 60 minutes (BS EN 197-1:2011). The setting time or working time of GPC is not well documented in the literature, with limited publications on this subject. Setting times can vary from minutes to up to four hours, depending on factors such as curing temperature and the chemical composition of the source material. Based on a previous study, the setting time for fly ash-based geopolymer without GGBS has been found to be around 1 500 minutes (Jang et al., 2014). In a prior study, setting time tests were performed to explore the impact of GGBS content on fly ash- and GGBS-based geopolymer mortar. The study examined geopolymer mixes with GGBS-to-binder ratios of 10%, 20%, 30%, 40%, and 50% (Rao & Rao, 2015).

As outlined by BS EN 480-2:2006, two measurements were taken: the initial and final setting times. The initial setting time was measured from the end of mixing until the needle penetrated to 4 mm from the base plate, while the final setting time was recorded when the needle penetrated to 2.5 mm. The findings revealed that adding GGBS to the mixture significantly reduced the setting time. For mixtures containing 10% GGBS, the initial setting time was shortened to 80 minutes and the final setting time to 150 minutes. As the GGBS content increased, the total setting time decreased considerably. With 20% GGBS,

the initial and final setting times were reduced to 58 minutes and 120 minutes, respectively. For 30% GGBS, these times dropped further to 42 minutes and 80 minutes. The setting time continued to decrease slightly when the GGBS content was increased from 30% to 40%.

In another study, different specimen series were labelled ‘A’, ‘B’, ‘C’, and ‘D’, with the numbers ‘100’, ‘150’, ‘200’, ‘250’, and ‘300’ representing various percentages of GGBS replacing fly ash by weight. The research explored how the setting time of alkali-activated fly ash-slag (AAFS) pastes varied with different slag replacement levels. The findings indicated that both the initial and final setting times decreased as the percentage of slag increased. Specifically, specimens with 10% slag had longer setting times compared to those with higher slag content. With increased slag, the initial setting time dropped sharply from 350 minutes to a range of 77 to 118 minutes, and the final setting time fell from 470 minutes to between 107 and 128 minutes.

2.8.2 Flow workability of geopolymer mortar/concrete

Workability, or flow, refers to the ease of working with freshly mixed concrete during the stages of handling, placing, compacting, and finishing. The slump test is commonly used to measure the workability of GPC, while the flow table test is employed for assessing the workability of geopolymer mortars. Generally, GPC exhibits lower workability compared to OPC concrete due to the sticky nature of the silicates present in geopolymer mixtures. However, it is still possible to achieve effective compaction of GPC using a vibrating table, even with a relatively low slump value. Consequently, the workability of GPC is evaluated based on its ability to be compacted effectively. GPC with a slump value of 90 mm or higher is considered highly workable, while concrete with slump values between 50 mm and 89 mm is categorised as having medium workability. In contrast, GPC with slump values below 50 mm is deemed to have low workability due to the increased effort required for compaction. Flow tests are conducted immediately after mixing (Fang et al., 2018). Usually, this test is conducted at room temperature; however, preliminary tests indicated that room temperature might significantly impact workability measurements,

likely due to changes in the viscosity of the alkali-activator solution, particularly the $Na_2O{\cdot}nSiO_2$ component (Yang et al., 2008).

In a previous study, mixtures were tested to evaluate the impact of substituting fly ash with slag, using GPC1 through GPC5, where slag was incorporated at 10%, 20%, 30%, 40%, and 50%, respectively. The findings revealed that mixtures with 10% and 20% slag had slump values that exceeded 90 mm, which classified them as highly workable GPCs. Mixtures with 30% and 40% slag had slump values ranging from 50 mm to 89 mm, which indicated medium workability. In contrast, the GPC with 50% slag was classified as having low workability due to a slump value below 50 mm. Additionally, the slump values decreased as the slag content increased, which demonstrated an inverse relationship between slag content and workability. This reduced workability in slag-rich concrete is attributed to the high concentration of calcium ions leached from the slag, which react rapidly with the alkaline activator to form C-S-H (Sunarsih et al., 2023). Similarly, another study investigated the flow value of AAFS pastes and the slump value of AAFS concrete with various slag contents. Both the flow value of AAFS pastes and the slump value of AAFS concrete were influenced by the replacement level of slag in the binder. The slump and flow values decreased with the increase in slag content in the mixture (Fang et al., 2018). This finding is consistent with the previously mentioned study.

2.8.3 Compressive strength of GPC

Compressive strength is a key mechanical property of concrete. For standard engineering applications, concrete must reach a compressive strength of at least 28 MPa in 28 days (ACI 318 M-05). Furthermore, to protect reinforcement from corrosion, the concrete should have a minimum compressive strength of 35 MPa (Fang et al., 2018). Fly ash-GPC achieves high early compressive strength, similar to that of OPC concrete. Factors such as high-temperature curing, high silicate concentrations, and very low water content contribute to this performance. This makes it suitable for structures that require high early strength, with reported compressive strengths ranging from 20 to 95 MPa (Olivia, 2011).

2.8.3.1 *Effect of the silica source / sodium hydroxide molar ratio on compressive strength*

A study explored how mixture parameters affect the compressive strength of fly ash-GPC mortars. In this study, Class F fly ash was activated with an 8 M sodium hydroxide + $Na_2O{\cdot}nSiO_2$ solution, using SS/SH ratios between 0.4 and 2.5. The aggregate-to-fly ash mass ratio was kept constant at 0.30, and curing was conducted at 90 °C for 24 hours. The findings showed that increasing the SS/SH ratio from 0.4 to 2.5 resulted in higher compressive strength of the mortars (Dhinakaran & Rajarajeswari, 2011). Another study produced similar results, where the silica source / sodium hydroxide ratio of the fly ash-GPC mixtures was adjusted from 0.5 to 3.0, while the sodium hydroxide concentration was maintained at 8 M. The results demonstrated that the compressive strength of fly ash-GPC mortars increased as the silica source / sodium hydroxide ratio was raised from 0.5 to 2.0. However, increasing the silica source / sodium hydroxide ratio beyond 2.0 to 3.0 led to a decrease in strength (Naghizadeh, 2019).

2.8.3.2 *Effect of sodium hydroxide concentration on compressive strength*

The effect of sodium hydroxide concentration on the compressive strength of AAFS concrete shows that increasing the sodium hydroxide concentration from 10 M (Series A) to 12 M (Series B) gradually enhances compressive strength. This improvement can be attributed to the reaction of internal silica, aluminium, and calcium components, which is facilitated by the increased breakage of T-O-T bonds (T: silica or aluminium) in fly ash and Ca-O and Si-O bonds in GGBS due to the higher alkalinity from the increased sodium hydroxide concentration (Fang et al., 2018). In another study, the compressive strength results for GPC mortars with various sodium hydroxide concentrations and a constant SS/SH ratio of 2.0 indicated that, for a liquid to solid (L/S) ratio of 0.3, the compressive strength increased from 33 MPa to 47 MPa as the sodium hydroxide concentration increased from 10 M to 14 M. This strength gain at higher sodium hydroxide concentrations is attributed to enhanced geopolymerisation at higher pH levels and increased alkali content. However, for mixes with L/S ratios of 0.4 and 0.5, the strength decreased when the sodium hydroxide concentration exceeded 12 M.

2.8.3.3 Effect of GGBS ratio on compressive strength

A study investigated the mechanical and microstructural properties of GPC mixes prepared with a combination of fly ash and slag cured at an ambient temperature. The results showed that increasing the GGBS content in the mix significantly improved the compressive strength, even at early curing ages. The three-day mean compressive strengths were 2.9 MPa, 10.4 MPa, 13.7 MPa, 18.6 MPa, and 25.9 MPa for mixtures with 10%, 20%, 30%, 40%, and 50% GGBS, respectively. At 28 days, mixtures with 20%, 30%, 40%, and 50% GGBS respectively achieved strengths that were 65%, 133%, 140%, and 162% higher compared to the mixture with 10% GGBS. This strength increase is attributed to the infilling of the porous microstructure of the geopolymer mortar with more hydration products, facilitated by the inclusion of the highly reactive slag particles (Al-Majidi et al., 2016). A similar trend was observed in a study that tested various combinations of fly ash and GGBS: 90% fly ash with 10% GGBS, 80% fly ash with 20% GGBS, and 70% fly ash with 30% GGBS. The ratios of sodium silicate / sodium hydroxide used were 2 and 2.5, and the alkaline liquid to binder ratio was set at 0.45. The results indicated that the geopolymer mortar gained strength even under ambient conditions, with compressive strength increasing as the proportion of GGBS in the mixture increased (Rajan & Ramujee, 2015).

2.8.3.4 Effect of curing period on compressive strength

The properties of hardened GPC are significantly affected by both curing duration and temperature. Since geopolymerisation reacts slowly at room temperature, GPC mixtures are typically cured at higher temperatures, between 35 and 90 °C, to accelerate the setting process and improve strength. An investigation was conducted into how curing duration impacts the mechanical properties of fly ash-GPC paste mixtures, using an 8 M sodium hydroxide + $Na_2O{\cdot}nSiO2$ alkali-activator. Paste samples, measuring 40 x 40 x 160 mm, were cured at 80 °C for periods of six, 15, or 24 hours and then left at ambient temperature for seven, 28, or 90 days. The findings revealed that extending the curing duration from six to 24 hours enhanced the seven-day compressive strength from 9 MPa to 29 MPa. Additionally, samples that were heat-cured for 24 hours and then aged at

room temperature for seven to 90 days achieved a compressive strength of 41 MPa. Similarly, the effect of curing temperature on the compressive strength of fly ash-GPC was investigated in a recent study. In the study, Class F fly ash was used as the raw material, activated using 14 M sodium hydroxide + $Na_2O{\cdot}nSiO2$ with 45% solid to liquid ratio and a solid to heat ratio of 2.1. The GPC mixtures were prepared at a constant L/S ratio of 0.5 and SS/SH ratio of 2.5. It was reported that the compressive strength of the concretes increased when the curing temperature was raised from 60 °C to 90 °C.

2.9 Microstructural analyses

The gel microstructure of GPC determines the structure of the pore network, which influences moisture control by increasing folds and pores at high temperatures. These changes in pore structure are believed to enhance resistance to disintegration and fragmentation at elevated temperatures, such as during a fire, by allowing trapped water vapour to be released more easily and reducing internal vapour pressure. Various techniques are employed to analyse the microstructure of silica-activated geopolymer paste or mortar. These techniques include XRD, X-ray fluorescence (XRF), magic-angle spinning nuclear magnetic resonance, SEM with energy-dispersive spectroscopy, transmission electron microscopy with energy-dispersive spectroscopy, FTIR, and thermogravimetry (Majidi, 2009). However, the most commonly used techniques in fly ash-GPC are SEM and XRD, as discussed below.

- SEM is an effective method for obtaining high-resolution images and analysing the microstructure of GPC. To prepare the concrete samples, they are cut or fractured to expose a fresh surface. The specimens are then coated with a thin layer of conductive material, such as gold or carbon, to improve imaging quality. SEM provides information about the morphology, pore structure, and interfacial bonding in the geopolymer matrix.
- XRD is a technique used to analyse the crystalline structure of materials, including GPC.
- XRD works on the principle that X-rays are directed at the sample, and a detector measures the diffracted rays at various angles. The instrument rotates the sample

and detector to cover a range of angles, which creates a complete diffraction pattern. The resulting diffraction pattern consists of peaks that correspond to the different crystalline phases present in the sample. Each peak represents a set of crystallographic planes in the material. The position (2θ) and intensity of these peaks are characteristic of crystalline phases.

The microstructure of geopolymer is influenced by the particle size distribution and chemical composition of the fly ash, the type and dosage of the alkaline activator, and the curing temperature. Fernández-Jiménez et al. (2005) examined the morphology of fly ash mixes using three different alkali activators: sodium hydroxide, sodium hydroxide combined with sodium silicate, and sodium hydroxide combined with sodium carbonate. The study revealed that the primary reaction product in all mixtures is aluminosilicate gel. In the mix activated solely with sodium hydroxide, a significant amount of unreacted fly ash was observed, which indicated a moderate degree of reaction. Conversely, the mixture activated with sodium hydroxide and sodium silicate resulted in a dense material with minimal porosity and excellent bonding between the paste and aggregates. The final mix activated with sodium hydroxide and sodium carbonate exhibited the most porous paste. XRD analysis revealed the presence of porous minerals called zeolites in all mixtures, with hydroxysodalite also forming in the mixture activated solely with sodium hydroxide. In another study, the microstructure of fly ash geopolymer activated using a combination of sodium hydroxide and sodium silicate also exhibited stronger bonding and better adhesion between the pastes. It also showed excellent connectivity between the gels and resulted in a high-strength material (Jo et al., 2007).

Chi and Huang (2013) examined the mechanical properties and binding mechanism of fly ash and slag-based geopolymer mortars. Their research included compressive strength tests, flexural strength tests, water absorption tests, drying shrinkage tests, as well as SEM and XRD analyses. The results indicated that the binding mechanism and properties of fly ash-slag-based geopolymer mortars were significantly influenced by the ratio of fly ash to slag and the dosage of sodium oxide. SEM and XRD analyses revealed that the hydration products of fly ash-slag-based geopolymer mortars mainly consist of amorphous alkaline aluminosilicate and low-crystalline C-S-H gel. The fly ash-slag-based

geopolymer mortars exhibited better mechanical properties, including compressive strength, flexural strength, and water absorption, compared to OPC mortars, except for drying shrinkage.

It is commonly accepted that variations in the mechanical characteristics of geopolymers are primarily due to changes in the internal microstructure. Consequently, several researchers have used SEM to analyse the microstructural creation and evolution that occur during temperature exposure (Duan et al., 2015; Zhang et al., 2016; Duan et al., 2017; Morsy et al., 2019). A related study confirmed that a system cured at a low temperature (20 °C) has more unreacted fly ash due to low adherence between particles. Similar conclusions were drawn for geopolymers cured at 30 °C, with the resulting material exhibiting more porous structures compared to that cured at 75 °C.

High-temperature curing leads to a greater degree of aluminosilicate gel formation, which enhances the final strength of the geopolymer. High-temperature curing is therefore recommended due to the resulting strong bond in the geopolymer paste (Jo et al., 2007). Similarly, Xiao et al. (2020) discovered that geopolymer cured at 40 °C and 98% relative humidity exhibited the most compact microstructure, which indicates the highest degree of geopolymerisation. However, geopolymer cured at 20 °C, with 45% relative humidity, and at 20 °C, with 98% relative humidity, retained more unreacted particles linked by cementitious gels.

Microstructure can provide insight into pore structures, but accurate porosity measurements often require specialised techniques. For instance, fly ash activated with sodium hydroxide and sodium silicate has been reported to exhibit porosities ranging from 20% to 40% (Škvára et al., 2006). Using the vacuum saturation technique, the porosity of fly ash geopolymer was found to be approximately 8.5% to 14% (Ravikumar et al., 2010). Pores larger than 200 nm, observed in geopolymer mixtures cured at 30 °C, highlight the influence of curing temperature on pore formation (Sindhunata et al., 2006). Higher curing temperatures and concentrations of activating agents tend to reduce pore size. A higher concentration of sodium hydroxide has thus been recommended to decrease geopolymer porosity.

Similarly, a study investigated the effects of the concentration of the activating agent (4 M, 6 M, or 8 M sodium hydroxide solution) and the activator-to-binder ratio (0.40, 0.50, or 0.60) on the compressive strengths, pore structure features, and microstructure of cement-free binder concretes containing Class F fly ash or GGBS as the sole binder. The results showed that the porosity of the concretes increased with the activator-to-binder ratio, as illustrated in Figure 2.16. Additionally, cement-free binder concretes made with fly ash and activated with 4 M sodium hydroxide exhibited the highest porosity values. Porosity decreased with higher activator concentration, due to improved activation efficiency and increased formation of reaction products. Similar trends were observed for cement-free binder concretes made with GGBS, which had lower porosities compared to those made with fly ash. The activator concentration had a lesser impact on the porosity of cement-free binder concretes made with GGBS than on those made with fly ash. Curing temperature and activator concentration are both critical parameters that must be carefully studied and adjusted to modify geopolymer porosity (Ravikumar et al., 2010).

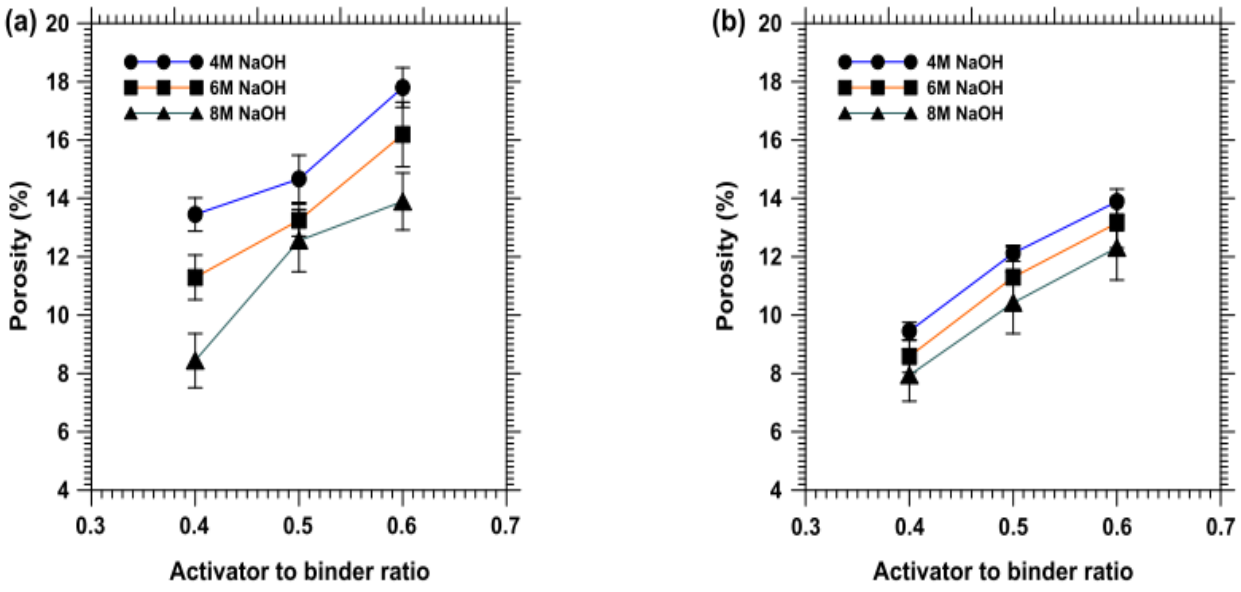

Figure 2.16: Porosities of cement-free binder concretes made using (A) fly ash and (B) GGBS
Source: Ravikumar et al. (2010)

2.10 Durability of geopolymer binders

Durability is defined as the capacity of concrete to resist aggressive environments such as weathering action, abrasion, and chemical attack while retaining its expected technical features, which are intended not to deteriorate over an extended service life (Amran et al., 2021). In moderate environments, concrete made with OPC has proven to be quite durable. However, it is recognised that severe exposure to sulphate, chloride, and acid may induce degradation in conventional concrete (Law et al., 2014; Živica et al., 2015; Amran et al., 2021). This has always presented a challenge, because it makes it susceptible to deterioration over time. Consequently, replacing OPC with GPC has become a viable option, as GPC generally offers better resistance to acids, water, and chemical ingress, as well as improved long-term performance. Several researchers have reported on the high resilience of geopolymer cements in harsh environments (Davidovits, 1994; Xu & Van Deventer, 2002; Thokchom et al., 2010; Živica et al., 2015). Additionally, these studies have shown that fly ash-based geopolymer cement is more resistant over the long term.

The durability of GPC is influenced by the type of precursor material used. Various precursors are required to create AABs, typically made using combinations of materials such as fly ash / slag, fly ash / metakaolin, and slag/metakaolin. A study examined the durability of GPC produced with GGBS, Class F fly ash, and alkaline activators at an ambient temperature, exposed to magnesium sulphate ($MgSO_4$) and sodium sulphate (Na_2SO_4) environments. In this study, GGBS was partially replaced with fly ash at levels ranging from 0% to 50%, using a constant 12 M alkali-activator solution. In the magnesium sulphate environment, the strength of GPC with GGBS decreased by 35%, whereas a 40% replacement of fly ash with GGBS demonstrated a strength gain of 10%. Similar trends were observed in the sodium sulphate environment, with the 40% fly ash replacement performing well. Consequently, it was concluded that a 40% partial replacement of fly ash with GGBS is ideal for achieving the desired durability properties in ambient-cured GPC.

Similarly, a study examined the durability performance of GPC composed of 80% fly ash and 20% GGBS, activated with sodium silicate and an 8 M sodium hydroxide solution.

The tests conducted included acid resistance, water absorption, sulphate resistance, and the rapid chloride penetration test. The findings revealed that GPC exhibited better acid resistance, higher sulphate resistance, and lower water absorption compared to OPC concrete. However, it demonstrated higher chloride penetration than OPC concrete (Naghizadeh et al., 2023). It is also vital to explore the durability of geopolymer binders when a silica-based waste material is used as an alkaline activator. In recent years, when an SF activator was applied, an interestingly high level of acid resistance in geopolymer was achieved (Xu & Van Deventer, 2000; Živica & Križma, 2013).

2.10.1 Chemical resistance of GPC

Concrete is held together by an alkaline hydrated cement paste with a pH of 11±1. As a result, it will dissolve in the presence of acids, which are often found in industrial waste, mining tailings, and some bodies of water (Bakharev, 2005; Živica & Križma, 2013). Chemical attack by acids can be particularly severe if the pH of the cement paste drops to 4, and even more so when the acid solution has a velocity capable of causing mechanical abrasion (Shill et al., 2020). The precise velocities that accelerate chemical attack vary and are difficult to determine. The most straightforward method for assessing the degree of attack would be to examine a variety of samples and compare the impact of different pH levels and velocities (Vafaei et al., 2018). The chemical resistance of cement paste is proportional to its permeability, with less permeable pastes exhibiting greater chemical resistance. PC also contains calcium hydroxide, which is the most soluble hydration product that dissolves when exposed to water, which increases the porosity and susceptibility of the paste (Bakharev, 2005).

Sulphate attack can occur when cement is exposed to sulphate-containing fluids, such as certain natural or contaminated groundwaters. In OPC, this type of attack can lead to strength loss, expansion, spalling of surface layers, and eventually disintegration. However, multiple references in the literature indicate that alkaline inorganic polymer cements, including alkali-activated metakaolin and fly ash, demonstrate excellent resistance to ordinary sulphate attack and seawater due to the absence of high-calcium phases (Thokchom et al., 2010).

The comparatively strong resistance to acidic media is an intriguing characteristic of GPC. Alkali-activated metakaolin or fly ash is said to be significantly more resistant to chemical attack by acids such as nitric acid (HNO_3), sulphuric acid (H_2SO_4), or hydrochloric acid (HCl) than PC mortar or concrete. According to Bakharev (2005), high-performance geopolymer materials (compressive strength above 60 MPa) deteriorate in acidic environments due to the production of cracks in the amorphous polymer matrix, whereas low-performance geopolymers (compressive strength below 40 MPa) deteriorate due to zeolite crystallisation and the formation of brittle grainy structures. The creation of aluminosilicate gel is critical for determining geopolymer stability. The crystalline geopolymer material created with sodium hydroxide is found to be more stable in the harsh environment of sulphuric and acetic acid solutions than the amorphous geopolymer material made with sodium silicate activator (Živica et al., 2015). A relevant study showed a clear SEM image of fly ash-based GPC under acid attack, as seen in Figure 2.17.

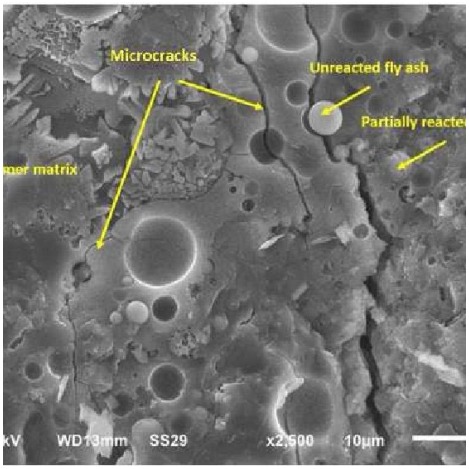

Figure 2.17: Visual appearance of concrete under acid attack

Source: Matalkah et al. (2016)

Several authors have investigated the acid resistance of geopolymer pastes and concrete (Bakharev, 2005; Arioz et al., 2012; Aiken et al., 2018). In most cases, the degree of deterioration is determined by the concentration of the acid solution and the duration of exposure. It has also been reported that fly ash-based geopolymer pastes retained a dense microstructure after three months in nitric acid. Observations from various studies suggest that the acid and alkaline resistance of a fly ash-based geopolymer is heavily influenced by its mineralogical makeup. A similar study that examined the impact of

sodium oxide content on geopolymer durability in sulphuric acid concluded that the specimen with the highest alkali concentration lost the most weight compared to the specimen with the lowest alkali level. Conversely, specimens with the lowest alkali concentration lost more strength. As a result, specimens with a greater alkali concentration outperformed those with a lower alkali content in terms of residual compressive strength (Thokchom et al., 2010; Živica et al., 2015).

2.10.2 Durability index tests

South African durability index tests include the oxygen permeability index, chloride conductivity index, and water sorptivity index (Alexander & Mackechnie, 2003; Alexander, 2004; Alexander et al., 2008; Alexander et al., 2018; Moore et al., 2021). Although these three index tests have been developed and validated in laboratories, they have not been widely applied to concrete in actual structures under typical site conditions. The durability index tests are conducted using circular discs prepared by coring and cutting the fly ash-GPC cubes (as illustrated in Figure 2.18). The oxygen permeability test determines the oxygen permeability index in the test specimens, while the chloride conductivity test assesses the chloride conductivity index. Furthermore, the sorptivity test establishes the water sorptivity index in the test specimens. These tests are conducted in accordance with the Durability Index Testing Manual (2018).

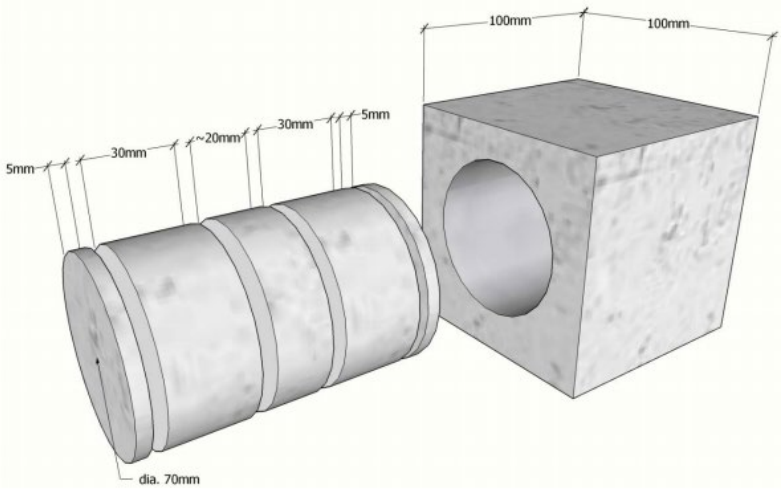

Figure 2.18: Details of cutting discs from 100 mm cube

Source: Alexander et al. (2018)

Before these tests can be conducted, it is essential to establish the range of results and the extent of variability that can be expected when applying the durability index tests, as shown in Table 2.1. The table is qualitative and has limitations, as it does not account for acceptable performance levels based on exposure conditions and the service environment of the structure. As a result, Table 2.1 may be considered overly simplistic. To address these limitations, the South African National Roads Agency Limited developed more detailed and advanced specifications.

Table 2.1: Recommended range for durability classifications using index values

Durability class	Oxygen permeability (log scale)	Sorptivity (mm/√*h*)	Conductivity (mS/cm)
Excellent	>10	<6	<0.75
Good	9.5-10	6-10	0.75-1.5
Poor	9.0-9.5	10-15	1.5-2.5
Very poor	<9	>15	>2.5

Source: Moore et al. (2021)

Table 2.2: Suggested durability classification table for sorptivity and porosity values

Sorptivity (mm/√*h*)	Porosity (%)	Durability classification
<6	<10	Excellent
6-10	<10	Excellent to good
	>10, <12	Good to poor
10-15	<12	Good to poor
	>12, <15	Poor to very poor
>15	-	Very poor

Source: Moore et al. (2021)

A recent study assessed the long-term strength development and durability performance of fly ash-GPC mixtures subjected to ambient curing at normal temperatures. The mixture was activated using combined sodium silicate and sodium hydroxide solutions mixed at a varied ratio of the former to the latter, ranging from 0.72 to 4.89. The ambient-cured fly ash-GPCs demonstrated significant strength gains of 60% to 90% over a one-year period. These concretes also showed good durability performance and a strong correlation between the oxygen permeability and water sorptivity indexes. However, the chloride conductivity index test indicated potential interferences from the ion fluxes in the pore solution of GPCs, which resulted in erratic results (Naghizadeh et al., 2023).

2.10.2.1 *Oxygen permeability index tests*

The oxygen permeability index test is used to assess the durability of concrete by measuring its ability to resist the penetration of oxygen. The oxygen permeability index test employs a falling head permeameter, with the index defined as the negative logarithm of the coefficient of permeability. Typical oxygen permeability index values range from 8.5 to 10.5 (on a logarithmic scale), where higher values indicate greater impermeability, which suggests potentially higher quality concrete (Moore et al., 2021). This test provides an indication of the concrete's microstructural quality and its susceptibility to deterioration processes such as carbonation and corrosion of embedded steel reinforcement. The oxygen permeability index test should be conducted after 28 days of curing to allow for substantial completion of the geopolymerisation process, which will result in a stable and mature microstructure.

A previous study used durability index test methods to evaluate the impact of repair materials on concrete durability. Five commercially available repair materials were examined, including two specialised coatings (masonry and carbothane aliphatic paints) and three repair mortars (general-purpose, cement-based, and epoxy resin). The oxygen permeability index and water sorptivity test methods were employed to assess and compare the performance of these materials. The results demonstrated that repair materials significantly enhanced concrete durability, and improved the oxygen permeability index durability classification of the samples from "Good" to "Excellent". The repaired concretes exhibited excellent oxygen permeability index values ranging from 10.10 to 10.35, compared to control samples with values between 9.7 and 10, depending on the surface preparation method (Parbhoo et al., 2012).

2.10.2.2 *Water sorptivity and porosity tests*

The water sorptivity index test measures the rate at which a wetting front progresses through concrete due to capillary suction (Moore et al., 2021). Lower water sorptivity index values suggest better potential durability of the concrete. This index is highly sensitive to the properties of the concrete's surface layer, which makes it a reliable indicator of the type and effectiveness of curing. When performing this test on surface-treated concretes

or concrete subjected to environmental factors such as carbonation or sea salts, care should be taken when interpreting the findings (Mackechnie & Alexander, 2000). The test also determines the specimen's water-penetrable porosity through vacuum saturation. When testing for porosity, it is assumed that all water-accessible pore volumes are filled, which leads to a mass change that can be expressed as a percentage of the specimen's volume. This, along with the measured rate of mass change from water absorption, determines the sorptivity. If the specimen is not fully saturated at this stage, some pores will remain empty. As a result, the measured porosity will be lower than the actual porosity. This leads to an incorrectly high sorptivity value, placing the concrete in a higher sorptivity classification, which suggests poorer durability and higher water absorption than it actually has (Moore et al., 2020). Furthermore, it has been found that this test technique is not applicable to concrete with a maximum nominal aggregate size greater than 26.5 mm. Concrete with larger aggregates tends to have a more heterogeneous structure, which leads to greater variability in test results. The test relies on a relatively uniform pore structure to provide consistent and reliable measurements

2.10.2.3 Chloride conductivity tests

The chloride conductivity index test assesses the immediate electrical current generated by the movement of chloride ions (Cl^-) through a standard specimen that has been pre-saturated in a 5 M sodium chloride solution. This is conducted using a two-cell conduction setup, where both sides of the specimen are in contact with the sodium chloride solution. The chloride conductivity index is indicative of the concrete's chloride diffusion characteristics (Moore et al., 2021). In the chloride conductivity test, chloride ions move through all pores of sufficient size, unlike the permeation process, which favours larger pores. The chloride conduction test therefore provides a good indication of the material's overall diffusivity and is sensitive to changes in pore structure and cement chemistry that might seem insignificant in the permeation process. Typical chloride conductivity index values for concrete range from very poor (>2.5 mS/cm) to excellent (<0.75 mS/cm), with lower values indicating better potential durability of the concrete (Gouws et al., 2001). A study evaluated the robustness of the chloride conductivity test, focusing on how concrete quality affects its sensitivity to selected test parameters. Three parameters were

investigated: (1) test duration (10, 40, and 120 seconds), (2) capillary voltage across the test specimen (7, 10, and 15 V), and (3) concentration of the sodium chloride solution (3 M and 5 M). One parameter was varied at a time. The results indicate that concretes with high chloride conductivity index values (>0.8 mS/cm) are generally sensitive to changes in sodium chloride solution concentration, capillary voltage, and test duration. For these concretes, the chloride conductivity index increases with higher capillary voltage, decreases with lower salt concentration, and shows random effects with longer test durations. Although not specified in the test standard, the study recommended limiting the test duration to less than 10 seconds once the electrical circuit is closed (Otieno, 2018).

2.11 Summary

This chapter presented information from the literature that is relevant to the topic of this study. Previous research on sodium silicate activators in GPC was gathered and critically discussed. There is a significant gap in research regarding the use of alternative silica sources in place of sodium silicate in geopolymers. Current studies do not fully explain how variations in silica source type, composition, and dissolution behaviour influence the fresh and hardened properties of geopolymer binders. This lack of systematic investigation limits the ability to optimise geopolymer formulations that do not rely on commercial sodium silicate. Furthermore, because the effects of alternative silica sources on geopolymer performance remain underexplored, there is a need for controlled experimental research to quantify their impact on reaction kinetics, microstructure development, and engineering properties. Addressing this gap is essential for developing cost-effective and sustainable activator systems for geopolymer production. It is important to evaluate whether these alternatives can achieve the same mechanical and durability properties as conventional sodium silicate-based geopolymers. Experimental studies are therefore being conducted to examine how different silica sources affect the performance of geopolymers as replacements for traditional sodium silicate.

CHAPTER 3:
METHODOLOGY

3.1 Introduction

This chapter presents the method used to assess the influence of alkali activators derived from different silica sources that will replace conventional sodium silicate in fly ash-based GPC. It also details the characteristics of the materials used in the experiment, including their physical and chemical properties. Additionally, it discusses the test methods and procedures employed. Based on the information acquired from the literature review, an experimental programme was developed.

The experimental programme was conducted at the Green Concrete Laboratory of the Department of Engineering Sciences at the University of the Free State in Bloemfontein, South Africa. The experiment was conducted in two phases. The first phase investigated the fresh and hardened properties of fly ash and fly ash/GGBS geopolymer mortar activated with sodium hydroxide and conventional sodium silicate solutions, which were used as control samples. Subsequently, conventional sodium silicate was replaced with alkaline activators derived from different waste materials to evaluate the effect of varying silica sources on the properties of fly ash-based geopolymer mortars. The investigation included setting time measurements, flow workability assessments, and compressive strength tests, all conducted in accordance with South African National Standards (SANS).

In the second phase, the GPC samples made using waste material-based alkali activators at optimum proportions were subjected to durability performance evaluation. The durability index test was conducted on the GPC samples to assess their resistance to various environmental factors and to evaluate their long-term performance.

The study also performed microstructural studies to provide potential explanations for the observations. Two techniques were used for microstructure characterisation: XRD and SEM. XRD analysis was employed to evaluate changes in the crystalline phases of the hardened binders due to the use of different alkaline activators. SEM analysis was

conducted to reveal the presence of unreacted particles, the geopolymerisation rate, and the formation of aluminosilicate gel in the material. Additionally, to characterise the various alternative silica source materials, XRF spectrometry was utilised. XRF is a well-established analytical technique that is widely used in industrial and research applications for elemental composition analysis. This test was used to establish the composition of all the raw materials. The composition of silica sources is imperative for determining and optimising the alkali-activator concentration.

3.2 Materials

The materials used in the experiment involved aluminosilicate raw materials (precursors), various alkali activators, and different types of aggregates to create GPC pastes and mortars. These components were mixed to form the geopolymer mixture, with the alkali activators initiating the geopolymerisation process, and the aggregates contribute to the overall properties of the final mortar and concrete. The physical, chemical, and mineralogical characteristics of the aluminosilicate raw materials used in this study are discussed in the following section.

3.2.1 Aluminosilicate raw materials (precursors)

Fly ash is a common precursor material used in geopolymers. Low-calcium Class F fly ash was employed as a precursor material in the first phase of this study. As outlined in Section 2.3.1 of the literature review, low-calcium content (Class F) fly ash is preferred over high-calcium content (Class C) fly ash. This preference is due to Class F fly ash containing a high amount of silica and alumina, which are essential for the geopolymerisation process. Conversely, Class C fly ash can lead to the formation of C-S-Hs, which may interfere with the development of the desired aluminosilicate gel network. For this study, Class F fly ash was sourced from Lethabo, a local coal-powered electricity station in South Africa. Fly ash consists of silt- and clay-sized glass particles, with particle sizes ranging from 0.1 to 2 000 µm. Fly ash that meets the criteria of 75% fineness, a loss on ignition of under 4%, and sulphur trioxide (SO_3) content below 3.0% is classified as fine ash according to the standards set by AS 3582.1. The finer particle

size of fly ash enhances its reactivity, increases the surface area, and improves the packing efficiency in the binder paste (Olivia, 2011). The chemical composition of fly ash was determined using the XRF technique, as detailed in Table 3.1. The mineralogical phase composition of fly ash was analysed using a PANalytical diffractometer. The XRD pattern obtained from the fly ash analysis showed distinct peaks corresponding to the presence of crystalline phases of quartz (SiO_2) and mullite ($Al_{4.68}Si_{1.32}O_{9.66}$). Other minerals, such as magnetite ($Fe_{24}O_{32}$) and marokite ($Ca_4Mn_8O_{16}$), were also present, although they were not as prominent. The presence of amorphous aluminosilicate phases in fly ash is indicated by the broad hump visible between 15 and 35 degrees. A significant amount of the amorphous aluminosilicate phase is primarily located in the outer layer of the fly ash spheres, which suggests that the outer surface of the fly ash particles contains a higher concentration of amorphous material. Quartz is predominantly found in the intermediate layer, while mullite is concentrated in the inner core of the particles.

Table 3.1: Chemical composition of the raw materials (percentage)

Oxides	Fly ash (%)	GGBS (%)	RHA (%)	GWP (%)	SF (%)
SiO_2	54.33	37.03	89.20	83.21	97.56
Al_2O_3	32.49	13.39	0.37	3.72	0.28
CaO	4.22	36.62	0.73	10.73	1.04
Fe_2O_3	3.34	0.61	0.60	1.97	0.12
MgO	0.92	8.00	1.53	1.09	0.29
TiO_2	1.64	0.63	0.03	0.20	-
MnO	0.04	0.87	0.14	0.04	-
Na_2O	1.83	0.23	0.10	3.52	0.23
K_2O	0.71	1.11	1.71	0.22	0.48
P_2O_5	0.52	-	1.08	0.06	-
LOI	0.56	0.19	3.88	4.55	-

A blend of fly ash and GGBS was also used as precursor material in the first and second phases of the study. Fly ash is low in calcium and highly amorphous, which makes it slower to react under ambient curing. GGBS is rich in calcium, which accelerates geopolymerisation and early strength development. Blending them creates a synergistic effect that improves both early and long-term strength. Moreover, adding slag to fly ash-based geopolymer mortar, even in small amounts, reduces the need for high-temperature curing. This is because the high calcium oxide content in the GGBS activates the formation of C-S-H gel, which improves strength and accelerates setting time, even when

the mortar is cured at ambient temperatures (Sunarsih et al., 2023). This study therefore adopted this blend. GGBS was supplied by AfriSam SA (Pty) Ltd. The average particle size of the GGBS was approximately 138 µm, and its specific surface area was around 0.106 m²/g. The XRD analysis of the GGBS material showed a wide diffusive amorphous hump in the 2θ range between 25° and 35°. This indicates that most of the material was in an amorphous state. Additionally, there were small reflections corresponding to various crystalline phases, including berlinite ($Al_6P_6O_{12}$), andradite ($Ca_{12}Fe_{7.54}Si_{12}O_{48}$), periclase ($Mg_4O_4$), rutile ($Ti_2O_4$), and quartz ($SiO_2$).

3.2.2 Alkaline activators

In preparing GPC, sodium hydroxide and sodium silicate are typically used as the alkali-activator solution. Consequently, at the stage where GPC samples were produced, the conventional alkali-activator mixture (sodium silicate and sodium hydroxide) served as the control sample. However, for geopolymer paste and mortar samples, sodium silicate was not used. The control mixes contained only sodium hydroxide, with no silica sources. The primary objective of the study was to substitute sodium silicate with alternative silica sources; the alkaline activator examined was therefore a combination of sodium hydroxide solution and alternative silica source materials. For each of the three alternative silica sources, three sodium hydroxide solutions were used. Trial mixes were conducted with different ratios of solid sodium hydroxide / silica sources. Ratios from 0 to 0.8 could not produce a sufficient alkaline solution for the production of the geopolymer mortars. The ratios were therefore adjusted, and a range of 1.0 to 1.5 was used at different molarities.

3.2.2.1 Sodium hydroxide

The sodium hydroxide flakes (98% purity) used in this experiment were obtained from Kiran Global in Benoni, Johannesburg. In this study, different sodium hydroxide concentrations of 6 M, 8 M, 10 M, and 12 M were utilised for the sodium hydroxide solution. This range was consistent with that used in previous studies similar to this one (Antoni et al., 2016; Kamseu et al., 2017). Once the sodium hydroxide solution was

prepared, alternative silica sources were immediately added to it. This step was crucial, as it ensured that the alternative silica sources dissolved properly in the alkaline solution. The dissolution process was a critical aspect of the study, as it influenced the interaction between the silica sources and the sodium hydroxide solution.

3.2.2.2 Sodium silicate

Sodium silicate was used as the activator for the GPC. It was supplied by Merck (Pty) Ltd with a composition of 64% water, 8.3% sodium oxide, and 27.7% silica, and was provided in solution form. The solution had a silicate modulus of 3.3 and a solid content of 36%. It was mixed with sodium hydroxide solutions of different concentrations, while the ratio of sodium silicate to sodium hydroxide varied from 0.72 to 4.89.

3.2.2.3 Alternative silica source materials

As a replacement for sodium silicate, alternative silica source materials such as RHA, SF, and GWP were used in the study. The alternative silica source materials were processed in the laboratory and characterised using XRF analysis, as shown in Table 3.1, and XRD analysis (see Appendix A9-A11) as follows:

(a) Rice husk ash (RHA)

RHA was obtained by calcination at 400 °C for one hour in a laboratory electric furnace, at a heating rate of 3 °C per minute, and was then sieved to achieve a particle size of 150 µm. The XRD pattern of RHA (Figure 3.1) revealed crystalline phases, including silicon and graphite. The presence of silicon in the RHA suggests a high content of silica, which is the primary component of RHA. This is expected, as rice husk is rich in silica, and when burned, the organic matter is removed, which leaves behind silica. However, the presence of graphite indicates that some carbonaceous materials remain, which suggests that not all the organic material was completely combusted during the burning process. This residual carbon can affect the properties of the ash, such as its reactivity and the purity of the silica content.

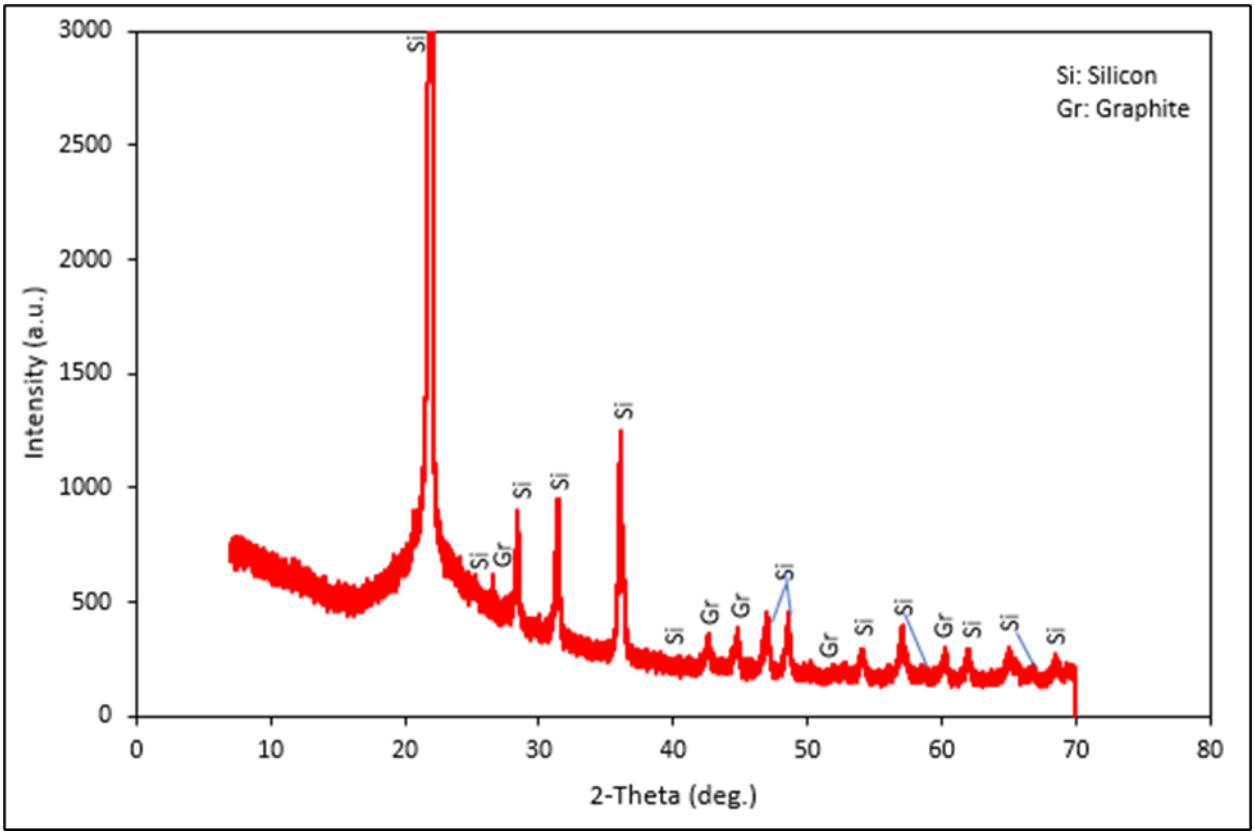

Figure 3.1: XRD pattern of RHA

(b) Glass waste powder (GWP)

Crushed glass waste material was sourced from Consol (Pty) Ltd. The glass waste was washed, milled, and sieved to obtain a particle size of 150 µm, which resulted in GWP. The XRD analysis of GWP (Figure 3.2) primarily revealed a crystalline phase, which showed minerals such as quartz (SiO_2), pigeonite $(Ca,Mg,Fe)(Mg,Fe)Si_2O_6$, and dolomite $(CaMg(CO_3)_2)$. The presence of quartz suggests that the GWP contains significant amounts of silica in a crystalline form. Pigeonite indicates that the glass may have originated from a material that contained components formed under high-temperature conditions, such as volcanic glass or certain types of manufactured glass that incorporate such minerals. Lastly, the presence of dolomite suggests that the GWP included carbonate materials, which implies that the raw materials used in the glass production process may have included dolomite.

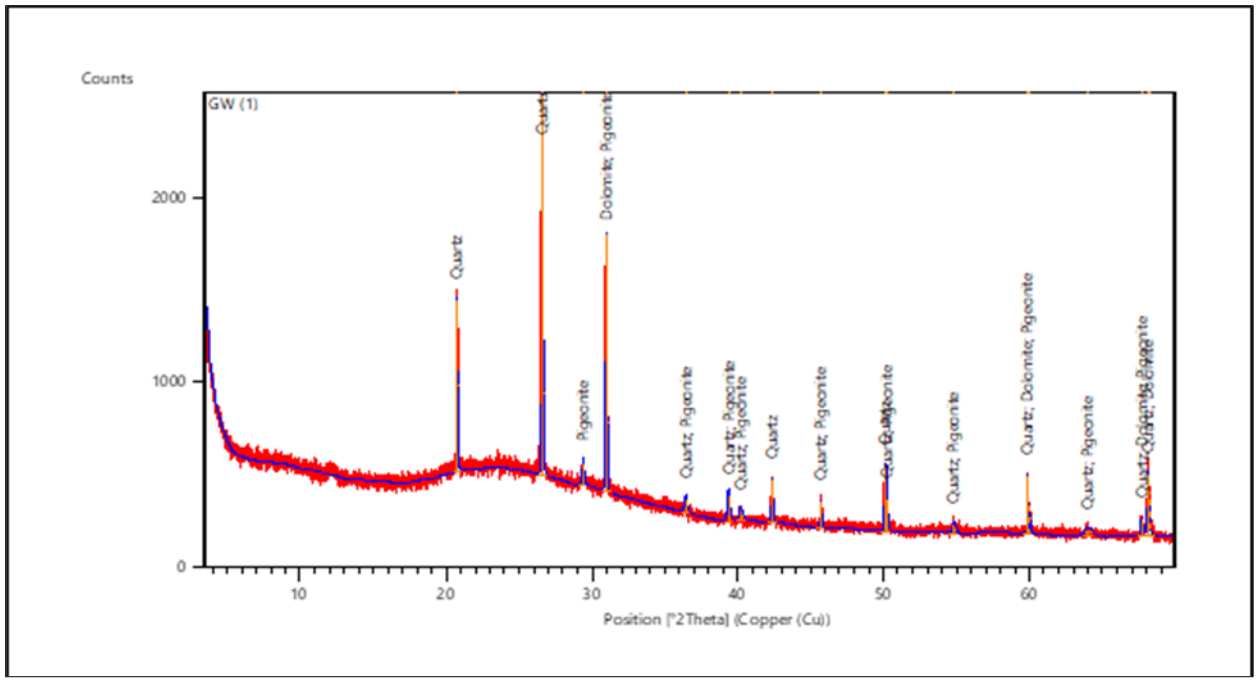

Figure 3.2: XRD pattern of GWP

(c) Silica fume (SF)

SF was obtained from Mapei South Africa Pty (Ltd) and was used without any pretreatment. This SF is a dark grey powder composed of amorphous silica in the form of spherical submicron-sized granules. The SF particles are extremely fine, with over 95% of them being smaller than 1 µm. The specific gravity of the SF is 2.2 g/cm³. Particle size plays a significant role both physically and chemically in concrete. Physically, the small particles fill the gaps between cement particles, while chemically, they undergo a pozzolanic reaction that enhances the concrete's mechanical strength (Mapei, 2023). The XRD pattern for SF shows a broad hump in the 2θ range between 15° and 30°, which indicates the amorphous phase in the structure. SF is primarily composed of amorphous silicon dioxide. This amorphous nature is responsible for its high reactivity. However, the pattern also contains some crystalline phases in addition to the predominantly amorphous phase. Silicon (Si_8), magnesioferite ($MgFe_2O_4$), and jadeite ($NaAlSi_2O_6$) are the minerals present in the crystalline phase of the structure.

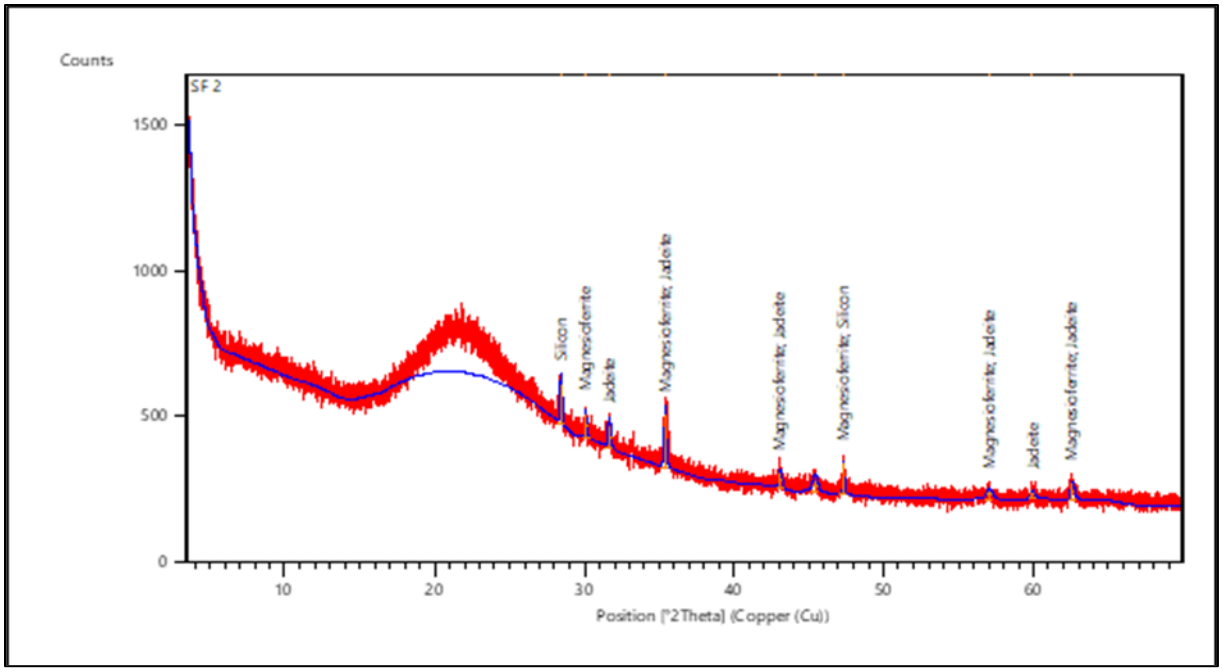

Figure 3.3: XRD pattern of SF

3.2.4 Aggregates

This study utilised both coarse and fine aggregates. Fine aggregate, specifically silica sand, was obtained from Sallies Silica (Pty) Ltd, while coarse aggregate was sourced from a local quarry in the Free State province. The silica sand sizes ranged from 0.6 to 1.8 mm. An optimal mix combination of fine, medium, and coarse silica sand was used as graded standard sand to prepare the mortar mixtures for compressive strength tests (Ekolu, 2014). The silica sand had a fineness modulus of 2.50 and a water absorption rate of 1.17%. The sand was categorised as fine (0 to 0.6 mm), medium (0.4 to 0.8 mm), and coarse (0.8 to 1.8 mm), as shown in Table 3.2. A well-graded mix of silica sand enhances workability by allowing smaller particles to fill the voids between larger particles, which results in a more cohesive and workable mix. Consequently, based on the study by Naghizadeh and Ekolu (2019), the proportions of 3, 1, and 4 were adopted in the order of fine, medium, and coarse respectively. The coarse aggregate used was crushed granite stones, incorporated into the final GPC mix (Phase 2 of the study). Granite is highly durable and resistant to weathering, which makes it suitable for use in various

environmental conditions. The aggregate was provided in 19 mm-sized stones, as adopted from similar studies (Hardjito, 2005; Naghizadeh, 2019).

Table 3.2: Fine aggregate grading

Grading	Fine	Medium	Coarse
Proportion (%)	37.5	12.5	50
Particle size (mm)	0 - 0.6	0.4 - 0.85	0.8 - 1.8

3.2.5 Admixture

A polycarboxylate-ether–based superplasticizer, SikaPlast 220VX, was incorporated into selected mixes to evaluate its influence on the workability of geopolymer concrete. Although originally formulated for Portland cement systems, the admixture was tested in this study to assess its behaviour in highly alkaline geopolymer environments. Previous research has shown that adding a high-range water-reducing admixture at dosages of up to approximately 2% of the fly ash mass can improve the workability of fresh geopolymer concrete (GPC) with minimal impact on the compressive strength of the hardened material (Triwulan et al., 2016). In this research, the solid-to-liquid ratio was adjusted to achieve optimal workability and strength in mortar samples, whereas the superplasticizer was used specifically for the concrete samples.

SikaPlast 220VX, sourced from SIKA S.A. (Pty) Ltd, Gauteng, was added only to the concrete mixtures (Phase 2 of the study). During mixing, it became evident that the concrete was excessively dry, which necessitated the addition of the superplasticizer. A dosage of approximately 2.9% by fly ash mass was added gradually until a workable consistency was achieved. This proportion resulted in acceptable workability, as verified by the slump test (see Section 3.5.1.2). The superplasticizer conforms to ASTM C494-12 (2012) requirements for Type A and Type F admixtures.

3.3 Preparation of the alkali activator solution and the hydrothermal process

The mass of sodium hydroxide solids in a solution depends on its concentration, which is expressed in molarity (M). For example, an 8 M sodium hydroxide solution contains 320 g of sodium hydroxide solids (in flakes or pellet form) per litre of solution, calculated as 8 x

40 = 320 g. The mass of sodium hydroxide solids constitutes only a fraction of the total mass of the sodium hydroxide solution, with water being the major component. Tables 3.3 to 3.5 provide the mixture proportions of the alkali-activator solution for different molarities, with materials measured in grams. To prepare 1 l of a 1 M sodium hydroxide solution, 40 g of solid sodium hydroxide was dissolved in 100 ml of tap water.

The sodium silicate activator was used as the control mix for the GPC binders. However, in this section, the focus is on the preparation of the alternative alkaline activator. The preparation of the alternative alkali-activator was conducted using a ratio of silica source to sodium hydroxide. The varying ratios chosen were 1, 1.1, 1.2, 1.3, 1.4, and 1.5, with different sodium hydroxide concentrations of 6 M, 8 M, 10 M, and 12 M, as shown in Tables 3.3 to 3.5. The following process was then conducted:

a) Sodium hydroxide flakes were dissolved in tap water to produce a solution of varying concentrations.
b) Once the sodium hydroxide solution was prepared, the silica sources were stirred into the solution.
c) This solution was placed in an oven at 100 °C for two hours and stirred for 10 seconds at 15-minute intervals. During the heat treatment in the oven, the chemical reaction of the solution with SF was accelerated more than in the other solutions, which resulted in bubbling, as shown in Figure 3.1B.
d) The final product obtained was a thick gel or a viscous liquid.

The gels were filtered into glass containers using a funnel and domestic chlorine-free filter paper for 24 hours at room temperature (see Figure 3.2B). This filtration was necessary to remove any undissolved solids or impurities that might be present after heating in the oven in order to ensure a uniform and consistent solution for accurate results regarding the performance of the GPC. Only about one-third of the solution was filtered. It is important to consider this factor for an accurate mix design. During the filtration process, some solutions experienced precipitation, which led to the crystallisation of the solution (see Figure 3.3). This could have been due to changes in temperature, pressure, or chemical reactions. The crystallised solutions had to be discarded and redone to achieve an uncontaminated solution that could lead to better mechanical properties and durability.

Table 3.3: Mix design for the alkali-activator solution using molarity of 6 M

Mix ID	Silica source / NaOH ratio	Silica source (g)	NaOH (g)	Water (g)	Alkali-activator produced (g)	Alkali-activator used (g)
CONTROL-6M	0	0	69	265	334	161
GWP-6M-1.0	1	69	69	265	403	161
GWP-6M-1.1	1.1	76	69	265	410	161
GWP-6M-1.2	1.2	82	69	265	416	161
GWP-6M-1.3	1.3	89	69	265	423	161
GWP-6M-1.4	1.4	96	69	265	430	161
GWP-6M-1.5	1.5	103	69	265	437	161
RHA-6M-1.0	1	69	69	265	403	161
RHA-6M-1.1	1.1	76	69	265	410	161
RHA-6M-1.2	1.2	82	69	265	416	161
RHA-6M-1.3	1.3	89	69	265	423	161
RHA-6M-1.4	1.4	96	69	265	430	161
RHA-6M-1.5	1.5	103	69	265	437	161
SF-6M-1.0	1	69	69	265	403	161
SF-6M-1.1	1.1	76	69	265	410	161
SF-6M-1.2	1.2	82	69	265	416	161
SF-6M-1.3	1.3	89	69	265	423	161
SF-6M-1.4	1.4	96	69	265	430	161
SF-6M-1.5	1.5	103	69	265	437	161

Table 3.4: Mix design for the alkali-activator solution using molarity of 8 M

Mix ID	Silica source / NaOH ratio	Silica source (g)	NaOH (g)	Water (g)	Alkali-activator produced (g)	Alkali-activator used (g)
CONTROL-8M	0	0	87	246	333	161
GWP-8M-1.0	1	87	87	246	420	161
GWP-8M-1.1	1.1	96	87	246	429	161
GWP-8M-1.2	1.2	105	87	246	438	161
GWP-8M-1.3	1.3	114	87	246	447	161
GWP-8M-1.4	1.4	122	87	246	455	161
GWP-8M-1.5	1.5	131	87	246	464	161
RHA-8M-1.0	1	87	87	246	420	161
RHA-8M-1.1	1.1	96	87	246	429	161
RHA-8M-1.2	1.2	105	87	246	438	161
RHA-8M-1.3	1.3	114	87	246	447	161
RHA-8M-1.4	1.4	122	87	246	455	161
RHA-8M-1.5	1.5	131	87	246	464	161
SF-8M-1.0	1	87	87	246	420	161
SF-8M-1.1	1.1	96	87	246	429	161
SF-8M-1.2	1.2	105	87	246	438	161
SF-8M-1.3	1.3	114	87	246	447	161
SF-8M-1.4	1.4	122	87	246	455	161
SF-8M-1.5	1.5	131	87	246	464	161

Table 3.5: Mix design for the alkali-activator solution using molarity of 10 M

Mix ID	Silica source / NaOH ratio	Silica source (g)	NaOH (g)	Water (g)	Alkali-activator produced (g)	Alkali-activator used (g)
CONTROL-10M	0	0	105	229	334	161
GWP-10M-1.0	1	105	105	229	439	161
GWP-10M-1.1	1.1	115	105	229	449	161
GWP-10M-1.2	1.2	126	105	229	460	161
GWP-10M-1.3	1.3	136	105	229	470	-
GWP-10M-1.4	1.4	147	105	229	481	161
GWP-10M-1.5	1.5	157	105	229	491	161
RHA-10M-1.0	1	105	105	229	439	161
RHA-10M-1.1	1.1	115	105	229	449	161
RHA-10M-1.2	1.2	126	105	229	460	161
RHA-10M-1.3	1.3	136	105	229	470	161
RHA-10M-1.4	1.4	147	105	229	481	161
RHA-10M-1.5	1.5	157	105	229	491	-
SF-10M-1.0	1	105	105	229	439	161
SF-10M-1.1	1.1	115	105	229	449	161
SF-10M-1.2	1.2	126	105	229	460	161
SF-10M-1.3	1.3	136	105	229	470	-
SF-10M-1.4	1.4	147	105	229	481	-
SF-10M-1.5	1.5	157	105	229	491	-

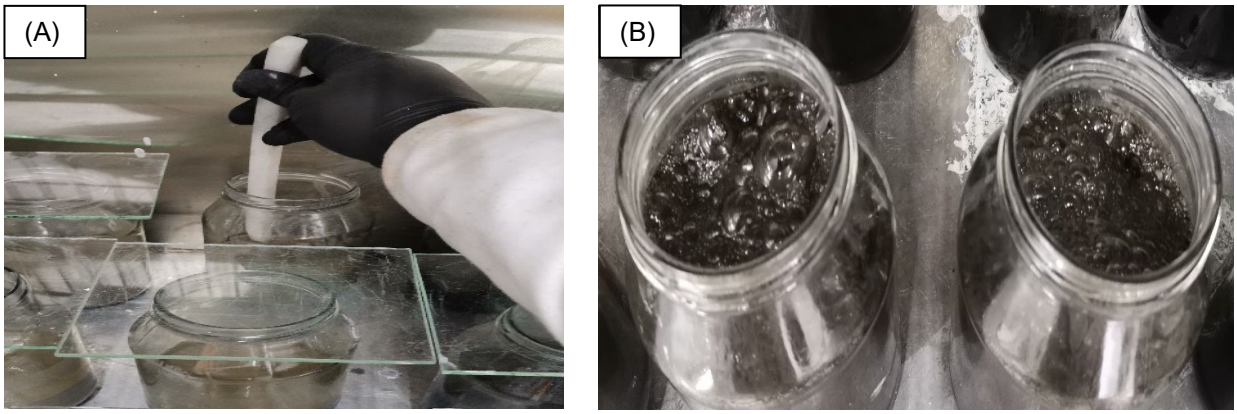

Figure 3.1: (A) Stirring solutions in the oven and (B) SF solution during heat treatment

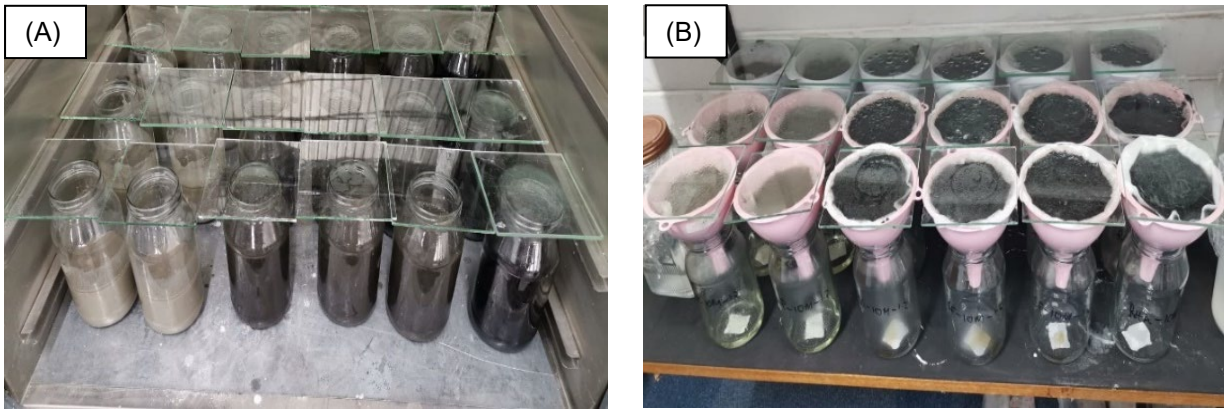

Figure 3.2: (A) Alkali-activator solution in the oven and (B) filtering the alkali-activator solution

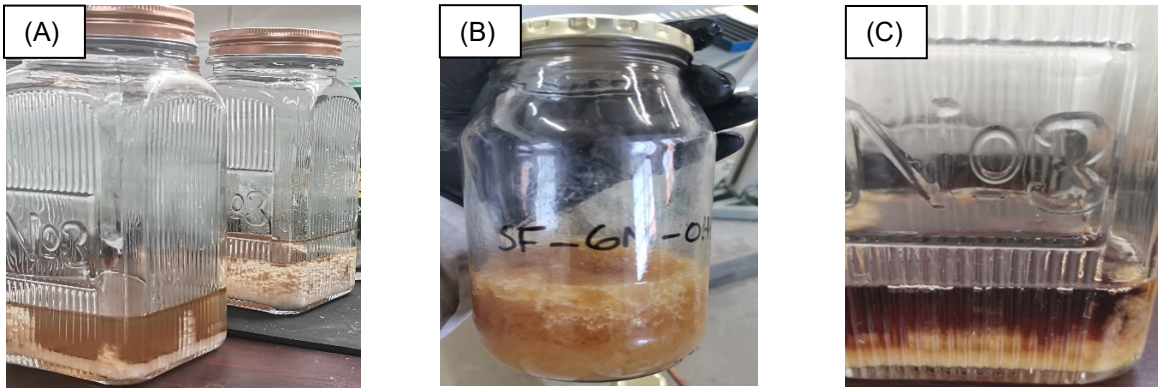

Figure 3.3: Crystallisation of (A) GWP, (B) SF, and (C) RHA

The 12 M activator was initially included in the mix design; however, during the trial period, it was discovered that the 12 M activator was too thick to be filtered effectively. As a result, it was discarded from the mix design. Difficulties were also encountered when filtering the 10 M activator solution with SF, GWP, and RHA for certain silica source / sodium hydroxide ratios. The GWP and SF did not filter through at a ratio of 1.3, and the SF failed to filter at a ratio of 1.4. Additionally, the SF and RHA did not filter at a ratio of 1.5. Given that there was sufficient data for other silica source / sodium hydroxide ratios, the 10 M solution was ultimately used in the mix design. Tables 3.6 to 3.8 clearly show which solutions could be filtered and which could not. During the filtration process, it was observed that the SF was the only alternative silica source that struggled to filter through in most of the mixes. Consequently, in addition to the filtered SF alkaline activator, an unfiltered SF alkaline activator was also prepared to produce geopolymer mortar

samples. This approach also facilitated a better understanding of the differences between the filtered and unfiltered activators.

Table 3.6: Filtration of the alkali-activator solution with GWP

Molarity	Solid silica source / sodium hydroxide ratio					
	1.0	1.1	1.2	1.3	1.4	1.5
6 M	Filtered	Filtered	Filtered	Filtered	Filtered	Filtered
8 M	Filtered	Filtered	Filtered	Filtered	Filtered	Filtered
10 M	Filtered	Filtered	Filtered	Not filtered	Filtered	Filtered
12 M	Not filtered	Not filtered	Not filtered	Not filtered	Not filtered	Not filtered

Table 3.7: Filtration of the alkali-activator solution with SF

Molarity	Solid silica source / sodium hydroxide ratio					
	1.0	1.1	1.2	1.3	1.4	1.5
6 M	Filtered	Filtered	Filtered	Filtered	Filtered	Filtered
8 M	Filtered	Filtered	Filtered	Filtered	Filtered	Filtered
10 M	Filtered	Filtered	Filtered	Not filtered	Not filtered	Not filtered
12 M	Not filtered	Not filtered	Not filtered	Not filtered	Not filtered	Not filtered

Table 3.8: Filtration of the alkali-activator solution with RHA

Molarity	Solid silica source / sodium hydroxide ratio					
	1.0	1.1	1.2	1.3	1.4	1.5
6 M	Filtered	Filtered	Filtered	Filtered	Filtered	Filtered
8 M	Filtered	Filtered	Filtered	Filtered	Filtered	Filtered
10 M	Filtered	Filtered	Filtered	Filtered	Filtered	Not Filtered
12 M	Not filtered	Not filtered	Not filtered	Not filtered	Not filtered	Not filtered

3.3.1 pH measurement of the alkali-activator solution

Measuring the pH of the alternative alkali-activator solutions was important for understanding the behaviour of different silica sources. It was necessary to ensure that the activator was alkaline enough to initiate the geopolymerisation process. Additionally, pH measurements helped in assessing the fresh properties, specifically the setting time and workability of the mortars. Higher alkalinity can speed up the reaction, which will lead to faster setting, including instances of flash setting observed in some of the trial mixes in this study.

The following method was used to measure the pH of the alternative alkaline activators: After filtering the activator solution, the portion intended to produce geopolymer mortar samples was measured. The remaining solution was used for pH measurement. This

leftover solution, corresponding to different silica sources at varying molarities and silica / sodium hydroxide ratios, was poured into small plastic containers and labelled accordingly.

The pH meter calibration was carried out to ensure accurate and reliable pH measurements. Standard buffer solutions with pH values of 4, 7, and 10 were used for this calibration. The pH meter was first rinsed with distilled water to eliminate any residue from previous measurements. The electrodes were then immersed in the different solutions, and the pH readings were recorded. The results are discussed in Chapter 4.

3.4 Sample preparation

3.4.1 Mortar samples

During the trial period, the L/S ratio was set at 0.5, based on previous research (Naghizadeh & Ekolu, 2018; 2019; 2022). However, this L/S ratio resulted in flash setting of some mixtures, particularly when using SF and RHA in the mix. To mitigate the problem of flash setting in fly ash-based mixtures containing RHA, SF, and GWP, the L/S ratio was reduced. Lowering the L/S ratio meant using less water in the mix, which helped to control the cementitious reaction, slow down the setting time, and maintain workability. In this case, adjusting the L/S ratio to 0.36 served as a balance between achieving sufficient strength development and avoiding flash setting in the mixture.

In the first phase, two sets (Set A and Set B) of different mortar mixtures were prepared by varying the silica sources / sodium hydroxide ratio and alkali-activator/binder ratio. The Set A mix contained a fly ash precursor, and the samples were used to determine the hardened properties of geopolymer mortar mixtures. The Set B mix contained fly ash / GGBS, and the samples were used to determine the fresh properties of geopolymer mortar mixtures (the Set B mix was also cast into moulds and tested for compressive strength). The mixes were prepared at a constant aggregate/binder ratio of 2.25, as based on similar previous studies (Naghizadeh & Ekolu, 2018; Kawalu et al., 2022).

In preparing the geopolymer mortar samples, the dry ingredients were first mixed in a mortar mixer (shown in Figure 3.4) at a low speed of 150 rpm for one minute.

Figure 3.4: Mortar mixing

3.4.1.1 Effect of silica source / NaOH ratio on the compressive strength

The alkali-activated solution was then added to the dry ingredients, and the mixture was further mixed for one minute at low speed, followed by an additional minute at a high speed of 400 rpm. The resulting mixture was initially used to investigate the setting time and flow workability measurements. Once these measurements were conducted, the same mixing procedure was followed for the compressive strength testing. The resulting mixture was cast into 50 x 50 mm moulds and compacted using 32 hand strokes per layer, followed by levelling the surface for a smooth finish. After casting, the specimens were covered with plastic film to prevent moisture loss and were immediately oven-cured at 80 °C for 24 hours (some specimens were ambient-cured and analysed at a later stage for microstructural studies). Following demoulding, the samples were cured at room temperature for an additional six days. The compressive strength of the samples was tested after seven days of curing in accordance with SANS 5863:2006. The samples were tested after seven days because geopolymer mortar tends to achieve significant strength within the first few days of curing. Testing at this interval provided quicker feedback than waiting 28 days, which allowed for a more efficient determination of the optimum mix design for different source materials.

3.4.1.2 Effect of NaOH concentration on the compressive strength

The following formula was used for the mix design of the geopolymer mortar samples in Tables 3.9 to 3.11:

3 cubes = 350 g fly ash + 788 g aggregate (C+M+F) + 161 g alkali-activator

Table 3.9: Mix design for fly-ash based geopolymer mortars using molarity of 6 M

Mix ID	ID of waste-based alkaline activator	Weight of waste-based alkaline activator (g)	NaOH flakes (g)	Silica source powder (g)	Water (g)	Concentration of NaOH	Fly ash (g)	Aggregates (g)		
								C*	M*	F*
CONTROL-6M	CTRL-6M-0.0	161	69	-	246	6M	350	394	98	296
M-GWP-6M	GWP-6M-1.0	161	69	69	246	6M	350	394	98	296
	GWP-6M-1.1	161	69	76	246	6M	350	394	98	296
	GWP-6M-1.2	161	69	82	246	6M	350	394	98	296
	GWP-6M-1.3	161	69	89	246	6M	350	394	98	296
	GWP-6M-1.4	161	69	96	246	6M	350	394	98	296
	GWP-6M-1.5	161	69	103	246	6M	350	394	98	296
M-RHA-6M	RHA-6M-1.0	161	69	69	246	6M	350	394	98	296
	RHA-6M-1.1	161	69	76	246	6M	350	394	98	296
	RHA-6M-1.2	161	69	82	246	6M	350	394	98	296
	RHA-6M-1.3	161	69	89	246	6M	350	394	98	296
	RHA-6M-1.4	161	69	96	246	6M	350	394	98	296
	RHA-6M-1.5	161	69	103	246	6M	350	394	98	296
M-SF-6M	SF-6M-1.0	161	69	69	246	6M	350	394	98	296
	SF-6M-1.1	161	69	76	246	6M	350	394	98	296
	SF-6M-1.2	161	69	82	246	6M	350	394	98	296
	SF-6M-1.3	161	69	89	246	6M	350	394	98	296
	SF-6M-1.4	161	69	96	246	6M	350	394	98	296
	SF-6M-1.5	161	69	103	246	6M	350	394	98	296

*C: coarse sand, M: medium silica sand, F: fine silica sand

Table 3.10: Mix design for fly-ash based geopolymer mortars using molarity of 8 M

Mix ID	ID of waste-based alkaline activator	Weight of waste-based alkaline activator (g)	NaOH flakes (g)	Silica source powder (g)	Water (g)	Concen-tration of NaOH	Fly ash (g)	Aggregates (g)		
								C	M	F
CONTROL-8M	CTRL-8M-0.0	161	87	-	246	8M	350	394	98	296
M-GWP-8M	GWP-8M-1.0	161	87	87	246	8M	350	394	98	296
	GWP-8M-1.1	161	87	96	246	8M	350	394	98	296
	GWP-8M-1.2	161	87	105	246	8M	350	394	98	296
	GWP-8M-1.3	161	87	114	246	8M	350	394	98	296
	GWP-8M-1.4	161	87	122	246	8M	350	394	98	296
	GWP-8M-1.5	161	87	131	246	8M	350	394	98	296
M-RHA-8M	RHA-8M-1.0	161	87	87	246	8M	350	394	98	296
	RHA-8M-1.1	161	87	96	246	8M	350	394	98	296
	RHA-8M-1.2	161	87	105	246	8M	350	394	98	296
	RHA-8M-1.3	161	87	114	246	8M	350	394	98	296
	RHA-8M-1.4	161	87	122	246	8M	350	394	98	296
	RHA-8M-1.5	161	87	131	246	8M	350	394	98	296
M-SF-8M	SF-8M-1.0	161	87	87	246	8M	350	394	98	296
	SF-8M-1.1	161	87	96	246	8M	350	394	98	296
	SF-8M-1.2	161	87	105	246	8M	350	394	98	296
	SF-8M-1.3	161	87	114	246	8M	350	394	98	296
	SF-8M-1.4	161	87	122	246	8M	350	394	98	296
	SF-8M-1.5	161	87	131	246	8M	350	394	98	296

Table 3.11: Mix design for fly-ash based geopolymer mortars using molarity of 10 M

Mix ID	ID of waste-based alkaline activator	Weight of waste-based alkaline activator (g)	NaOH flakes (g)	Silica source powder (g)	Water (g)	Concen-tration of NaOH	Fly ash (g)	Aggregates (g)		
								C	M	F
CONTROL-10M	CTRL-10M-0.0	161	105	-	246	10M	350	394	98	296
M-GWP-10M	GWP-10M-1.0	161	105	105	246	10M	350	394	98	296
	GWP-10M-1.1	161	105	115	246	10M	350	394	98	296
	GWP-10M-1.2	161	105	126	246	10M	350	394	98	296
	GWP-10M-1.3	161	105	136	246	10M	350	394	98	296
	GWP-10M-1.4	161	105	147	246	10M	350	394	98	296
	GWP-10M-1.5	161	105	157	246	10M	350	394	98	296
M-RHA-10M	RHA-10M-1.0	161	105	105	246	10M	350	394	98	296
	RHA-10M-1.1	161	105	115	246	10M	350	394	98	296
	RHA-10M-1.2	161	105	126	246	10M	350	394	98	296
	RHA-10M-1.3	161	105	136	246	10M	350	394	98	296
	RHA-10M-1.4	161	105	147	246	10M	350	394	98	296
	RHA-10M-1.5	161	105	157	246	10M	350	394	98	296
M-SF-10M	SF-10M-1.0	161	105	105	246	10M	350	394	98	296
	SF-10M-1.1	161	105	115	246	10M	350	394	98	296
	SF-10M-1.2	161	105	126	246	10M	350	394	98	296
	SF-10M-1.3	161	105	136	246	10M	350	394	98	296
	SF-10M-1.4	161	105	147	246	10M	350	394	98	296
	SF-10M-1.5	161	105	157	246	10M	350	394	98	296

The study aimed to determine the optimal mix proportions for replacing sodium silicate with alternative silica sources, with the focus on achieving the best compressive strength performance. To gain a better understanding, additional mixes not initially included in the design were also examined. Specifically, mixes with 4 M, 5 M, and 7 M concentrations for various silica sources were tested at a silica source / sodium hydroxide ratio of 1.3, as shown in Table 3.12. This evaluation was conducted to provide a clear indication of

compressive strength development in this type of geopolymer, using a consistent average ratio.

Table 3.12: Mix design of additional mixes

Mix ID	Silica source / NaOH ratio	Weight of waste-based alkaline activator (g)	NaOH (g)	Silica source (g)	Water (g)	Concentration of NaOH	Fly ash (g)	Aggregates (g)		
								C	M	F
M-GWP-4M	1.3	161	48	62	285	4M	350	394	98	296
M-RHA-4M	1.3	161	48	62	285	4M	350	394	98	296
M-SF-4M	1.3	161	48	62	285	4M	350	394	98	296
M-GWP-5M	1.3	161	59	76	275	5M	350	394	98	296
M-RHA-5M	1.3	161	59	76	275	5M	350	394	98	296
M-SF-5M	1.3	161	59	76	275	5M	350	394	98	296
M-GWP-7M	1.3	161	78	102	255	7M	350	394	98	296
M-RHA-7M	1.3	161	78	102	255	7M	350	394	98	296
M-SF-7M	1.3	161	78	102	255	7M	350	394	98	296

3.4.2 Optimum proportions

The samples were labelled to differentiate them during testing; for example, SF-6M-1.3 represents the components of the sample mix (SF – silica fume, 6M – NaOH concentration, 1.3 – optimum silica source / sodium hydroxide ratio). The “M” in front of the Mix ID name is an abbreviation for mortar. Based on the compressive strength test results for all mixes, SF-10M-1.2 achieved the highest compressive strength. However, using a 10 M solution to produce geopolymer mortars would be costly. SF-6M-1.3 was therefore chosen as the optimal mix because it had the lowest molarity while still providing high compressive strength. For ease of reference, the optimal activator mix was named “alternative activator”.

3.4.2.1 Effect of GGBS ratio on the compressive strength

A blend of fly ash and GGBS was used as precursor material in the first and second phases of the study to enhance the workability of the mixes, as mentioned in Section

3.2.1. At this stage of the study, it was important to evaluate how the incorporation of GGBS would affect the mechanical properties of the geopolymer samples. The same mixing procedure outlined previously in this section was followed; however, the dry ingredients (GGBS, fly ash, and aggregates) were activated using an alternative activator. Both the fresh and hardened properties were evaluated using this mix. The proportion of GGBS in the binder varied at 0%, 20%, 30%, and 40%, as shown in Table 3.13. According to the literature review in Chapter 2, this is the acceptable range for GGBS incorporation in fly ash-based geopolymer mortars. The literature indicated that incorporating GGBS beyond 40% negatively affects the compressive strength of the geopolymer; the range was thus limited to 40% in this study.

Table 3.13: Mix design for fly ash/GGBS geopolymer pastes/mortars

Mix ID	Silica source / NaOH ratio	SF (g)	NaOH (g)	Water (g)	SF-based alkali-activator (g)	L/S ratio	Fly ash (g)	GGBS (g)	Aggregates (g)		
									C	M	F
0% GGBS	1.3	0	33	128	161	0.36	350	0	394	98	295
20% GGBS	1.3	43	33	128	204	0.36	280	70	394	98	252
30% GGBS	1.3	43	33	128	204	0.36	245	105	394	98	252
40% GGBS	1.3	43	33	128	204	0.36	210	140	394	98	252

Once the optimum proportions for Set A and Set B mortar mixes were established, additional mortar samples were prepared to determine the effect of GGBS under different curing conditions. These samples were subjected to both ambient and oven curing for seven days.

Specifically, the investigation compared mixes with different properties such as the following:

- A control mix (only a sodium hydroxide activator) that was ambient-cured;
- A 0% GGBS mix (alternative activator but no GGBS) that was oven-cured; and
- An optimum GGBS mix (alternative activator with optimum GGBS percentage) that was both oven-cured and ambient-cured.

The samples were tested for compressive strength to evaluate their mechanical performance. They were also subjected to SEM analysis to study their microstructural characteristics and to understand how GGBS and curing conditions influence the geopolymerisation process.

3.4.3 Concrete samples

In the second phase, further investigations were conducted on ambient-cured concrete samples made from fly ash / GGBS activated with an alternative activator and the addition of a superplasticiser. The inclusion of superplasticisers enhances the workability of the geopolymer paste by improving its plastic and hardening properties, which results in higher compressive strength. Compressive strength is influenced by the pore structure of the hardened superplasticiser paste, mainly comprising micropores, which leads to a denser structure. In the mortar mixes, no superplasticiser was added because mortar mixes primarily consist of fine aggregates, binder, and water. This composition typically provides sufficient workability without the need for additional admixtures such as superplasticisers. In contrast, concrete contains both coarse and fine aggregates, along with binder and water. The inclusion of coarse aggregates often reduces the workability of the mix, especially with lower water-to-binder ratios required for higher strength. A control mix, obtained from a similar study, activated with a higher molarity of 8 M sodium silicate, was used as the acceptable standard. This stage of testing was designed to evaluate the performance of blended fly ash / GGBS GPC activated with an alternative activator. The optimum GGBS proportion was determined based on the fresh and hardened properties examined in the first phase of the study, which included tests for setting time, flow workability, and compressive strength of the fly ash / GGBS geopolymer mortars. The compressive strength of fly ash / GGBS was measured using proportions of 0%, 20%, 30%, and 40% GGBS (see Appendix A). Although 40% yielded the highest compressive strength, the literature review in Section 2.3.3 indicated that this ratio might reduce some of the long-term benefits associated with fly ash, such as improved durability. The incorporation of 30% GGBS was thus chosen to achieve a balance between strength, workability, and durability.

The GPC was produced using a design method that involves combining dry ingredients with alkaline solutions, as shown in Table 3.14. The aggregates used for the GPC samples included 19 mm granite stones as coarse aggregate and silica sand as fine aggregate. An aggregate-to-fly ash ratio of 2.25 was maintained during the production of the GPC samples. Initially, dry ingredients, such as aggregates and fly ash / GGBS, were stirred for three minutes until well blended. After the initial mixing of the dry materials, the alternative activator was slowly poured into the mixture. A superplasticiser of 130 g was also added during mixing. Following the addition of the alternative activator and superplasticiser, the mixture was mixed for an additional four minutes. The resulting mixture was dark grey and cohesive. A slump test was conducted immediately after mixing. After conducting the slump test, the mixture was poured into 100 x 100 mm cubic moulds. The GPC specimens were then cured in ambient conditions at 20±2 °C. Ambient curing was chosen for the concrete samples (instead of oven curing) as it is more practical, especially for larger structural applications. GPC samples can achieve sufficient strength and durability through ambient curing due to the presence of coarse aggregates, which contribute to the internal curing process.

Table 3.14: Mix design for ambient-cured concrete samples

Mix no.	Alkali-activator			Total activator (g)	70% fly ash (g)	30% GGBS (g)	Super-platiciser (g)	Aggregate (g)	
	SF-based alkali-activator (g)	Sodium silicate (g)	8 M NaOH (g)					C	F
1	0	2 434	1 466	3 900	4 550	1 950	130	16 250	14 623
2	3 900	0	0	3 900	4 550	1 950	130	16 250	14 623

3.5 Characterisation techniques

In this study, various tests were conducted on geopolymer mortar and concrete samples to evaluate their fresh and hardened properties. For the mortar samples, tests were performed to assess flow workability, setting time, and compressive strength. In contrast, the concrete samples were primarily tested for compressive strength and durability. All

laboratory tests adhered to ASTM and SANS standards. The following sections detail the specific test procedures used in this research, with durability discussed in Section 3.7.

3.5.1 Workability measurement

Workability refers to the ease of working with newly mixed concrete during the processes of handling, placing, compacting, and finishing. In this study, workability was assessed for both mortar and concrete samples. The flow table test was used to measure workability for the mortar samples, while the slump test was employed for the concrete samples in accordance with ASTM standards.

3.5.1.1 Mortar samples

The flow workability of fresh mortar was assessed using Set B mortar samples that contained fly ash / GGBS and the alternative activator, as detailed in Section 3.4.1. At this stage, it was important to evaluate the impact of GGBS on the flow workability of fresh geopolymer mortars. The measurement was carried out using the flow table apparatus shown in Figure 3.5, in accordance with ASTM C-230 (2008). The flow test was performed immediately after mixing. The flow of the mix was determined by measuring the diameter of the mortar spread on the flow table along four lines marked on the table surface, using a calliper. This measurement was taken after 25 jolts, as specified in the standard procedure. A minimum of 110 ± 5% was set for the flow workability of the geopolymer mortars. Temperature has a significant impact on the viscosity of the alkali-activation solution; all workability measurements were therefore conducted at room temperature.

Figure 3.5: Flow table apparatus

3.5.1.2 Concrete samples

The workability of fresh GPC was assessed using the slump test in accordance with ASTM C143-12. The slump test is a standard procedure used in concrete construction to evaluate the consistency and workability of freshly mixed concrete. It measures the degree to which a concrete mixture can flow or spread, which is crucial for determining whether the concrete can be easily placed and moulded at a construction site. As outlined in Section 3.4.2, the alternative activator was used to produce the GPC samples. At this stage, various silica source mixes with different proportions had been eliminated, and the alternative activator-based mix was used to evaluate the durability properties. Based on the GGBS proportion results, a mix of 70% fly ash and 30% GGBS was determined to be the most suitable percentage for incorporation into the binder content.

A metal slump cone was used, as shown in Figure 3.6. The cone was placed on level ground and filled with three layers of fresh concrete. Each layer was penetrated 25 times using a steel rod. Once the concrete was compacted, the top was levelled with the same steel rod, and the base of the cone was wiped clean of any spilled concrete. The cone was then pulled up straight without twisting for three to seven seconds. The slump was measured from the top of the mould to the original centre of the concrete.

Figure 3.6: Concrete slump test equipment

3.5.2 Setting time measurement

The setting time behaviour of fresh mortar is crucial as it dictates the time available for transporting, casting, and compacting the GPC. The setting time measurement was conducted on the Set B mortar to assess the effect of GGBS on the setting time of the fresh geopolymer mortar. Measurements were taken immediately after the mixing procedure, using a Vicatronic automatic recording (Vicat) apparatus, as shown in Figure 3.7. This device can determine the initial and final setting times of cement or mortars. The measurement of the setting times of the mortar was performed in accordance with ASTM C-807 (2020).

Figure 3.7: Vicatronic automatic recording apparatus (Vicat)

A layer of geopolymer mortar approximately 20 mm thick was placed in the mould and paddled with a tamper. A total of 14 strokes were applied around the outside of the mould and four strokes to the centre of the specimen. The mortar was levelled with the top of the mould. Then, using the modified Vicat apparatus shown above, the needle was brought into contact with the surface of the mortar, and the setscrew was tightened. The movable indicator was set to the upper zero mark on the scale, or alternatively, an initial reading could be taken. The initial setting time began when the liquid phase was added to the binder and continued until the paste started losing its plasticity. The rod was released quickly by loosening the setscrew to allow the needle to settle for 30 seconds. The penetration of the needle was measured at this time and every 30 minutes thereafter until the needle failed to penetrate to the bottom of the mould. Penetration tests were then conducted every 10 minutes until a penetration of 10 mm or less was achieved. The results were recorded, and by interpolation, the time at which a penetration of 10 mm was obtained was determined. The difference, in minutes, between the time of contact of dry and wet ingredients during the mortar mixing procedure and the time at which a penetration of 10 mm was achieved is the setting time.

3.5.3 Compressive strength test

Compressive strength measures a concrete's ability to withstand axial loads or pressure without failing. It is typically expressed in pounds per square inch or megapascals and is a critical property, especially in structural and load-bearing applications. Compressive strength is often used as an indicator of other mechanical properties of concrete, as several properties, such as tensile strength, flexural strength, and durability, tend to correlate well with the concrete's compressive strength (Olivia, 2011).

3.5.3.1 Mortar samples

Compressive strength testing was performed on the geopolymer mortar samples, each measuring 50 x 50 mm, in accordance with ASTM C109 (2021). The compressive strength results are presented and discussed in detail in Chapter 4. Approximately 63 samples of the Set A mix were tested. The compressive strength test was conducted after the geopolymer mortar samples had been cured for seven days. After casting, the mortar samples were covered with a plastic film to prevent moisture loss. The samples were oven-cured at 80 °C for 24 hours before being demoulded and cured at room temperature for another six days. Compressive strength testing was therefore conducted after the geopolymer mortar samples had been cured for seven days. An Automatic Max testing machine, shown in Figure 3.8, was used to determine the ultimate strength of the geopolymer mortar. Three 50 x 50 mm cube samples were crushed by being subjected to a compressive load at a rate of 180 kN/min, and the load at failure was determined to calculate the compressive strength of the geopolymer mortar. The reported compressive strength values are averages (of at least three) of the results obtained from individual samples.

Figure 3.8: Automatic Max testing machine for compressive strength test

3.5.3.2 Concrete samples

(a) Effect of the curing period on the compressive strength

The 100 x 100 mm cubic samples shown in Figure 3.9 were cured at ambient temperature for three, seven, 28, and 90 days before being crushed. The samples underwent a compressive strength test in accordance with ASTM C109 (2021), and the results are presented and discussed in Chapter 4. After completing the compressive strength test, the samples that were cured for 28 days were prepared for the concrete durability index tests.

Figure 3.9: 100 x 100 ambient-cured GPC samples

3.6 Microstructural studies

In addition to studying the mechanical properties of geopolymer mortars, microstructural and analytical studies were conducted to understand the variation in the hardened properties of fly ash and fly ash / GGBS geopolymer mortars activated with different silica sources. Two techniques were employed for microstructural characterisation: XRD and SEM. These techniques provide insight into the internal structure and composition of the geopolymers. The compressive strength test determines the maximum compressive load that the geopolymer samples can withstand before fracturing. After the Set A mix samples were fractured and the seven-day compressive strength was recorded, the fractured samples were then used for XRD analysis. The samples used for the XRD analysis are shown in Table 3.17.

Both Set A and Set B geopolymer samples were subjected to SEM analysis. For the Set B samples, an unfiltered alternative activator solution was used to thoroughly examine the reaction in the geopolymer matrix. Consequently, different labels were assigned to these samples. The sample label S6-1.3 OF represents (S – silica fume, 6 – 6 M molarity, 1.3 – silica source / NaOH ratio, O – oven-cured, F – filtered activator solution), while 30-7D AU denotes (30-30% GGBS incorporation, 7D – 7 days cured, A – ambient curing condition, U – unfiltered activator solution). Initially, the Set A mix samples were examined to understand the reaction of various alternative silica source materials at different

molarities, specifically focusing on geopolymers activated with 6 M and 8 M sodium hydroxide concentrations. The aim was to ensure that the SEM analysis results aligned with the compressive strength findings. Following this, SEM analysis was conducted on the Set B mix geopolymer mortar samples, as detailed in Table 3.17. The alternative activator mix sample with 30% GGBS incorporation was compared to a sample without GGBS to evaluate the impact of GGBS on geopolymerisation. Additionally, the curing period of this optimal sample was analysed at seven and 28 days for both ambient and oven-cured samples.

Table 3.15: Geopolymer mortar samples used for microstructural studies

Technique	Sample name (Set A)	Silica source	NaoH molarity	Silica source / NaOH ratio	Curing duration	Curing method	Filtered/ Unfiltered
XRD & SEM	S6-1.3 OF	SF	6M	1.3	7 days	Oven	Filtered
	S6-1.3 OU	SF	6M	1.3	7 days	Oven	Unfiltered
	S8-1.3 OF	SF	8M	1.3	7 days	Oven	Filtered
	G6-1.3 OF	GWP	6M	1.3	7 days	Oven	Filtered
	G8-1.3 OF	GWP	8M	1.3	7 days	Oven	Filtered
	R6-1.3 OF	RHA	6M	1.3	7 days	Oven	Filtered
	R8-1.3 OF	RHA	8M	1.3	7 days	Oven	Filtered
	Sample name (Set B)	**Silica source**	**GGBS / fly ash %**	**Silica source / NaOH ratio**	**Curing duration**	**Curing method**	**Filtered/ Unfiltered**
SEM	30-7D OU	SF	30/70	1.3	7 days	Oven	Unfiltered
	00-7D OU	SF	0/100	1.3	7 days	Oven	Unfiltered
	30-7D AU	SF	30/70	1.3	7 days	Ambient	Unfiltered
	30-28D AU	SF	30/70	1.3	28 days	Ambient	Unfiltered

3.6.1 X-ray diffraction (XRD)

The XRD analysis was first performed to identify the minerals present in the raw materials used to produce geopolymers. This step was crucial for understanding the existing phases before the geopolymerisation process and determining whether these phases changed or remained unchanged after the process was complete. For the geopolymerised samples, about 2 g of sample was used from the fractured samples of compressive strength testing. The solvent extraction method was employed to suspend the geopolymer reaction after seven days, as the XRD analysis would be conducted the

following day. The samples were immersed in 80 ml of acetone for a duration of 30 minutes each. After this process, the geopolymer mortar samples were finely cut using a saw blade, to a thickness of 1 to 2 mm. Proxy samples were used for this analysis. The XRD technique was used to determine the mineralogical composition of crystalline materials. When a crystalline mineral is subjected to X-rays of a specific wavelength, the layers of atoms refract the rays, which produces a pattern of peaks that is unique to the material. The horizontal scale (diffraction angle) of a typical XRD pattern represents crystal lattice spacing, while the vertical scale (peak height) represents diffracted ray intensity. The XRD analysis was completed using a PANalytical Empyrean with a Cu-anode X-ray tube, operating at 45 kV and 40 mA. The configuration employed Bragg-Brentano geometry focused along with a Theta-Theta goniometer. High-Score was used for interpretation, along with the International Centre for Diffraction Data-PDF2 2021 database. Samples were scanned between 3.5° and 70° 2θ.

3.6.2 Scanning electron microscope (SEM)

SEM analysis was conducted on both raw materials and synthesised geopolymers. The analysis was initially performed on the powdered form of the raw alternative silica source materials to examine the characteristics of the particles comprising the raw material. This analysis aids in understanding the material's reactivity both during and after the geopolymerisation process. For the geopolymer samples, the solvent extraction method was used to suspend the geopolymer reaction after seven and 28 days, as the SEM analysis would be conducted the following day. The samples were immersed in 80 ml of acetone for a duration of 30 minutes each. After this process, the geopolymer mortar samples were finely cut to a thickness of 1 to 2 mm using a saw blade. Proxy samples were placed on double-sided carbon tape on a glass section and carbon coated using a Quorum Q150 sputter coater to prevent dust from contaminating the SEM machine and causing blemished or tarnished images. The accelerating voltage of the filament was set to 20 kV. This analysis was also conducted to understand the bonding and the extent of geopolymerisation using various silica sources. A magnification range of x100 to x1500 was used to achieve better surface topography analysis of the samples with optimal spatial resolution.

3.7 Durability

Durability index tests were employed to measure the durability characteristics of GPC prepared with an alternative activator mix. This approach consisted of three tests: oxygen permeability, water sorptivity, and chloride conductivity. The oxygen permeability index and chloride conductivity are test methods that have been shown to be effective in characterising concrete durability, according to the study by Beushausen and Alexander (2008). These methods are comparable to other internationally accepted methods for concrete durability characterisation and can provide valuable information about the material properties of concrete. The tests were performed in accordance with the Durability Index Testing Manual and SANS.

Concrete samples of varying mixes containing 0%, 20%, 30%, and 40% GGBS were cured for 28 days. The samples were cored and cut into 70 x 30 mm circular discs, as shown in Figure 3.10 (SANS 3001-CO3-1:2015; Alexander et al., 2018). A reference mix from a related study was used for comparison. In the related study, nine mixes (13, 16, 20, 34, 39, 53, 58, 77, and 79) were used for durability index testing. These mixes utilised fly ash as the binder material and were activated with a combination of sodium silicate and sodium hydroxide solutions, with no GGBS included. The ratio of sodium silicate to sodium hydroxide ranged from 0.72 to 4.89. Furthermore, these nine mix samples were cured under ambient conditions for a duration of one year (Naghizadeh et al., 2023). Among these mixes, Mix 13 exhibited similar physio-chemical characteristics to the mix used in the current study and achieved a high compressive strength of 70 MPa. Mix 13 was therefore selected as the reference mix for this study.

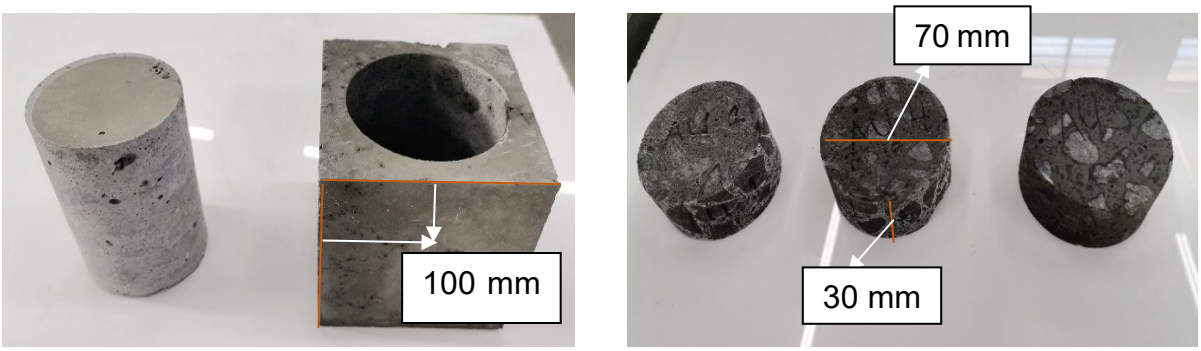

(A) (B)

Figure 3.10: (A) A cored concrete sample and (B) Concrete samples cut into circular discs

3.7.1 Oxygen permeability test

The oxygen permeability test is a method to assess the durability of concrete, particularly its resistance to the penetration of oxygen, which can lead to other forms of deterioration, such as corrosion of steel reinforcement (Salvoldi et al., 2015). The aim of this test is to establish the coefficient of permeability *k* and the average oxygen permeability index. This method is applied to concrete samples prepared by coring and cutting concrete cubes in the laboratory. Four 70 x 30 mm circular discs of the SF-based mix were used for this test. The samples were placed in an oven to dry at 50 °C for seven days before testing. After this period, the samples were placed in a desiccator to cool for two to four hours. Following cooling, the samples were removed from the desiccator, and testing was conducted in accordance with SANS 3001-CO3-2:2015. The thickness and diameter of each sample were measured to an accuracy of 0.02 mm using a Vernier calliper. Permeability cells with a volume of 5 L and a pressure tolerance range of 0 kPa to 120 kPa were used (see Figure 3.11). The average of each set of four readings was calculated and recorded. A sample was placed in the compressible collar within the rigid sleeve, with the exterior face facing downwards. The sample, collar, and rigid sleeve were then positioned on top of the permeability cell to cover the hole. Once the hole was covered, the solid ring and cover plate were placed on top of the collar to ensure that no gaps were visible between the collar and the sleeve. The top screw on the cover plate was tightened to prevent gas leakage. The oxygen inlet and outlet valves were opened, and the valve of the oxygen supply tank was adjusted to between 100 kPa and 120 kPa to allow oxygen to flow through the permeability cell for five seconds. After this interval,

the oxygen outlet valve was closed to ensure that there were no leaks. The pressure in the cell was increased to (100 ± 5) kPa, and the inlet valve was closed. Subsequently, eight readings were recorded at 15-minute intervals until the pressure dropped to (50 ± 2.5) kPa. The readings were recorded using the Observer Ⅱ system, and the data were exported from its application. Once the readings were successfully captured, the oxygen permeability index for each sample was calculated using Excel worksheets. It was noted that the spreadsheet returned a result of “Invalid” for pressures exceeding 105 kPa.

Figure 3.11: Permeability cells for oxygen permeability index testing

3.7.2 Water sorptivity test

The water sorptivity index test assesses the speed at which a wetting front advances through concrete due to capillary suction (Moore et al., 2020). This test also enables the measurement of the water-penetrable porosity of the samples, which is crucial for interpreting the water sorptivity results. While the test is straightforward to perform, it is essential to appropriately pre-condition the samples to ensure a repeatable moisture state at the start of the test.

Three 70 x 30 mm circular disc samples of the same mix as oxygen permeability index were used for this test. The samples were wrapped in 1.5 layers of Sellotape and placed in an oven to dry at 50 °C for 12 hours. After this period, the samples were placed in a

desiccator to cool for two hours. Meanwhile, 10 layers of paper towel were folded and placed on a tray, then saturated with water until it was visible on the top surface. Calcium hydroxide solution was poured onto the paper towels and levelled to eliminate all air bubbles.

The samples were removed from the desiccator, and after 30 minutes, they were weighed to an accuracy of 0.01 g and recorded as the dry mass. The samples were then immediately placed with the outer face on the wet paper towels, and the stopwatches were started. The samples were weighed again after immersion in the solution. They were then gently patted with a damp absorbent paper towel to ensure they were moist but did not have free water on the outer face. The saturated mass was recorded at three-, five-, seven-, nine-, 12-, 16-, 20-, and 25-minute intervals.

Once the last measurement was taken, the stopwatches were stopped, and the samples were placed back in the oven for another 12 hours with the submerged surface facing upwards. After this period, the samples were placed in a vacuum tank at a pressure of 75 to 80 kPa for three hours. The tank was filled with calcium hydroxide solution to cover the samples, as shown in Figure 3.12. The vacuum was re-established to between 75 and 80 kPa for one hour. After one hour, the vacuum was released, and air was allowed to enter for 18 hours.

Following 18 hours of soaking in the solution, the samples were dried and weighed to obtain the vacuum-saturated mass. A standard spreadsheet was developed to perform the calculations, and the sorptivity index was established as the average of the valid individual test determinations.

Figure 3.12: Water sorptivity index samples in a vacuum tank filled with calcium hydroxide solution

3.7.3 Chloride conductivity

Chloride conductivity measures the rate at which chloride ions can penetrate a concrete sample. These ions can enter concrete through various mechanisms, including diffusion and capillary action, potentially leading to the corrosion of steel reinforcement within the concrete (Gouws et al., 2001). Three 70 x 30 mm circular disc samples of the same mix as for the oxygen permeability index and water sorptivity index tests were used for this test. The samples were placed in an oven to dry at 50 °C for seven days before testing. After drying, the samples were removed from the oven and immediately placed in a desiccator for two hours to cool. The thickness and diameter of each sample were measured and recorded to an accuracy of 0.02 mm using a Vernier calliper. The dry mass was calculated and recorded by determining the average of each set of readings. The samples were then placed in a vacuum tank at a pressure of 75 to 80 kPa for three hours. The tank was filled with sodium chloride solution to cover the samples. The vacuum was re-established to between 75 and 80 kPa for one hour. After one hour, the vacuum was released, and air was allowed to enter for 18 hours. Following the 18-hour soaking period

in the solution, the samples were dried and weighed to obtain the vacuum-saturated mass.

After obtaining the vacuum-saturated mass, the test commenced. The connection points of the conduction cells (shown in Figure 3.13) were unscrewed, and the plastic tubes were filled with sodium chloride solution. The sample was placed in the collar, ensuring that one face was against the plastic lip of the rigid ring. Once the sample was positioned, the anode and cathode sections of the cell were tightly screwed into the central portion. The assembled test rig was then placed upright on a horizontal surface. Both the anode and cathode compartments were filled with 5 M sodium chloride solution, and the holes were sealed with cap screws to prevent any leakage. After sealing, the ammeter and voltmeter were connected, and the direct current power supply was adjusted until the voltage across the sample was approximately 10 V. The current and voltage readings were recorded from the ammeter and voltmeter within 10 seconds. Once the readings were taken, the power supply was switched off, and the chloride conductivity index was determined as the average of the three samples.

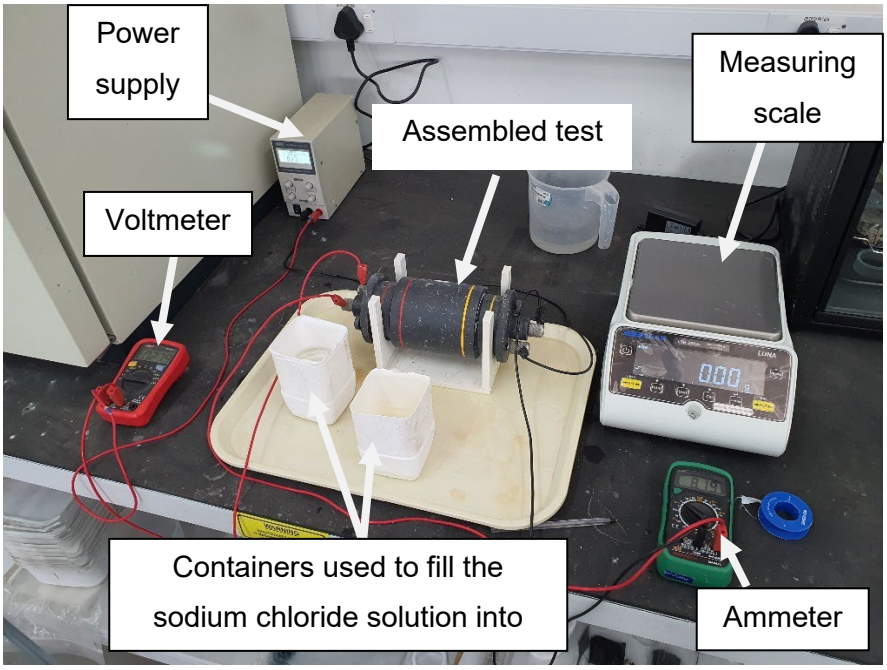

Figure 3.13: Chloride conductivity test equipment

3.8 Summary on the methodology of the study

The study was conducted in two phases. In Phase 1, the fresh and hardened properties of the geopolymer mortar samples were investigated. For this purpose, two sets of mixes were prepared. Set A included only fly ash as the precursor material, while Set B contained both fly ash and GGBS. The Set A mix was used to determine the hardened properties of the geopolymer samples, particularly compressive strength. Based on the compressive strength results for Set A, an optimum mix, referred to as the alternative activator-based mix, was established. After determining the optimum mix, the fresh properties were assessed. Setting time and flow workability were measured using both the fly ash / GGBS and the alternative activator mix. To determine the acceptable GGBS proportion, the Set B mix samples underwent the same casting, curing, and compressive strength testing processes as the Set A samples. The acceptable GGBS proportion was established, which completed Phase 1.

In Phase 2, GPC samples were produced using the alternative activator-based mix and the optimal GGBS proportion. A superplasticiser was also added to the mix. Fifteen GPC moulds, each measuring 100 x 100 mm, were cast and cured under ambient conditions for three, seven, 28, and 90 days. The 28-day ambient-cured samples (three in total) were cored and cut according to SANS 3001-CO3-1:2015 for durability index testing. Nine discs (70 x 30 mm) were obtained from the cores. Four of these discs were used for the oxygen permeability index test, and the three valid discs from the oxygen permeability index test were further tested for the water sorptivity index. The remaining four discs were used for the chloride conductivity index test. The durability characteristics were then compared to those of the sodium silicate mix.

The microstructural studies were conducted using XRD and SEM analyses. These studies aimed to understand the hardened properties of fly ash and the properties of the fly ash / GGBS mixture. For the XRD analysis, six geopolymer samples with different silica sources (GWP, SF, RHA) at two molarities (6 M and 8 M) were selected. The samples maintained a constant silica source / sodium hydroxide ratio of 1.3, utilised a filtered solution, and were oven-cured. This analysis evaluated changes in the crystalline phases of the hardened binders resulting from the use of different alkaline activators. The

SEM analysis examined the mixes of Sets A and B under various conditions to identify unreacted particles, assess the rate of geopolymerisation, and observe the formation of aluminosilicate gel in the material.

CHAPTER 4:
RESULTS AND DISCUSSION

4.1 Introduction

Replacing conventional sodium silicate with waste-based materials in the alkaline activator of geopolymer binders requires evaluating several internal and external factors. Consequently, a comprehensive experimental programme was conducted to understand the interrelationships between these factors. An experimental programme was designed to address the key factors that influence the production of waste-based geopolymers. The previous chapter outlined this programme, focusing on the materials used, their characteristics, mix proportions, and the preparation of the geopolymer samples. Additionally, it explained the various test methods used to assess strength, workability, setting time, durability, and microstructural analysis.

This chapter presents and discusses the results of the experimental study on waste-based geopolymer mortar and concrete. Section 4.1 examines the effects of various parameters on compressive strength. The silica source / sodium hydroxide ratio and sodium hydroxide concentration play a crucial role in determining the optimal proportions for the waste-based geopolymer mix. GGBS was added to reduce the need for high-temperature curing and to accelerate the setting time of the samples under ambient conditions. Consequently, different proportions of GGBS were evaluated. Additionally, the curing duration of the samples influenced compressive strength, which warrants a discussion of this parameter. Flow workability is detailed in Section 4.2, while the measurements of setting time and pH levels of the alkali-activator solution for the fly ash-based geopolymer mortar samples are presented in Sections 4.3 and 4.4. Section 4.5 demonstrates the durability index test of the 28-day cured concrete samples. Lastly, the results of microstructure and mineralogical analysis of the fly ash-based geopolymer mortar samples, using XRD and SEM, are presented in Section 4.6.

4.2 Compressive strength of mortar samples

This section presents the results of the compressive strength tests, based on the parameters outlined in Section 4.1. Each compressive strength value represents the average of three specimens, with error bars indicating ±1.0 standard deviation. Detailed test results can be found in Appendix B. The results highlight the effects of the silica source / sodium hydroxide ratio, sodium hydroxide concentration, GGBS proportions, and curing period on compressive strength.

4.2.1 The effect of silica source / sodium hydroxide ratio on the compressive strength

Figure 4.1 (A to C) shows the effect of the silica source / sodium hydroxide ratio on the seven-day compressive strength of geopolymer mortar made with GWP, SF, and RHA at different sodium hydroxide molarities of 6 M, 8 M, and 10 M. Figure 4.1A indicates that the compressive strength of GWP (18 MPa) at a silica source / sodium hydroxide ratio of 1 is low compared to the control mix. This observation can be attributed to the high calcium content in GWP, which can interfere with the geopolymerisation process. Calcium-rich materials tend to support the formation of C-A-S-H phases rather than the sodium-aluminosilicate gel typical of geopolymers. This difference between reaction products can reduce the overall degree of geopolymerisation, thus leading to a less cohesive matrix and lower compressive strength (Wang et al., 2023). GWP demonstrated better performance with an average strength of 19 MPa across the varying silica source / sodium hydroxide ratios, compared to RHA's average strength of 13 MPa at a 6 M sodium hydroxide concentration. However, as shown in Figures 4.1B and 4.1A, RHA outperformed GWP, achieving average strengths of 42 MPa and 78 MPa, respectively. Overall, GWP exhibited the lowest strengths compared to both SF and RHA, as seen in Figures 4.1A to 4.1C. In Figure 4.1A, the RHA sample displayed lower compressive strength than the control sample across ratios from 1 to 1.5. However, as the sodium hydroxide concentration increases to 8 M (Figure 4.1B) and 10 M (Figure 4.1C), the RHA sample shows a general improvement, surpassing the control sample's strength at these ratios. This outcome can be attributed to the addition of RHA, which

increases the volume of capillary pores and results in a less compact structure and lower strength compared to the control sample. These findings are consistent with a study that examined GPC produced by replacing cement with fly ash and RHA (Prabu et al., 2014). The study found that in the early phase, adding ground RHA reduced the cement content by 10% to 20%, which led to an increase in capillary pores, the accumulation of calcium hydroxide at the interface, and ultimately resulted in lower strength compared to specimens without ground RHA. Furthermore, as shown in Figures 4.1B and 4.1C, RHA showed an increasing trend of 73% and 11%, respectively, up to a silica source / sodium hydroxide ratio of 1.2. At this point, a sudden decrease of 7% and 4%, respectively, was observed, followed by an immediate increase to a ratio of 1.3. Overall, RHA achieved its highest strength at a ratio of 1.3 across Figures 4.1A and 4.1B. Lastly, SF displayed significantly higher strength than the control mix, as well as other silica sources (GWP and RHA). As illustrated in Figure 4.1A, the trend for SF strength showed an increase from a ratio of 1 to 1.3, followed by a decrease from 1.3 to 1.5. As shown in Figure 4.1B, the strength of SF followed a polynomial trend, where the values fluctuated, with the lowest strength of 84 MPa achieved at a ratio of 1.5 and the highest strength of 90 MPa achieved at both ratios 1.1 and 1.4. Due to a lack of data for SF in Figure 4.1C, the highest strength recorded was 101 MPa at ratios 1.1 and 1.2. Generally, SF outperformed the other two silica sources evaluated (GWP and RHA). This finding may be attributed to the tiny particle size (<1 μm) of the SF, which promotes a high rate of dissolution in the sodium hydroxide solution during the production of the alkali-activator, which results in a faster reaction of silica in the mixture. The results of this investigation revealed a positive correlation between the compressive strength of the geopolymer mixture and the silica source / sodium hydroxide ratio, which generally increased from 1 to 1.3. However, as the ratio exceeded 1.3, the compressive strength decreased. This aligns with a study where the effects of SF on the compressive strength of geopolymer-based ultra-high-performance concrete were investigated (Wang et al., 2022). In the study, low-calcium fly ash and calcium aluminate cement were activated by a combination of sodium hydroxide and sodium silicate solution to produce geopolymer binders. The effects of the calcium aluminate cement content, alkaline solution to binder ratio, and sodium hydroxide concentration on the flowability and compressive strength of geopolymer binders were

studied. The SF dosage varied from 5% to 30% of the total binder weight, and the Taguchi method was used to determine the optimum mix proportions. The addition of SF resulted in a trend of initial increase followed by a subsequent decrease in compressive strength for mixes with 20% calcium aluminate cement content.

This trend is noticeable in compressive strength at seven days of age. As the dosage of SF increases from 0% to 5%, the compressive strength rises from 50.6 MPa to 56.4 MPa. However, it then decreases to 43.5 MPa when the SF content is increased to 20%. The findings of this study indicate that SF exhibits better compressive strength compared to GWP and RHA. Furthermore, despite the lack of data in Figure 4.1C, most silica sources achieved the highest compressive strength at a silica source / sodium hydroxide ratio of 1.3. In conclusion, the compressive strength of SF-based activator samples initially increases as the silica source / sodium hydroxide ratio rises from 1.0 to 1.3. This is attributed to an optimal balance between silica content and alkalinity, which promotes efficient geopolymerisation and enhances the formation of the aluminosilicate gel structure, which leads to higher strength. However, beyond a ratio of 1.3, the excess silica content can disrupt this balance. Higher silica levels may hinder the dissolution process necessary for a proper reaction with the alkali, which can lead to incomplete polymerisation and increased porosity, which will ultimately reduce compressive strength.

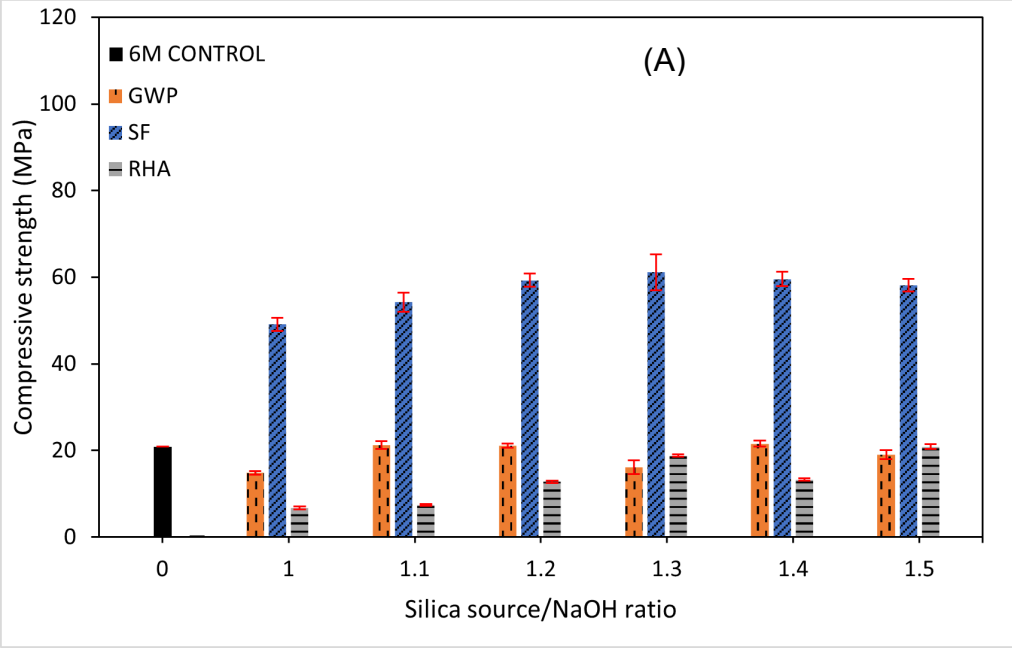

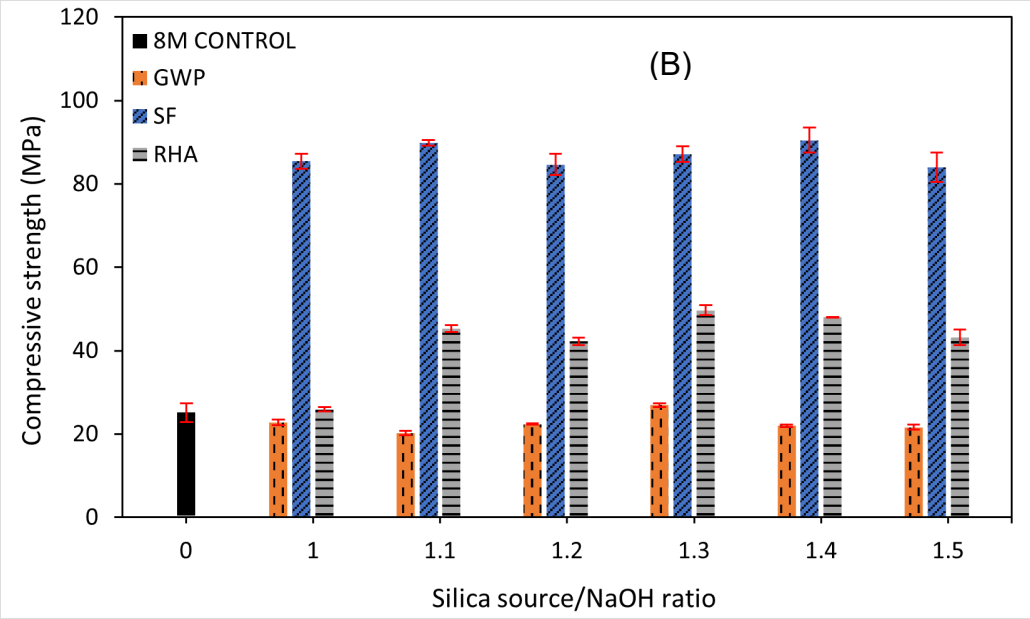

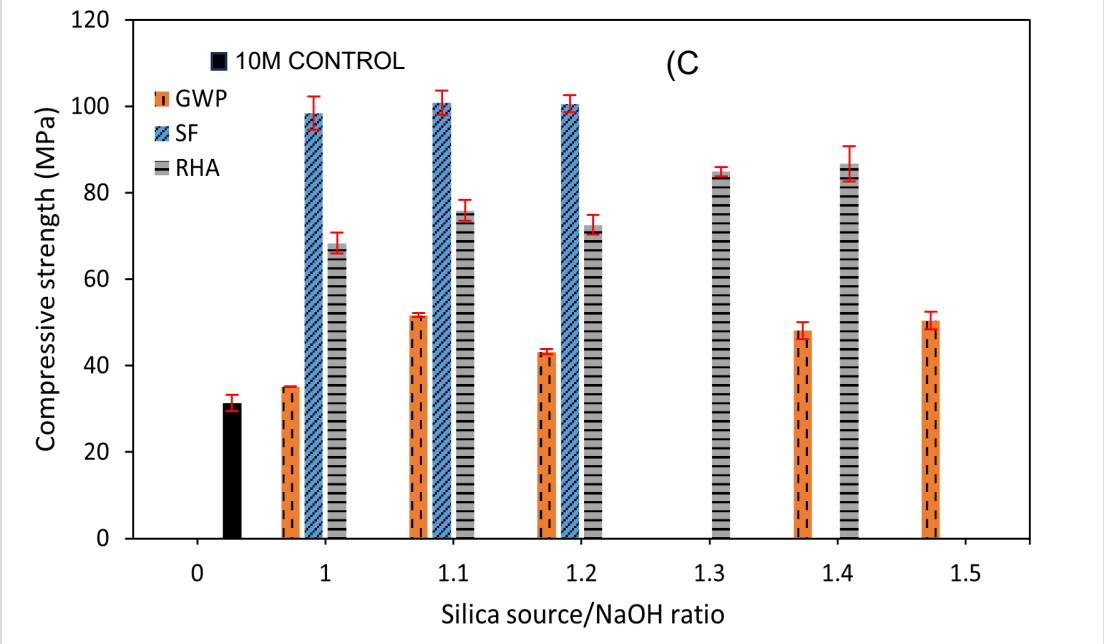

Figure 4.1: Seven-day compressive strength of geopolymer mortars made using filtered alkali-activator of (A) silica source + 6 M sodium hydroxide, (B) silica source + 8 M sodium hydroxide, and (C) silica source + 10 M sodium hydroxide

4.2.2 The effect of the sodium hydroxide concentration on compressive strength

Figure 4.2 shows that the compressive strength of geopolymer mortars made with activators from different silica sources at varying sodium hydroxide concentrations

increases as the sodium hydroxide concentration rises, maintaining a constant silica source / sodium hydroxide ratio of 1.3. The control sample exhibited the lowest compressive strength of 10 MPa at a sodium hydroxide concentration of 4 M, while the highest strength was recorded at 10 M. This suggests that compressive strength increases with the molarity of sodium hydroxide. The strength of the control sample slightly decreased from 6 M to 7 M, with a minor change from 21 MPa to 20 MPa, which was likely due to minor inconsistencies in the mixing process. Overall, however, the strength trend generally appears to increase as the molarity rises. Furthermore, the strength of the control sample increased by 28% from 8 M to 10 M, whereas the compressive strength of mortars using RHA-based alkali activators significantly increased by 68% as the sodium hydroxide concentration rose from 8 M to 10 M. According to recent studies, this increase in strength is attributed to the faster dissolution of RHA in higher sodium hydroxide concentrations (Tong et al., 2018; Handayani et al., 2021). The GWP and RHA samples achieved the lowest strength of 1 MPa at a 4 M sodium hydroxide concentration. Unlike other silica sources, SF demonstrated high strength (greater than the control sample) from the lowest molarity of 4 M up to 8 M. SF achieved its highest strength of 87 MPa at 8M. GWP and RHA exhibited significant strength increases of 24% and 56%, respectively, from 7 M to 10 M sodium hydroxide concentrations, although this increase was still less significant compared to that of the SF sample. At 8 M, the compressive strength of GWP, SF, and RHA (27 MPa, 87 MPa, and 50 MPa, respectively) surpassed that of the control sample (25 MPa), which makes 8 M a potentially viable sodium hydroxide concentration compared to the other concentrations. Since the 10 M solutions for SF and GWP could not pass through filters, no readings were obtained. However, RHA and the control samples reached their highest strengths of 85 MPa and 31 MPa at 10 M, which implies that the GWP and SF samples might also have reached their peak strength at this concentration.

This increase in strength at higher sodium hydroxide concentrations results from stronger geopolymerisation at higher pH values and alkali content (Torres-Carrasco & Puertas, 2015; Naghizadeh & Ekolu, 2018; Vora & Dave, 2013). At higher concentrations of sodium hydroxide, more active species of the raw materials are dissociated, which leads to a greater degree of dissolution of the fly ash. This, in turn, creates more reactive sites

for the formation of geopolymer gels and results in a denser and more uniform microstructure in the final geopolymer product (Hamidi et al., 2016). Although there is a lack of data for the 10 M sodium hydroxide concentration, it can be observed that there is a substantial variation in the strength development of the various mixtures as the sodium hydroxide concentration increases. The results in this section indicate that SF samples consistently achieved the highest compressive strength, regardless of increases in sodium hydroxide concentration, which demonstrates the superior performance of SF compared to other silica sources. SF was therefore chosen as the optimal silica source material for this study. Additionally, while 8 M was identified as the most effective sodium hydroxide concentration, 6 M was selected as the optimal molarity due to its lower cost and sufficient compressive strength. Overall, comparing the different mixtures showed that silica sources can be effectively activated and contribute to geopolymerisation, which results in substantial strength gains.

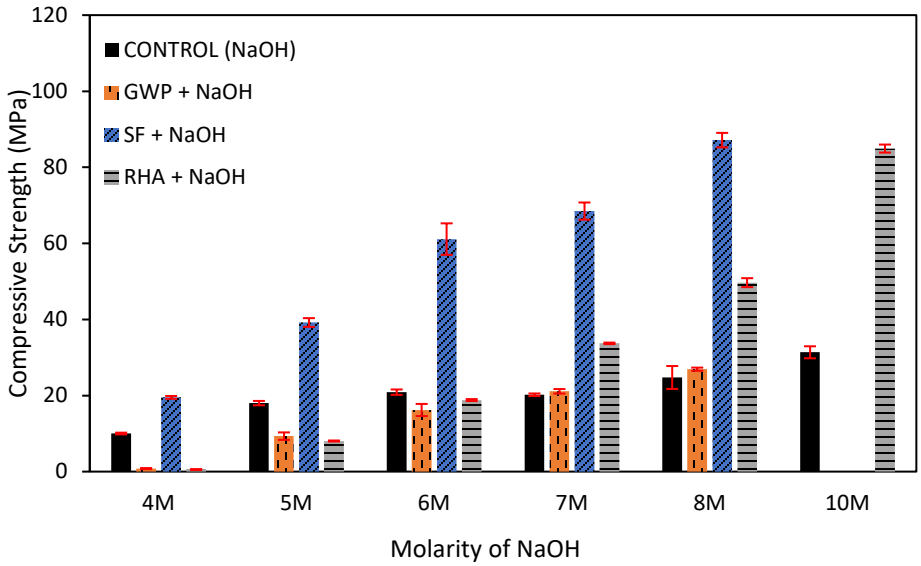

Figure 4.2: Seven-day compressive strength of geopolymer mortars made with activators from different silica sources at varying sodium hydroxide concentrations

4.2.3 The effect of the GGBS ratio on compressive strength

The results in Figure 4.3 demonstrate an increase in compressive strength with higher GGBS content. When 20% GGBS was added, the 28-day ambient-cured mix showed an

increase from 30 MPa to 54 MPa, while the seven-day ambient-cured mix also showed a strength gain from 3 MPa to 25 MPa. The presence of GGBS in the mix leads to the formation of C-S-H phases alongside the geopolymer product, which ultimately contributes to improved strength development. This is because the formation of C-S-H phases enhances the overall strength and durability of the concrete (Banchhor et al., 2022). The increase in compressive strength is more pronounced in the early stages of curing, which indicates that GGBS has a significant impact on the early stages of strength development in alkali-activated mortars. This is because the nucleation effect of calcium ions is most pronounced in the early stages of curing, and the early formation of C-S-H phases contributes to the rapid development of strength in the mix. The results also show that the highest strengths of 49 MPa and 82 MPa were recorded after seven and 28 days of ambient curing, respectively. The high strengths were observed at 40% GGBS content. A similar trend was noted in a study by Lemougna et al. (2020), where the compressive strength of specimens made with 50% slag and 50% volcanic ash increased with slag addition in the system, which reached an optimal value of 85 MPa after 28 days of curing. This observation aligns with the findings by Rafeet et al. (2017), who examined the effects of paste volume, water content, and precursor blend on the consistency, setting time, and compressive strength of AAC made with fly ash and GGBS. Their study aimed to establish a suitable mix design procedure and demonstrated that GGBS content significantly influenced compressive strength. Compressive strengths ranged from 12 MPa to 20 MPa for 100/0 fly ash / GGBS mixes, 30 MPa to 40 MPa for 80/20 mixes, 50 MPa to 60 MPa for 60/40 mixes, and 65 MPa to 75 MPa for 30/70 mixes. Higher GGBS content also enhanced early-age strength, with the seven-day to 28-day strength ratio increasing from about 60% for 80/20 mixes to 80% for 30/70 mixes. Based on the analysis of the results, the 60% fly ash / 40% GGBS ratio achieved the highest strength. However, as indicated in the literature review in Chapter 2, 40% GGBS incorporation can show a reduction in the strength development of geopolymer mortars. The 70% fly ash / 30% GGBS ratio was therefore selected as the optimum mix. It is worth noting that the exact impact of GGBS on the strength development of alkali-activated mortar/concrete may depend on the specific mix design and curing conditions used.

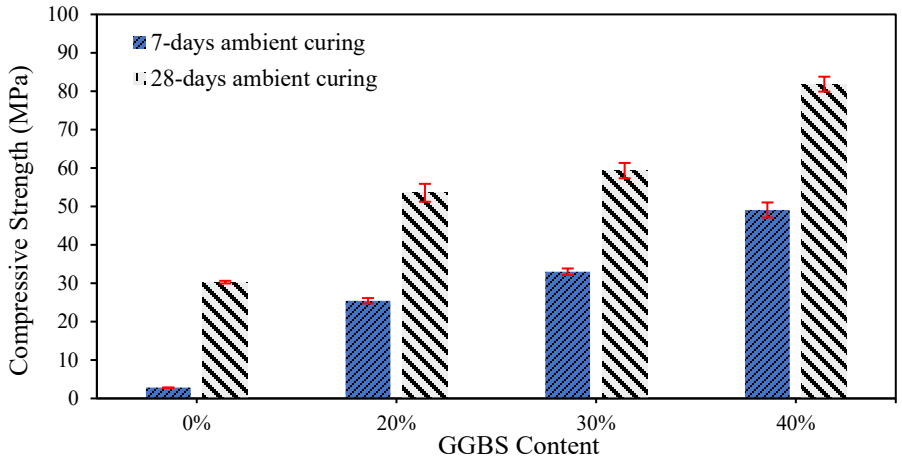

Figure 4.3: Seven- and 28-days compressive strength of geopolymer mortars made with an alternative activator and varying contents of GGBS

4.2.4 The effect of the curing period on compressive strength

The curing period can significantly affect the properties and performance of GPC. This section focuses on assessing the effect of curing duration on concrete samples rather than mortar samples. With the optimal mix proportions established, the effect of the curing period on the final concrete product was evaluated at three, seven, 28, and 90 days. The GPC samples consisting of 70% fly ash and 30% GGBS activated with an alternative activator (SF-6M-1.3) were compared against geopolymer samples of 70% fly ash and 30% GGBS activated with a conventional activator (sodium silicate-8M-1.3) from a similar study. The purpose of the comparison in this section is not to optimise molarity itself, but to benchmark the performance of the alternative activator (SF-6M-1.3) against a conventional activator expected to demonstrate strong performance under typical, industry-accepted conditions. Since previous studies (Katti et al. 2016; Patil & Joshi 2025) have shown that 8 M NaOH yields sufficiently high reaction kinetics and improved mechanical performance in 70% fly ash–30% GGBS mixes, it provides a more robust reference point than 6 M. Sodium silicate was mixed with sodium hydroxide at concentrations ranging from 8 M to 12 M, with the sodium silicate to sodium hydroxide solution ratio varying from 0.72 to 4.89. A ratio of 1.3 was selected for comparison. Although the study did not use a 6 M concentration, the 8 M concentration still provided insight into the performance of waste-based alkaline activators in relation to conventional

activators, particularly since the conventional activator was expected to perform well at higher molarity. Figure 4.4 shows a comparison of GPC made with an alternative activator and a conventional activator. It is common to observe that as the curing period increases, the compressive strength of the GPC also increases, which results in a similar trend seen in Figure 4.4. At three days of ambient curing, both GPCs are still weak and brittle; however, the alternative activator concrete achieves a higher initial strength of 21 MPa, while the conventional activator concrete attains an initial strength of 18 MPa. After seven days of ambient curing, the strengths of the alternative and conventional activator concretes were nearly similar, reaching 31 MPa and 33 MPa, respectively. There was a significant average percentage increase of 101.71% for both concretes from seven days to 28 days of ambient curing. This is because early curing, such as at three or seven days, primarily initiates the hardening process, while the most substantial material densification and strength gain occur during the seven- to 28-day period. At 90 days of ambient curing, the GPCs reach their ultimate strength. The highest strength achieved is with the conventional activator concrete at 81 MPa, while the alternative activator concrete reaches a strength of 76 MPa. Beyond 90 days, the strength gained is typically limited. The 30% GGBS substitution may also contribute to the increasing trend, as slag not only reduces the initial setting time of the geopolymer cured at ambient temperature but also increases compressive strength due to the synergistic formation of C-A-S-H/N-A-S-H gel (Lemougna et al., 2020). It was expected that the conventional activator concrete would achieve higher compressive strength in all curing periods since it was made with a higher molarity than the alternative activator concrete. However, based on the results, it can also be observed that the alternative activator concrete provided results that are very close to, and almost the same as, those of the conventional activator concrete. This indicates that the optimum proportions of the alternative activator were efficient and effective in replacing the conventional activator in fly ash / GGBS GPC.

Research shows that various studies have found both sodium silicate- and sodium hydroxide-based activators to be appropriate choices when considering the mechanical properties of geopolymer materials made from GGBS and fly ash (Oti et al., 2024). Sodium silicate-based activators have been demonstrated to effectively initiate the reaction between GGBS and fly ash, leading to the formation of geopolymer gels, which

contribute to the development of mechanical properties, including compressive strength. Similarly, the inclusion of SF also improves the compressive strength of geopolymer mixtures (Bajpai et al., 2020). These results align with a recent study that showed that compressive strength increased with the addition of SF. At 20% SF inclusion, the compressive strength at seven and 28 days was 22.2% and 34.3% higher, respectively, compared to mixes without SF (Wang et al., 2022). This phenomenon can be attributed to the fact that SF is rich in amorphous silica, which is highly reactive. This reactivity enhances the strength properties of the material. The presence of amorphous silica in SF positively affects the overall performance of the GPC (Chakraborti, 2010).

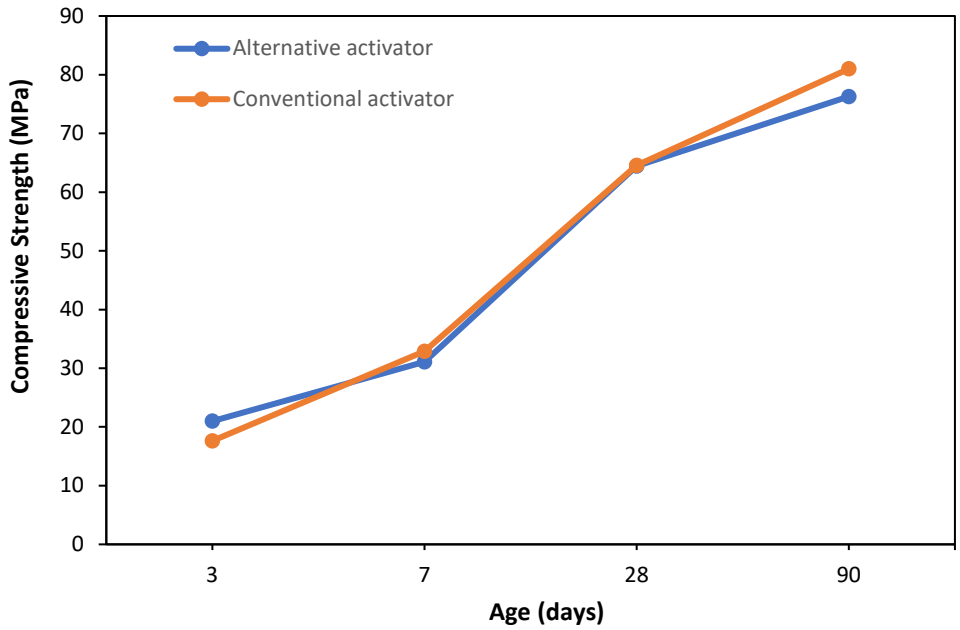

Figure 4.4: Three-, seven-, 28-, and 90-day compressive strengths of GPC made with alternative activator and conventional activator + 30% GGBS cured at an ambient temperature

4.3 Flow workability measurement

Figure 4.5 presents the flow workability results for the fly ash / GGBS geopolymer mortars. The mortar mix activated using the alternative activator was compared to the mix activated with the conventional activator at different GGBS proportions of 0%, 20%, 30%, and 40%. The conventional mix used for comparison was adopted from a related study,

as discussed in Section 4.2.4. In Figure 4.5, the flow initially measured 162 mm for both mortars activated with the alternative and conventional activators in the absence of GGBS. This indicates that changes in flow are influenced by the quantity of GGBS incorporated into the mix. The flow of the mix decreased with increasing GGBS dosage for the alternative activator, while the conventional activator displayed an opposite pattern. However, a slight increase in flow occurred at 20% GGBS for the alternative activator and at 40% GGBS for the conventional activator. According to previous studies, the reduction in flow workability of geopolymer mixtures containing GGBS can be attributed to the difference in particle shape between fly ash and GGBS. Specifically, fly ash typically has spherical particles that act as bearings. These enhance the workability of the mixture, while GGBS contains more angular particles that can reduce the workability of the mixture (Al-Majidi et al., 2016). Additionally, an increase in the proportion of GGBS and a reduction in the proportion of fly ash can further negatively impact the workability of the geopolymer mixture. In general, it was observed that the flow decreased by up to 13.2% with GGBS dosages ranging from 0% to 30%. A similar study that utilised fly ash and GGBS to develop concrete, activated with sodium hydroxide and sodium silicate, demonstrated that higher GGBS percentages lead to an increase in the stiffness of the GPC mix (Kumar & Mishra, 2021). In Figure 4.5, the trend also shows that the flow of mortars activated with a conventional activator increased, while the flow of mortars activated with an alternative activator decreased. This can be attributed to the fact that sodium silicate acts as a flow-enhancing agent due to its water content and dispersive properties, whereas SF, on the other hand, reduces workability due to its high water demand, reactivity, and particle characteristics (Chakraborti, 2010). The results highlighted the performance of SF as an alternative activator in relation to fresh properties, particularly flow workability. While the conventional activator demonstrated higher flow values, especially with 20% GGBS, the alternative activator achieved its highest flow when no GGBS was present in the mix. According to the ASTM standards, the recommended range for geopolymer mortar flow workability is 140 to 200 mm. Based on this range, it is evident that the inclusion of GGBS reduces the flow of the alternative activator, which results in a flow value that is lower compared to the conventional activator. However, for some mixes with the conventional activator, the flow value is

higher than the recommended range. This could indicate that the conventional mix with 20% and 30% GGBS inclusion was found to be too runny. It can therefore be concluded that, in terms of flow workability, an SF plus sodium hydroxide activator with no GGBS present in the mix would be a viable replacement for a sodium silicate plus sodium hydroxide activator.

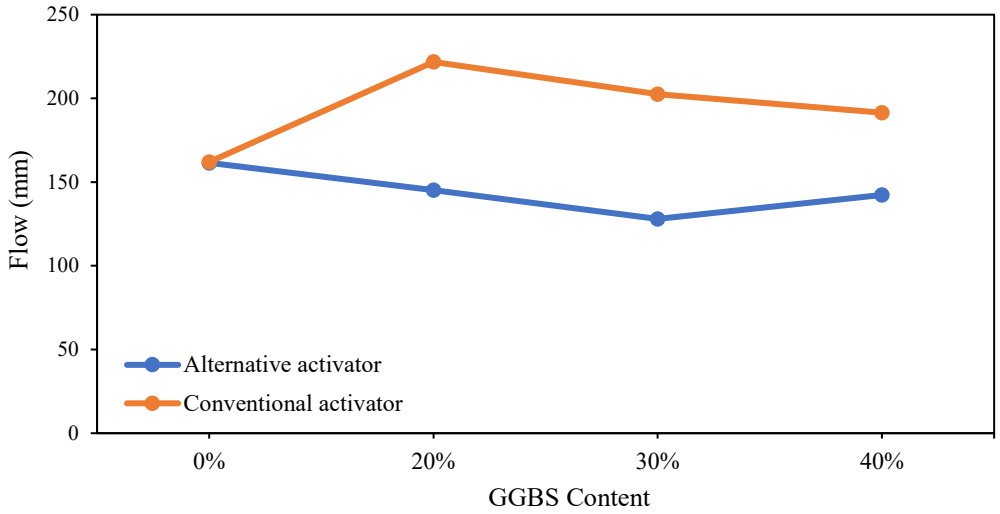

Figure 4.5: Workability of geopolymer mortar mixes made with an alternative activator and conventional activator with varying contents of GGBS

4.4 Setting time measurement

The fresh binder's setting time behaviour is critical, as it influences the time allowed for transporting, casting, and compacting the AAC. Figure 4.6 illustrates the initial and final setting times of a geopolymer mix activated with an alternative activator and varying contents of GGBS. The results indicate that the mix with 0% GGBS takes longer to set, with initial and final setting times of 439 and 1 270 minutes, respectively. This phenomenon aligns with a related study that examined the fresh and hardened properties of alkali-activated fly ash / slag paste using superplasticisers. In that study, binders were prepared by dry mixing slag and fly ash at five different slag-to-binder ratios: 0, 0.3, 0.5, 0.7, and 1. The alkali-activator consisted of a combination of sodium hydroxide solution and sodium silicate solution. The findings indicated that the setting time for fly ash-based geopolymer without GGBS was approximately 1 500 minutes, which aligns closely with the results presented in Figure 4.6 (Jang et al., 2014). This prolonged setting time can be

attributed to the absence of GGBS, as fly ash alone lacks sufficient calcium to significantly accelerate the geopolymerisation process. Instead, the reaction relies on aluminosilicate dissolution and polymerisation, which occur more slowly under ambient curing conditions. However, the results also show that both the initial and final setting times of other geopolymer mixes decrease as the GGBS content increases. Adding GGBS to the binder significantly reduces the binder's setting time. This is due to the presence of high-calcium oxide and the surface area of slag particles in the structure (Haruna et al., 2020). This finding demonstrates that incorporating GGBS into geopolymers activated with the alternative activator results in shorter setting times under ambient conditions. Given that similar results were reported for geopolymers activated with a conventional activator in the literature, it can be concluded that the alternative activator serves as a suitable replacement for the conventional activator in terms of setting time.

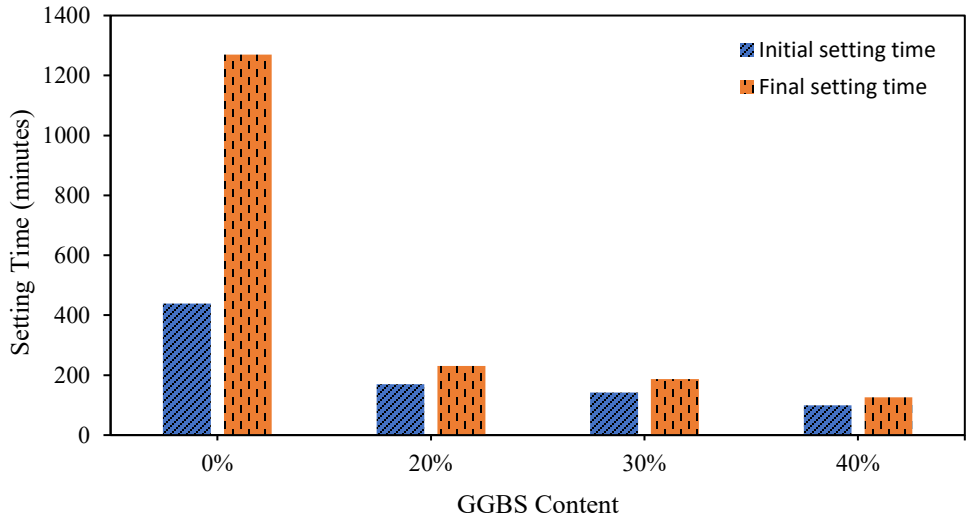

Figure 4.6: Initial and final setting times for geopolymer mixes made with an alternative activator and varying contents of GGBS under ambient conditions

4.5 pH levels of the alkali-activator solution

Figure 4.7 presents the results for the pH levels of GWP, RHA, and SF activator solutions prepared using 6 M sodium hydroxide at varying silica source / sodium hydroxide ratios. The pH levels of an alkali-activator solution can vary depending on several factors, such as the specific type of silica source, the concentration of sodium hydroxide, and the ratio

of silica to sodium hydroxide. However, in general, higher sodium hydroxide concentrations can lead to higher pH levels, while a higher silica source / sodium hydroxide ratio can lead to lower pH levels. In Figure 4.7, a similar phenomenon was observed with respect to the silica source / sodium hydroxide ratio. The pH values of GWP, RHA, and SF solutions decreased as the silica source / sodium hydroxide ratio increased. The initial pH value at a ratio of 0 was 14.19 for all three silica sources. At a silica source / sodium hydroxide ratio of 1.0, the GWP solution achieved the highest pH level of 13.97, while the RHA and SF solutions were at 13.87 and 13.77 respectively. At a ratio of 1.3, the GWP solution led with a pH level of 13.85, followed by the RHA and SF solutions with pH levels of 13.80 and 13.33, respectively. At a ratio of 1.5, the trend was similar for the GWP, RHA, and SF solutions, which reached pH levels of 13.80, 13.60, and 12.89, respectively. These findings support a similar study, which reported that RHA at a silica / sodium hydroxide ratio of 1.5 and a 6 M sodium hydroxide concentration had a pH of around 13.60, which correlates with the latter statement (Duxson et al., 2007). In this case, the observed decrease in the pH values of the alkali-activator solutions containing GWP, RHA, and SF, as the silica source / sodium hydroxide ratio increased, was due to the consumption of hydroxide ions by the silica source at higher ratios (Han et al., 2023).

The relationship between compressive strength and the pH of the activator solution, as shown in Figure 4.7, corresponds with the observed effects of the silica source / sodium hydroxide ratio on compressive strength. Figure 4.7 indicates that the GWP reached the highest pH level (13.83) but achieved the lowest average strength (16 MPa) compared to the RHA and SF, as discussed in Section 4.2.1. The RHA followed with a pH of 13.78 and a compressive strength of 19 MPa, while the SF recorded a pH of 13.63 and the highest strength of 61 MPa. As noted in the literature review under Section 2.7, the optimal pH range for effective polymerisation and higher strength in GPC fresh mixes is between 13 and 14 (Khale & Chaudhary, 2007), which aligns with the pH range observed in this study. The findings of this section demonstrate that the pH levels of the activators, derived from various silica sources, contribute to enhanced compressive strength. This suggests that these silica sources are a viable and effective alternative to conventional activators.

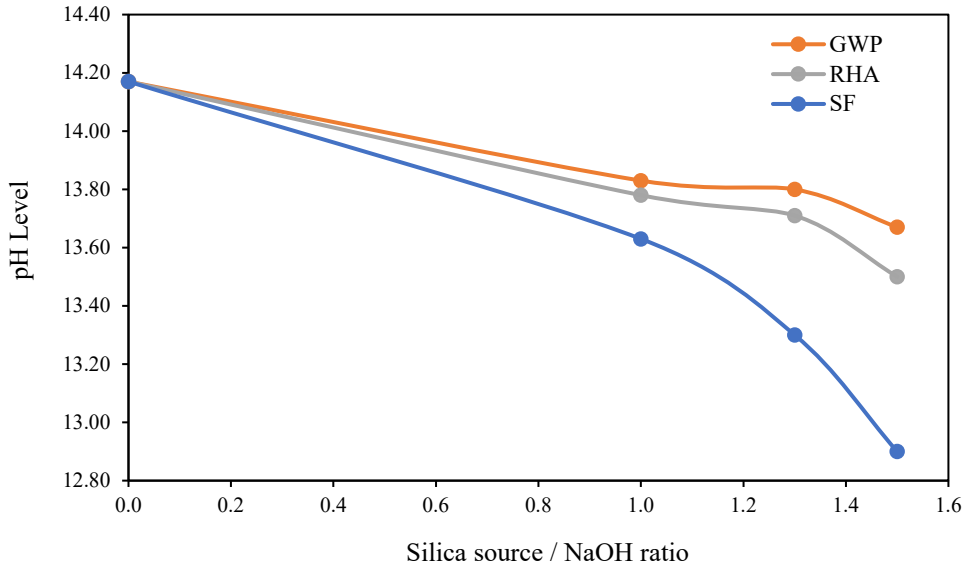

Figure 4.7: pH Levels of different silica sources prepared using 6 M sodium hydroxide at varying silica source / sodium hydroxide ratios

4.6 Durability testing of concrete samples

Durability index testing was performed on the 28-day ambient-cured GPC samples. Although the durability index approach is not commonly employed outside South Africa, Beushausen and Alexander (2008) conducted a comparison with globally recognised methods for characterising concrete durability. The purpose of the durability index testing was to assess variations in the durability characteristics of binary fly ash / GGBS GPC using an alternative activator. The selected samples had different GGBS contents, which ranged from 0% to 40%. The 0% GGBS samples indicated that the mix contained only fly ash as a binder material, with no GGBS included. These samples demonstrated average compressive strengths of 30 MPa, 54 MPa, 59 MPa, and 82 MPa at 28 days, respectively. The reference mix (Mix 13) was obtained from a recent study, as mentioned in Section 3.7. Mix 13 had similar physico-chemical characteristics as the alternative activator mix in this study. The reference samples were ambient-cured for one year. Ambient curing of the GPCs resulted in significant long-term strength improvements of 60% to 90%, with normal pore structure characteristics and good durability performance. However, the chloride conductivity test produced inconsistent results, possibly due to

variations in ion flux (Naghizadeh et al., 2023). In this study, the results of the durability index tests for the 28-day ambient-cured GPC with varying GGBS proportions are detailed in Table 4.1. Figure 4.8 (A to C) outlines the criteria for “good” durability, which is defined as an oxygen permeability index within the range of 9.5 to 10, a water sorptivity index between 6 to 10 mm/hr$^{0.5}$, and a chloride conductivity index from 0.75 to 1.50 mS/cm.

Table 4.1: Durability index test results

Sample ID	Oxygen permeability	Water sorptivity (mm/hr$^{0.5}$)	Effective porosity (%)	Chloride conductivity (mS/cm)	Compressive strength (MPa)
0% GGBS	10.1	3.9	13.4	3.3	30
20% GGBS	10.3	3.1	12.0	2.3	54
30% GGBS	9.2	5.8	12.3	2.4	59
40% GGBS	9.9	4.4	10.2	1.0	82
Mix 13	9.8	5.7	9.98	2.26	70

4.6.1 Oxygen permeability index

Figure 4.8 shows that the permeability of the concrete was rated as good to excellent for all GGBS percentages, except for the 30% GGBS mix. The oxygen permeability index values for 0%, 20%, and 40% GGBS exceeded that of Mix 13, which was ambient-cured for one year. Specifically, the 0% and 20% GGBS mixes slightly exceeded the “good” criterion and fell within the “excellent” range, which achieved oxygen permeability index values of 10.1 and 10.3, respectively. However, the 30% GGBS mix was classified as “poor”, with an oxygen permeability index of 9.2. This poor performance can be attributed to uneven gel formation. Fly ash contributes to the formation of a denser matrix through aluminosilicate gel, while GGBS supplies calcium, which promotes the formation of C-A-S-H gel. At 30% GGBS inclusion, the combination may result in irregular gel formation or increased porosity, which will lead to a lower oxygen permeability index value (Bondar et al., 2017). Additionally, the trend showed an increase after the 30% GGBS mix, returning to the “good” criterion at 40% GGBS incorporation. Furthermore, the compressive strengths for the different mixes align with the oxygen permeability index results, with the exception of the 30% GGBS mix. The highest compressive strength, reaching 82 MPa, was attained at an oxygen permeability index of 9.9 and a GGBS content of 40%. These

results align with a previous study in which higher oxygen permeability index values indicated greater resistance to gas penetration (Alexander et al., 2008). It can thus be inferred that elevated oxygen permeability index values correspond to enhanced resistance to gas penetration. Furthermore, the study demonstrated that a denser microstructure, often associated with higher compressive strength, contributes to lower permeability and, consequently, higher oxygen permeability index values (Alexander et al., 2008). The compressive strength of the 40% mix exceeded that of Mix 13 by 16%, despite the 40% mix being ambient-cured for only 28 days, compared to the one-year ambient curing of Mix 13. Typically, Mix 13 would be expected to exhibit higher compressive strength due to the extended curing period. However, while the strength of the other mixes was slightly lower than that of Mix 13, the 40% mix stood out by outperforming Mix 13. This indicates that, regardless of the GGBS incorporation, the alternative activator mix used in this study was a viable replacement for the conventional mix in GPC.

4.6.2 Water sorptivity and porosity indexes

According to the durability classification in Table 2.1, water sorptivity is classified as “excellent” if it is less than 6. Figure 4.8B illustrates the “excellent” performance of all mixtures. The 0%, 20%, and 40% mixes had lower water sorptivity index values compared to Mix 13, although all mixes, including Mix 13, were classified as “excellent”. The 20% mix achieved the best water sorptivity index of 3.1 mm/hr$^{0.5}$, while the 30% mix obtained the weakest water sorptivity index of 5.8 mm/hr$^{0.5}$. This can be attributed to the formation of a dense and cohesive microstructure that minimised interconnected pores, which reduced water absorption and sorptivity. In contrast, the poor performance of the 30% GGBS mix could be due to uneven gel formation, which might result in an inconsistent and less compact microstructure, as mentioned in Section 4.6.1. These defects increased the permeability of the matrix and allowed for greater water ingress, thus resulting in higher water sorptivity for the 30% GGBS mix. This result aligns with the findings of the oxygen permeability index test in Section 4.6.1, where the 20% mix achieved the highest oxygen permeability index value and the 30% mix achieved the lowest oxygen permeability index value. A closer analysis of the results indicated a relationship between

the oxygen permeability and sorptivity values, where mixtures with good or poor oxygen permeability index results demonstrated corresponding performance levels in the water sorptivity index testing. However, the relationship between the oxygen permeability index and water sorptivity index is not a straightforward linear correlation; instead, it followed a parabolic curve. As a result, for samples in the poor durability category, the water sorptivity index increased as the oxygen permeability index values decreased. Conversely, for concretes with good to excellent durability, both the oxygen permeability and water sorptivity index values were within the same performance category.

Porosity has not yet been directly considered as an independent durability parameter within the range of the durability index parameters. However, sorptivity and porosity share an inverse relationship. Laboratory observations have revealed that high or low sorptivity values can correspond to either high or low porosity values, and vice versa. Figure 4.8D illustrates that the 0% GGBS mix had the highest porosity at 13.4%, which is classified as poor to very poor, while the 40% mix had the lowest porosity at 10.2%, which is classified as good to poor. The 20% GGBS mix achieved a porosity value of 12% (good to poor), whereas the 30% mix recorded 12.3% (poor to very poor). Mix 13 achieved a porosity value of 9.98%, which is classified as excellent. In comparison, the lowest porosity value from this study was 10.2%, which falls under the classification of good to poor. This indicates that the conventional activator mix performed better in terms of porosity than the alternative activator mix. However, the alternative activator mix demonstrated a compressive strength 15.79% higher than that of the conventional activator mix. This aligns with findings from the literature review, which highlight that conventional activation promotes better porosity due to faster and more efficient geopolymerisation, which results in a denser matrix. However, the alternative activator, enhanced with GGBS, produced higher compressive strength due to the formation of both N-A-S-H and C-A-S-H gels, even with slightly higher porosity. These findings suggest that concrete with lower porosity and a given sorptivity rate is likely to exhibit greater durability, as higher porosity indicates greater pore connectivity. Porosity and sorptivity must therefore be considered together, as both influence durability (Moore et al., 2021). Moreover, the trends for porosity and sorptivity align, with values decreasing from 0% to 20% GGBS, increasing from 20% to 30%, and decreasing again at 40%. This pattern was

consistent across both parameters. A comparison can also be made between mixes without GGBS, specifically Mix 13 and the 0% GGBS mix. The results revealed that conventional activation still outperformed alternative activation by 29%. However, in this case, the compressive strength of the alternative activation was significantly lower than that of the conventional activation by 80%. This difference may be attributed to the absence of GGBS and the longer curing period of Mix 13. The findings in this section indicate that the alternative activated mix samples were more porous than the conventional mix samples. Additionally, the alternative activated mix samples demonstrated a higher wetting rate than the conventional mix samples. This suggests that the conventional mix was more durable in terms of porosity, while the alternative mix offered greater durability concerning water sorptivity.

4.6.3 Chloride conductivity index

The chloride conductivity index results are displayed in Figure 4.8C. A lower index indicates greater potential durability of the concrete (Gouws et al., 2001). Most of the results fell within the category of poor durability, characterised by values that exceed 1.5 mS/cm. The highest chloride conductivity value of 3.3 mS/cm was reported for 100% fly-ash-based GPC with no GGBS. In contrast, the 40% mix displayed the most favourable outcome, with the lowest chloride conductivity value of 1.0 mS/cm, which meets the criteria for good chloride conductivity. This demonstrates that substituting fly ash with slag considerably decreases chloride ion permeability in GPC samples. These findings are consistent with a study that discovered that GPC samples prepared with 100% fly ash showed lower resistance to chloride ion entry (Bellum et al., 2022). Furthermore, the results revealed that at 0% GGBS, the chloride conductivity value was 37% higher than that of Mix 13. The higher chloride conductivity value in the alternative activation reflected a less dense matrix with more interconnected pores, which facilitated easier chloride ion transport compared to the denser and less permeable structure produced by conventional activation. These findings align with a prior study, which reported that geopolymer specimen MGP-31 (silica / aluminium ratio = 2.1), containing the lowest SF content of 2.75%, exhibited the highest bulk density of 1905.30 kg/m³. Conversely, geopolymer specimen MGP-41, with a higher SF content of 11% (silica / aluminium ratio = 2.3),

demonstrated a lower bulk density of 1 732.88 kg/m³ (Chakraborti, 2010). According to the results, it can be understood that GPC produced with a blend of fly ash and GGBS may exhibit good chloride conductivity (with lower conductivity indicating better resistance) at 40% GGBS and above. Additionally, GPC activated with the alternative activator allows for greater chloride ion penetration due to its less dense matrix and higher pore connectivity compared to the conventional activator. The conventional activator therefore served as the most viable option in terms of potential durability against chloride ion ingress.

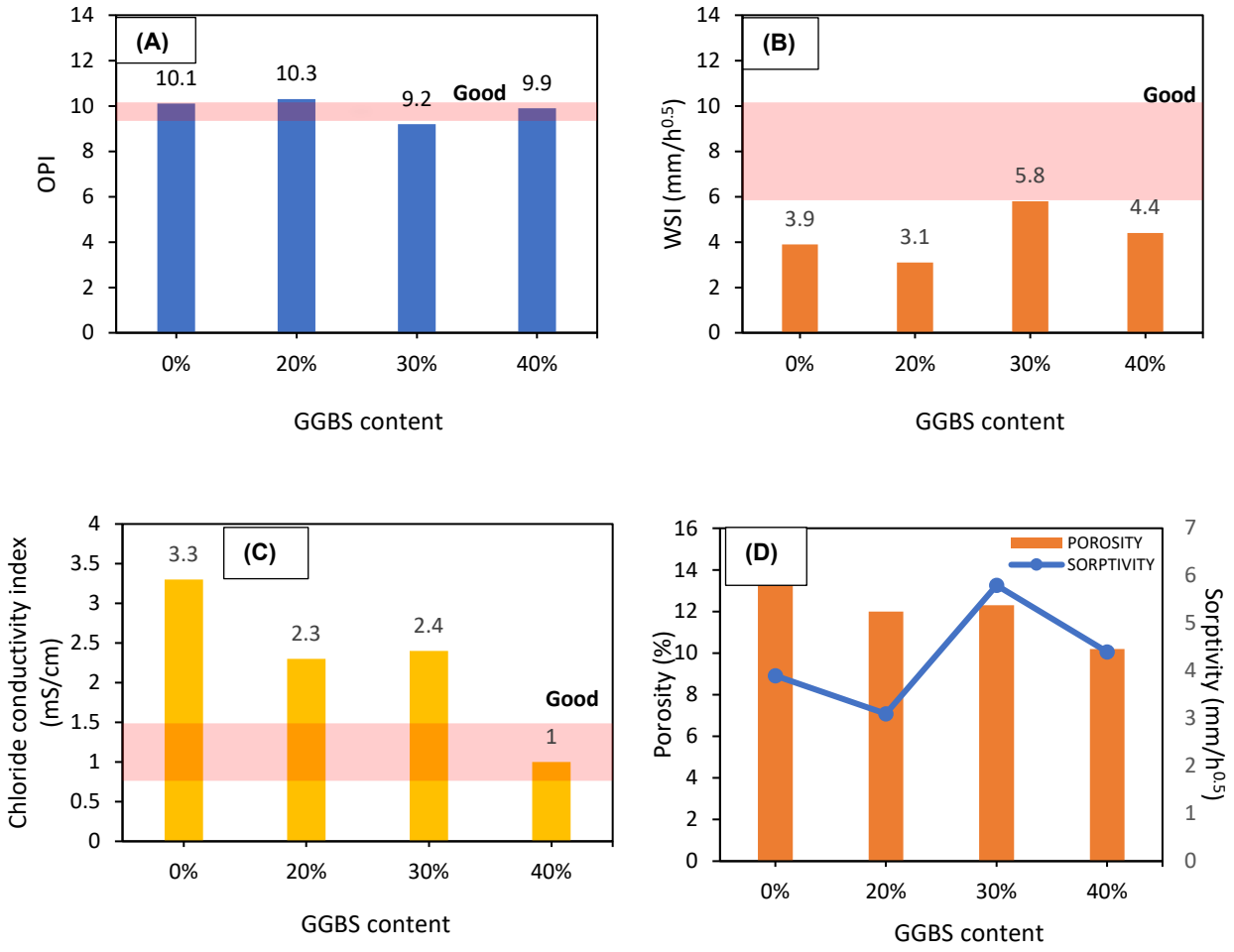

Figure 4.8: (A) Oxygen permeability index, (B) water sorptivity index, (C) chloride conductivity index, and (D) sorptivity vs porosity index

4.7 Analytical studies

Two techniques were employed for microstructure characterisation: XRD and SEM. XRD analysis was conducted on seven-day oven-cured Set A mix mortar samples, as detailed in Section 3.6 and Table 3.17. These samples were activated using filtered and unfiltered activators derived from different silica sources (GWP, RHA, and SF) with sodium hydroxide concentrations of 6 M and 8 M, while maintaining a constant silica source / sodium hydroxide ratio of 1.3. As the optimal silica source had already been identified based on compressive strength results in Section 4.2, it was necessary to compare this silica source with others at different molarities using XRD analysis. Mixes with a molarity of 10 M provided limited data for the 1.3 ratio and were therefore excluded from this

investigation. SEM analysis was performed on both Set A and Set B geopolymer mortar samples. For Set B, an unfiltered alternative activator solution was used to provide a more detailed examination of the reactions in the geopolymer matrix. Additionally, the effect of GGBS concerning curing conditions was also investigated using SEM analysis, as mentioned in Section 3.4.2.

4.7.1 XRD results

XRD analysis was conducted on fly ash geopolymer mortar samples to investigate the potential development of new crystalline phases and changes in existing phases before and after geopolymerisation. As shown in Figure 4.9, the prominent peaks identified in all geopolymer samples correspond to quartz and mullite. These peaks are also present in the XRD pattern of the fly ash raw material (see Appendices A7 to A11). The strong peaks attributed to quartz and mullite are likely due to unreacted fly ash particles present in the geopolymer mixture. No significant changes in the patterns of the SF-6M-OF and SF-6M-OU samples suggest that the method (filtered or unfiltered) of preparing the alkaline solution did not influence the formation of new phases. Notably, sample GWP-8M-OF exhibited new peaks corresponding to leucite ($K(AlSi_2O_6)$) and spinel ($MgAl_2O_4$) at angles of 2θ = 16.282° with a *d*-spacing of 5.4395 Å and 2θ = 64.355° with a *d*-spacing of 1.4465 Å, respectively. GWP often has a more amorphous structure and higher solubility in alkaline environments than crystalline silica sources such as RHA and SF. This promotes the dissolution of silica and alumina, which facilitates the formation of secondary crystalline phases such as spinel and leucite during geopolymerisation (Zheng et al., 2022). The presence of leucite and spinel can limit the extent of amorphous gel formation, which results in a less cohesive matrix with lower compressive strength (27 MPa) compared to other samples, as seen in Figure 4.2.

The XRD pattern of the raw materials (fly ash, GWP, SF, and RHA) indicated an amorphous phase, as evidenced by the presence of broad humps. For fly ash, SF, and RHA, the hump appeared in the 2θ range between 15° and 30°, as shown in Appendices A7, A10, and A11. For GWP, the hump was observed in the 2θ range between 20° and 30°. However, after undergoing geopolymerisation using fly ash and filtered/unfiltered

alkali-activator solution, there was minimal evidence of an amorphous phase in the resulting material. This suggests that the geopolymerisation process transforms the amorphous phases present in the raw materials into crystalline phases (Toniolo, 2018). Furthermore, the crystalline phases, namely quartz and mullite, which were initially present in the fly ash, appeared to remain unchanged after activation. This observation confirms that during the geopolymerisation synthesis, the amorphous component of the fly ash is the most reactive phase involved in the process, while the crystalline phases undergo minimal alteration. A similar observation was noted in the aforementioned study, where the XRD analyses showed no change in the crystalline phases (Toniolo, 2018). It can be concluded that there was no impact on the filtration of the SF mix with respect to XRD analysis. Additionally, variations in the sodium hydroxide concentration had no effect on the XRD peaks, as no phase changes were detected. The only change observed was the formation of new elements in the GWP samples. These new elements had a negative effect on the compressive strength, with the result that the GWP demonstrated the lowest strength across the study. SF was therefore the most suitable silica source compared to the other silica sources, due to its stable phases and higher compressive strength.

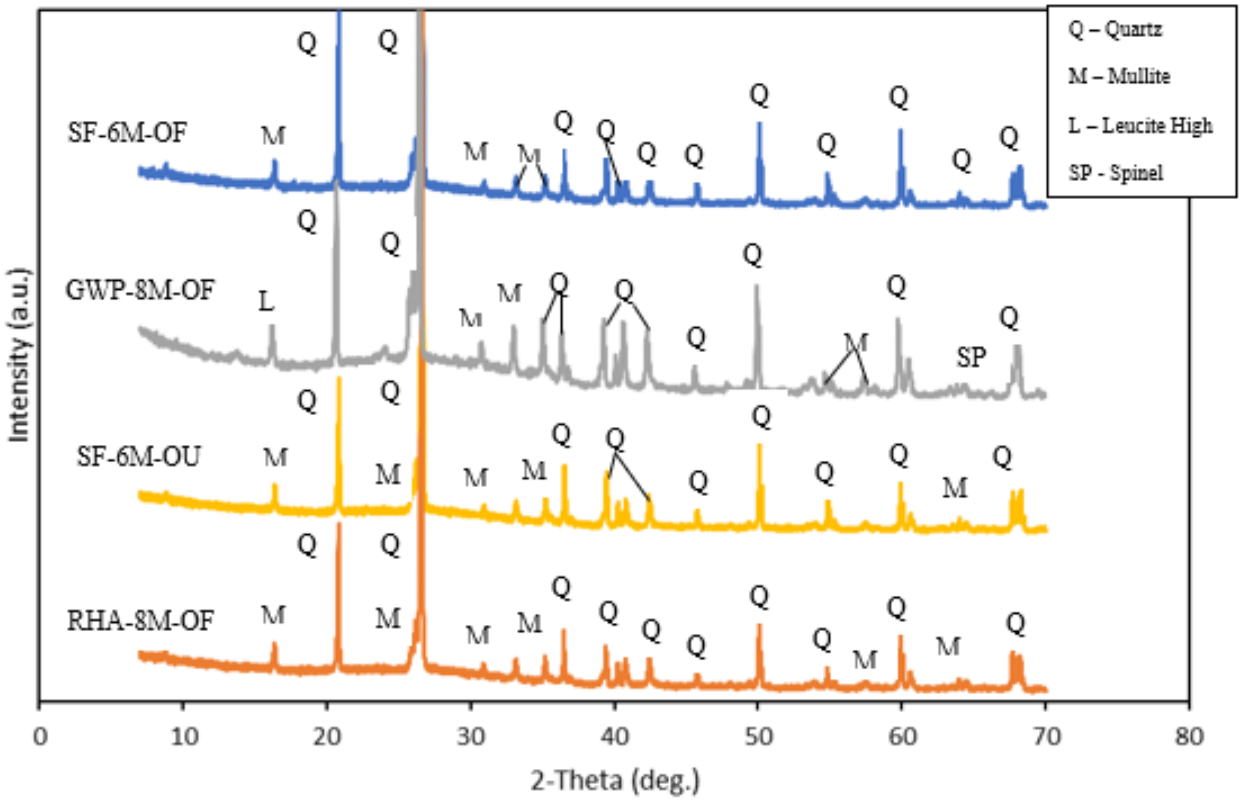

Figure 4.9: XRD analysis of geopolymer mortar samples

4.7.2 SEM results

SEM analysis was conducted to examine the microstructure of the raw materials (GWP, SF, and RHA) and the geopolymerised mortar samples from the Set A and Set B mixes. The Set A samples were prepared using fly ash as the precursor and activated with 6 M and 8 M solutions of different silica sources, maintaining a constant silica source / sodium hydroxide ratio of 1.3. In contrast, the Set B samples used a fly ash / GGBS blend as the precursor and were activated with both filtered and unfiltered alternative activators. The samples underwent various curing methods, with some being oven-cured and others being ambient-cured for seven days.

Figure 4.10 shows micrographs of the raw materials: RHA, SF, and GWP, all at x1500 magnification. Figure 4.10A displays fine particles with uneven sizes resulting from the high combustion temperature of the rice husks (Basri et al., 2020). Some of these particles adhered together to form an agglomerated gel-like structure due to the presence of

amorphous silica and the manner in which it forms during the combustion process of rice husks, as well as the high surface energy and free hydroxide groups on the silica surface (Basri et al., 2020). Furthermore, the agglomerated structure is typically the result of incomplete burning or uneven distribution of silica particles, which causes them to cluster together. Figure 4.10A also shows clusters of silica particles, which are attributed to their amorphous nature and high surface area. These characteristics correspond to the XRD peaks for RHA shown in Appendix A11, which confirms its effectiveness as a silica source for geopolymerisation. The amorphous structure of RHA enhances its reactivity, which makes it a viable replacement for sodium silicate. Similarly, the SEM micrograph in Figure 4.10B reveals that the particles of raw SF appear as agglomerates that consist of extremely fine primary particles. The SF is also composed of rounded particles with high sphericity. The small particle size increases the specific surface area of the SF, which renders it more chemically reactive (Uzbas & Aydin, 2020). Furthermore, the absence of crystalline features supports SF's effectiveness as a highly reactive pozzolanic material. These characteristics make SF highly reactive and beneficial as an activator, particularly in enhancing the microstructure and durability of GPC.

In contrast, Figure 4.10C shows that GWP consists of angular particles with sharp edges and smooth surfaces. Unlike SF and RHA, GWP particles are generally non-porous, as evidenced by the lack of internal voids or porosity in the micrograph. The smooth surface and lack of porosity in the GWP may limit its reactivity compared to more porous materials such as SF and RHA. Furthermore, its amorphous nature is advantageous for participating in geopolymerisation, which forms C-S-H or N-A-S-H. These microstructural features of GWP help to assess its role in enhancing the physical and chemical properties of GPC (Xiao et al., 2020).

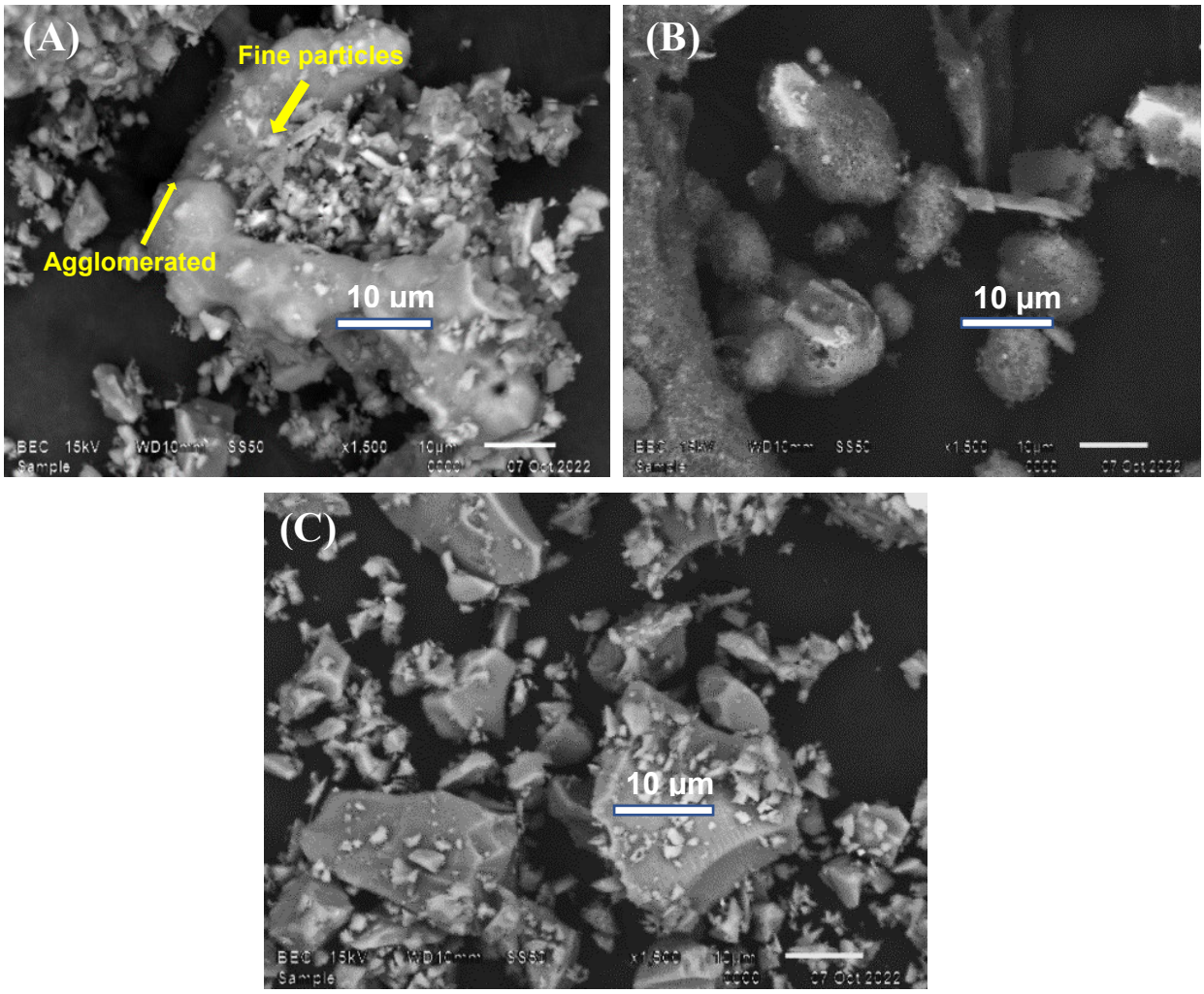

Figure 4.10: SEM features of raw materials of A) RHA, B) SF, and C) GWP

Figure 4.11 represents the microstructure observed through SEM analysis. It reveals significant changes corresponding to variations in 6 M and 8 M molarity of different silica sources. Across all samples, there was an evident presence of both spherical particles, likely undissolved fly ash particles, which are evenly dispersed in the amorphous geopolymeric matrix. Figure 4.11B displays a denser matrix and a lower amount of unreacted fly ash compared to Figure 4.11A. This can be attributed to the fact that higher sodium hydroxide concentrations promote greater dissolution of fly ash particles, and the geopolymeric gel formed at higher sodium hydroxide concentrations tends to have better connectivity between particles, which leads to improved compressive strength from 61 MPa to 87 MPa for SF-6M-OF and SF-8M-OF, respectively (Wang et al., 2022). Furthermore, Figure 4.11B exhibits a very distinct and strong interfacial transition zone

(ITZ) phase. This is attributed to the spherical shape of the SF particles, which promote uniform packing in the concrete matrix. This uniformity helps to bridge the gap between the aggregate and binder, which enhances the overall microstructure and leads to a more distinct ITZ phase. As a result, the bond strength and durability at the aggregate-paste interface are improved. Figure 4.11C displays a higher presence of unreacted fly ash particles and a less densely packed binder matrix compared to Figure 4.11A. This observation aligns with the findings regarding compressive strength, which indicate that RHA results in lower strength than SF. However, Figure 4.11D shows a more efficient dissolution of fly ash compared to Figure 4.11C. The micrographs for lower molarity samples show more distinct white spherical fly ash particles that have not been fully incorporated into the gel matrix, while higher molarity samples show a cohesive structure with fewer visible fly ash particles. This result can also be linked to the higher concentrations of sodium hydroxide, which, in turn, result in elevated compressive strength. Specifically, the compressive strengths for Mix RHA-6M-OF and Mix RHA-8M-OF were measured at 19 MPa and 50 MPa, respectively. In Figure 4.11E, a porous binder matrix is evident, along with a higher amount of unreacted fly ash particles compared to Figures 4.11A to 4.11F. The observed pore structure in the mortars containing glass particles is likely due to the presence of aluminium in the glass composition. During the reaction with sodium hydroxide, the aluminium in the glass reacts, which leads to the formation of dihydrogen gas (H_2) and sodium aluminate ($NaAl_2O_2$) (Kawalu et al., 2022). This chemical reaction contributes to the creation of pores in the binder matrix, which can influence the material's properties, such as permeability and mechanical strength. Overall, the 8 M samples showed better gel formation and fewer unreacted particles, regardless of the silica source. The higher sodium hydroxide concentration accelerates geopolymerisation, which improves microstructural integrity. Furthermore, the SF exhibited the most uniform and reactive behaviour, followed by RHA and GWP. This aligns with the compressive strength results in Section 4.2.

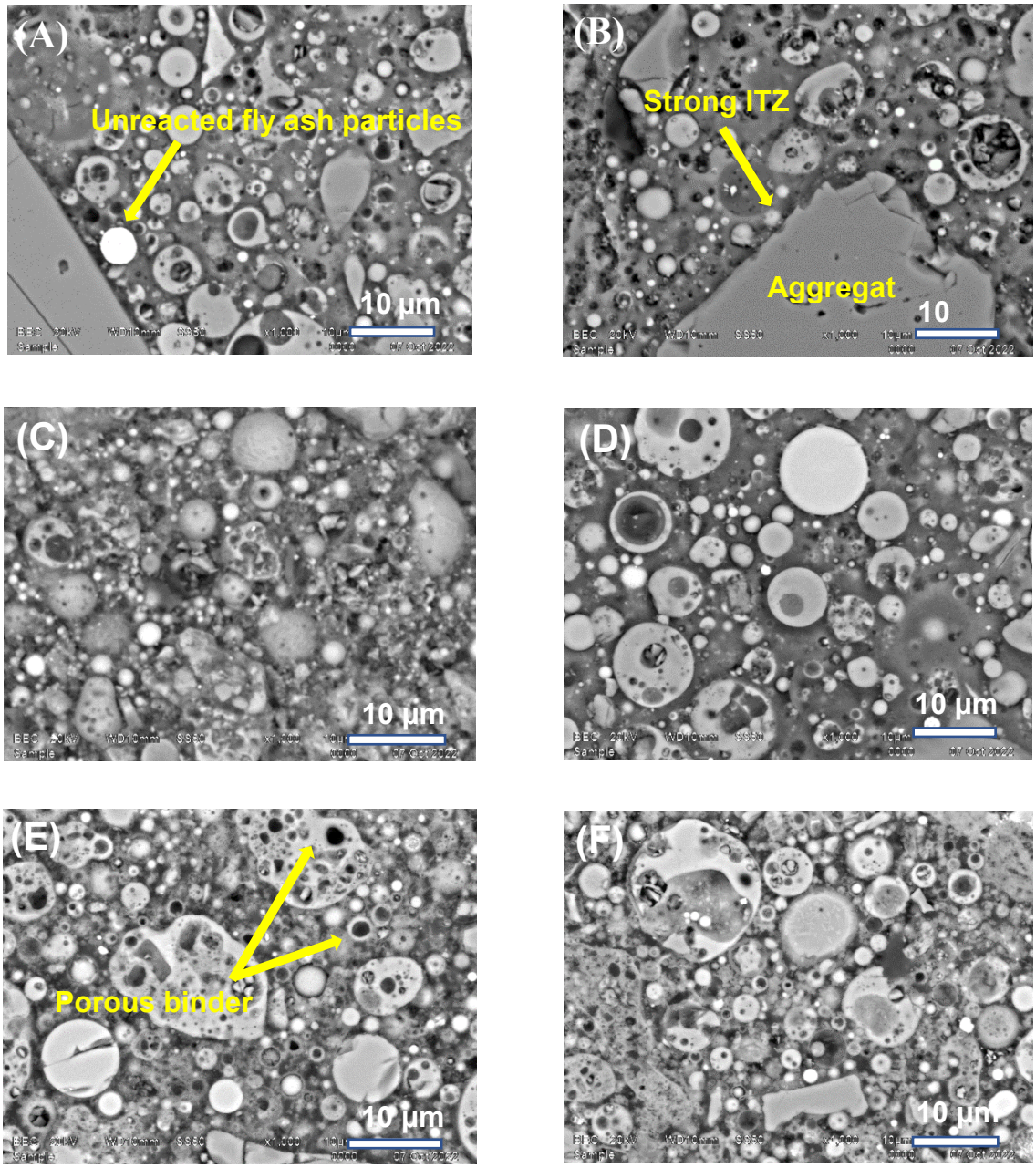

Figure 4.11: SEM features of fly ash geopolymer mortars activated using filtered activators of A) SF-6M-OF, B) SF-8M-OF, C) RHA-6M-OF, D) RHA-8M-OF, E) GWP-6M-OF, and F) GWP-8M-OF

Figure 4.12 presents the microstructure observed through SEM analysis of seven-day oven-cured fly ash / GGBS geopolymer samples based on 0% GGBS and 30% GGBS activated with a 6 M sodium hydroxide unfiltered SF activator solution. Figure 4.12A shows that most particles appear spherical in shape, with a few irregular particles present, which suggests a relatively smooth surface texture. In contrast, Figure 4.12B reveals

particles with rough and angular shapes, which indicates a rougher surface texture. The rough and angular particles in the blended fly ash and GGBS geopolymer samples arise from the mechanical grinding process of GGBS and its interaction with the fly ash during geopolymerisation. This angularity can also contribute to improved mechanical interlocking in the matrix due to the presence of C-A-S-H gel, which enhances compressive strength and durability (Haruna et al., 2020). A study by Banchhor et al. (2022) concluded that materials with rough and angular surfaces, like those in Figure 4.12B, tend to have higher water absorption capacities than materials with smoother surfaces, such as those in Figure 4.12A. This is because the irregular surface features provide more sites for water to adhere to or be absorbed. Based on the SEM images and the characteristics described, it can therefore be concluded that blended fly ash / GGBS geopolymers are more likely to have a higher water absorption capacity than geopolymers based solely on fly ash. A similar phenomenon was observed in the durability results (see Section 4.6), where the porosity of the 70% fly ash / 30% GGBS sample was better than that of the 100% fly ash / 0% GGBS sample. In this case, the findings showed that the sample with no GGBS absorbed more water than the sample with GGBS. Additionally, the compressive strength results were consistent with this observation. As shown in Section 4.2, mixes that contain a blend of GGBS and fly ash exhibited higher compressive strength than those without GGBS. It can therefore be concluded that the 30% GGBS mix is more suitable compared to the 0% GGBS mix.

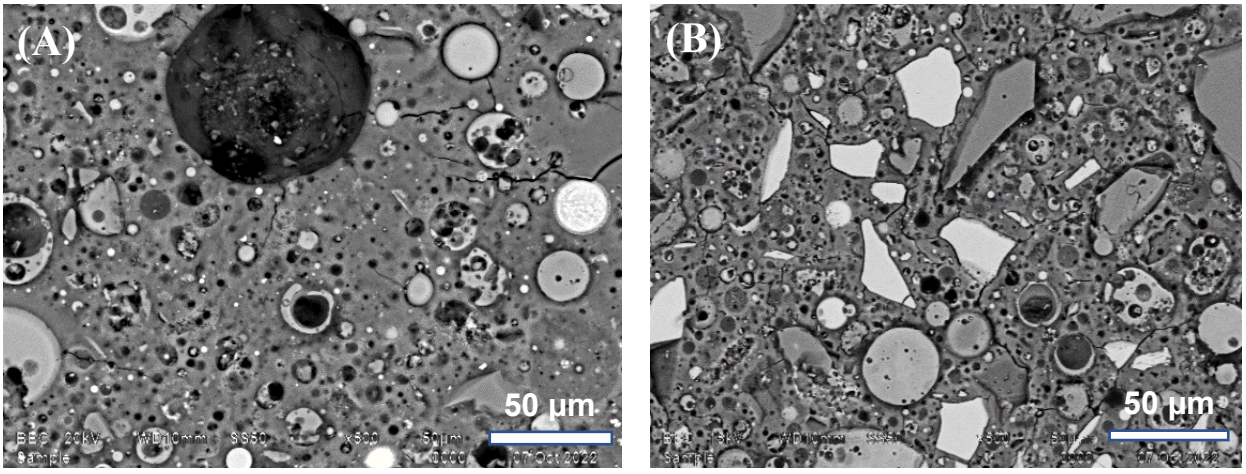

Figure 4.12: SEM features of seven-days oven-cured unfiltered geopolymer mortars based on A) 100% fly ash-0% GGBS and B) 70% fly ash-30% GGBS

Figure 4.13 shows the microstructure of fly ash / GGBS geopolymer mortar samples prepared using an unfiltered alternative activator. The mortar samples were cured at ambient temperature and in an oven for seven and 28 days. Figure 4.13A reveals the initial stages of geopolymerisation by showing the formation of reaction products and a binding matrix between the fly ash and GGBS particles. The presence of GGBS introduces an additional supply of calcium, which leads to the formation of an extra binding product. This, in turn, affects the setting behaviour of the geopolymer mixture (Bouaissi et al., 2019). This conclusion aligns with the setting time results, which showed a significant reduction when GGBS was incorporated into the mix (see Section 4.4). Additionally, the microstructure in Figure 4.13A exhibits some porosity, which can lead to reduced compressive strengths. The SEM micrograph in Figure 4.13B shows further development of the geopolymer structure, with densification of the matrix and reduced porosity compared to Figure 4.13A. These findings align with the durability results highlighted in Section 4.6. However, Figure 4.13B also reveals microcracks, which may have originated from the mechanical testing process, as these samples had already undergone compressive strength testing.

The SEM analysis of a seven-day ambient-cured sample (see Figure 4.13A) and a seven-day oven-cured sample (see Figure 4.13C) exhibited differences primarily in microstructural characteristics and the extent of geopolymerisation. Figure 4.13A reveals distinct unreacted fly ash and GGBS particles, which resulted in a less cohesive gel matrix with visible voids and incomplete gel formation, while Figure 4.13C shows a more uniform and compact gel network with fewer visible voids as the fly ash and GGBS particles were incorporated into the gel matrix. In the case of Figure 4.13A, the microstructure shows the initial stages of geopolymerisation and matrix formation between the particles. However, the curing process is slower under ambient conditions; the degree of geopolymerisation and hydration may therefore be relatively limited (Rao & Kumar, 2020). On the other hand, the sample in Figure 4.13C was subjected to higher temperatures during the curing process, which accelerated the geopolymerisation reaction. As a result,

the microstructure demonstrates more advanced stages of geopolymerisation and hydration compared to the sample in Figure 4.13A. Additionally, the binding matrix between particles was denser. Overall, it can be concluded that ambient curing results in a less dense and less reactive microstructure with visible unreacted particles, while oven curing facilitates a more homogeneous and densely packed structure that leads to improved mechanical properties and durability. To obtain optimal results for this specific mix, the samples should therefore be oven-cured for seven days or, alternatively, cured under ambient conditions for 28 days or longer.

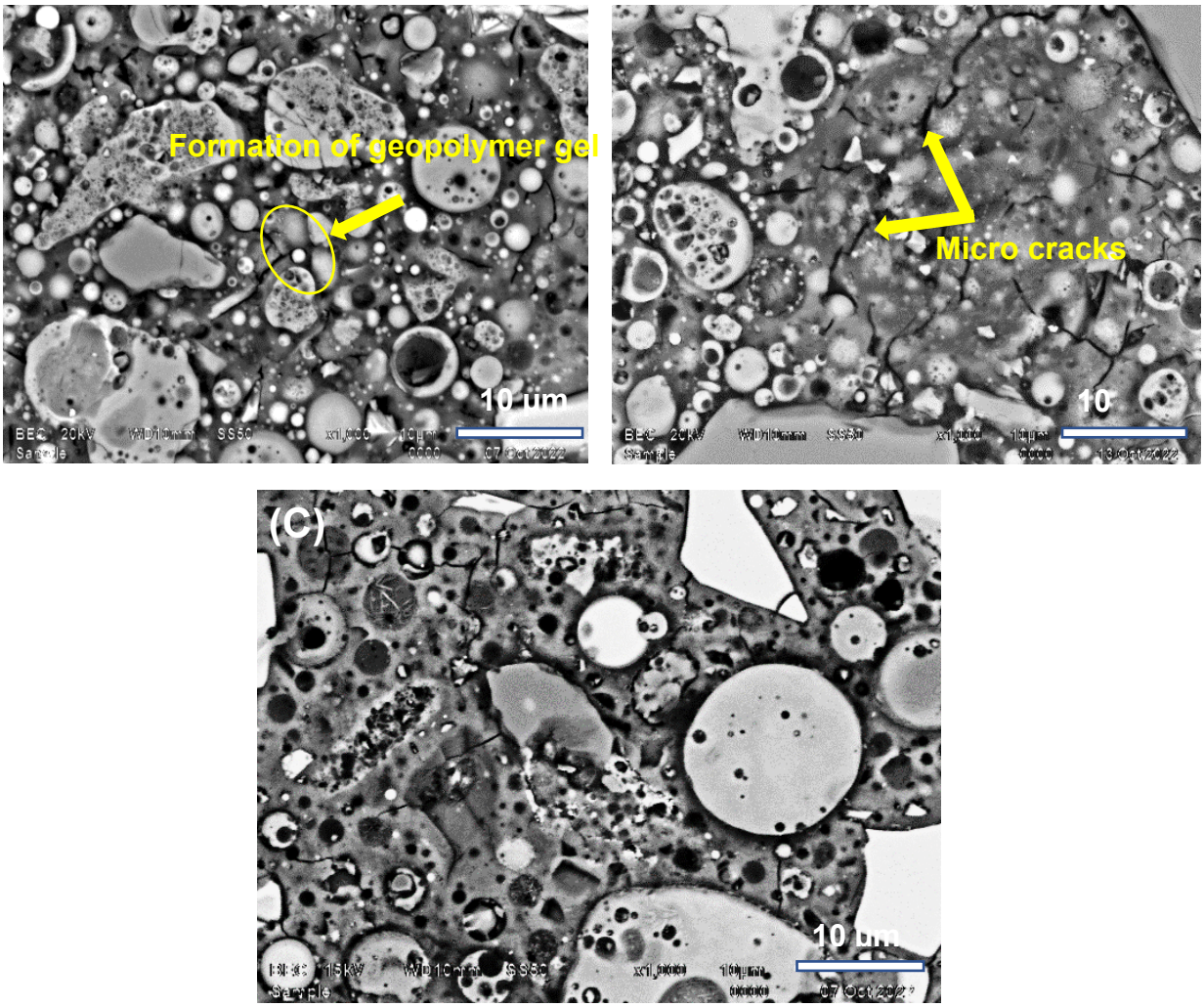

Figure 4.13: SEM features of 30% GGBS unfiltered geopolymer mortars based on A) seven days ambient-cured, B) 28 days ambient-cured, and C) seven days oven-cured

4.8 Summary of the results and discussion

The test results outlined above highlight the variations in the compressive strength, microstructure, and durability of the hardened concrete. Additionally, fresh properties such as workability and setting time were examined. The influence of curing conditions was also analysed as part of the hardened properties. Compressive strength served as a key benchmark for evaluating various parameters to determine the optimum mix. These parameters included the effect of the silica source / sodium hydroxide ratio, the effect of sodium hydroxide concentration, the effect of the GGBS ratio, and the impact of the curing period. A conventional mix (activated with sodium silicate and sodium hydroxide) was used as a reference for assessing the effect of the curing period.

Once the optimum mix was identified, the fresh properties were evaluated, with workability compared to the conventional mix. The durability of the optimum mix was then assessed using durability index tests, including oxygen permeability, water sorptivity, and chloride conductivity. Furthermore, the microstructural properties of mortar samples containing different silica sources were investigated to better understand variations in the geopolymer matrix. XRD and SEM analyses were conducted, with XRD results presented for both the raw materials (GWP, RHA, and SF) and geopolymerised mortars activated with different silica sources at 6 M and 8 M sodium hydroxide concentrations, maintaining a constant silica source / sodium hydroxide ratio of 1.3. All the results were analysed and discussed throughout this chapter. The conclusions of the results are discussed further in Chapter 5.

CHAPTER 5:
CONCLUSIONS AND RECOMMENDATIONS

5.1 Conclusions

This chapter presents the conclusions drawn from the results and discussions in Chapter 4, which assessed the influence of alkali activators derived from different silica sources intended to replace conventional sodium silicate in fly ash and fly ash / GGBS-based GPC. This assessment was conducted by determining the optimum mix based on both fresh and hardened properties. Various parameters, including sodium hydroxide concentration, silica source / sodium hydroxide ratio, and GGBS ratio, influenced the fresh and hardened properties of the geopolymer mortars. The effect of each parameter was therefore measured based on compressive strength. The following were the significant findings:

- The findings from this study demonstrated a positive correlation between the compressive strength of the geopolymer mixture and the silica source / sodium hydroxide ratio, which increased from 1 to 1.3. However, when the ratio surpassed 1.3, the compressive strength began to decrease, particularly for SF and RHA. Hence, 1.3 was concluded to be the optimum ratio. Furthermore, among the three silica sources, SF achieved the highest strengths compared to RHA and GWP. The best-performing silica source was thus identified as SF. In this case, two aspects of the optimum mix (the silica source material and the silica source / sodium hydroxide ratio) were established.

- The concentration of sodium hydroxide plays a significant role in the geopolymerisation process and directly influences the properties of fly ash-based geopolymer mortars. The results indicated that compressive strength improves with increasing sodium hydroxide concentration while maintaining a constant silica source to sodium hydroxide ratio of 1.3. This is due to the formation of a more compact and homogeneous gel matrix. However, excessively high concentrations (above 10 M or 12 M) may lead to rapid setting and cracking due to shrinkage,

which compromises overall performance. Selecting the appropriate sodium hydroxide concentration is therefore critical for achieving a balance between workability, strength, and durability. Six M was therefore selected as the optimal sodium hydroxide concentration. In this case, the molarity of the optimum mix was established.

- The impact of varying GGBS ratios was also examined. The findings revealed that the highest strengths, reaching 49 MPa after seven days and 82 MPa after 28 days of ambient curing, were attained with a 40% increase in GGBS content. It can therefore be concluded that high GGBS content results in higher compressive strength. This finding not only supports the inclusion of GGBS in the optimum mix but also indicates how much GGBS should be incorporated. Although the 40% GGBS mix achieved the highest strengths, the literature review suggests that this mix can sometimes lead to early strength reduction. A 30% GGBS mix was thus chosen as the optimum GGBS proportion. In this case, the ratio of fly ash to GGBS in the optimum mix was established. GGBS was included in the mix for better workability, faster curing under ambient conditions, and enhancement of compressive strength, as observed in this case.

- Furthermore, the impact of the curing period on 70% fly ash / 30% GGBS GPC was analysed by comparing mixes activated with the conventional activator (sodium silicate + 8 M sodium hydroxide) and the alternative activator (SF + sodium hydroxide) under ambient conditions for three, seven, 28, and 90 days. The highest strength recorded was 81 MPa for the conventionally activated concrete, while the alternative activated concrete achieved a strength of 76 MPa. Although the alternative activator, at a lower concentration of 6 M, obtained a lower compressive strength than the conventional activator at a higher concentration of 8 M, it still demonstrated outstanding performance. In this case, the alternative activated mix proved to be a viable replacement for the conventionally activated mix in GPC with respect to compressive strength. Samples were thoroughly prepared to assess the fresh properties of fly ash / GGBS geopolymer mortar

mixtures using the optimal mix. Workability, setting time, and pH (activator solution) measurements were used as indicators to evaluate these fresh properties. The proportion of GGBS in the binder varied, ranging from 0% to 40%.

- The flow workability results for the 8 M conventional sodium silicate mixes showed an initial increase in flow at a 20% GGBS dosage, followed by a sudden decrease as the GGBS dosage increased further. In contrast, the 6 M alternative activator demonstrated a consistent decrease in flow workability with increasing GGBS dosage. According to the ASTM standards, the recommended range for geopolymer mortar flow workability is 140 mm to 200 mm. Based on the results of this study, the alternative activator achieved the best flow performance of 150 mm when no GGBS was included in the mix. Meanwhile, two of the conventional activator mixes (with 20% and 30% GGBS) exhibited excessively high, runny flow workability. The alternative activator with 0% GGBS was therefore deemed a viable replacement for the conventional activator.

- The setting time results for the alternative active mix indicated longer setting periods under ambient conditions when no GGBS was included. The addition of GGBS to the mix significantly reduced both the initial and final setting times. It can thus be concluded that incorporating GGBS into the binder significantly decreased the setting time. According to the literature review, the conventional activated mix without GGBS achieved a setting time of approximately 1 500 minutes, which aligns with the results of this study. It can therefore be concluded that the alternative activator mix is a suitable (if not better) replacement for the conventional mix concerning setting time performance.

- The pH levels of the alkaline solutions were assessed to determine whether any of the silica sources in this study could serve as suitable replacements for conventional sodium silicate. The solutions analysed had the same sodium hydroxide molarity (6 M) and varied silica source / sodium hydroxide ratios ranging from 1.0 to 1.5. The results showed that the pH values of GWP, RHA, and SF

solutions decreased as the silica source / sodium hydroxide ratio increased. This reduction is attributed to the consumption of hydroxide ions by the silica source at higher ratios. Additionally, the findings revealed that the silica source with the highest pH values (GWP) yielded the lowest compressive strength, while the source with the lowest pH values (SF) produced the highest compressive strength. According to the literature, the recommended pH range for geopolymer solutions is between 13 and 14, which is consistent with the range observed in this study. It can therefore be concluded that all three silica sources (GWP, SF, and RHA) are viable alternatives to conventional sodium silicate.

- In this study, fly ash-based geopolymers incorporating GGBS were synthesised and analysed. Key emphasis was placed on examining the correlation between the mechanical properties of the samples and their composition and microstructure. The durability characteristics and microstructural analyses were investigated and discussed. The durability characteristics were evaluated using the oxygen permeability index test, the water sorptivity index test, and the chloride conductivity test. For this analysis, Mix 13 (prepared with a conventional activator and adopted from a similar study) served as the reference mix. The oxygen permeability index results for mixes with 0%, 20%, and 40% GGBS content showed a higher resistance to gas penetration compared to Mix 13. The permeability of these mixes was rated as good to excellent for all GGBS levels, except for the 30% GGBS mix, which exhibited poorer performance, likely due to uneven gel formation. The mix with 40% GGBS achieved the highest compressive strength of 82 MPa at an oxygen permeability index of 9.9. This indicates that a denser microstructure, which is typically associated with higher compressive strength, contributes to the lower permeability observed in samples with higher oxygen permeability index values.

- Furthermore, the observed trends in water sorptivity indicated results similar to those of the oxygen permeability index. All the mixes, except for the 30% GGBS mix, achieved “excellent” performance. The 20% mix obtained the best water

sorptivity index of 3.1 mm/hr$^{0.5}$, which can be attributed to the formation of a dense and cohesive microstructure that minimises interconnected pores, which reduces water absorption and sorptivity. However, the 30% mix exhibited the weakest water sorptivity index of 5.8 mm/hr$^{0.5}$ due to uneven gel formation. This inconsistency results in a less compact microstructure, which increases matrix permeability and allows greater water ingress and subsequently leads to higher water sorptivity in the 30% GGBS mix.

- Porosity and sorptivity are interconnected factors that significantly influence durability. The 0% GGBS mix exhibited the highest porosity at 13.4%, which was rated as poor to very poor, while the 40% GGBS mix recorded the lowest porosity at 10.2%, which was rated as good to poor. The 20% GGBS mix achieved a porosity value of 12% (good to poor), whereas the 30% GGBS mix registered 12.3% (poor to very poor). Mix 13, using the conventional activator, achieved a porosity value of 9.98%, which was classified as excellent. This suggests that the conventional activator mix outperformed the alternative activator mix in terms of porosity. However, the alternative activator mix exhibited a compressive strength that was 15.79% higher than the conventional mix, which was attributed to the formation of both N-A-S-H and C-A-S-H gels. It can thus be concluded that alternative activator mix samples are more porous and exhibit a higher wetting rate than conventional mix samples. Additionally, the results suggested that exceeding a GGBS content threshold, potentially around 30% or 40%, may negatively impact the geopolymerisation process.

- The chloride conductivity index results indicated that the 100% fly ash-based GPC (with no GGBS) exhibited the highest chloride conductivity value of 3.3 mS/cm. In contrast, the 40% GGBS mix achieved the most favourable outcome, recording the lowest chloride conductivity value of 1.0 mS/cm, which falls within the range for good chloride conductivity. This highlights that replacing fly ash with slag significantly reduces chloride ion permeability in GPC. Additionally, GPC activated with the alternative activator exhibited greater chloride ion penetration due to a

less dense matrix and higher pore connectivity compared to the conventional activator. As a result, the conventional activator proved to be the most viable option compared to the alternative activator in this case.

- The XRD analysis revealed consistent quartz and mullite peaks in both the raw materials and fly ash geopolymer mortar samples, which indicated minimal changes to the crystalline phases during geopolymerisation. The amorphous phase of fly ash was identified as the most reactive component. No significant differences were observed in the XRD patterns of the SF-6M-OF and SF-6M-OU samples, which suggested that the filtration of the alkaline solution and variations in sodium hydroxide concentration did not affect phase formation. However, the GWP samples exhibited the formation of new elements that reduced compressive strength, which made SF the most suitable silica source due to its stable phases and higher strength.

- The SEM analysis highlighted that increasing sodium hydroxide molarity in fly ash-based and fly ash / GGBS-based geopolymers reduced the number of unreacted fly ash particles and created a denser matrix. Higher GGBS content led to rougher surfaces and greater water absorption. SF proved to be the most effective silica source, followed by RHA and GWP. Blended GGBS and fly ash mixes, particularly the 30% GGBS mix, achieved higher compressive strength than mixes without GGBS. Curing methods significantly impacted the microstructure; ambient curing resulted in a less reactive and less dense matrix, while oven curing produced a more compact structure that enhanced the mechanical properties and durability. Optimal results were achieved with seven days of oven curing or at least 28 days of ambient curing.

- Overall, replacing sodium silicate with an alkali-activator solution of SF/6 M sodium hydroxide at a 1.3 ratio was concluded to be the most effective alternative. This conclusion is mainly supported by findings related to compressive strength and durability. The incorporation of GGBS also resulted in improved mechanical

properties of fly ash-based geopolymers, based on acceptable fresh properties such as workability and setting time. Additionally, the durability index test results confirmed that the optimal mix samples are durable in various environments, except under chloride conditions. Therefore, the results achieved are considered satisfactory and indicate a positive impact on the overall performance of the materials.

5.2 Recommendations

The following recommendations are made:

5.2.1 Standardisation of Activator Preparation Across All Mixes

- Future studies should adopt uniform preparation protocols for both conventional and alternative activator systems. Using a conventional activator sourced from previous studies introduces variability in concentration, purity, and preparation methods. To minimise bias and ensure comparability, both activators should be prepared in-house under identical conditions, using matched molar ratios, mixing durations, and curing regimes. This standardisation will improve replicability and allow more accurate evaluation of performance differences attributable to silica source alone.

5.2.2 Comprehensive Screening of All Potential Silica Sources

- Only a subset of silica sources was fully evaluated in the present study. To strengthen the scientific basis for selecting optimal alternatives to sodium silicate, future work should include:
  - full mechanical testing (early age and long term)
  - fresh-state behaviour (workability, setting time, rheology)
  - durability performance (permeability, sorptivity, chloride ingress, shrinkage, chemical resistance)

A multi criteria assessment framework rather than focusing on early test results alone will allow the identification of silica sources that may perform better at later ages or under specific curing conditions.

5.2.3 Optimisation Studies on L/S Ratio for Alternative Activators

- The observation that liquid to solid (L/S) ratios above 0.45 resulted in flash setting highlights the need for systematic optimisation. Future studies should:
  - investigate a range of L/S ratios below 0.45, for example 0.35–0.45
  - analyse the effect of L/S ratio on reaction kinetics using calorimetry
  - correlate setting behaviour with microstructural development through XRD, FTIR, or SEM

This work would help establish a scientifically grounded L/S range for safe, workable mixes when adopting alternative silica sources.

5.2.4 Increased Sample Size for Durability Index Testing

- Durability assessment requires multiple concrete discs per test, and sample losses during coring/cutting can compromise statistical reliability. Future studies should prepare a larger batch of ambient cured specimens, especially when testing unfamiliar activators. This ensures robust datasets for durability indices such as:
  - oxygen permeability
  - water sorptivity
  - chloride conductivity

Increasing sample size will also improve the confidence level of results and make them more comparable to standard durability classifications.

5.2.5 Microstructural and Chemical Characterisation of Reaction Products

- To better understand why certain silica sources perform differently, future research should incorporate comprehensive microstructural analysis, including:
  - SEM/EDS for morphology and elemental distribution
  - XRD for crystalline phases
  - FTIR or NMR for gel chemistry identification

These tests will provide insight into the geopolymerisation mechanism for each silica source and help explain the relationships between activator chemistry, setting behaviour, and long term performance.

5.2.6 Long Term Durability and Environmental Exposure Testing

- While standard durability indices offer valuable insights, real world performance requires extended testing, such as:
  - accelerated carbonation
  - sulfate and acid resistance
  - freeze-thaw cycling
  - thermal stability and fire exposure

These tests are essential for determining whether alternative silica sources remain viable under harsh environmental conditions.

5.2.7 Economic and Sustainability Assessments

- Given that one of the motivations for alternative silica sources is sustainability, future studies should include:
  - life cycle assessment (LCA)
  - cost benefit analysis
  - availability and supply chain considerations

This will help determine whether the alternative silica sources are not only technically feasible but also economically and environmentally advantageous.

REFERENCES

Abdullah, M. M. A., Hussin, K., Bnhussain, M., Ismail, K. N. & Ahmad, M. I. (2011) 'Chemical reactions in the geopolymerisation process using fly ash-based geopolymer: A review', *Australian Journal of Basic and Applied Sciences*, 5(7), pp. 1199–1203.

Abdullah, M. M. A., Kamarudin, H., Mohammed, B., Nizar, K. I., Rafiza, A. R. & Zarina, Y. (2011) 'The relationship of NaOH molarity, Na_2SiO_3/NaOH ratio, fly ash/alkaline activator ratio, and curing temperature to the strength of a fly ash-based geopolymer', *Advanced Materials Research*, 328–330, pp. 1475–1482. doi:10.4028/www.scientific.net/AMR.328-330.1475.

ACI 318M-05 (2005) *Building Code Requirements for Structural Concrete and Commentary*. https://pulukcu.com/wp-content/uploads/2018/10/ACI-318-Metric-2005.pdf.

Adjei, S., Elkatatny, S., Aggrey, W. N. and Abdelraouf, Y. (2021) 'Geopolymer as the future oil-well cement: A review', *Journal of Petroleum Science and Engineering*, 208(PB), 109485. doi:10.1016/j.petrol.2021.109485.

Aiken, T. A., Kwasny, J., Sha, W. & Soutsos, M. N. (2018) 'Effect of slag content and activator dosage on the resistance of fly ash geopolymer binders to sulfuric acid attack', *Cement and Concrete Research*, 111, pp. 23–40.

Al Bakri, M. M., Mohammed, H., Kamarudin, H., Niza, K. I. & Zarina, Y. (2011) 'Review of fly ash-based geopolymer concrete without Portland cement', *Journal of Engineering and Technology Research*, 3, pp. 1–4.

Albidah, A., Alghannam, M., Abbas, H., Almusallam, T. & Al Salloum, Y. (2021) 'Characteristics of metakaolin-based geopolymer concrete for different mix design parameters', *Journal of Materials Research and Technology*, 10, pp. 84–98. doi:10.1016/j.jmrt.2020.11.104.

Alexander, K., Ballim, M. & Stanish, Y. (2008) 'A framework for use of durability indexes in performance-based design and specifications for reinforced concrete structures', *Materials and Structures*, 41, pp. 921–936. https://doi.org/10.1617/s11527-007-9295-0.

Alexander, M. (2004) 'Durability indexes and their use in concrete engineering', in *Proceedings of the Conference: International RILEM Symposium on Concrete Science and Engineering: A Tribute to Arnon Bentur*, pp. 9–22. https://www.researchgate.net/publication/269152809_Durability_indexes_and_their_use_in_concrete_engineering.

Alexander, M., Ballim, Y. & Mackechnie, J. M. (2018) 'Durability Index Testing Procedure Manual', *Research Monograph No.4*. https://www.scribd.com/document/455609588/Durability-Index-Testing-Procedure-Manual

Alexander, M. & Mackechnie, J. (2003) 'Concrete mixes for durable marine structures', *Journal of the South African Institution of Civil Engineering*, 45(2), pp. 20–25.

Aliabdo, A. A., Abd Elmoaty, A. E. M. & Salem, H. A. (2016) 'Effect of water addition, plasticizer and alkaline solution constitution on fly ash based geopolymer concrete performance', *Construction and Building Materials*, 121, pp. 694–703. doi:10.1016/j.conbuildmat.2016.06.062.

Aliques-Granero, J., Tognonvi, M. T. & Tagnit-Hamou, A. (2019) 'Durability study of AAMs: Sulfate attack resistance', *Construction and Building Materials*, 229, 117100. https://doi.org/10.1016/j.conbuildmat.2019.117100.

Al-Majidi, M. H., Lampropoulos, A., Cundy, A. & Meikle, S. (2016) 'Development of geopolymer mortar under ambient temperature for in situ applications', *Construction and Building Materials*, 120, pp. 198–211. doi:10.1016/j.conbuildmat.2016.05.085.

Al-Majidi, M. K. H. (2017) Development of Fibre Reinforced Geopolymer Concrete (FRGC) Cured Under Ambient Temperature for Strengthening and Repair of Existing Structures. Doctoral Dissertation, University of Brighton.

Amran, M., Al Fakih, A., Chu, S.H., Fediuk, R., Haruna, S., Azevedo, A. & Vatin, N. (2021) 'Long-term durability properties of geopolymer concrete: An in-depth review', *Case Studies in Construction Materials*, 15(July), e00661. doi:10.1016/j.cscm.2021.e00661.

Amritphale, S., Bhardwaj, P. & Gupta, R., (2019) Advanced geopolymerization technology. In *Geopolymers and Other Geosynthetics*, edited by M. Alshaaer & H. Y. Jeon. London: IntechOpen. doi:10.5772/intechopen.87250.

Antoni, A., Wijaya, S. W. & Hardjito, D. (2016) 'Factors affecting the setting time of fly ash-based geopolymer', *Materials Science Forum*, 841(January), pp. 90–97. doi:10.4028/www.scientific.net/MSF.841.90.

Antoni, S. W., Wijaya, J. S., Sugiarto, A. & Hardjito, D. (2016) 'The use of borax in deterring flash setting of high calcium fly ash based geopolymer', *Material. Science Forum*, 857, pp. 416–420.

Arioz, E., Arioz, O. & Mete Kockar, O. (2012) 'An experimental study on the mechanical and microstructural properties of geopolymers', *Procedia Engineering*, 42, pp. 100–105. doi:10.1016/j.proeng.2012.07.399.

Assi, L., Ghahari, S., Deaver, E., Leaphart, D. & Ziehl, P. (2016) 'Improvement of the early and final compressive strength of fly ash-based geopolymer concrete at ambient conditions', *Construction and Building Materials*, 123, pp. 806–813. doi:10.1016/j.conbuildmat.2016.07.069.

Assi, L. N., Carter, K., Deaver, E. & Ziehl, P. (2020) 'Review of availability of source materials for geopolymer/sustainable concrete', *Journal of Cleaner Production*, 263, 121477. doi:10.1016/j.jclepro.2020.121477.

AS 3582.1 (1998) *AS 3582.1-1998: Supplementary Cementitious Materials for Use With Portland and Blended Cement, Part 1: Fly Ash*. https://www.standards.org.au/standards-catalogue/standard-details?designation=as-3582-1-1998.

ASTM (2008) *ASTM C230/C230M-08: Standard Specification for Flow Table for Use in Tests of Hydraulic Cement*. https://store.astm.org/c0230_c0230m-08.html.

ASTM (2008) *ASTM C403/C403M-08: Standard Test Method for Time of Setting of Concrete Mixtures by Penetration Resistance*. https://store.astm.org/c0403_c0403m-08.html.

ASTM (2012) *ASTM C143/C143M-12: Standard Test Method for Slump of Hydraulic-Cement Concrete*. https://standards.iteh.ai/catalog/standards/astm/7ea197bd-7856-4937-a4bd-8b61f868f6
c1/astm-c143-c143m-12?srsltid=AfmBOooOC2pXZIb5-
qL52JdOwnHBFaTFd3BQo1FuoOgGk
NoA-R7mZ1xB.

ASTM (2012) *ASTM C494/C494M-12: Standard Specification for Chemical Admixtures for Concrete*. https://store.astm.org/c0494_c0494m-12.html.

ASTM (2020) *ASTM C807-20: Standard Test Method for Time of Setting of Hydraulic Cement Mortar by Modified Vicat Needle*. https://store.astm.org/c0807-21.html.

ASTM (2021) *ASTM C 109/C 109M-21: Standard Test Method for Compressive Strength of Hydraulic Cement Mortars (Using 2-in. or [50 mm] Cube Specimens)*. https://store.astm.org/
c0109_c0109m-21.html.

Azad, N. M. & Samarakoon, S. M. S. M. K. (2021) 'Utilization of industrial by-products/waste to manufacture geopolymer cement/concrete', *Sustainability (Switzerland)*, 13(2), pp. 1–22. doi:10.3390/su13020873.

Babor, D. T., Plian, D. & Judele, L. (2009) 'Environmental impact of concrete', *Bulletin of the Polytechnic Institute of Jassy, Constructions. Architecture Section*, 4, pp. 27–36.

Bajpai, R., Shrivastava, A. & Singh, M. (2020) 'Properties of fly ash geopolymer modified with red mud and silica fume: A comparative study', *SN Applied Sciences*, 2(11), pp. 1–16. doi:10.1007/s42452-020-03665-3.

Bakharev, T. (2005) 'Resistance of geopolymer materials to acid attack', *Cement and Concrete Research*, 35(4), pp. 658–670.

Banchhor, S., Murmu, M. & Deo, S. V. (2022) 'Combined effect of fly-ash and GGBS on performance of alkali activated concrete', *Journal of Building Pathology and Rehabilitation*, 7(1), pp. 1–6. doi:10.1007/s41024-022-00170-5.

Basri, M. S. M., Mustapha, F., Mazlan, N. & Ishak M. R. (2020) 'Optimization of rice husk ash-based geopolymers coating composite for enhancement in flexural properties and microstructure using response surface methodology', *Coatings*, 10(2), pp. 1–18. doi:10.3390/coatings10020165.

Bellum, R. R., Venkatesh, C. & Choudhary, S. (2022) 'Effect of slag on strength , durability and microstructural characteristics of fly ash-based geopolymer concrete', *Journal of Building Pathology and Rehabilitation*, 7(1), 25. doi:10.1007/s41024-022-00163-4.

Bernal, S. A., Rodriguez, E. D., Kirchheim, A. P. & Provis, J. L. (2016) 'Management and valorisation of wastes through use in producing alkali-activated cement materials', *Journal of Chemical Technology and Biotechnology*, 91(9), pp. 2365–2388. doi:10.1002/jctb.4927.

Bernal, S. A., Rodriguez, E. D., Mejia de Gutierrez, R. & Provis, J. L. (2015) 'Performance at high temperature of alkali-activated slag pastes produced with silica fume and rice husk ash based activators', *Materiales de Construcción*, 65(318), 3049.

Beushausen, H. & Alexander, M. G. (2008) 'The South African durability index tests in an international comparison', *Journal of the South African Institution of Civil Engineering*, 50(1), pp. 25–31.

Bianco, I., Tomos, B. A. D. & Vinai, R. (2021) 'Analysis of the environmental impacts of alkali-activated concrete produced with waste glass-derived silicate activator – A LCA study', *Journal of Cleaner Production*, 316(5), 128383.

Bilgil, A. (2018) 'Geopolymers and their uses: Review', *IOP Conference Series: Materials Science and Engineering*, 373, 012019. doi:10.1088/1757-899X/374/1/012019.

Billong, N., Oti, J. & Kinuthia, J. (2021) 'Using silica fume based activator in sustainable geopolymer binder for building application', *Construction and Building Materials*, 275, 122177. doi:10.1016/j.conbuildmat.2020.122177.

Bondar, D., Nanukutta, S. V., Soutsos, M. N., Basheer, P. A. M. & Provis, J. L (2017) 'Suitability of alkali activated GGBS/fly ash concrete for chloride environments', *American Concrete Institute, ACI Special Publication*, 320, pp. 421–434.

Bouaissi, A., Li, L. & Al Bakri Abdullah, M. M. (2019) 'Mechanical properties and microstructure analysis of FA-GGBS-HMNS based geopolymer concrete', *Construction and Building Materials*, 210, pp. 198–209. doi:10.1016/j.conbuildmat.2019.03.202.

BS EN (2006) *BS 480-2:2006: Admixtures for Concrete, Mortar and Grout. Test Methods – Determination of Setting Time*. https://knowledge.bsigroup.com/products/admixtures-for-concrete-mortar-and-grout-test-methods-determination-of-setting-time.

BS EN (2011) *BS 197-1:2011: Cement – Composition, Specifications and Conformity Criteria for Common Cements*. https://knowledge.bsigroup.com/products/cement-composition-specifications-and-conformity-criteria-for-common-cements.

Carreño-Gallardo, C., Tejeda-Ochoa, A., Perez-Ordonez, O. I., Ledezma-Sillas, J. E., Lardizabal-Gutierrez, D., Prieto-Gomez, C., Valenzuela-Grado, J. A., Robles Hernandez, F. C. & Herrera-Ramirez, J. M. (2018) 'In the CO_2 emission remediation by means of alternative geopolymers as substitutes for cements', *Journal of Environmental Chemical Engineering*, 6(4), pp. 4878–4884. doi:10.1016/j.jece.2018.07.033.

Chakraborti, P. (2010) *Performance of Geopolymer Mortar Prepared by Blending Silica Fume With Fly Ash Civil*.

Chi, M. & Huang, R. (2013) 'Binding mechanism and properties of alkali-activated fly ash/slag mortars', *Construction and Building Materials*, 40, pp. 291–298

Chindaprasirt, P., Chareerat, T. & Sirivivatnanon, V. (2007) 'Workability and strength of coarse high calcium fly ash geopolymer', *Cement and Concrete Composites*, 29(3), pp. 224–229.

Chindaprasirt, P., Homwuttiwong, S. & Jaturapitakkul, C. (2007) 'Strength and water permeability of concrete containing palm oil fuel ash and rice husk-bark ash', *Construction and Building Materials*, 21(7), pp. 1492–1499.

Chindaprasirt, P. & Ridtirud, C. (2020) 'High calcium fly ash geopolymer containing natural rubber latex as additive', *International Journal of GEOMATE*, 18(69), pp. 124–129. doi:10.21660/2020.69.9321.

Cong, P. & Cheng, Y. (2021) 'Advances in geopolymer materials: A comprehensive review', *Journal of Traffic and Transportation Engineering (English Edition)*, 8(3), pp. 283–314. doi:10.1016/j.jtte.2021.03.004.

Cyr, M., Idir, R. & Poinot, T. (2012) 'Properties of inorganic polymer (geopolymer) mortars made of glass cullet', *Journal of Materials Science*, 47(6), pp. 2782–2797. doi:10.1007/s10853-011-6107-2.

Davidovits, J. (1989) 'Geopolymers and geopolymeric materials', *Journal of Thermal Analysis*, 35(2), pp. 429–441.

Davidovits, J. (1991) 'Geopolymers – Inorganic polymeric new materials', *Journal of Thermal Analysis*, 37(8), pp. 1633–1656. doi:10.1007/BF01912193.

Davidovits, J. (1994) 'Geopolymers: Man-made rock geosynthesis and the resulting development of very early high strength cement', *Materials Eduucation*, 16(2–3), pp. 1–25.

Davidovits, J. (2013) *Geopolymer Cement: A Review*. https://www.geopolymer.org/wp-content/uploads/GPCement2013.pdf.

Davidovits, J. (2018) 'Geopolymeric reactions in archaeological cements and in modern blended cements', *Geopolymer '88*, 1, pp. 93–106. https://www.researchgate.net/profile/Joseph-Davidovits/publication/284676426_Ancient_and_modern_concretes_what_is_the_real_difference/links/5be2b96892851c6b27aca353/Ancient-and-modern-concretes-what-is-the-real-difference.pdf.

Delgado-Plana P, Bueno-Rodríguez S, Pérez-Villarejo L, Eliche-Quesada D. (2025) 'Synthesis of solid sodium silicate from waste glass and utilization on one-part alkali-activated materials based on spent oil filtering earth.', Environ Sci Pollut Res Int., 32(48), pp. 27763-27785.

Dhinakaran, G. & Rajarajeswari, A. (2011) 'Compressive strength of fly ash-based geopolymer mortar', *IUP Journal of Structural Engineering*, IV(4), pp. 65–74.

Duan, P., Yan, C., Zhou, W. & Luo, W. (2015) 'Thermal behavior of Portland cement and fly ash–metakaolin-based geopolymer cement pastes', *Arabian Journal for Science and Engineering*, 40, pp. 2261–2269.

Duxson, P. (2007) 'Geopolymer technology: The current state of the art', *Journal of Materials Science*, 42(9), pp. 2917–2933. doi:10.1007/s10853-006-0637-z.

Duxson, P., Fernández-Jiménez, A., Provis, J. L., Lukey, G. C., Palomo, A. & Van Deventer, J. S. J. (2007) 'Geopolymer technology: The current state of the art', *Journal of Materials Science*, 42(9), pp. 2917–2933. https://doi.org/10.1007/s10853-006-0637-z.

Ekolu, S. (2014) *Potential South African Standard Sand for Cement Mortar Testing and Research*. https://ujcontent.uj.ac.za/esploro/outputs/bookChapter/Potential-South-African-standard-sand-for/999922207691.

Environmental, Health and Safety Solutions (2021) 'Sodium silicate', *Environmental, Health and Safety (EHS)*, 1, pp. 1–7.

Fang, G., Ho, W. K., Tu, W. & Zhang, M. (2018) 'Workability and mechanical properties of alkali-activated fly ash-slag concrete cured at ambient temperature', *Construction and Building Materials*, 172, pp. 476–487. doi:10.1016/j.conbuildmat.2018.04.008.

Faris, M. A., Al Bakri Abdullah, M. M., Sandu, A. V., Ismail, K. N., Moga, L. M., Neculai, O. & Muniandy, R. (2017) 'Assessment of alkali activated geopolymer binders as an alternative of portlant cement', *Materiale Plastice*, 54(1), pp. 145–154. doi:10.37358/mp.17.1.4806.

Fatima, R., Naseer, S., Gilani, M. R. H. S., Aamir, M. & Akhtar, J. (2023) Metal hydroxides. In *Sustainable Materials for Electrochemical Capacitors*, edited by T. A. Inamuddin & S. M. Adnan. Wiley Online Library, pp. 33–64.

Fernández-Jiménez, A., Palomo, A. & Criado, M. (2005) 'Microstructure development of alkali-activated fly ash cement: A descriptive model', *Cement and Concrete Research*, 35(6), pp. 1204–1209. doi:10.1016/j.cemconres.2004.08.021.

Fifinatasha, S. N., Mustafa Al Bakri, A. M., Kamarudin, H., Zarina, Y., Rafiza, A. R. & Liyana, J. (2013) 'Reviews on the different sources materials to the geopolymer performance', *Advances in Environmental Biology*, 7(S12), pp. 3835–3842.

Food and Agriculture Organization (FAO) (2018) *FAO Rice Market Monitor (RMM), April 2018*. https://openknowledge.fao.org/items/7b5d292f-ef49-4cb3-9746-919970ecab68.

Gouws, S. M., Alexander, M. G. & Maritz, G. (2001) 'Use of durability index tests for the assessment and control of concrete quality on site', *Concrete Beton*, 98(April), pp. 5–16.

Granizo, M., LuzBlanco-Varela, M. T. & Martínez-Ramírez, S. (2007) 'Alkali activation of metakaolins: Parameters affecting mechanical, structural and microstructural properties', *Journal of Materials Science*, 42(9), pp. 2934–2943.

Grubb, J. A., Limaye, H. S. & Kakade, A. M. (2007) 'Testing pH of concrete: Need for a standard procedure', *Concrete International*, 29, pp. 78–83.

Hamidi, R. M., Man, Z. & Azizli, K. A. (2016) 'Concentration of NaOH and the effect on the properties of fly ash-based geopolymer', *Procedia Engineering*, 148, pp. 189–193. doi:10.1016/j.proeng.2016.06.568.

Han, W., Lv, Y., Wang, S., Qiao, J., Zou, C., Su, M. & Peng, H. (2023) 'Effects of Al/Na and Si/Na molar ratios on the alkalinity of metakaolin-based geopolymer pore solutions', *Materials*, 16(5), 1929. doi:10.3390/ma16051929.

Handayani, L., Abdullah, A., Aprilia, S., Rahmawati, C., Mustafa Al Bakri, A. M., Aziz, I. H. & Azimi, E. A. (2021) 'Synthesis of sodium silicate from rice husk ash as an activator

to produce epoxy-geopolymer cement', *Journal of Physics: Conference Series*, 1845, 012072. doi:10.1088/1742-6596/1845/1/012072.

Hanjitsuwan, S., Hunpratub, S., Thongbai, P., Maensiri, S., Sata, V. & Chindaprasirt, P. (2014) 'Effects of NaOH concentrations on physical and electrical properties of high calcium fly ash geopolymer paste', *Cement and Concrete Composites*, 45(0958–9465), pp. 9–14.

Hardjito, D. (2005) Studies on Fly Ash-Based Geopolymer Concrete. Doctoral Dissertation, Curtin University of Technology.

Hariz, Z., Al Bakri Abdullah, M. M., Hussin, K., Ariffin, N. & Bayuaji, R. (2017) 'Review on various types of geopolymer materials with the environmental impact assessment', *MATEC Web of Conferences*, 97, 01021.

Haruna, S., Mohammed, B. S. & Wahab, M. M. (2020) 'Effect of GGBS slag on setting time and compressive strength of one-part geopolymer binders', *Journal of Infrastructure & Facility Asset Management*, 2(2) pp. 149–159. doi:10.12962/jifam.v2i2.7640.

Heath, A. & Paine, K. (2014) 'Minimising the global warming potential of clay based geopolymers', *Journal of Cleaner Production*, 78(0959–6526), pp. 75–83.

Heath, A., Paine, K. & McManus, M. (2014) 'Minimising the global warming potential of clay based geopolymers', *Journal of Cleaner Production*, 78, pp. 75–83.

Jang, J. G., Lee, N. K. & Lee, H. K. (2014) 'Fresh and hardened properties of alkali-activated fly ash/slag pastes with superplasticizers', *Construction and Building Materials*, 50(0950–0618), pp. 169–176.

Jegan, M., Annadurai, R. & Kannan Rajkumar, P. R. (2023) 'A state of the art on effect of alkali activator, precursor, and fibers on properties of geopolymer composites', *Case Studies in Construction Materials*, 18(May), e01891. doi:10.1016/j.cscm.2023.e01891.

Jo, B., Park, S. & Park, J. (2007) 'Properties of concrete made with alkali-activated fly ash lightweight aggregate (AFLA)', *Cement and Concrete Composites*, 29, pp. 128–135.

Joshi, S. V. & Kadu, M. S. (2012) 'Role of alkaline activator in development of eco-friendly fly ash based geo polymer concrete', *International Journal of Environmental Science and Development*, 3(5), pp. 417–421. doi: 10.7763/ijesd.2012.v3.258.

Kaduku, T., Daramola, M. O., Obazu, F. O. & Iyuke, S. E. (2015) 'Synthesis of sodium silicate from South African coal fly ash and its use as an extender in oil well cement applications', *Journal of the Southern African Institute of Mining and Metallurgy*, 115(12), pp. 1175–1182. doi:10.17159/2411-9717/2015/v115n12a5.

Kamseu, E., Beleuk a Moungam, L. M., Cannio, M., Billong, N., Chaysuwan, D., Melo, C. & Leonelli, C. (2017) 'Substitution of sodium silicate with rice husk ash-NaOH solution in metakaolin based geopolymer cement concerning reduction in global warming', *Journal of Cleaner Production*, 142, pp. 3050–3060. doi:10.1016/j.jclepro.2016.10.164.

Karthiyaini, S. (2016) 'Physicochemical propertiesof alkali activated fly ash based geopolymer concrete: A review', *International Journal of Earth Sciences and Engineering*, 9(6), pp. 2419–2426.

Katti, M., Jagadeesh, B and Katti, N. (2016) 'Experimental Investigation of Geopolymer Concrete Using Fly Ash And GGBS.' Pp. 404-410.

Kawalu, N., Naghizadeh, A. & Mahachi, J. (2022) 'The effect of glass waste as an aggregate on the compressive strength and durability of fly ash-based geopolymer mortar', *MATEC Web of Conferences*, 361, 05007. doi:10.1051/matecconf/202236105007.

Keawthun, M., Krachodnok, S. & Chaisena, A. (2014) 'Conversion of waste glasses into sodium silicate solutions', *International Journal of Chemical Sciences*, 12(1), pp. 83–91.

Khale, D. & Chaudhary, R. (2007) 'Mechanism of geopolymerization and factors influencing its development: A review', *Journal of Materials Science*, 42(3), pp. 729–746. doi:10.1007/s10853-006-0401-4.

Kumar, G. & Mishra, S. S. (2021) 'Effect of GGBFS on workability and strength of alkali-activated geopolymer concrete', *Civil Engineering Journal (Iran)*, 7(6), pp. 1036–1049. doi:10.28991/cej-2021-03091708.

Lahoti, E. M., Tan, K. H. & Yang, E. (2019) 'A critical review of geopolymer properties for structural fire-resistance applications', *Construction and Building Materials*, 221, pp. 514–526.

Lancellotti, I., Catauro, M., Ponzoni, C., Bollino, F. & Leonelli, C. (2013) 'Inorganic polymers from alkali activation of metakaolin: Effect of setting and curing on structure', *Journal of Solid State Chemistry*, 200, pp. 341–348.

Law, D. W., Adam, A. A., Molyneaux, T. K., Patnaikun, I. & Wardhono, A. (2014) 'Long term durability properties of class F fly ash geopolymer concrete', *Materials and Structures/Materiaux et Constructions*, 48(3), pp. 721–731. doi:10.1617/s11527-014-0268-9.

Lee, N. K., An, G. H., Koh, K. T. & Ryu, G. S. (2016) 'Improved reactivity of fly ash-slag geopolymer by the addition of silica fume', *Advances in Materials Science and Engineering*, 2016, 2192053. doi:10.1155/2016/2192053.

Lemougna, P. N., Nzeukou, A., Aziwo, B., Tchamba, A. B., Wang, U., Melo, C. & Cui, X. (2020) 'Effect of slag on the improvement of setting time and compressive strength of low reactive volcanic ash geopolymers synthetized at room temperature', *Materials Chemistry and Physics*, 239(June), 122077. doi:10.1016/j.matchemphys.2019.122077.

Leong, H. Y., Leong Ong, D. E., Jay, G. & Sanjayan, A. N. (2016) 'The effect of different Na_2O and K_2O ratios of alkali activator on compressive strength of fly ash based-geopolymer', *Construction and Building Materials*, 106(0950–0618), pp. 500–511.

Li, C., Sun, H. & Li, L. (2010) 'A review: The comparison between alkali-activated slag (Si + Ca) and metakaolin (Si + Al) cements', *Cement and Concrete Research*, 40(9), pp. 1341–1349. doi:10.1016/j.cemconres.2010.03.020.

Lima, J. S., Apolonio, P. H., Marinho, E. P., Vasconcelos, E. A., Nóbrega, A. C. V. & Freitas, J. C. O. (2021) 'Use of rice husk ash to produce alternative sodium silicate for geopolymerization reactions', *Ceramica*, 67(381), pp. 58–64. doi:10.1590/0366-69132021673812891.

Lin, K., Shiu, H., Shie, J., Cheng, T. & Hwang, C. (2012) 'Effect of composition on characteristics of thin film transistor liquid crystal display (TFT-LCD) waste glass-metakaolin-based geopolymers', *Construction and Building Materials*, 36, pp. 501–507.

Ling, Y. (2018) Proportion and Performance Evaluation of Fly Ash-Based Geopolymer and its Application in Engineered Composites. Doctoral Dissertation, Iowa State University.

Lloyd, N. A. & Rangan, B. V. (2010) Geopolymer concrete with fly ash. In *Proceedings of the Second International Conference on Sustainable Construction Materials and Technologies*, edited by J. Zachar, P. Claisse, T. Naik & G. Ganjian. Ancona: UWM Center for By-Products Utilization. pp. 1493–1504.

Lowitt, S. (2020) *Towards the Decarbonisation of the South African Cement Industry: Opportunities and Challenges*. https://www.tips.org.za/research-archive/sustainable-growth/green-economy-2/item/3888-towards-the-decarbonisation-of-the-south-african-cement-industry-opportunities-and-challenges.

Luukkonen, T., Abdollahnejad, Z., Yliniemi., J., Kinnunen, P. & Illikainen, M. (2018) 'Comparison of alkali and silica sources in one-part alkali-activated blast furnace slag mortar', *Journal of Cleaner Production*, 187, pp. 171–179. doi:10.1016/j.jclepro.2018.03.202.

Mackechnie, J. R. & Alexander, M. (2000) Practical considerations for rapid chloride conductivity testing. In *Proceedings of the Second International RILEM Workshop on Testing and Modelling the Chloride Ingress Into Concrete*, edited by C. Andrade & J. Kropp. pp. 451–459. France: RILEM Publications SARL.

Majidi, B. (2009) 'Geopolymer technology, from fundamentals to advanced applications: A review', *Materials Technology*, 24(2), pp. 79–87. doi:10.1179/175355509X449355.

Maochieh Chi, R. H. (2013) 'Binding mechanism and properties of alkali-activated fly ash/slag mortars', *Construction and Building Materials*, 40, pp. 291–298.

Mariyappan, V., and Somasundaram, K., (2025) The Synergy of Low-NaOH Activation and Carbon Sequestration in Sustainable Red Mud Based Geopolymer, School of Civil Engineering, Vellore Institute of Technology, Chennai-600127, India. https://doi.org/10.30955/gnj.07964

Mapei (2023) *MAPEPLAST SF (Microsil DM)*. https://cdnmedia.mapei.com/docs/librariesprovider2/products-documents/1_00780_mapeplast-sf_en_930440a5f5dc4b45bffe38cdd7f59edb.pdf?sfvrsn=4887e675_0.

Matalkah, F., Soroushian, P., Balachandra, A. & Peyvandi, A. (2016) 'Characterization of alkali-activated nonwood biomass ash–based geopolymer concrete', *Journal of Materials in Civil Engineering*, 29(4), 04016270.

McLellan, B. C., Williams, R. P., Janine, L., Van Riessen, A. & Corder, G. D. (2011) 'Costs and carbon emissions for geopolymer pastes in comparison to ordinary Portland cement', *Journal of Cleaner Production*, 19(9–10), pp. 1080–1090.

Mishra, J., Nanda, B., Patro, S. K. & Krishna, R. S. (2022) 'Sustainable fly ash based geopolymer binders: A review on compressive strength and microstructure properties', *Sustainability (Switzerland)*, 14(22). doi:10.3390/su142215062.

Mohamed Ismail, A. A., Kannadasan, K., Pichaimani, P., Arumugam, H. & Muthukaruppan, A. (2020) 'Synthesis and characterisation of sodium silicate from spent foundry sand: Effective route for waste utilisation', *Journal of Cleaner Production*, 264, 121689. doi:10.1016/j.jclepro.2020.121689.

Monnin, C. & Dubois, M. (2005) 'Thermodynamics of the LiOH + H_2O system', *Journal of Chemical & Engineering Data*, 50(4), pp. 1109–1113.

Moore, A. J., Bakera, A. T. & Alexander, M. G. (2020) 'Water sorptivity and porosity testing of concrete', *Concrete Beton*, 162, pp. 13–16.

Moore, A. J., Bakera, A. T. & Alexander, M. G. (2021) 'A critical review of the water sorptivity index (WSI) parameter for potential durability assessment: Can WSI be considered in isolation of porosity?', *Journal of the South African Institution of Civil Engineering*, 63(2), pp. 27–34. doi:10.17159/2309-8775/2021/v63n2a4.

Morsy, M. S., Rashaad, A. M., Shoukry, H. & Mokhtar, M. M. (2019) 'Potential use of limestone in metakaolin-based geopolymer activated with H3PO4 for thermal insulation', *Construction and Building Materials*, 229, 117088.

Mucsi, G. & Ambrus, M. (2018) *Raw Materials for Geopolymerisation*. https://www.researchgate.net/publication/328009917_Raw_Materials_for_Geopolymerisation.

Naghizadeh, A. (2019) Mix Design and Alkali Resistance of Fly Ash Geopolymer Binders. Doctoral Dissertation, University of Johannesburg.

Naghizadeh, A. & Ekolu, S.O. (2017) 'Pozzolanic materials and waste products for formulation of geopolymer cements in developing countries: A review,' *Concrete Beton*, 151(November), pp. 22–31.

Naghizadeh, A. & Ekolu, S. O. (2018) Effect of mix parameters on strength of geopolymer mortars-experimental study. In *Proceedings of the 6th International Conference on Durability of Concrete Structures, ICDCS 2018*, pp. 315–319. https://docs.lib.purdue.edu/cgi/viewcontent.cgi?article=1256&context=icdcs.

Naghizadeh, A. and Ekolu, S. O. (2019) 'Method for comprehensive mix design of fly ash geopolymer mortars', *Construction and Building Materials*, 202, pp. 704–717. doi:10.1016/j.conbuildmat.2018.12.185.

Naghizadeh, A. & Ekolu, S. O. (2022) 'Activator-related effects of sodium hydroxide storage solution in standard testing of fly ash geopolymer mortars for alkali–silica

reaction', *Materials and Structures/Materiaux et Constructions*, 55(1), pp. 1–16. doi:10.1617/s11527-021-01875-8.

Naghizadeh, A., Ekolu, S. O., Tchadjie, L. N. & Solomon, F. (2023) 'Long-term strength development and durability index quality of ambient-cured fly ash geopolymer concretes', *Construction and Building Materials*, 374(March), 130899. doi:10.1016/j.conbuildmat.2023.
130899.

Nikolov, A., Rostovsky, I. & Nugteren, H. (2017) 'Geopolymer materials based on natural zeolite', *Case Studies in Construction Materials*, 6(March), pp. 198–205. doi:10.1016/j.cscm.2017.03.001.

Occidental Chemical Corporation (2013) 'Product stewardship summary: Liquid sodium silicates', *Product Stewardship Journal*, pp. 1–5. https://www.oxy.com/siteassets/documents/
chemicals/stewardship/liquid-sodium-silicates.pdf.

Okoye, F. N., Durgaprasad, J. & Singh, N. B. (2016) 'Effect of silica fume on the mechanical properties of fly ash based-geopolymer concrete', *Ceramics International*, 42, pp. 3000–3006.

Olivia, M. (2011) Durability Related Properties of Low Calcium Fly Ash Based Geopolymer Concrete. Doctoral Dissertation, Curtin University.

Oti, J., Adeleke, B. O., Mudiyanselage, P. R. & Kinuthia, J. (2024) 'A comprehensive performance evaluation of GGBS-based geopolymer concrete activated by a rice husk ash-synthesised sodium silicate solution and sodium hydroxide', *Recycling*, 9(2), 23.

Otieno, M. (2018) 'Sensitivity of the rapid chloride conductivity index test to concrete quality and changes in various test parameters', *Cement and Concrete Composites*, 86(0958–9465), pp. 110–116.

Oyebisi, S. O., Owolabi, E. F., Owamah, H. I., Oluwafemi, J. O. & Ayanbisi, O. W. (2021) 'Strength prediction of GPC using alkali pH, salinity, temperature, and conductivity as

continuous predictors', *IOP Conference Series: Materials Science and Engineering*, 1107(1), 012145. doi:10.1088/1757-899x/1107/1/012145.

Palomo, A., Grutzeck, M. W. & Blanco, M. T. (1999) 'Alkali-activated fly ashes: A cement for the future', *Cement and Concrete Research*, 29(8), pp. 1323–1329. doi:10.1016/S0008-8846(98)00243-9.

Parbhoo, P., Lyimo, H. & Ekolu, S. O. (2012) Effect of repair materials on durability indexes of concrete. In *Concrete Repair, Rehabilitation and Retrofitting III – Proceedings of the 3rd International Conference on Concrete Repair, Rehabilitation and Retrofitting, ICCRRR 2012*, pp. 1017–1022. https://ujcontent.uj.ac.za/esploro/outputs/journalArticle/Effect-of-repair-materials-on-durability/9913102707691.

Park, S. K., Wook, J. B. & Park, M. S. (2007) 'Strength and hardening characteristics of activated fly ash mortars', *Magazine of Concrete Research*, 2(59), pp. 121–129.

Passuello, A, Rodríguez, E. D. & Hirt, E. (2017) 'Evaluation of the potential improvement in the environmental footprint of geopolymers using waste-derived activators', *Journal of Cleaner Production*, 166, pp. 680–689.

Passuello, A., Rodríguez, E. D., Hirt, E., Longhi, M., Bernal, S. A., Provis, J. L. & Kirchheim, A. P. (2017) 'Evaluation of the potential improvement in the environmental footprint of geopolymers using waste-derived activators', *Journal of Cleaner Production*, 166, pp. 680–689. doi:10.1016/j.jclepro.2017.08.007.

Patil, S., & Joshi, D.A. (2025) 'Design of highly workable geopolymer concrete for rigid pavement by experimental investigation.' Innov. Infrastruct. Solut. 10(7)

Poomritphale, S., Bhardwajja, S. S., Gupta, R., Mazen, A. & Jeong, H. (2020) Advanced geopolymerization technology. In *Geopolymers and Other Geosynthetics*, edited by M. Alshaaer & H. Y. Jeon. InTechOpen. https://www.intechopen.com/chapters/67922.

Prabu, B., Shalini, A. & Kishore Kumar, S. (2014) 'Rice husk ash based geopolymer concrete – A review', *Chemical Science Review and Letters*, 3(10), pp. 288–294.

https://www.researchgate.net/publication/284309050_Rice_husk_ash_based_geopolymer_concrete_-_A_Review.

Provis, J. L. & Van Deventer, J. S. J. (2007) 'Geopolymerisation kinetics. 2. Reaction kinetic modelling', *Chemical Engineering Science*, 62, pp. 2318–2329.

Provis, J. L. & Van Deventer, J. S. J. (Eds.). (2009) *Geopolymers: Structure, Processing, Properties and Industrial Applications*. Cambridge: Woodhead Publishing.

Qaidi, S., Najm, H. M., Abed, S. M., Ahmed, H. U., Al Dughaishi, H., Al Lawati, J., Sabri, M. M., Alkhatib, F. & Milad, A. (2022) 'Fly ash-based geopolymer composites: A review of the compressive strength and microstructure analysis', *Materials*, 15(20), 7098. doi:10.3390/ma15207098.

Rahim, R. H. A., Azizli, K. A., Man, Z., Rahmiati, T. & Nuruddin, M. F. (2014) 'Effect of sodium hydroxide concentration on the mechanical property of non sodium silicate fly ash based geopolymer', *Journal of Applied Sciences*, 14(3), pp. 3381–3384.

Rafeet, A., Vinai, R., Soutsos, M. & Sha, W. (2017) 'Guidelines for mix proportioning of fly ash/GGBS based alkali activated concretes', *Construction and Building Materials*, 147, pp. 130–142. doi:10.1016/j.conbuildmat.2017.04.036.

Rajan, B. R. & Ramujee, K. (2015) 'Strength & development of fly ash and GGBS based geopolymer mortar', *International Journal of Engineering and Advanced Technology (IJRAET)*, 3(1), pp. 42–45.

Rajan, H. S. & Kathirvel, P. (2021) 'Sustainable development of geopolymer binder using sodium silicate synthesized from agricultural waste', *Journal of Cleaner Production*, 286, 124959. doi:10.1016/j.jclepro.2020.124959.

Rao, A. K. & Kumar, D. R. (2020) 'Comparative study on behaviour of GPC using silica fume and fly ash with GGBS exposed to elevated temperature and ambient curing conditions', *Materials Today*, 27, pp. 1833–1837.

Ravikumar, D., Peethamparan, S. & Neithalath, N. (2010) 'Structure and strength of NaOH activated concretes containing fly ash or GGBFS as the sole binder', *Cement and Concrete Composites*, 32(6), pp. 399–410. doi:10.1016/j.cemconcomp.2010.03.007.

Reynolds-Clausen, K. & Singh, N. (2019) 'South Africa's power producer's revised coal ash strategy and implementation progress', *Coal Combustion and Gasification Products*, 11(1), pp. 1–10. doi:10.4177/CCGP-D-18-00015.1.

Ridtirud, C., Chindaprasirt, P. & Pimraksa, K. (2011) 'Factors affecting the shrinkage of fly ash geopolymers', *International Journal of Minerals, Metallurgy and Materials*, 18(1), pp. 100–104. doi: 10.1007/s12613-011-0407-z.

Rivera, J. F., Cuarán-Cuarán, Z. I., Vanegas-Bonilla, N. & Mejía de Gutiérrez, R. (2018) 'Novel use of waste glass powder: Production of geopolymeric tiles', *Advanced Powder Technology*, 29(12), pp. 3448–3454. doi:10.1016/j.apt.2018.09.023.

Rodríguez, E. D., Bernal, S. A., Provis, J. L., Paya, J. & Monzo, J. M. (2013) 'Effect of nanosilica-based activators on the performance of an alkali-activated fly ash binder', *Cement and Concrete Composites*, 35(1), pp. 1–11.

Rupesh Kumar, D. & Krishna Rao, A. (2020) 'Comparative study on the behaviour of GPC using silica fume and fly ash with GGBS exposed to elevated temperature and ambient curing conditions', *Materials Today: Proceedings*, 27, Part 2(2214–7853), pp. 1833–1837.

Salvoldi, M., Beushausen, B. & Alexander, H. (2015) 'Oxygen permeability of concrete and its relation to carbonation', *Construction and Building Materials*, 85, pp. 30–37. https://doi.org/10.1016/j.conbuildmat.2015.02.019.

Sambucci, M., Sibai, A. & Valente, M. (2021) 'Recent advances in geopolymer technology: A potential eco-friendly solution in the construction materials industry', *Journal of Composites Science*, 5, pp. 1–30.

Samson, G., Cyr, M. & Gao, X. X. (2017) 'Formulation and characterization of blended alkali-activated materials based on flash-calcined metakaolin, fly ash and GGBS',

Construction and Building Materials, 144, pp. 50–64. doi:10.1016/j.conbuildmat.2017.03.160.

SANS 3001-CO3-1:2015 (2015) *Civil Engineering Test Methods Part CO3-1: Concrete Durability Index Testing – Preparation of Test Specimens*, *South African National Standard*.

SANS 3001-CO3-2 (2015) *Civil Engineering Test Methods Part CO3-2: Concrete Durability Index Testing – Oxygen Permeability Test*, *South African National Standard*.

SANS 5863:2006 (2006) *Concrete Tests – Compressive Strength of Hardened Concrete*. https://www.scribd.com/document/357100671/SANS-5863.

Shill, S. K., Al-Deen, S. & Mahmud Ashraf, W. H. (2020) 'Resistance of fly ash based geopolymer mortar to both chemicals and high thermal cycles simultaneously', *Construction and Building Materials*, 239, 117886.

Sindhunata, J., Van Deventer, S. J., Lukey, G. & Xu, H. (2006) 'Effect of curing temperature and silicate concentration on fly-ash-based geopolymerization', *Industrial & Engineering Chemistry Research*, 45(10), pp. 3559–3568.

Singh, B., Ishwarya, G., Gupta, M. & Bhattacharyya, S. K. (2015) 'Geopolymer concrete: A review of some recent developments', *Construction and Building Materials*, 85, pp. 78–90. doi:10.1016/j.conbuildmat.2015.03.036.

Singh, N. B., Kumar, M. & Rai, S. (2019) 'Geopolymer cement and concrete: Properties', *Materials Today: Proceedings*, 29, pp. 743–748. doi:10.1016/j.matpr.2020.04.513.

Singh, N. B. & Middendorf, B. (2020) 'Geopolymers as an alternative to Portland cement: An overview', *Construction and Building Materials*, 237, 117455. doi:10.1016/j.conbuildmat.2019.
117455.

Škvára, F (2011) 'Alkali activated material – Geopolymer', *ICT Prague*, 02, pp. 68–72.

Škvára, F., Kopecký, L., Nìmeèek, J. & Bittnar, Z. (2006) 'Microstructure of geopolymer concrete based on fly ash', *Ceramics − Silikáty*, 50(4), pp. 208–215. https://www.osti.gov/etdeweb/biblio/20862289.

Sore, S. O., Messan, A., Prud'Homme, E., Escadeillas, G. & Tsobnang, F. (2020) 'Comparative study on geopolymer binders based on two alkaline solutions (NaOH and KOH)', *Journal of Minerals and Materials Characterization and Engineering*, 8(6), pp. 407–420. doi:10.4236/jmmce.2020.86026.

Sunarsih, E. S., As'ad, S., Sam, A. R. M. & Kristiawan, S. A (2023) 'Properties of fly ash-slag-based geopolymer concrete with low molarity sodium hydroxide', *Civil Engineering Journal (Iran)*, 9(2), pp. 381–392. doi:10.28991/CEJ-2023-09-02-010.

Tajudin, M. A., Faris, M. A., Al Bakri Abdullah, M. M., Sandu, A. V., Nizar, K., Moga, L., Neculai, O. & Muniandi, R. (2017) 'Assessment of alkali activated geopolymer binders as an alternative of portlant cement', *Materiale Plastice*, 54(1). pp. 145–154. http://psasir.upm.edu.my/id/eprint/60942/.

Tang, S. W., Yao, Y., Andrade, C. & Li, Z. J. (2015) 'Recent durability studies on concrete structure', *Cement and Concrete Research*, 78(Part A), pp. 143–154. doi:10.1016/j.cemconres.
2015.05.021.

Tchakoute, H. K., Elimbi, A., Yanne, E. & Djangang, C. N. (2013) 'Accepted manuscript', *Cement & Concrete Composites*.

Thokchom, S., Ghosh, P. & Ghosh, S. (2010) 'Performance of fly ash based geopolymer mortars in sulphate solution', *Journal of Engineering Science and Technology Review*, 3(1), pp. 36–40. doi:10.25103/jestr.031.07.

Tong, K. T., Vinai, R. & Soutsos, M. N. (2018) 'Use of Vietnamese rice husk ash for the production of sodium silicate as the activator for alkali-activated binders', *Journal of Cleaner Production*, 201, pp. 272–286. doi:10.1016/j.jclepro.2018.08.025.

Toniolo, N. (2018) *Novel Geopolymers Incorporating Silicate Waste*. https://www.researchgate.net/publication/330872748_Novel_geopolymers_incorporating_silicate_waste.

Torres-Carrasco, M. & Puertas, F. (2015) 'Waste glass in the geopolymer preparation: Mechanical and microstructural characterisation', *Journal of Cleaner Production*, 90(0959–6526), pp. 397–408.

Triwulan, M., Wigestika, P. & Ekaputri, J. J. (2016) 'Addition of superplasticizer on geopolymer concrete', *ARPN Journal of Engineering and Applied Sciences*, 11(24), pp. 14456–14462.

Turner, L. K. & Collins, F. G. (2013) 'Carbon dioxide equivalent (CO_2-e) emissions: A comparison between geopolymer and OPC cement concrete', *Construction and Building Materials*, 43, pp. 125–130. doi:10.1016/j.conbuildmat.2013.01.023.

Uzbas, B. & Aydin, A. C. (2020) 'Microstructural analysis of silica fume concrete with scanning electron microscopy and x-ray diffraction', *Engineering, Technology and Applied Science Research*, 10(3), pp. 5845–5850. doi:10.48084/etasr.3288.

Vafaei, M., Allahverdi, A., Dong, P. & Bassim, N. (2018) 'Acid attack on geopolymer cement mortar based on waste-glass powder and calcium aluminate cement at mild concentration', *Construction and Building Material*, 193, pp. 363–372.

Vinai, R. & Soutsos, M. (2019) 'Production of sodium silicate powder from waste glass cullet for alkali activation of alternative binders', *Cement and Concrete Research*, 116, pp. 45–56. doi:10.1016/j.cemconres.2018.11.008.

Vora, P. R. & Dave, U. V. (2013) 'Parametric studies on compressive strength of geopolymer concrete', *Procedia Engineering*, 51, pp. 210–219. doi:10.1016/j.proeng.2013.01.030.

Wang, F., Sun, X., Tao, Z. & Pan, Z. (2022) 'Effect of silica fume on compressive strength of ultra-high-performance concrete made of calcium aluminate cement/fly ash based

geopolymer', *Journal of Building Engineering*, 62, 105398. doi:10.1016/j.jobe.2022.105398.

Wang, Q., Zhu, L., Lu, C., Liu, Y., Yu, Q. & Chen, S. (2023) 'Investigation on the effect of calcium on the properties of geopolymer prepared from uncalcined coal gangue', *Polymers*, 15(5), 1241.

Xiao, R., Polaczyk, P., Zhang, M., Jiang, X., Zhang, Y., Huang, B. & Hu, W. (2020) 'Evaluation of glass powder-based geopolymer stabilized road bases containing recycled waste glass aggregate', *Transportation Research Record*, 2674(1), pp. 22–32. doi:10.1177/0361198119898695.

Xie, J. & Kayali, O. (2013) 'Effect of water content on the development of fly ash-based geopolymers in heat and ambient curing conditions', *Sustainable Construction Materials and Technologies*, 2013, pp. 1–9.

Xu, H. & Van Deventer, J. S. (2000) 'The geopolymerisation of alumino-silicate minerals', *International Journal of Mineral Processing*, 59(3), pp. 247–266.

Xu, H. & Van Deventer, J. S. (2002) 'Microstructural characterisation of geopolymers synthesized from kaolinite/stilbite mixtures using XRD, MAS-NMR, SEM/EDX, TEM/EDX and HREM', *Cement and Concrete Research*, 32, pp. 1705–1716.

Xu, H. & Van Deventer, J. S. (2003) 'The effect of alkali metals on the formation of geopolymeric gels from alkali-feldspars', *Colloids and Surfaces A*, 216, pp. 27–44.

Xiaohong, Y., Weiling, Z. & Qiao, Y. (2008) 'The viscosity properties of sodium silicate solutions', *Journal of Solution Chemistry*, 37(1), pp. 73–83.

Yang, X., Zhu, W. & Yang, Q. (2008) 'The viscosity properties of sodium silicate solutions', *Journal of Solution Chemistry*, 37, pp. 73–83.

Zerfu, K. & Ekaputri, J. J. (2016) 'Review on alkali-activated fly ash based geopolymer concrete', *Materials Science Forum*, 841, pp. 162–169. doi:10.4028/www.scientific.net/MSF.841.162.

Zheng, C., Wang, J., Liu, H., GangaRao, H. & Liang, R. (2022) 'Characteristics and microstructures of the GFRP waste powder/GGBS-based geopolymer paste and concrete', *Reviews on Advanced Materials Science*, 61(1), pp. 117–137. doi:10.1515/rams-2022-0005.

Živica, V. (2006) 'Effectiveness of new silica fume alkali activator', *Cement and Concrete Composites*, 28(1), pp. 21–25. doi:10.1016/j.cemconcomp.2005.07.004.

Živica, V. & Križma, M. (2013) 'Acidic-resistant slag cement', *Magazine of Concrete Research*, 65(18), pp. 1073–1080.

Živica, V., Palou, M. T. & Križma, M. (2015) 'Geopolymer cements and their properties: A review', *Building Research Journal*, 61(2), pp. 85–100. doi:10.2478/brj-2014-0007.

Zuda, L., Pavlík, Z., Rovnaníková, P., Bayer, P. & Černý, R. (2006) 'Properties of alkali activated aluminosilicate material after thermal load', *International Journal of Thermophysics*, 27(4), pp. 1250–1263. doi:10.1007/s10765-006-0077-7.

APPENDICES

Appendix A: Additional Results

This section provides additional results for the experiments conducted in Phase 1 and Phase 2 of the study. It also includes the durability and microstructural analysis results that were not shown in the dissertation.

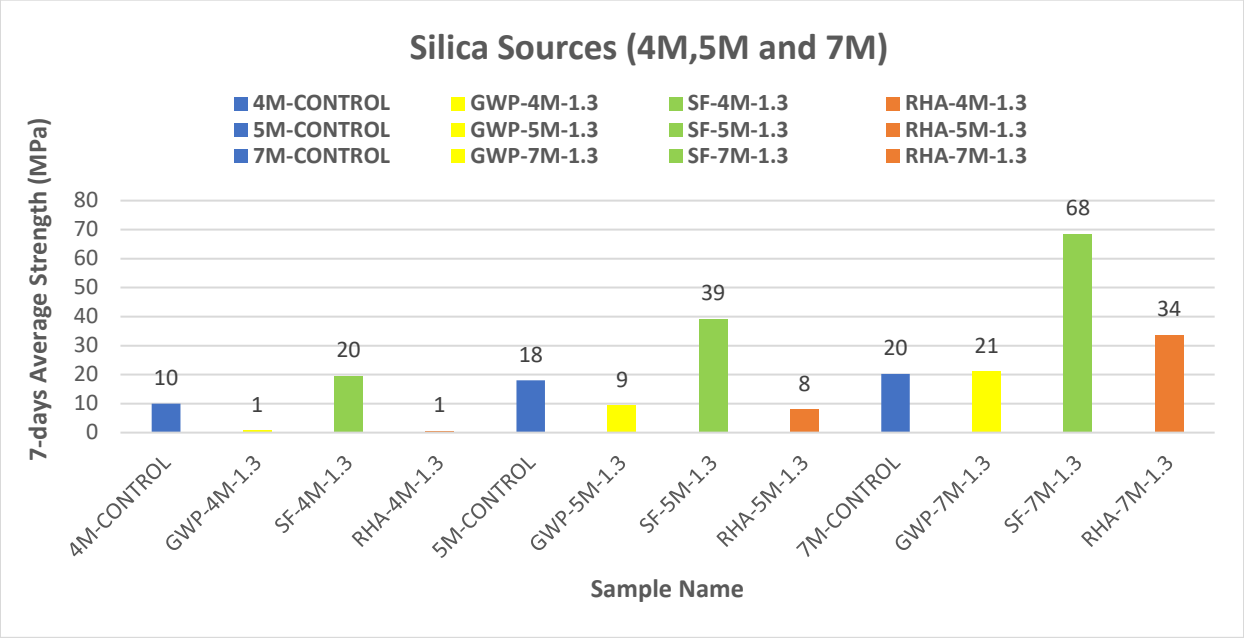

Figure A1: Compressive strength test results of additional mixes described in Table 3.12

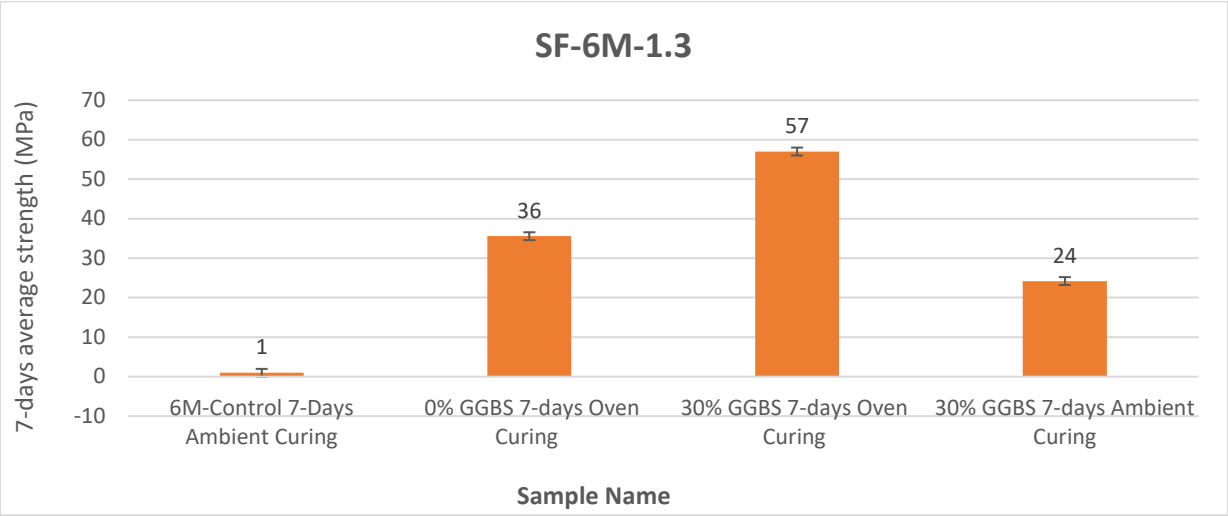

Figure A2: Compressive strength test results of optimum mortar samples described in Section 3.4.2

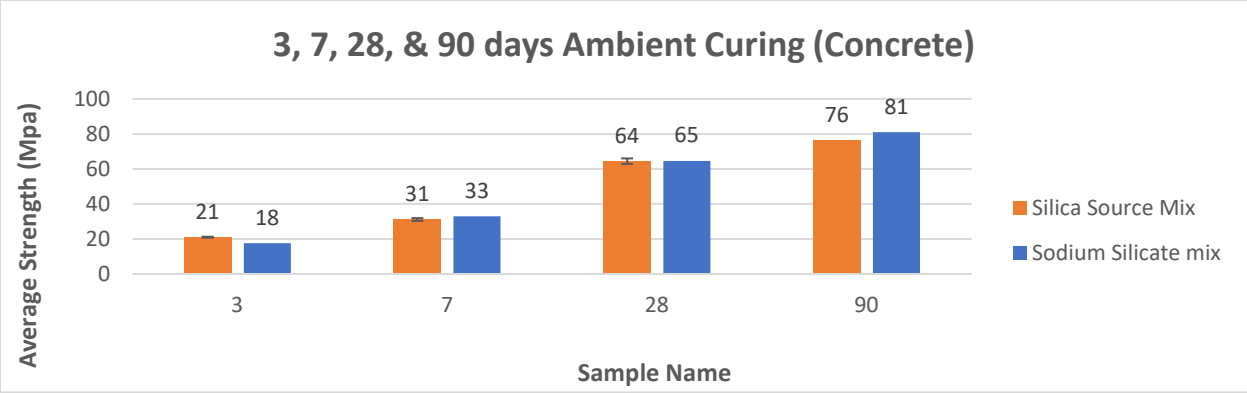

Figure A3: Compressive strength test results of conventional and alternative mixes under ambient curing

Concrete Permeability
Test 2

File Name :-	AU-1
Client:-	
Reference:-	
Description:-	
Date Tested:-	24 Oct 2022
Purge Time (Secs):-	5.00
1st Reading (Min);-	15.00
Record Interval (Min):-	15.00
Stop kPa (kPa):-	5.0
Stop Test (Hrs):-	2.00
Working Pressure (kPa):-	100.0

Reading No	kPa	kPa drop per Min
0	95.5	0.0
1	80.2	1.0
2	68.5	0.8
3	58.7	0.7
4	50.5	0.5
5	44.3	0.4
6	38.9	0.4
7	33.5	0.4
8	29.7	0.3
9	26.2	0.2
Stop	2.0	kPa

Concrete Permeability
Test 3

File Name :-	AU-4
Client:-	
Reference:-	
Description:-	
Date Tested:-	24 Oct 2022
Purge Time (Secs):-	5.00
1st Reading (Min);-	15.00
Record Interval (Min):-	15.00
Stop kPa (kPa):-	5.0
Stop Test (Hrs):-	2.00
Working Pressure (kPa):-	100.0

Reading No	kPa	kPa drop per Min
0	95.3	0.0
1	88.8	0.4
2	81.5	0.5
3	75.6	0.4
4	70.2	0.4
5	64.5	0.4
6	59.8	0.3
7	55.7	0.3
8	51.0	0.3
9	45.8	0.3
Stop	2.0	kPa

Concrete Permeability
Test 4

File Name :-	AU-3
Client:-	
Reference:-	
Description:-	
Date Tested:-	24 Oct 2022
Purge Time (Secs):-	5.00
1st Reading (Min):-	15.00
Record Interval (Min):-	15.00
Stop kPa (kPa):-	5.0
Stop Test (Hrs):-	2.00
Working Pressure (kPa):-	100.0

Reading No	kPa	kPa drop per Min
0	95.6	0.0
1	88.7	0.5
2	82.6	0.4
3	77.1	0.4
4	71.4	0.4
5	66.6	0.3
6	62.5	0.3
7	57.6	0.3
8	53.9	0.2
9	48.1	0.4
Stop	2.0	kPa

Concrete Permeability
Test 3

File Name :-	AU-5
Client:-	
Reference:-	
Description:-	
Date Tested:-	24 Oct 2022
Purge Time (Secs):-	5.00
1st Reading (Min):-	15.00
Record Interval (Min):-	15.00
Stop kPa (kPa):-	5.0
Stop Test (Hrs):-	2.00
Working Pressure (kPa):-	100.0

Reading No	kPa	kPa drop per Min
0	95.5	0.0
1	86.9	0.6
2	79.1	0.5
3	72.6	0.4
4	65.7	0.5
5	60.4	0.4
6	55.7	0.3
7	50.7	0.3
8	46.6	0.3
9	41.7	0.3
Stop	2.0	kPa

Concrete Permeability
Test 2

File Name :-	AU-6
Client:-	
Reference:-	
Description:-	
Date Tested:-	24 Oct 2022
Purge Time (Secs):-	5.00
1st Reading (Min):-	15.00
Record Interval (Min):-	15.00
Stop kPa (kPa):-	5.0
Stop Test (Hrs):-	2.00
Working Pressure (kPa):-	100.0

Reading No	kPa	kPa drop per Min
0	95.3	0.0
1	82.2	0.9
2	72.4	0.7
3	64.4	0.5
4	58.0	0.4
5	52.4	0.4
6	46.7	0.4
7	42.4	0.3
8	38.2	0.3
9	34.0	0.3
Stop	2.0	kPa

Figure A4: Durability: Oxygen permeability index test results

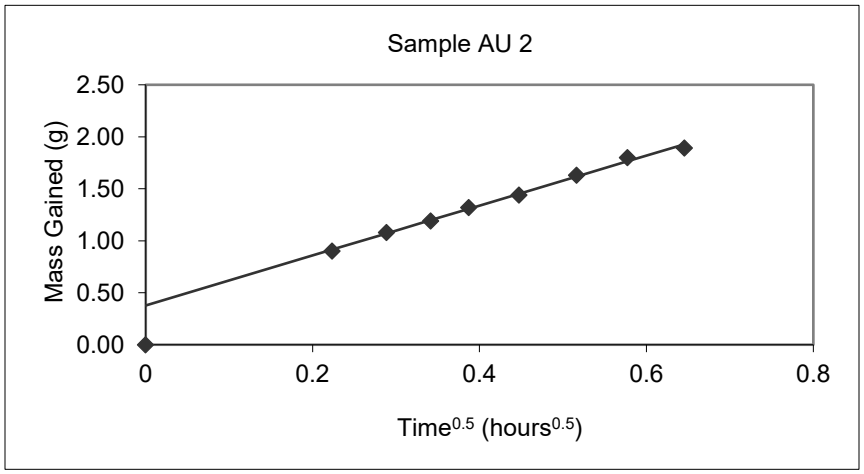

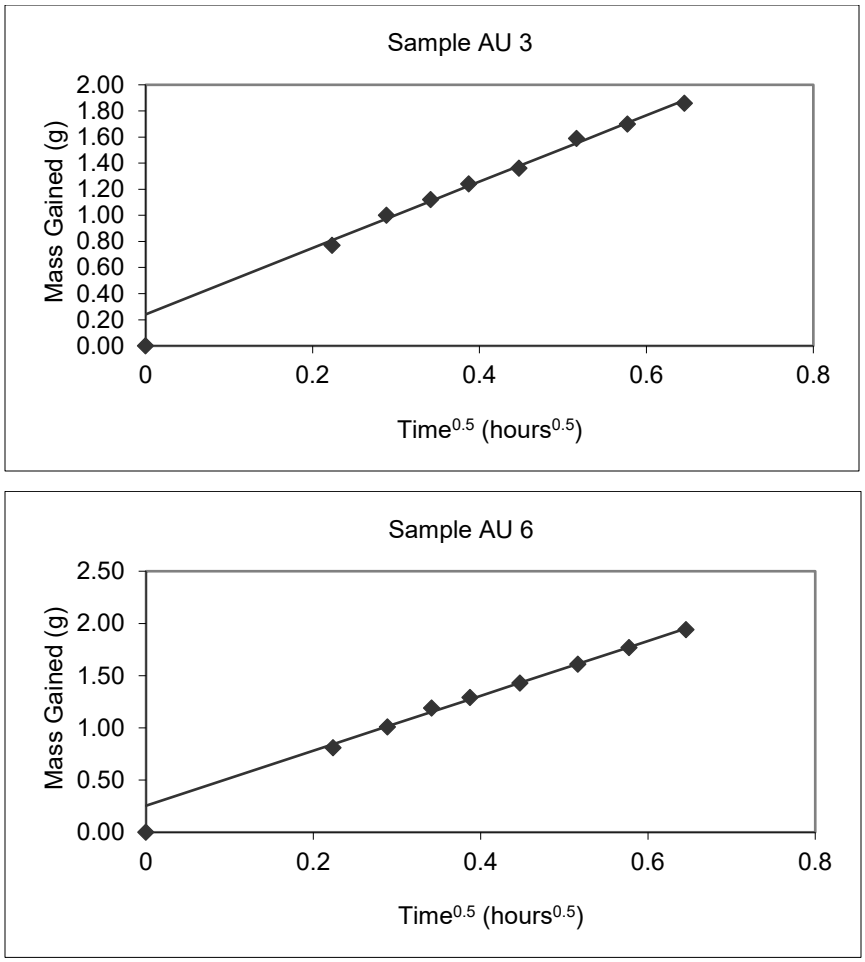

Figure A5: Durability: Water sorptivity index test results

	AU 1	AU 4	AU 5	AU - 4		
Mix 1	a	b	c'x	d	Mean	COV. (%)
Avr. Tickness (cm)	30.005	29.410	29.760	29.41		
Avr. Dia. (cm)	68.41	68.320	68.295	68.320		
A (cm^2)	36.761	36.664	36.637	36.664		
V- Supply	10.00	10.00	10.00	10.00		
V- Luggin	8.02	8.04	8.17	8.04		
i- Current-Supply (mA)	255	227.000	212.000	227.000		
dv = Vsupply-V luggin	1.980	1.960	1.830	1.960		
CC (mS/cm) = i.t/dv.A	105.120	92.901	94.101	92.901		
					96.26	6.17

Figure A6: Durability: Chloride conductivity index test results

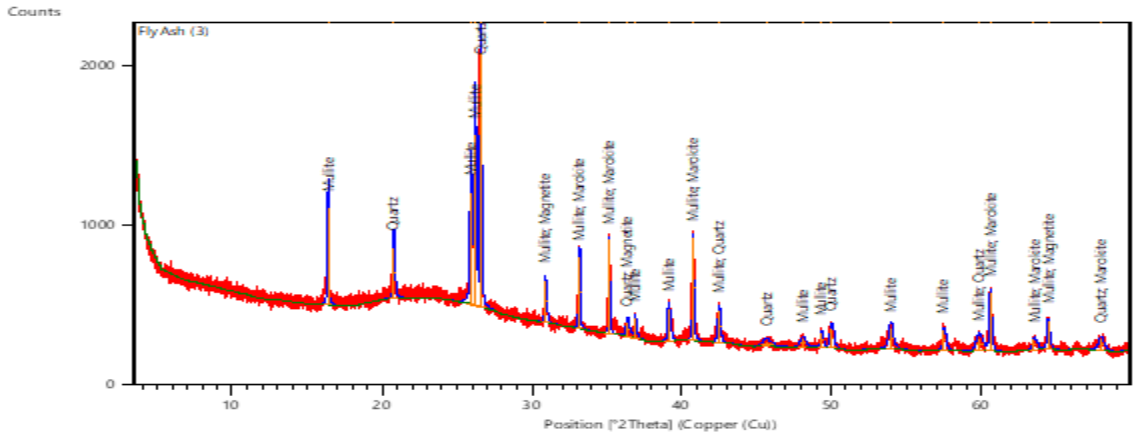

Peak List: (Bookmark 3)

Pos. [°2Th.]	Height [cts]	FWHM Left [°2Th.]	d-spacing [Å]	Rel. Int. [%]
16.3706	611.88	0.0866	5.41483	38.41
20.7886	318.46	0.1260	4.27298	19.99
25.9159	705.30	0.1417	3.43806	44.28
26.1958	1072.59	0.1260	3.40196	67.33
26.5689	1592.96	0.0787	3.35503	100.00
30.9004	264.33	0.0945	2.89390	16.59
33.1587	448.32	0.1102	2.70179	28.14
35.1757	591.87	0.0630	2.55135	37.16
36.4191	83.96	0.2519	2.46705	5.27
36.9388	124.96	0.1260	2.43353	7.84
39.1660	205.20	0.1574	2.30012	12.88
40.7792	650.04	0.0787	2.21278	40.81
42.5122	205.45	0.1574	2.12650	12.90
45.6713	34.28	0.7557	1.98649	2.15
48.0677	48.50	0.3779	1.89291	3.04
49.3629	95.88	0.1260	1.84623	6.02
50.0188	125.61	0.2204	1.82355	7.89
53.9406	128.18	0.3149	1.69987	8.05
57.5093	128.44	0.1889	1.60258	8.06
59.8400	83.78	0.4408	1.54561	5.26
60.5751	369.21	0.1102	1.52861	23.18
63.5246	65.64	0.2519	1.46456	4.12
64.4454	181.67	0.1260	1.44584	11.40

Figure A7: Details of the peaks obtained in the XRD pattern related to fly ash

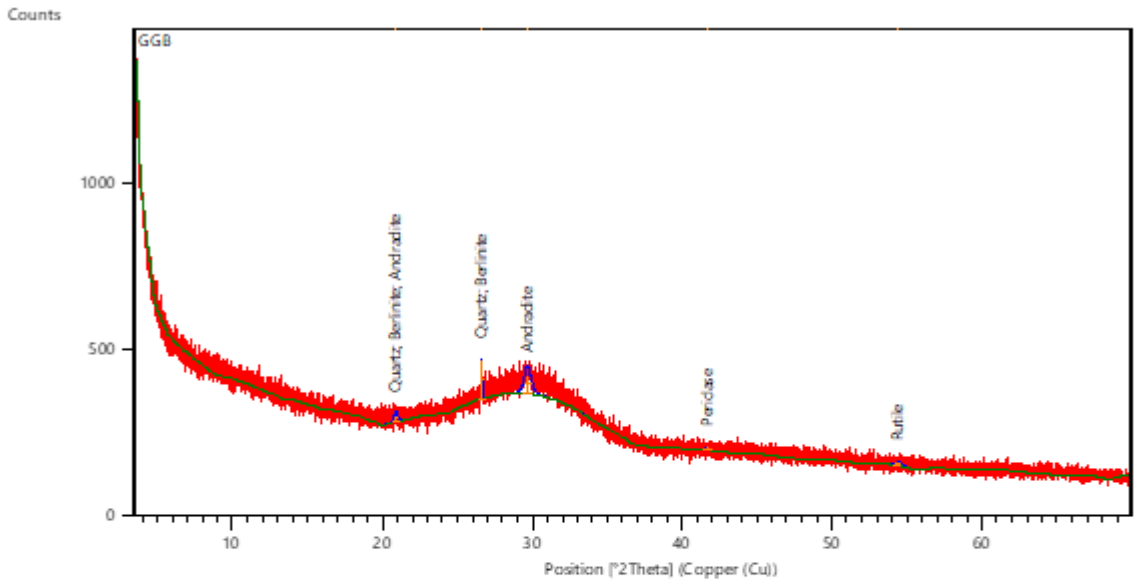

Peak List: (Bookmark 3)

Pos. [°2Th.]	Height [cts]	FWHM Left [°2Th.]	d-spacing [Å]	Rel. Int. [%]
20.8790	22.26	0.1889	4.25468	18.83
26.6037	118.25	0.0288	3.34795	100.00
29.6383	58.17	0.5038	3.01419	49.19
41.6685	6.83	0.0945	2.16759	5.78
54.3660	9.97	0.3779	1.68757	8.43

Figure A8: Details of the peaks obtained in the XRD pattern related to GGBS

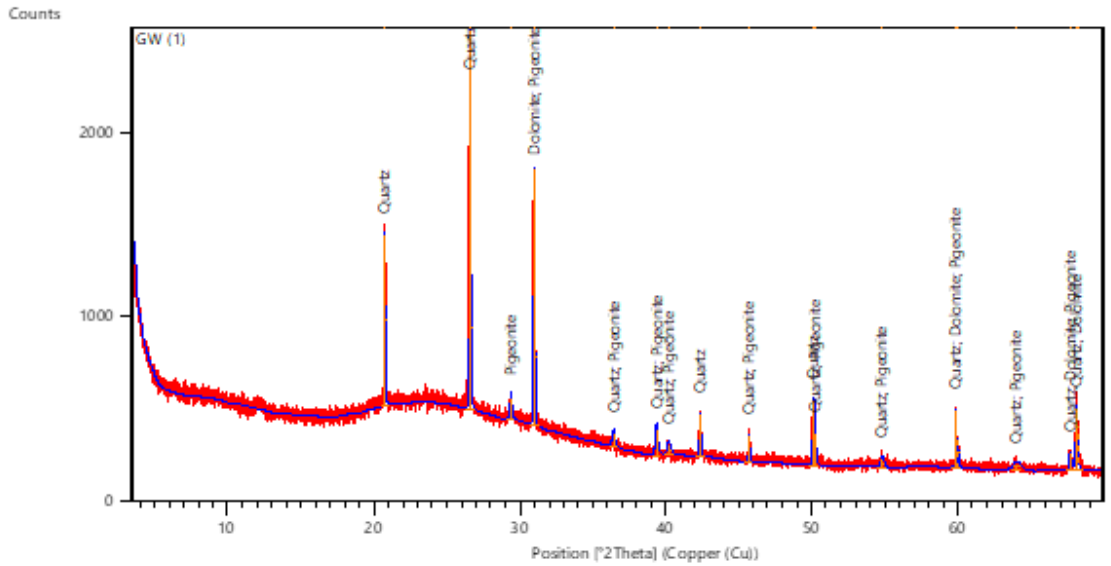

Peak List: (Bookmark 3)

Pos. [°2Th.]	Height [cts]	FWHM Left [°2Th.]	d-spacing [Å]	Rel. Int. [%]
20.7856	932.39	0.0315	4.27359	45.35
26.5710	2055.78	0.0384	3.35199	100.00
26.6374	885.16	0.0288	3.35209	43.06
29.3474	118.04	0.1536	3.04089	5.74
30.9417	1403.78	0.0336	2.88774	68.28
31.0117	735.18	0.0288	2.88854	35.76
36.4433	75.75	0.1920	2.46343	3.68
39.3732	146.14	0.1536	2.28660	7.11
40.2189	53.30	0.2304	2.24045	2.59
42.3701	229.35	0.0480	2.13154	11.16
45.7083	141.05	0.0576	1.98333	6.86
50.0752	347.67	0.0480	1.82012	16.91
50.2086	175.39	0.0768	1.81560	8.53
54.8200	51.95	0.2304	1.67327	2.53
59.8682	314.35	0.0576	1.54367	15.29
60.0370	161.32	0.0768	1.54356	7.85
63.9752	32.50	0.4608	1.45412	1.58
67.6556	95.50	0.0960	1.38369	4.65
68.0726	343.37	0.0576	1.37623	16.70
68.2569	250.16	0.0576	1.37637	12.17

Figure A9: Details of the peaks obtained in the XRD pattern related to GWP

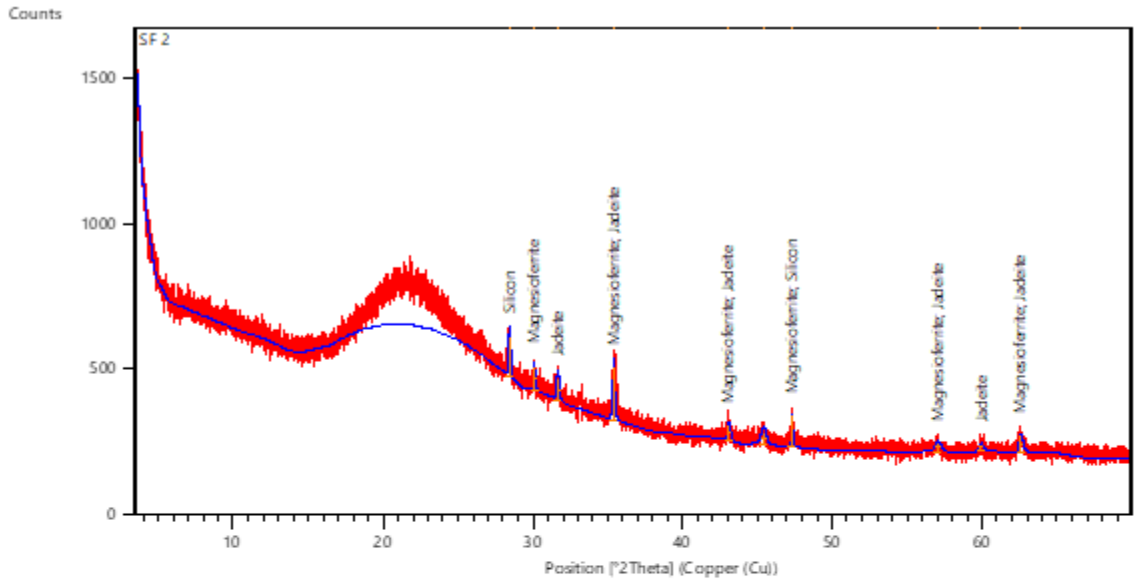

Peak List: (Bookmark 3)

Pos. [°2Th.]	Height [cts]	FWHM Left [°2Th.]	d-spacing [Å]	Rel. Int. [%]
28.4105	141.56	0.1260	3.14160	76.19
30.0842	88.26	0.0945	2.97053	47.50
31.6349	78.28	0.1889	2.82836	42.13
35.4132	185.80	0.1260	2.53478	100.00
43.0800	53.55	0.1889	2.09978	28.82
45.3956	43.91	0.3779	1.99791	23.63
47.2829	107.11	0.0576	1.92089	57.65
57.0163	27.53	0.3779	1.61526	14.82
59.9277	25.52	0.1889	1.54356	13.74
62.5535	60.62	0.1889	1.48493	32.62

Figure A10: Details of the peaks obtained in the XRD pattern related to SF

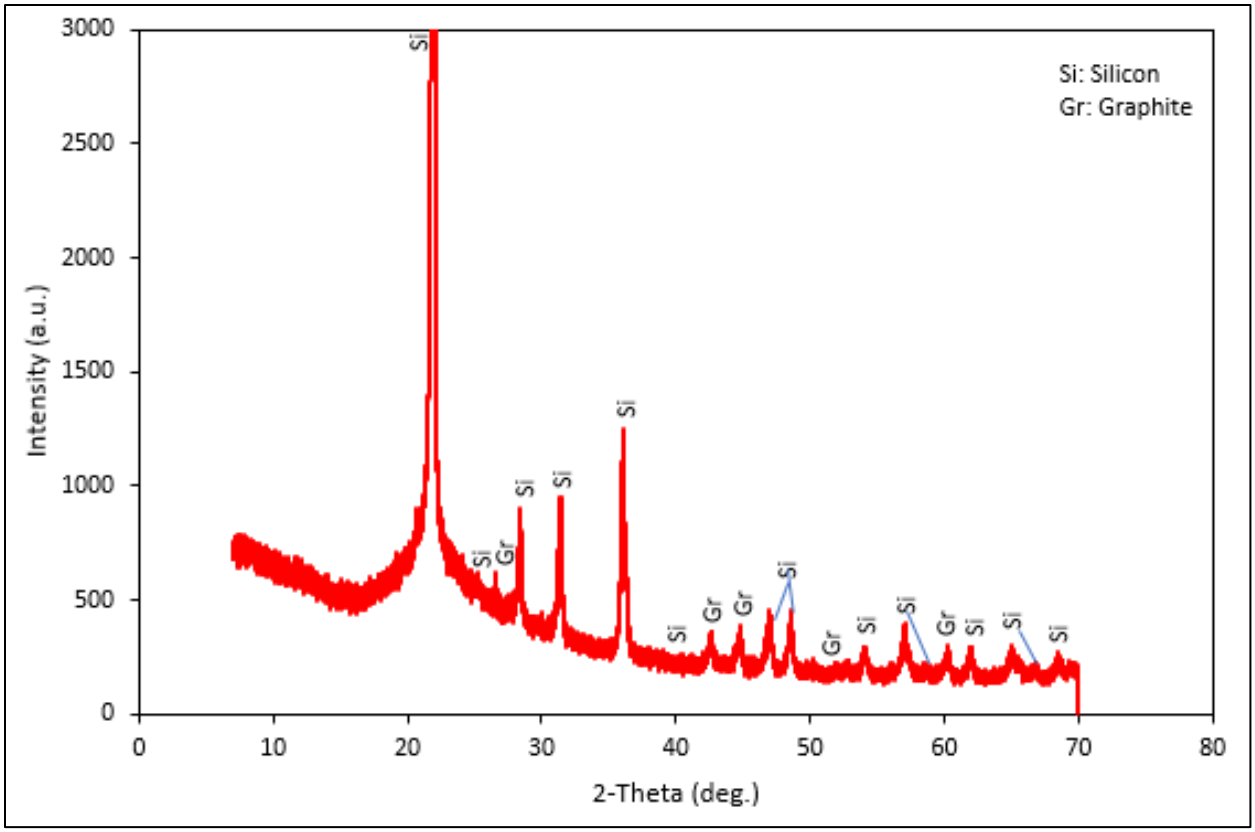

Figure A11: XRD pattern related to RHA

Appendix B: Journal Paper

Published journal paper emanating from this dissertation.

TECHNICAL PAPER

Effect of waste-derived alkali activators on compressive strength of fly ash geopolymer mortar

Ntebaleng Lekhera [1], Abdolhossein Naghizadeh [2] and Rakesh Gopinath [3,4]

(1) Faculty of Engineering, Information Technology and Built Environment, Central University of Technology, South Africa
(2) Department of Engineering Sciences, University of the Free State, South Africa
(3) School of Energy, Construction and Environment, Coventry University, UK
(4) School of Civil and Environmental Engineering, University of the Witwatersrand, South Africa

ABSTRACT

Portland cement (PC) production causes significant carbon emissions. Geopolymer technology is one of the alternative binders to PC in concrete. Although the elimination of lime calcination reduces the environmental impact of the production process in geopolymer binders, several studies have questioned the use of conventional sodium silicate as an activator. The environmental impacts of sodium silicate production are related to the elevated temperatures of up to 1300 °C associated with its production, which results in an increased carbon footprint. This study focuses on replacing sodium silicate with waste-derived alkali activators (WAA) based on silica fume, rice husk ash and glass-waste powder. WAA were prepared using sodium hydroxide solution through a hydrothermal method at 100 °C. The silica source/NaOH mass ratio varied from 1.0 to 1.3, while the concentration of NaOH was 6 M, 8 M or 10 M. Geopolymer mortars were prepared at a constant aggregate/fly ash ratio and alkali activator/fly ash ratio of 2.25 and 0.46, respectively. The 7-day compressive strength results indicated that mortar prepared with a silica fume-based activator gave the optimum strength of 87 MPa at a silica source/NaOH mass ratio of 1.3 and NaOH concentration of 8 M. Thus, WAA can effectively replace the conventional sodium silicate in geopolymer mortars.

Keywords: Waste-derived alkali activators; Compressive strength; Geopolymer; Sodium silicate; Silica fume.

1. INTRODUCTION

Concrete is a highly prevalent construction material recognized for its superior properties such as exceptional longevity, cost-effectiveness, and adaptability [1]. The primary constituent of concrete is Portland cement (PC) which is responsible for its binding capabilities. PC-based concrete usage is staggering, with global utilization exceeding 10 billion tons annually, making PC the second most utilized substance worldwide, after water [2]. Studies have demonstrated that PC has adverse environmental effects, attributable to the high temperatures necessary for its production process, resulting in the release of carbon dioxide (CO_2) emissions into the atmosphere. To mitigate the environmental impact of PC, alternative "green" approaches and solutions, such as geopolymers, have been developed. Several years of comprehensive research and development efforts have focused on investigating the engineering, thermal, microstructural, and durability characteristics of geopolymer concrete as a sustainable substitute for PC. Geopolymer binders have exhibited properties similar to PC, indicating its potential as a viable replacement. Some studies have also found that geopolymer binders outperform PC concretes in terms of durability, including acid attack, chloride attack, shrinkage, alkali-silica reaction (ASR), and fire attack. Furthermore, fresh concrete properties such as setting time and workability are critical aspects that should be considered when using concrete in construction [3, 4].

Geopolymers are typically synthesized by the reaction of alumino-silicate precursors and alkaline activators at moderate temperatures. These precursors encompass both naturally occurring pozzolans and industrial by-products. Among the various aluminosilicates employed, industrial by-products, such as fly ash, ground granulated blast furnace slag (GGBS), silica fume, and rice husk ash, are currently the most extensively utilized. Additionally, sodium/potassium hydroxide and sodium/potassium silicate solutions are the most used alkaline activators. Several studies have indicated that a blend of sodium hydroxide (NaOH) and sodium silicate solution is the most effective alkaline activator for geopolymer production, owing to its rapid dissolution and superior interaction with source materials. Nevertheless, conventional silicate-based alkali activators, like sodium silicate, used in geopolymer synthesis contribute significantly to the high carbon footprint, attributable to the elevated temperatures up to 1300 °C required for their production. However, studies have demonstrated that the replacement of sodium silicate with waste-derived alkali activators (WAA), such as silica fume (SF), rice husk ash (RHA), and glass waste powder (GWP), can serve as a means to mitigate the current level of CO_2 emissions [3, 5].

Research conducted by Tambichik et al. [7] indicates a significant increase in the amount of waste generated by the agricultural and industrial sectors. Incorporating this waste material in concrete production provides an alternative to mitigate the adverse environmental effects of conventional concrete, along with the challenge of limited landfill space. Venyite et al. [8] conducted a study utilizing a RHA-based activator for sodium silicate synthesis at a local level, aiming to reduce the energy consumption and cost associated with commercial sodium silicate production. Furthermore, the study also explored the usage of RHA as the only alkali activator in the geopolymerization of raw and calcined laterites. The findings show that the adoption of the hydrothermal process (a chemical reaction in solvents caused by heating or elevated temperatures) greatly improves the dissolution of RHA in NaOH. The prepared RHA/NaOH activator was also comparable to the commercial sodium silicate, which concluded that the produced RHA-based sodium silicate is efficient for laterite geopolymerization. Further research on GWP and SF has